The Discovery of a Novel Chemical Scaffold that Binds Dengue Virus Non-structural Protein 5

by

Brittany Lauren Speer

Department of Pharmacology
Duke University

Date:_____

Approved:

_____
Timothy Haystead, Supervisor

_____
Mariano Garcia-Blanco

_____
Micah Luftig

_____
Donald McDonnell

_____
Dennis Thiele

A Dissertation submitted in partial fulfillment of
the requirements for the degree of Doctor
of Philosophy in the Department of
Pharmacology in the Graduate School
of Duke University

2013

ABSTRACT

The Discovery of a Novel Chemical Scaffold that Binds Dengue Virus Non-structural Protein 5

by

Brittany Lauren Speer

Department of Pharmacology
Duke University

Date:_____

Approved:

_____
Timothy Haystead, Supervisor

_____
Mariano Garcia-Blanco

_____
Micah Luftig

_____
Donald McDonnell

_____
Dennis Thiele

An abstract of a dissertation submitted in partial fulfillment of the requirements for the degree of Doctor of Philosophy in the Department of Pharmacology in the Graduate School of Duke University

2013

Abstract

Dengue viruses (DENV) are mosquito-borne flaviviruses that pose a continued and growing threat to global health. There are estimated to be 390 million DENV infections each year, and because there is no vaccine or approved therapeutic treatment, developing a small-molecule treatment is imperative. Possible small-molecule drug therapies for DENV could be immune system modulators, inhibitors of DENV-required host factor, or inhibitors of a viral gene product. In this study, we chose to take the latter approach and focused our drug discovery efforts on the most highly conserved flaviviral protein, non-structural protein 5 (NS5). NS5 contains two major domains, each with different enzymatic activities. The N-terminus has methyltransferase activity, and the C-terminus, an RNA-dependent RNA polymerase (RdRp). The activities of both domains are purine-dependent, and therefore both domains contribute to the purine-binding properties of NS5. Inhibition of either of these domains in NS5 results in inadequate propagation of DENV, and the purine-binding domains present ideal drug targets for disrupting these activities. These factors make NS5 protein an ideal candidate target for our small-molecule library screen.

A high-throughput fluorescence-based screen was employed to identify anti-DENV compounds based on their ability to competitively bind NS5. The screen was performed by binding green fluorescent protein NS5 fusion protein (GFP-NS5) to immobilized ATP resin, and then performing parallel elutions using over 3,000 distinct

compounds. One compound in particular, HS-205020, was able to competitively elute GFP-NS5 from the ATP resin and also exhibited antiviral activity in both the U937+DC-SIGN human monocyte cell line and BHK-21 cells. Additionally, HS-205020 was able to inhibit DENV NS5 RNA polymerase activity in vitro. HS-205020 is chemically distinct from the majority of previously reported NS5 inhibitors, which are nucleoside analogs that can cause severe toxicity in animal studies. In contrast, over the concentration range that produced anti-DENV effects, HS-205020 showed comparable cell viabilities to ribavirin, an FDA approved hepatitis C virus (HCV) therapeutic. These findings support HS-205020 as a potential dengue antiviral candidate, and its chemical scaffold represents as an ideal starting compound for future structure-activity relationship studies.

Dedication

This dissertation in its entirety is dedicated to Cornelis Hagers, my grandfather, Opa. Although you are not here to witness this milestone in my life, I know you'd be proud. You were a tough man, but you had plenty of attributes that I'm proud to say I inherited. Ik hou van je. Here's to you, Opa!

Contents

Abstract iv

Dedication vi

Abbreviations xi

Table xiii

List of Figures xiv

Acknowledgements xviii

1. Introduction: Dengue virus 1

1.1 Background & Significance 1

1.2 Epidemiology 1

1.3 Pathogenesis 3

1.3.1 Virulence 4

1.3.2 Dengue virus life cycle 5

1.3.3 Gene products of DENV 9

1.3.3.1 Structural proteins 10

1.3.3.2 Nonstructural proteins 12

1.4 Anti-dengue treatment efforts 19

1.4.1 Vaccine efforts 20

1.4.1.1 Live attenuated virus vaccines 21

1.4.1.2 Live chimeric virus vaccines 22

1.4.1.3 Inactivated virus vaccines 23

1.4.1.4 Live recombinant and DNA vaccines 25

1.4.2 Drug discovery efforts 26

1.5 Hypothesis 29

2. Materials and Methods 29

2.1 Materials 29

2.2 Methods 31

2.2.1 Cell Culture 31

2.2.2 Dengue virus stock preparation 32

2.2.3 Metabolic Labeling of DENV-infected and mock-infected mammalian cells 33

2.2.3.1 Post-infection time frame determination 33

2.2.3.2 Metabolic labeling of HuH7 cells 33

2.2.3.3 Metabolic labeling of U937+DC-SIGN cells 35

2.2.4 Expression of GFP-fusion proteins 35

2.2.5 Fluorescence-based small-molecule drug screen 36

2.2.6 Flow cytometry-based assay to measure percent DENV infection in a monocytic cell line 39

2.2.6.1 Optimization of DENV infection vs. MOI 42

2.2.7 Focus-forming unit assay 44

2.2.8 EC_{50} determination using cell-based flaviviral immunodetection (CFI) assay 46

2.2.9 Viability Assays 48

2.2.10 RNA-dependent RNA polymerase (RdRp) assay 50

2.2.11 *In vitro* Hepatitis C virus assays 51

2.2.12 Statistical Analyses 53

3. Identification of purine-utilizing proteins that are differentially expressed during DENV infection 53

3.1 Twenty-four hour time course in DENV-infected human liver cells 58

3.2 DENV-infection in human monocytic cells 62

3.3 Comparison of the DENV purinomics profile with published DENV proteomic studies 65

3.4 ATP binding profile of GFP-NS5 69

4. A fluorescence-based small-molecule screen identifies novel anti-DENV candidates 73

4.1 Identification of lead compounds that disrupt the binding of GFP-NS5 to immobilized ATP 74

5. *In vitro* DENV antiviral assays 84

5.1 Flow cytometric anti-DENV assay 86

5.2 Quantifying the titer of infectious DENV using a focus-forming unit assay 92

5.3 Independent viability assay to determine cytotoxicity of lead compounds in the absence of DENV 97

5.4 Determination of EC_{50} for top 3 lead compounds in a cell-based flaviviral immunodetection (CFI) assay 100

6. HS-205020 preferentially binds the RNA-dependent RNA polymerase (RdRp) of DENV and reduces enzymatic activity *in vitro* 104

6.1 Elution profiles of NS5 methyltransferase and polymerase domains. 105

6.2 Determination of IC_{50} of HS-205020 against the DENV NS5 polymerase 111

7. HS-205020 activity in a cell culture model of Hepatitis C virus 113

7.2 A Flaviviridae member: Hepatitis C Virus 114

7.3 HS-205020 reduces production of infectious virus but not percent infection for HCV 115

8. Conclusions 119

9. Future Directions 123

Appendix A 129

Appendix B 133

Appendix C 135

Appendix D 137

Appendix E 140

References 161

Biography 171

Abbreviations

ATP	Adenosine triphosphate
BSA	Bovine serum albumin
DC-SIGN	Dendritic cell specific ICAM3-grabbing non-integrin
DENV	Dengue virus
DENV2-NGC	Dengue virus type-2 New Guinea C strain
DHF	Dengue hemorrhagic fever
DMSO	Dimethylsulfoxide
DSS	Dengue shock syndrome
DTT	Dithiothreitol
EC_{50}	Half maximal effective concentration
FAS	Fatty acid synthase
FBS	Fetal bovine serum
FFA(U)	Focus-forming unit assay (focus-forming units)
GFP	Green fluorescent protein
HCV	Hepatitis C virus
HEPES	4-(2-hydroxyethyl)-1-piperazineethanesulfonic acid
HRP	Horseradish peroxidase
IC_{50}	Half maximal inhibitory concentration
JEV	Japanese encephalitis virus

LSWB	Low stringency wash buffer
NS5	Non-structural protein 5
NS5b	Non-structural protein 5b (HCV)
PBS	Phosphate buffered saline
PFA	Paraformaldehyde
PVDF	Polyvinylidene difluoride
RdRp	RNA-dependent RNA polymerase
TBEV	Tick-borne encephalitis virus
TBS	Tris-buffered saline
TBST	Tris-buffered saline + 0.1% Tween

Table

Table 1: Partial list of host proteins that have been shown to be up- or down-regulated in response to DENV infection in previous studies. As specified, ten of the identified proteins are capable of binding and utitlizing ATP. 67

List of Figures

Figure 1: Map of dengue transmission. The countries are ranked according to the presence, likelihood, or absence of DENV, as shown by color-code. The extremes are shown in green, which represents absence of DENV, and red, which represents confirmed presence of DENV. The red pins denote recently reported cases (confirmed or probable) of dengue fever, DHF, or DSS. Modified from (Freifeld, 2013) 3

Figure 2: DENV life cycle. After a DENV- infected Aedes mosquito bites a human, the virus must enter the host cells in order to replicate. Upon endocytosis, viral proteins are translated from the viral (+)ssRNA, followed by replication of the viral genome. The new viral components are then packaged within an immature virion, which is modified by cleavage to a mature virion prior to budding out of the host cell. Numbers shown represent pH. 8

Figure 3: DENV polyprotein. The three structural proteins are located at the amino terminus, and the seven non-structural proteins extend from the structural proteins to the carboxy terminus. After translation of the large of the one large polyprotein, individual DENV proteins are released via proteolytic processing by both host and viral proteases. 9

Figure 4: Overview of fluorescence-based small molecule drug screen. Crude cell lysate from HEK293 cells overexpressing GFP-NS5 was bound to ATP resin. Resin was aliquoted into 96-well plates and small-molecule solutions or soluble ATP was added. Fluorescence of eluted proteins was measured on a plate reader and compounds capable of yielding a fluorescence greater than 2.5-fold over background were flagged as lead compounds. Modified from (Carlson et al., 2013). 37

Figure 5: Optimization of DENV percent infection vs. multiplicity of infection in U937+DC-SIGN cells. A total of $2.5x10^4$ cells were plated in each well of a 96-well plate in a total volume of 250uL of RPMI+/+. After 24 h, cells are re-suspended in DENV2-NGC virus to the indicated MOI. The next day, cells were subjected to immunofluorescence to determine the percent DENV infection. 43

Figure 6: Schematic of [^{35}S]-metabolic labeling to identify purine-utilizing proteins that are up- or down-regulated in response to DENV infection. As described in Materials and Methods (Chapter 2), DENV2-NGC virus was added to HuH7 cells or U937+DC-SIGN cells. The radiolabeled amino acid mixture was added in equal quantities to either -infected HuH7 cells, mock-infected. After a 2 hour label, the cells in both samples are collected for analysis 57

Figure 7: Late Time Points in DENV Infection (12 – 24 hours post-infection): [^{35}S] autoradiogram showing purine-binding proteins in DENV-infected cells (V) and uninfected control cells (NV), from 12 to 24 hours post-infection. Protein bands that showed increased expression levels in DENV-infected cells over time (and compared to controls) were excised, and proteins were and identified using mass spectrometry. 59

Figure 8: ATP-capture of DENV proteins NS5 and NS3 from DENV-infected (24 h p.i.) or control U937+DC-SIGN cells. Both NS proteins bind ATP-resin and eluted with 100 mM ATP. Control, or mock-infected protein samples are labeled as C and virus-infected samples as V. It is probable that the band directly beneath NS3 in the V lane is a degradation product of NS3. Additionally, the two bands present below the 25 kDa marker in the V lane were identified by MS as IgG, 40S ribosomal protein and unnamed proteins. The unnamed proteins may be degradation products of viral proteins that are present in low quantities and below the detection threshold. All other proteins identified were host ATP-binding proteins or unidentified based on copy number. 64

Figure 9: Elution profile of GFP-NS5. Crude HEK293 lysate containing GFP-NS5 was added to ATP resin to isolate purine-binding proteins. Soluble ATP was then added to elute proteins bound to the the resin. Levels of GFP-NS5 in the eluted samples were measured by fluorescence detection (A) and Western blot (B) with α-GFP antibody. The Western blot sample correlates to the fluorescence data point directly above it (0-100 mM ATP). Full length GFP-NS5 protein is approximately 130 kDa. (n=3, SEM) 72

Figure 10: Heat map displaying hits from the library screen against GFP-NS5. The library consisted of 47 96-well plates containing compounds. In the heat map, each plate is labeled with a heading containing our unique plate identifier. Instead of listing raw fluorescence data, the heat map conveys relative fluorescence within a plate, with high levels of fluorescence being dark red, low levels being dark blue, and the median level being white. Hues within these three color confines represent a fluorescence value between the highest and median value or median value and lowest value. Each plate had three positive control wells containing increased concentrations of soluble ATP (0 mM, 20 mM, and 60 mM) in the absence of test compound (wells F1, G1, and H1, respectively). The well shown with a black border corresponds to the lead compound, HS-205020. Wells shown in gray are empty. 81

Figure 11: Representative GFP-NS5 Western blot showing eluted samples from the small-molecule screen. The lane designated as “EN009 F7” (from plate EN009, well F7) represents a typical example of a “strong” eluter. This eluate contains high levels of GFP-NS5, therefore the corresponding compound was considered a strong lead compound. Lane “EN008 G5” shows lower levels of GFP-NS5, and is a typical example

of “weak” lead compound. “EN008 G4” shows a typical “absent” eluter (no detectable GFP-NS5)..... 82

Figure 12: Flow chart summarizing the progression from 3,391 anti-DENV2 candidate compounds to one lead compound to be used in further analysis. The small-molecule library consisted of 3,391 candidate compounds, of which 95 were selected as lead compounds based on fluorescence signal in the small-molecule screening assay. Of those 95 lead compounds, only 50 were considered to be strong eluters of GFP-NS5, based on the Western-blot data showing high levels of GFP-NS5 protein in the corresponding eluates. A database search confirmed that 18 compounds were unique lead compounds for GFP-NS5 (showing no overlap with the unrelated proteins detected in previous screens). After subsequent anti-DENV assays measuring antiviral activity and cell toxicity, one lead compound (HS-205020) was chosen on the basis of its strong anti-DENV activity and minimal cell toxicity *in vitro*..... 83

Figure 13: Molecular structures of the six lead compounds. These compounds were identified using a fluorescence-based small-molecule purinomics screen (Chapter 4) to identify drug candidates capable of interfering with the purine-binding activity of DENV NS5 protein. The progression from 3, 391 compounds to the six lead compounds was accomplished by screening against GFP-NS5 fusion protein reversibly bound to immobilized-ATP resin, followed by Western blot analysis confirming elution of GFP-NS5, and finally, concentration-dependent elutions of GFP-NS5 from immobilized-ATP resin using the candidate compounds. 84

Figure 14: DENV- and mock-infected cell controls for the 48 h DENV compound screen. The four quandrants, or categories are confirmed by analyzing the DENV-infected cells and mock-infected cells. The mock-infected cells (left plot) shows a negligible cell population in the two infected quadrants and the DENV-infected cells (right plot) has a subpopulation of cells that are positive for the DENV stain. 89

Figure 15: Flow cytometric analysis of reduction in percent infection with lead compounds. Cells were pre-treated with lead compounds at 0.5 μM, 10 μM, 50 μM, and 100 μM, or comparable volumes of DMSO vehicle (negative control). The positive control was the compound C75, which is a FAS inhibitor that has been shown to inhibit DENV. Antibody targeted against DENV E protein was used to monitor percent infection, and fixable viability stain was used to simultaneously monitor cell viability. Only HS-206507, HS-203033, and HS-205020 significantly decreased the percent infection without increasing the nonviable cells by 50% or greater..... 91

Figure 16: Focus-forming assay to determine production of infectious virus in the presence of candidate compounds. The compound-containing media from the previous

DENV percent infection flow cytometry based assay (Fig. 15) were used in the FFA in triplicate. HS-205020 demonstrated a significant reduction in FFU/mL compared with the DMSO negative control (47- fold and 121- fold at 50 μM and 100 μM, respectively), and also resulted in a lower viral titer than the positive controls, ribavirin and C75. (n=3, SEM) 96

Figure 17: Resazurin viability assay. Non-infected U937+DC-SIGN cells were plated in 96-well plates and treated with compounds at the concentrations indicated. After a 24-hour exposure to the compound, resazurin was added to each well. The resulting fluorescence was measured and used to determine the percentage of viable cells relative to DMSO controls. The results show that the viability of cells treated with HS-203033 or HS-205020 was comparable to those treated with the drug ribavirin. (n=3, SEM) 99

Figure 18: Cell-based *Flavivirus* immunodetection assay. BHK-21 cells were infected with DENV2-TSV01 in the presence of the screen hits. After infection, the compounds remained in the culture media. The viability was measured by cell number (red line) and percent infection (black line) by immunofluorescence as described (E-protein antibody, 4G2). (A) DMSO control. (B) The positive control, celgosivir, strongly inhibited DENV propagation. (C) HS-203033 was ineffective at reducing the percent infection in these cells. (D-E) The close proximity between the viability curve and percent infection for HS-206507 made this compound a lower priority than HS-205020 (EC_{50} = 55.65 μM) (n=3, SEM) Courtesy of Subhash Vasudevan, Duke-NUS 103

Figure 19: Relative ATP and HS-205020 elution profiles of truncated, domain-based, GFP-NS5 proteins. (A) The methyltransferase domain (blue), polymerase domain (red), and full-length GFP (black) proteins were eluted from immobilized-ATP resin with increasing concentrations of soluble ATP or HS-205020, and all three proteins showed a concentration-dependent elution profile. HS-205020 eluted the polymerase domain, GFP-NSF (406-900), to the greatest extent, exhibiting the largest increase in elution at 500 μM HS-205020. (B) Western blot analysis to confirm the presence of GFP fusion proteins in the eluate. Control samples (LSWB) are shown in lane 1 of each blot. Lanes 2, 3, and 4 in each blot correspond to concentrations of ATP or HS-205020 indicated in the graphs. The results corresponded to the elution profiles for each truncated GFP-NS5 protein and full-length GFP-NS5. (C) Quantification of the percent of total protein that was either eluted with 100 mM ATP (blue), did not bind the immobilized-ATP resin initially (black), or was retained on the resin after the addition of 100 mM ATP (red). 110

Figure 20: Inhibition of DENV RdRp activity by HS-205020. The *in vitro* activity of DENV RdRp was monitored in the presence of 8 concentrations of HS-205020 ranging from 0 to 300 μM (0,0.1, 0.3, 1, 3, 10, 30, 100, and 300 μM). Results were plotted on a semi-log curve to determine the IC_{50} for HS-205020. Starting at approximately 30 μM of

test compound, a reduction in polymerase activity was noted, with a drastic decrease observed between 100 μM and 300 μM HS-205020. The calculated IC_{50} of HS-205020 in this assay is $\log_{10}2.01 = 102$ μM. Courtesy of Subhash Vasudevan, Duke-NUS. 113

Figure 21: HS-205020 activity in HCV-infected HuH7.5 cells (A) Assay measuring percent infection in HuH7.5 cells treated with HS-205020. The results demonstrated no significant reduction in the percent infection with treatment compared with DMSO control. (n=3, SEM) (B) The $TCID_{50}$ assay using the supernatants from the experiment in (A) did show a significant reduction in infectious virus compared with the DMSO control, at 50 μM, 75 μM, and 100 μM HS-205020 (19.9-, 25.1-, and 39.8-fold reduction in $TCID_{50}$ values, respectively) (* $p < 0.5$). The $TCID_{50}$ findings suggest that HS-205020 may have a broad spectrum activity within *Flaviviridae.* (n=3, SEM)..... 118

Figure 22: Five SAR-based analogs to HS-205020 128

Acknowledgements

I would like to acknowledge Tim Haystead and Mariano Garcia-Blanco for the guidance over the years. You've taught me so much, especially how to persevere and be optimistic. Also, to all the Haystead and Garica-Blanco lab members, thank you for the collaboration, advice, and support. I would also like to give a special thanks to my committee: Dr. Micah Luftig, Dr. Donald McDonnell, and Dr. Dennis Thiele for their mentorship over the course of my studies at Duke.

My family: Mom, Dad, and Erica (and my friends who I also consider my family)- thank you for the endless love, support, and encouragement. You have shown me that with a little courage, advice, and love, I can conquer anything in my life. An extra thanks to my Mom who still answers my phone calls despite assuming the role of a complaint department during my college and graduate school years.

I would like to acknowledge some scientific idols from my past; my two advisors at The College of New Jersey: Dr. David Hunt and Dr. Donald Hirsh. You both have contributed immensely to my growth as a scientist and instilled in me a scientific curiosity and knowledge base that led to my successful completion of graduate school. Dr. Hunt (aka “renegade”), you can now cash that $20 check!

To my soon-to-be husband, Greg, you have been and continue to be an invaluable source of love, support, and laughs through the tough times.

1. Introduction: Dengue virus

1.1 Background & Significance

Historically, all four dengue viruses, DENV(1- 4), are believed to have originated in monkeys. Between 100 and 800 years ago, the independent viruses began replicating and adapting to human cells (CDC, 2012). Subsequently, human infections started occurring during this time in Southeast Asia and possibly Africa. It was not until World War II when DENV progressed from a geographically limited disease of minor importance to an emerging disease (Ooi and Gubler, 2009). The causes of the dissemination of DENV are attributed to a dramatic increase in soliders' world travel, which is believed to have caused an accidental spread in the *Aedes* mosquito vector across the globe (Rogers et al., 2006). During the 1980s, more severe cases of DENV infection emerged in South America, the Caribbean, and Southeast Asia, now called Dengue shock syndrome (DSS) and Dengue hemorrhagic fever (DHF) (San Martin et al., 2010). The history of DENV illustrates the progression of the virus from a geographically limited human infection (restricted to Africa and Southeast Asia) to a global health pandemic with an estimated 390 million infections occurring annually worldwide (Bhatt et al., 2013).

1.2 Epidemiology

Within the past fifty years, the incidence of DENV has increased thirty-fold. In that time, DENV has emerged as one of the most important global health concerns and is

now the fastest spreading vector-borne disease in the world (WHO, 2013). The uncontrolled increase in the incidence of DENV can be attributed to rapid urbanization, population growth, high rates of travel, lack of vector control measures, global warming and an insufficient public health system (Lashley, 2002). Currently, DENV is considered endemic in over 100 countries in Africa, the Americas, Asia, the Caribbean, and the Pacific.

The United States is not impenetrable to dengue virus. In fact, dengue virus is already endemic in Puerto Rico and parts of Hawaii, and has been identified in the southernmost tips of Texas and Florida. Additionally, the more northern sections of the US remain susceptible, and DENV infection still poses a threat, as evidenced by the fact that the DENV-carrying mosquito vector, *Aedes albopictus*, has been found as far north as Minnesota (Novak, 1992).

As shown in Figure 1, DENV remains prevalent in areas close to the equator (± 35 degrees in latitude from the equator). Not surprisingly, this geographical "belt" also corresponds to the preferred breeding ground of the *Aedes* mosquito (Vilibic-Cavlek et al., 2012).

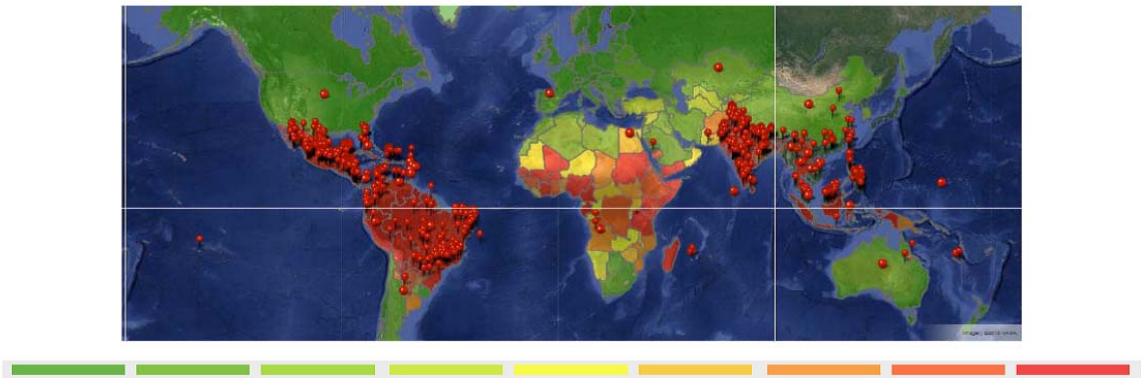

Figure 1: Map of dengue transmission. The countries are ranked according to the presence, likelihood, or absence of DENV, as shown by color-code. The extremes are shown in green, which represents absence of DENV, and red, which represents confirmed presence of DENV. The red pins denote recently reported cases (confirmed or probable) of dengue fever, DHF, or DSS. Modified from (Freifeld, 2013)

1.3 Pathogenesis

A bite from a DENV-infected *Aedes* mosquito introduces the virus into the host, and the virus will replicate at the localized bite site or in nearby lymph nodes. The first line of target cells in the human include the skin Langerhan's cells and dendritic cells (DC). Dendritic cells are a part of a group of potent antigen presenting cells (APC) that express multiple pathogen recognition receptors; the most relevant one for my studies being the dendritic cell specific ICAM3-grabbing non-integrin (DC-SIGN) receptor. DC-SIGN is an attachment factor for DENV virions. Dengue virus is able to replicate within DC, macrophages, and monocytes, thus producing a level of serum viremia within the human host. Once DENV is in the serum, it can infiltrate into organs and tissues (Fang et

al., 2013). Depending on the risk factors possessed by the human host, the viral disease can be asymptomatic, mild-moderate dengue fever (DF) or a more severe manifestation of the disease known as dengue hemorrhagic fever (DHF) or dengue shock syndrome (DSS) (Tang and Ooi, 2012).

Risk factors for DHF or DSS include: pre-existing DENV immunity, virus genotype, order of infecting serotypes, young or old age, and compromised immune system. Given these risk factors, it has hypothesized that both viral virulence and host immune responses most likely determine the severity of the disease (Tang and Ooi, 2012).

1.3.1 Virulence

Each serotype has been previously isolated from DHF/DSS patients over the years, which indicates that increased virulence (manifesting as DHF or DSS) could be caused by any of the four serotypes. Within a serotype, viruses can be further classified by genotype (the sequence of nucleic acids). A DENV2 genotype was found in the Caribbean (originated in Southeast Asia) in 1981 which resulted in an epidemic of DHF that continues to be a problem in Latin America today. This newer DENV2 strain in Latin America swept the area, and resulted in a reduction in the infections caused by their previous, less virulent DENV3 native strain. The DENV2 strain was then shown to possess different growth characteristics compared to non-DHF and non-DSS viruses; it is able to replicate very efficiently in human target cells and within the *Aedes* mosquito

vector. With an enhanced replication in the vector, a mosquito bite is capable of delivering a higher titer of virus. The potent bite combined with the increased efficiency of this DENV2 strain to replicate in human host cells may provide an explanation for why the genotype of DENV2 causes severe DENV disease (Carrington et al., 2005).

1.3.2 Dengue virus life cycle

DENV is an arbovirus, meaning it is transmitted by an arthropod vector, which in the case of DENV is the *Aedes* mosquito. Arboviruses are able to replicate in both the arthropod vector and the recipient cells. The transmission of the virus from the mosquito to the human is via a bite. A mosquito bite transmits DENV from the mosquito salivary glands to the human. The DENV life cycle is summarized visually in Figure 2. Once the virions reach primary target cells in the human (e.g., Langerhans, monocytes, macrophages), the virions must have an interaction with a mammalian surface cell factor or receptor (e.g., DC-SIGN, mannose receptor, C-type lectin domain family 5, member A, among others) prior to cell entry. Over the past several years, more and more mammalian cell surface receptors that interact with DENV have been identified, suggesting that DENV can exploit several different attachment factors (Fang et al., 2013). DENV and other flaviviruses use receptor-mediated endocytosis for cell internalization. The number of DENV permissive cell lines is large (monocytes, macrophages, dendritic cells, and the cell lines K562, U937+DC-SIGN, THP-1, HepG2, HuH7, HUVEC, ECV304, Raji, HSB-2, Jurkat, LoVo, LLC-MK2, C6/36, BHK-21), which suggests the virus may

bind to a universal attachment factor, or be able to exploit a wide array of cell surface receptors to mediate endocytosis (Tan and Alonso, 2009) (Fig. 2).

After virion internalization by endocytosis, the virus is contained in early endosomes. DENV-containing early endosomes are acidified by the host transmembrane protein, vacuolar ATPase (v-ATPase), which causes a conformational change in the DENV envelope protein resulting in fusion between virion surface and endosome membrane. Upon fusion between the endosome and virion envelope, the DENV RNA genome is released (Perera et al., 2008). The 11 kilobase positive-sense single stranded RNA viral genome is translated into one large polyprotein on the host ribosomes (Rodenhuis-Zybert et al., 2010). The polyprotein is cleaved by both host and viral proteases to release 10 total viral proteins. The 10 viral proteins are further classified into 3 structural proteins [capsid (C), premembrane (prM), and envelope (E)] and 7 nonstructural (NS) proteins (NS1, NS2A, NS2B, NS3, NS4A, NS4B, and NS5). Following the translation and proper folding of the proteins, the NS proteins are able to initiate and aid in the replication of the viral genome. The C protein packages the newly synthesized viral RNA into a nucleocapsid. The nucleocapsid is coated in the endoplasmic reticulum (ER) lumen with prM and E proteins.

As the immature virion travels through the secretory pathway within the trans-Golgi network (TGN), the environment becomes mildly acidic (pH approximately 5.7-6.0) triggering a disruption in the surface proteins of the virion. This better exposes the

cleavage site within the prM protein (Perera and Kuhn, 2008). The cleavage site within the prM protein [Arg-X-(Lys/Arg)-Arg (where X is any amino acid)] is targeted for cleavage by the host enzyme, furin. Furin cleavages the prM protein into two peptide fragments, called pr and M. The latter peptide, M, remains on the virion surface and pr, although often excluded from mature virions, does remain associated with the E protein to protect E from the acidic-driven fusion with the TGN membranes (Che et al., 2013). Prior to virion release by exocytosis, the pr peptide dissociates from its protective location on the E protein, and the surface of the mature virion is now smooth as the proteins lay flat. The mature virions can then bud, and be released into the extracellular milieu and go on to infect more susceptible cells. (Perera and Kuhn, 2008) (Fig. 2).

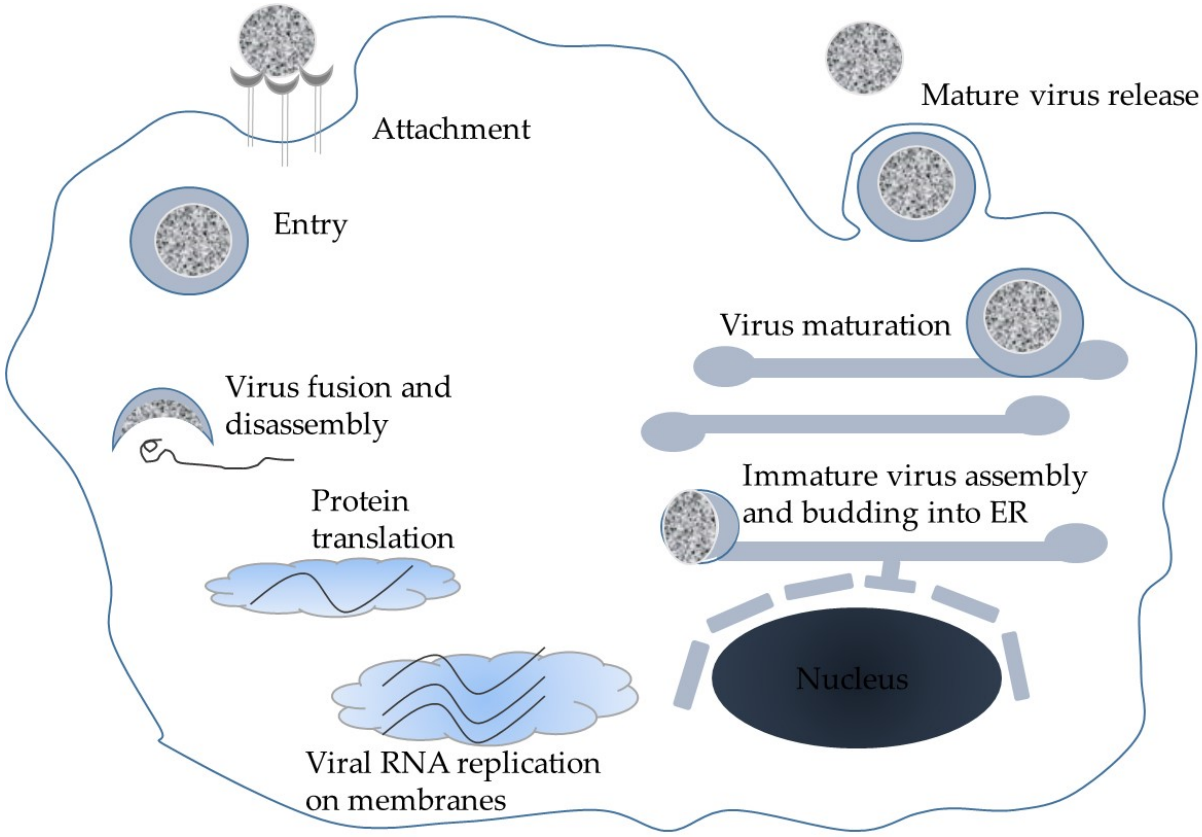

Figure 2: DENV life cycle. After a DENV- infected Aedes mosquito bites a human, the virus must enter the host cells in order to replicate. Upon endocytosis, viral proteins are translated from the viral (+)ssRNA, followed by replication of the viral genome. The new viral components are then packaged within an immature virion, which is modified by cleavage to a mature virion prior to budding out of the host cell. Numbers shown represent pH.

1.3.3 Gene products of DENV

The DENV polyprotein that is translated from the positive sense single sense RNA [(+)ssRNA] contains a total of 10 viral proteins. From the N-terminus to the C-terminus, the arrangement of the proteins in the polyprotein is shown in Figure 3.

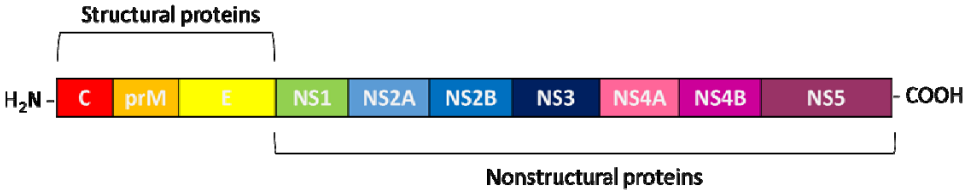

Figure 3: DENV polyprotein. The three structural proteins are located at the amino terminus, and the seven non-structural proteins extend from the structural proteins to the carboxy terminus. After translation of the large of the one large polyprotein, individual DENV proteins are released via proteolytic processing by both host and viral proteases.

1.3.3.1 Structural proteins

There are three structural proteins total, all of which are located on the N-terminus of the polyprotein. There include: capsid, premembrane, and envelope (C, prM, E, respectively).

1.3.3.1.1 C protein

The structural proteins are located on the N-terminus portion of the viral polyprotein. The C protein is initially translated in a precursor form. Both host signal peptidase and the viral NS2B/NS3 protease are required to generate the mature, very basic C protein. The mature C protein contains many basic amino acids flanking a hydrophobic domain in the center (Ma et al., 2004). The center domain is able to interact with cellular membranes and is believed to be implicated in virion assembly. A second cleavage by the serine protease of NS3 produces the mature, 100 amino acid long, C protein (Markoff et al., 1997). The mature C protein contains a hydrophobic region flanked on both sides by highly basic residues. The basicity of the mature C protein enhances its ability to interact with RNA (Alcaraz-Estrada, 2010). Approximately 180 C proteins interact with one copy of viral RNA to aid in the formation of the nucleocapsid. On the other hand, the hydrophobic domain interacts with cellular membranes. The C protein is highly resilient to mutations in the terminal regions and in the hydrophobic region to a lesser degree, which may explain the divergence in amino acid sequence across the *Flavivirus* genus (Markoff et al., 1997). During DENV infection, the C protein localizes to the nucleus, although the function of the nuclear localization is not fully

understood, but has been implicated in apoptosis (Netsawang et al., 2010, Markoff et al., 1997).

1.3.3.1.2 prM protein

The premembrane (prM) protein is a 21 kDa protein that is cleaved by the host protein, furin, into two smaller peptides, pr and M. prM protein is incorporated into the virion surface structure in the secretory pathway in the trans-Golgi network (TGN). With the progressively increasing acidic environment in the secretory pathway, the conformation of the virion surface proteins changes in such a way to expose the cleavage site in prM (Perera and Kuhn, 2008). Furin cleaves prM into pr and M, and M remains intact on the now smooth exterior of the virion. Pr may remain associated with E to continue to protect the virion surface from acidic exposure (which similarly to early viral events, is known to cause fusion with host membraneous structures). Prior to exocytosis, the pr peptide is removed from the mature virion. Occassionally, the cleavage of prM is not performed, in which case an immature, non-infectious DENV virion would be released (Rodenhuis-Zybert et al., 2011).

1.3.3.1.3 E protein

The 50 kDa E protein and the M protein form the proteinaceous outer coat of the dengue particle. E protein has three domains: domain I, domain II, and domain III. Domain I is located in the center of the E protein structure which includes the N-terminus. Domain II contains a dimerization domain that is important for the conformational changes of the DENV virion during transit through the TGN.

Additionally, domain II has a small hydrophobic domain that is able to initiate fusion with host cell membrane receptors. Glycosylation of two specific residues in domain II (Asn67 and Asn153) is important for DENV infectivity in human cells, but not mosquito cells. Domain III is the IgG-like region that is inundated with serotype-specific antibody neutralization sites suggesting this region interacts with receptor sites on the host cell.

As previously stated (1.3.2 Dengue life cycle), E protein binds uncleaved prM to form a heterodimer in the TGN. After cleavage of "pr," 180 E polypeptides assume the conformation of 90 homodimers in a head-to-tail format that results in a smooth virion surface. Further rotational rearrangements of the E proteins result in the virion surface exposure of fusion peptides.

1.3.3.2 Nonstructural proteins

The seven nonstructural (NS) proteins are nestled between the E protein and the C-terminus of the polyprotein. Unlike the structural proteins, the NS proteins do not comprise the structural features of the virion. Instead, the NS proteins have roles in RNA propagation, RNA cap formation, helicase activity, protease activity, and are active in host immune response modulation.

1.3.3.2.1 NS1

NS1 is a 45-50 kDa glycoprotein that is highly immunogenic and is essential for viral propagaton. During the translation of the viral polyprotein, NS1 assumes a homodimeric conformation that interacts with NS4A in the replication complex (Chua et

al., 2005). NS1 also binds to viral dsRNA intermediates, but its exact role in the replication process is yet to be understood (Muller and Young, 2013). Additionally, the NS1 dimers have been shown to localize to the cell surface and be secreted from the human host cells and form hexamers. This is the only DENV protein that has been observed in the extracellular milieu of human host cells. The function of circulating extracellular NS1 is not completely known; however, it may be useful as an indicator of the likelihood that the infection will progress to DHF. A serum analysis for NS1 of seventy-seven DENV2-infected children in Thailand (1995-2000) showed a correlation between increased levels of NS1, higher viremia levels, and increased chance of developing DHF (Libraty et al., 2002).

NS1 is not secreted from DENV-infected mosquito cells, which may help to explain the lack of overt pathology in the mosquito. The data from the study in Thailand combined with the mosquito cell data suggest NS1 is a virulence factor. Another important study supports the role of NS1 as a virulence factor. In this study, the introduction of antibodies directed against NS1 have been shown to cross-react with human platelets and endothelial cells, which leads to cell damage and an inflammatory response (Lin et al., 2006). This suggests that higher levels of NS1 leads to a greater number of antibodies produced against it, and subsequently causes inflammation and more destruction to platelets and endothelial cells. These latter two occurrences describe a more severe case of dengue, likely DHF or DSS.

Intracellular flaviviral NS1 has been shown to interact with a truncated (at N-terminus) form of STAT3β (Chua et al., 2005). Initially there was evidence that NS1 also inhibited TLR3- mediated signaling (Wilson et al., 2008), but that has been challenged in the past 3 years (Baronti et al., 2010). In addition to the direct interaction of NS1 and STAT3β, it has been shown that high levels of NS1 causes an elevation in both TNFα and IL-6. Increased plasma levels of both of these cytokines are correlated with severe manifestations of dengue fever: DHF and DSS. Because TNFα and IL-6 are either upstream of downstream of STAT3 signaling, the regulation of these cytokines may in fact be attributed to NS1 (Chua et al., 2005).

1.3.3.2.2 NS2A

NS2A is a hydrophobic protein of approximately 22 kDa that is known to associate with the ER membrane (Perera and Kuhn, 2008). By means of a mutagenesis study on NS2A, it was determined that one particular residue, arginine 84, is essential for adequate DENV RNA synthesis. When residue arginine 84 is switched to glutamate, there is a reduction in viral RNA synthesis and virion production. Interestingly, with a residue change of Arg84 to Ala84, no difference was observed in the levels of RNA produced, but there was a decrease in production of virions (Xie et al., 2013). These findings support at least two roles for NS2A: support viral RNA synthesis and aid in the production of mature infectious virions.

1.3.3.2.3 NS2B

NS2B is an approximately 14 kDa membrane-associated protein. The most important known role of NS2B is as a cofactor for serine protease activity of NS3 (Niyomrattanakit et al., 2004). Membrane association occurs through the hydrophobic regions of NS2B. It is believed that this membrane association restricts its cofactor, the protease, NS3, to assume only the proper conformation to perform the correct cleavages (Sampath and Padmanabhan, 2009).

1.3.3.2.4 NS3

NS3 is located in the perinuclear convoluted membrane structures which are composed of portions of the ER and golgi apparatus. NS3 is an approximately 68 kDa multifunctional protein. As a full length protein, NS3 is required for the assembly of infectious virions (Xu et al., 2005).

The N-terminus harbors the viral serine protease domain and associates with NS2B to cleave the following junctions in the polyprotein: NS2A-NS2B, NS2B-NS3, NS3-NS4A, and NS4B-NS5. The NS3 protease is the only virally encoded protease in the DENV genome.

The C-terminus contains an NTPase and RNA helicase each with several conserved motifs commonly shared amongst nucleotide binding proteins that take part in cellular functions ranging from coupling NTP hydrolysis with directional movement and genomic duplex destabilization. The helicase activity of NS3 is believed to have one or multiple roles including unraveling secondary structures; resolving RNA duplexes;

separating double-stranded RNA intermediates formed during RNA synthesis; and acting as a translocase and removing viral RNA-bound proteins. Without the helicase, RNA synthesis would not occur seamlessly and viral propagation would not occur.

In order to melt secondary structures, energy must be invested, and in this case the energy arises from the hydrolysis of ATP. Therefore, all RNA helicases have ATPase activity; in the case of flaviviral RNA helicases, they can hydrolyze any nucleoside triphosphate (known as NTPase), but purines are preferred over pyrimidine nucleoside triphosphates.

An additional enzyme activity on the C-terminus end is a 5'-RTPase, which is the first of three sequential enzymatic reactions needed to add the 5'-cap to the viral RNA. Using mutational analyses and competition assays using ATP analogs, it was discovered that both the NTPase and 5'-RTPase share the same active site.

1.3.3.2.5 NS4A

NS4A is one of the most poorly characterized of the DENV proteins. This 16 kDa NS protein is highly hydrophobic and is associated with membranes via four specific hydrophobic anchors. Membrane studies have shown that the N-terminus of NS4A is located in the cytoplasm and the C-terminus has been shown to be localized in the ER lumen (Miller et al., 2007). The center region of the protein contains three transmembrane domains (Nemesio et al., 2012). NS4A co-localizes with E, NS3, and NS4B in the hepatocellular carcinoma cells, HuH7. Specifically, NS4A exhibited a dot-like staining overlapping that of dsRNA, which is an intermediate of RNA replication,

suggesting a role involved in viral replication. When a truncated form of NS4A (minus the C-terminal region) is introduced into cells, membrane rearrangements resembling those of DENV replication complexes. Full length NS4A introduced into uninfected cells, did not induce this membrane alteration (Miller et al., 2007). This suggests a proteolytic cleavage of this C-terminal region may occur in response to DENV infection to promote the formation of the membranous viral replication complexes (Miller et al., 2007).

1.3.3.2.6 NS4B

NS4B is a 27 kDa transmembrane protein that helps aid in the anchoring of the viral replication complex to the ER membrane along with the viral proteins, NS2A and NS4A (Miller et al., 2007). NS4B has been shown to have two significant functions in dengue pathogenesis: association with NS3 and mediation of interferon response.

First, NS4B forms a protein-protein complex with NS3, which triggers the release of single-stranded RNA and enhances the helicase activity of NS3. When DENV type-2 is grown in cells in the presence of a published NS4B inhibitor, NITD-618, a point mutation is observed, proline 104 to lysine 104 (Xie et al., 2011). This mutation is nestled in the transmembrane domain of NS4b and thus not directly implicated in the association of NS4B and NS3 (Grant et al., 2011). However, proline is known to have significant effects on secondary protein structure, so its mutation to lysine may potentially have caused a conformational change in the overall protein structure. This modified secondary structure is believed to prevent correct NS4B-NS3 complex

formation, and reduces viral RNA replication by means of decreased NS3 enzymatic activity (Miller et al., 2006).

The second known function of NS4B is as an antagonist of the host interferon response (Grant et al., 2011). When all 10 viral proteins were tested for their ability to block the interferon response in human cells, NS4B was the protein that most potently inhibited this response. Additional studies demonstrated that NS4B effectively blocked the interferon-induced cascade, which when intact is anti-viral, by interfering with the messenger protein, STAT1 (Munoz-Jordan et al., 2003).

1.3.3.2.7 NS5

NS5 is an approximately 105 kDa multifunctional protein and is the largest and most conserved flaviviral protein. On the N-terminal domain there is an S-adenosylmethionine methyltransferase, while the C-terminal domain is an RNA-dependent RNA polymerase (RdRp). Methyltransferase activity is required for methylating the N7 and 2'-O positions on the viral RNA cap. The DENV RNA cap structure is formed by the actions of RNA triphosphatase of NS3, and the guanylyltransferase, N7- methyltransferase, and 2'-O methyltransferase of NS5. The methyltransferase domain contains two binding sites that act consecutively: one site is the methyl donor and the second site binds guanine base of the RNA to form the cap. An inhibitor of nucleotide binding could therefore prevent efficient capping activity of the viral RNA, jeopardizing the integrity of the RNA (Courageot et al., 2000; Idrus et al., 2012) as observed with ribavirin (Takhampunya et al., 2006).

Additionally, NS5 plays a role in antagonizing the IFN signaling, a key component in the innate immune response. The DENV NS proteins NS2A, NS4A, and NS4B have all be shown to anatagonize the IFN process, with NS4B being the most potent. However, the reduced levels of STAT2, an IFN signaling molecule, could not be explained by the function of those DENV NS proteins. It was demonstrated that NS5 is capable of binding STAT2 and thus inhibiting the IFN signaling. This is yet another way that DENV is able to evade the host innate immune response (Hannemann et al., 2013).

The peptide region nestled between the methyltransferase and RdRp domain has been shown to bind NS3. The NS5/NS3 complex is localized in the viral replication complexes where they aid in the propagation of DENV by means of viral replication (Rawlinson et al., 2006). Once the complex disassembles (viral replication ceases), NS5 is targeted to nuclear localization. NS5 undergoes multiple phosphorylation events and is imported to the nucleus where its exact role is still in question. Recent studies have shown that NS5 protein of different serotypes of DENV may be exclusively found in the cytoplasm. This supports the idea that the nuclear localization of NS5 is an ancillary part of the life cycle and is serotype-specific (Hannemann et al., 2013).

1.4 Anti-dengue treatment efforts

Dengue virus is the most prevalent arthropod-borne viral disease in humans. Approximately 2.5-3 billion individuals live in dengue virus endemic areas. Currently,

there are no approved anti-DENV virus medications or vaccines (Back and Lundkvist, 2013).

1.4.1 Vaccine efforts

Licensed human vaccines exist for several viruses within the same genus as DENV. These include yellow fever virus, Japanese encephalitis virus, and tick-borne encephalitis virus. Although DENV is the most prevalent *Flavivirus* with respect to worldwide disease incidence, the development of an anti-DENV vaccine has been complicated by both the risk of vaccine-mediated virus enhancement of disease manifestations in sequential DENV infections and the need to provide long term immunity against all four DENV serotypes simultaneously (Heinz and Stiasny, 2012a).

Additionally, the vaccine should be safe for use in infants and cost-effective to cater to many poorer populations that frequently suffer from DENV infections. Many obstacles exist that make development of a DENV vaccine a challenge including incomplete knowledge of complicated DENV pathogenesis and poor animal model options. Nonhuman primates and mice are most commonly used as models for DENV infection in the laboratory setting. However, DENV does not replicate well in nonhuman primates and the animals do not exhibit signs of disease. Generally, *in vivo* DENV vaccine research would start in the more cost-effective animal model, the mouse. Immunocompetent mice are suitable for determining initial efficacy tests of the immunogenicity of a DENV vaccine. However, DENV does not replicate well in these

mice. The AG129 mouse, an interferon receptor (IFN-α, β, and γ) deficient mouse, is an excellent host for DENV in terms of replication and exhibition of signs of classic DENV disease. Recent study described a mouse model that could be infected with DENV via intravenous, intraperitoneal, intracerebral, and intradermal incoculation, and the mouse displayed signs of DENV as determined by liver pathology, neurological manifestation, thrombocytopenia, and hemorrhage. Additionally, studies are underway to better adapt the AG129 mouse and a severe combined immune deficient (SCID)-tumor mouse model for testing with DENV vaccines (Zompi and Harris, 2012, Yauch and Shresta, 2008).

Current DENV vaccine efforts can be split into four cateogies: (1) live attenuated virus vaccines; (2) live chimeric virus vaccines; (3) inactivated virus vaccines; (4) live recombinant, DNA, and subunit vaccines (Wan et al., 2013). Live virus vaccines (1, 2, and 4) have progressed to clinical trials, but problems arose in the trials including unequal immunity of the four serotypes and virus interference in a tetravalent (four serotypes) preparation. Non-viral vaccines demonstrated high safety profiles with no chance of emerging virulence; however, no non-viral vaccine has been able to evenly balance the levels of antibodies against a viral protein in all four serotypes (viral proteins may not be well conserved across serotypes) (Heinz and Stiasny, 2012a).

1.4.1.1 Live attenuated virus vaccines

Live attenuated virus vaccines are weakened forms of the virus that are still capable of inducing an adaptive immune response to the constituents of the virus,

including structural and nonstructural proteins (Wan et al., 2013). The weakened virus can still replicate in the body, but its replication is self-limiting so no disease effects are observed in vaccinated individuals. A very successful example of a live attenuated virus vaccine directed against a *Flavivirus* is the yellow fever vaccine 17D (YFV 17D) (Monath, 2008). Unfortunately, an equally successful live attenuated virus vaccine against DENV has yet to be made.

A recent approach in the development of a DENV live attenuated virus vaccine utilized site-directed mutagenesis to cause attenuation of the virus. A deletion of 30 nucleotides in the 3'-untranslated region of DENV4 was able to attenuate DENV4, and similarly the same deletion in DENV1 was successful (McArthur et al., 2008). However, the nucleotide deletion in DENV2 and DENV3 significantly reduced the immunogenicity, making it far less successful in terms of use in a vaccine. To circumvent the troubles with DENV2 and DENV3, the deletion mutant of DENV4 was used as a genetic template for DENV2 and DENV3. The four resulting monovalent DENV vaccines were used to create a tetravalent admixture which is currently in clinical studies (Durbin et al., 2011).

1.4.1.2 Live chimeric virus vaccines

Live chimeric virus vaccines piggyback on the past successes of a licensed vaccine by modifying the existing genes within original vaccine to target-specific genes. Sanofi Pasteur developed ChimeriVax tetravalent vaccine (CVD1-4), a DENV vaccine

that utilized the YFV 17D vaccine as a backbone for a live chimeric DENV vaccine. The genes encoding the premembrane protein (prM) and envelope protein (E) of DENV for each of the four serotypes was incorporated into the chimeric vaccine (Wan et al., 2013).

In pre-clinical studies, the tetravalent vaccine, CVD1-4, was genetically stable, less neurovirulent than YFV 17D (Barban et al., 2007), and demonstrated immunogenicity in nonhuman primates (Guirakhoo et al., 2004). The phase I studies, demonstrated that CVD1-4 displayed a good safety profile and low viremia levels. However, upon testing in phase II studies it was discovered that CVD1-4 only imparted approximately a 30% efficacy against DENV1, 3, and 4 serotypes, without providing any detected protection against DENV2, the most pathogenic of all serotypes (Sabchareon et al., 2012). An effective DENV vaccine must protect against all four serotypes (tetravalent) in order to reduce the risk of antibody-dependent enhancement (ADE). ADE is a phenomenon in which serotype specific antibodies against a previous DENV infection result in a severe secondary infection when infected with a different serotype. Sanofi would have to modify its tetravalent ChimeriVax dengue vaccine to minimize the risk of causing ADE and subject the vaccine to more clinical trials down the road.

1.4.1.3 Inactivated virus vaccines

As the name implies, inactivated virus vaccines contain virus that have been subjected to extreme conditions, including heat or abrasive chemicals, to deem it non-virulent. This approach in developing vaccines carries three inherent strengths. First,

there is no possibility of infection or virulence upon introduction into the body. Secondly, inactivated virus vaccines are generally more heat and time tolerant and would be preferable for distributing to a greater number of people. Lastly, inactivation of multiple serotypes should, in principle, would be easy to attain by balancing the serotypes to elicit a proportional immune response from each serotype (Wan et al., 2013). However, DENV virions do not contain nonstructural (NS) proteins, so the vaccine would not impart immunity against the seven NS protein.

In the pursuit for a DENV vaccine, the route of developing an inactivated virus vaccine was highly considered due to the above advantages and the fact that two licensed vaccines targeting flaviviruses fall within this category (TBEV and JEV) (Del Angel and Valle, 2013).

Initial efforts in producing an inactivated DENV vaccine was hindered by an inability of the vaccine to elicit a high titer of anti-DENV antibodies in mice. Subsequent research efforts resulted in a several prospective inactivated dengue virus vaccines, one being tetravalent dengue purified inactivated vaccine (DPIV; GlaxoSmithKline Biologicals). DPIV was produced from purified high titers of DENV, incorporating one representative strain from each serotype into the final vaccine. In phase I studies, immunization of nonhuman primates have been promising thus far, but challenges still lie ahead if the vaccine makes it to future human clinical trials and further optimization (Roehrig, 2013).

1.4.1.4 Live recombinant and DNA vaccines

Advances in cell and molecular biology have spurred vaccine efforts developed around recombinant proteins, DNA vaccines, and subunit containing vaccines. As an exterior, structural protein, the E protein is often used as the antigen. Live vectors including adenoviruses, alphaviruses, and vaccinia can be genetically engineered to express DENV E protein, and subsequently cause an immunogenic response to the E protein (Wan et al., 2013). Additional systems have been used to express recombinant DENV E protein including yeast and insect cells. The purified protein can then be tested for its ability to evoke an immune response in an animal model.

The DENV protein NS1 has also been explored as vaccine component. As a NS protein, NS1 does not contribute to ADE; however, anti-NS1 antibodies did protect mice in a DENV challenge. Anti-NS1 antibodies are protective because they trigger complement mediated lysis of DENV-infected cells (Wan et al., 2013). NS1 can be expressed in similar systems as E including a DNA vaccine or recombinant vaccinia virus.

Problems were encountered with vaccines producing or containing DENV NS1. Anti-NS1 antibodies demonstrated cross-reactivity with host proteins causing pathogenic effects *in vivo*. In order to produce a safe DENV NS1-based vaccine, the cross-reactive epitopes in full length NS1 would have to be deleted or modified to eliminate the interaction with host proteins (Lu et al., 2013).

1.4.2 Drug discovery efforts

There are no approved therapeutics or vaccine for DENV (Cregar-Hernandez et al., 2011, Deng et al., 2012). Although several inhibitors of DENV targeting host and/or viral proteins have been reported and published, few have progressed to human clinical trials, and none have reported positive results from phase I trials. Two of the DENV inhibitors that made it to Phase I trials include balapiravir and celgosivir, a viral polymerase inhibitor and host alpha-glucosidase inhibitor, respectively (Nguyen et al., 2013). Another notable compound targeting a host factor is and ETAR, which is an inhibitor to inosine-5′-monophosphate dehydrogenase (IMPDH).

A highly published and effective anti-DENV compound *in vitro* is ribavirin. Ribavirin is a prodrug that is phosphorylated to ribavirin triphosphate in mammalian cells and is currently FDA approved for the treatment of HCV, but never as a monotherapy; it is always coupled with pegylated interferon. The anti-flaviviral activities of ribavirin are thought to be through inhibition of the viral NS5 RNA polymerase by mimicking GTP (Stevens et al., 2009). Ribavirin repeatedly exhibits anti-DENV effects in cell culture, but results in mouse models have been poor (McDowell et al., 2010).

There are 3 ways to approach developing a DENV antiviral agent. First is the development of an inhibitor to a required host factor (e.g., celgosivir). Second is a compound that is able to boost or modulate the immune response such that the immune

system is able to better clear the virus. One such compound, poly-IC-IC, received an orphan drug designation in the US in 2003, but its progress is still listed as in clinical trials. Third is the direct targeting of a viral protein. This latter approach carries the advantage of potentially fewer side effects than in the targeting of a host factor which is likely required for other important cellular functions.

In selecting a viral target, properties including conservation across DENV serotypes and the viruses within the same *Flavivirus* genus were considered. Of the virally encoded non-structural (NS) proteins NS5 is the most highly conserved and has two distinct targetable domains. The N-terminus has a methyltransferase (MTase) domain that has been targeted by 2-thioxothiazolidin-4-ones, S-adenosyl-L-homocysteine (SAH) derivatives, aurintricarboxylic acid, and to a lesser extent Ribavirin and ETAR (McDowell et al., 2010, Stahla-Beek et al., 2012, Stevens et al., 2009, Lim et al., 2011). The 2-thioxothiazolidin-4-one class, although observed to reduce viral replication, was labelled as a "promiscuous" or "sticky" class of molecules in HTS assays. Structurally, these derivatives are Michael acceptors, which may lead to reactivity of the molecule with a protein and enhance toxicity (Stahla-Beek et al., 2012). By docking studies, aurinticarboxylic acid derivatives are believed to bind to the proposed RNA binding site of the MTase(Stevens et al., 2009). The remaining MTase inhibitors are not novel scaffolds but are either nucleoside mimetics (such as ribavirin and ETAR) or mimic a known endogenous cellular substrate (SAH analogs). The remaining NS5 RdRp

inhibitors include both non-nucleoside and nucleoside compounds. One allosteric, non-nucleoside inhibitor of the DENV RdRp is N-sulfonylanthranilic acid. This compound is believed to affect DENV RNA replication, but no toxicity studies have been reported (Yin et al., 2009a). Two nucleoside inhibitors are NITD008 (and the similar analog, NITD449) and 7-deaza-2'-C-methyladenosine. Both are ATP mimetics and subsequently caused severe toxicity in animal studies by week two (Niyomrattanakit et al., 2010, Yin et al., 2009c).

Published NS3 helicase inhibitors include the quinolone derivatives, among others. These compounds are interesting in that in addition to exhibiting anti-DENV effects, presumed to be mediated through inhibitory action on the NS3 helicase, these compounds have also shown non-classical biology in HCV. Research has shown these derivatives have anti-HCV activity by inhibition of NS3 helicase and NS5B RdRp (Ahmed and Daneshtalab, 2012, Deng et al., 2012). Currently, there are no known inhibitors of NS1, NS2(A/B) or NS4(A/B) proteins. Although the literature presents a breadth of both targets and lead compounds, the fact is that there are still no approved DENV therapeutics. Additionally, the possibility of targeting a viral protein that is well conserved across flaviviruses or the *Flaviviridae* presents an opportunity of creating a broad spectrum anti-*Flavivirus* or anti-*Flaviviridae*. The lack of drugs that are capable of treating or preventing DENV coupled with the rapid spread of this arbovirus, strongly suggests that there is an unmet need to define novel scaffolds targeting the NS proteins.

1.5 Hypothesis

A small-molecule drug screen directed against a purine-binding dengue virus type-2 protein, non-structural protein 5, will reveal potential drug-candidate compounds capable of inhibiting dengue virus while exhibiting minimal toxicity *in vitro*.

2. Materials and Methods

2.1 Materials

All chemicals were obtained from Sigma-Aldrich (St. Louis, MO) unless otherwise noted. Cyanogen bromide (CNBr)-activated Sepharose 4B used to generate the γ-phosphate-linked ATP-Sepharose resin was purchased from Amersham Pharmacia/GE Healthcare Life Sciences (United Kingdom). The aqueous mixture containing [^{35}S]-methionine and [^{35}S]-cysteine (Easy tag EXPRESS^{35}S) used for metabolic labeling of proteins was obtained from Perkin Elmer (Waltham, MA). Compounds comprising the small-molecule library were purchased from various sources, with the primary sources being Enamine (Kiev, Ukraine) and ChemDiv (San Diego, CA). All solutions were prepared using distilled, deionized ultrapure water (>18 MΩ) purified by a Milli-Q water purification system (Millipore, Bedford, MA).

Dengue virus type-2 New Guinea C strain (DENV2-NGC), *Aedes albopictus* C6/36 cell line, African green monkey (Vero) cell line, and human hepatoma HuH7 and HuH7.5 cell line were generously provided by Mariano Garcia-Blanco (Duke University Medical Center). BHK-21 fibroblast cells were used as described previously (Rathore et

al., 2011) by Subhash Vasudevan (Duke-NUS). Human monocytic cell line, U937, constitutively expressing DC-SIGN (U937+DC-SIGN) was kindly provided by Aravinda De Silva (University of North Carolina at Chapel Hill). Human embryonic kidney (HEK293) cell line was obtained from American Type Culture Collection (ATCC, CRL-1573, Manassas, VA).The hepatitis C virus strain JFH1 and interferon alpha (IFN-α) were kindly provided by Shelton Bradrick (Duke University Medical Center). Constructs expressing NS5 fused to green fluorescent protein (GFP-NS5) were a gift from David Jans (Monash University, Clayton, Australia). All NS5 cDNA (truncated versions and full length sequence) was derived from the Dengue type-2 Townsville strain and were cloned into the pEPI-eGFP vector. The DNA sequence of pEPI-eGFP-NS5(1-900) is shown in Appendix A. All tissue culture media and supplements were obtained from Gibco (Carlsbad, CA) unless otherwise noted. The RNA substrate, 3′UTR-U_{30} (5′-bio-U_{30}-AACAGGUUCU*AGAACCUGUU*-3′), used in the polymerase assay was purchased from Dharmacon (Lafayette, CO). The 2-[2-benzothiazoyl]-6-hydroxybenzothiazole-ATP (BBT-ATP) was synthesized by and purchased from Jena Bioscience GmbH (Jena, Germany). Calf-intestinal alkaline phosphatase (CIP) was purchased from Promega (Madison, WI). BBT fluorescence was monitored by either Tecan SafireII or InfiniteR M1000 plate reader (Tecan, Durham, NC).

Corning FiltrEX 96-well filter plates with 0.2μm hydrophilic polyvinylidene difluoride (PVDF) membrane were purchased from Corning (Glendale, AZ). PVDF

Western-blotting membranes (0.2 μm) were purchased from BioRad (Hercules, CA). All polyacrylamide gels used for protein analysis were purchased from Bio-Rad (Berkeley, CA). Rabbit (polyclonal) anti-GFP antibody (G1544) was purchased from Sigma Aldrich (St. Louis, MO). Horseradish peroxidase (HRP)-conjugated goat anti-rabbit IgG antibody (7074) was purchased from Cell Signaling (Danvers, MA). Primary mouse monoclonal anti-Hepatitis C virus core antibody (C7-50, ab2740) was purchased from Abcam (Cambridge, MA). Primary mouse monoclonal 4G2 antibody directed against DENV envelope protein was produced using a hybridoma and was generously provided by Mariano Garcia-Blanco (Duke University Medical Center). Enhanced chemiluminescence (ECL) detection kit was purchased from Thermo Scientific Pierce (Pittsburg, PA). VIP substrate staining kit was purchased from Vector Laboratories (Vector Labs, Burlingame, CA).

2.2 Methods

2.2.1 Cell Culture

Aedes albopictus C6/36 cells (ATCC) were cultured at 28°C and 5% CO_2 in minimal essential medium (MEM) supplemented with 10% fetal bovine serum (FBS), 5 mM HEPES (pH 7.5), 1 mM sodium pyruvate, 0.1 mM non-essential amino acids, and penicillin/streptomycin (100 U/mL and 100 μg/mL, respectively). Human hepatoma HuH7 cells, African green monkey kidney Vero cells, BHK-21 fibroblast cells, and human embryonic kidney HEK293 cells were cultured at 37°C and 5% CO_2 in Dulbecco's

Modified Eagle Medium (DMEM) supplemented with 10% FBS and 1x penicillin/streptomycin. Human monocytic U937 cells constitutively expressing DC-SIGN (U937+DC-SIGN) were cultured at 37°C and 5% CO_2 in complete Roswell Park Memorial Institute (RPMI-1640) medium supplemented 10% FBS, 1% L-glutamine, 50 mM beta-mercaptoethanol, 0.1 mM non-essential amino acids, and 1x penicillin/streptomycin.

2.2.2 Dengue virus stock preparation

To prepare DENV2 viral stocks, *Aedes albopictus* C6/36 cells were seeded into T-150 (150 cm^2) tissue-culture flasks at a cell density of $1x10^6$ cells/mL. After a 24-hour incubation, each flask was inoculated with 500 μL of DENV2 virus in 4.5 mL serum-free culture medium. Following a 1-hour incubation period with swirling every 15 min, a total of 15 mL of culture medium supplemented with 2% FBS and 5 mM HEPES was added. After 48 hours of incubation, the culture medium was removed and replaced with fresh complete culture medium containing 2% FBS. Following a 72-hour incubation, the culture medium was collected and centrifuged at 4,000 rpm for 5 minutes to remove any C6/36 cell debris. The cleared supernatants containing virus were then aliquoted in 1 mL fractions and stored at -80°C.

2.2.3 Metabolic Labeling of DENV-infected and mock-infected mammalian cells

Metabolic labeling of actively translated proteins during DENV- and mock-infection was performed in two mammalian cell types: HuH7 and U937+DC-SIGN.

2.2.3.1 Post-infection time frame determination

The length of a DENV life cycle in both HuH7 and U937+DC-SIGN cells was determined to be approximately 20-24 h based on consecutive timed interval focus-forming unit assays (unpublished results, Mariano Garcia-Blanco). Determining the cell-specific length of viral life cycle entails infecting the cells with DENV at an MOI of 1 for 1 h, then washing away the viral media, and replacing it with fresh complete cell culture media. At each 2 hour time interval, the media was collected and virus was quantified. The p.i. time that yielded the peak in infectious viral load marks the end of the life cycle.

2.2.3.2 Metabolic labeling of HuH7 cells

HuH7 cells were seeded into 15-cm tissue culture plates. Twenty-four hours later, a time course experiment commenced. At time 0, DENV at a multiplicity of infection (MOI) of 10 was added to half of the plates (infected), and an equivalent volume of a non-viral mock infection medium was added to the other half of the plates (mock-infected). The mock medium used for the HuH7 cells was the same as the complete medium that was used to culture the *Aedes albopictus* cell line (C6/36; ATCC), which was the same cell line used to propagate the DENV2-NGC virus. Two hours prior to the collection of a time point, the cell media was spiked with 440 μCi of a mixture of

[^{35}S]-methionine and [^{35}S]-cysteine amino acids (Easy tag EXPRESS^{35}S; Perkin Elmer, Waltham, MA).

To collect cells at each time point, the media was removed, and the cell monolayer was washed with PBS (3 x 10 mL). The cell monolayer was then flash frozen in the plate by placing it on dry ice saturated with ethanol. The frozen cells were then collected in 3 mL of mammalian cell lysis buffer (0.1% Triton; 150 mM NaCl; 60 mM $MgCl_2$; 25 mM Tris·HCl, pH 7.5; 1 μM Microcystin [Cayman Chemical, Ann Arbor, MI], 1 mM DTT, and 1x protease inhibitor tablet [Roche, Florence, SC]) by scraping. The lysed cell milieu was centrifuged, and the protein supernatants were collected and passed over the ATP resin. The resin was washed with low-stringency wash buffer (LSWB) (Tris, 50 mM, pH 7.5; NaCl, 150 mM; and $MgCl_2$, 60 mM at 3× resin volume). Purine-binding proteins are boiled off of the resin with 5x SDS running buffer.

The matched virus- and mock-infected time course samples were loaded into a 10% Tris-HCl gel (BioRad, Hercules, CA) and subjected to SDS-PAGE. The gels were silver stained to visualize protein bands and then dried on a heated gel dryer. The dried gel was exposed to film (Blue Devil Film; Genesee, San Diego, CA) for 7 days, and protein bands containing [^{35}S]-Met/Cys were imaged, exised, trypsinized and identified by matrix-assisted laser desorption/ionization time-of-flight mass spectrometry (MALDI-TOF MS). The MS analysis was performed by David Loiselle (Haystead MS Facility, Duke University Medical Center).

2.2.3.3 Metabolic labeling of U937+DC-SIGN cells

U937+DC-SIGN cells were subjected to a similar experimental procedure as HuH7 cells with the following exceptions. The human monocytic cells were infected with DENV at a MOI of 5 or with "mock" media (*Aedes Albopictus* C6/36 cell culture media), and cells were incubated in for 22 h. At 22 h post infection, 300 μCi of [^{35}S]-methionine/cysteine was added to both the virus-infected (V) and the mock-infected control (C) cells. Following a 2-hour incubation, samples were collected in the same manner as described above. Lysates were passed over the ATP-resin to capture purine-binding proteins. To elute proteins bound to the resin, three different conditions were used. Elution was performed by either: 1) adding 100 mM soluble ATP to the resin and collecting the eluate; 2) adding 100 mM soluble ATP, discarding this initial eluate, and then adding 5x SDS running buffer, boiling for 2 minutes, and collecting the eluate; or 3) adding 5x SDS running buffer only boiling for 2 minutes, and collecting the eluate.

2.2.4 Expression of GFP-fusion proteins

The preparation of the DNA constructs of full-length or truncated NS5 with an N-terminal GFP tag has been previously described (Rawlinson et al., 2009b). Each DNA construct was amplified in *E. coli* DH5α and purified according to the instructions in the Plasmid Maxi Kit (Qiagen, Venlo, NL). The concentration of the purified plasmid was measured using a UV-Vis spectrophotometer (Shimadzu, Kyoto, Japan).

Each 15 centimeter plate of confluent HEK293 cells was transfected with a mixture of 30 μg of GFP-NS5 DNA and 10 μL of transfection reagent (Xtreme Gene HP; Roche, Indianapolis, Indiana). After a 36 hour transfection period, the HEK293 cell monolayer was flash-frozen in an ethanol/dry ice bath, and cells were scraped off of the plate in 5 mL of lysis buffer (0.1% Triton; 150 mM NaCl; 60 mM $MgCl_2$; 25 mM Tris·HCl, pH 7.5; 1 μM microcystin; 1 mM DTT; and 1x protease inhibitor[Roche, Florence, SC]). The crude lysates were clarified by centrifugation at 4,000 rpm for 5 minutes. Clarified lysate was used for all subsequent screening and titration experiments.

2.2.5 Fluorescence-based small-molecule drug screen

A collection of 10,000 compounds was initially selected from commercially available compounds using previously described parameters (Fadden et al., 2010b). The collection of 10,000 compounds was analyzed by a group of medicinal chemists, who eliminated approximately 6,000 of these compounds based on structural liabilities including general reactivity with proteins side chains. A final total of 3,379 compounds were selected for the screen, and individual compounds were purchased from various commercial sources as described in Materials. The candidate compounds were prepared as 10 mM solutions in dimethylsulfoxide (DMSO) and a final volume of 100 μL was plated into 96-well plates.

ATP-Sepharose resin was prepared as previously described (Graves et al., 2002). A schematic outlining the screening protocol is shown in Figure 4.

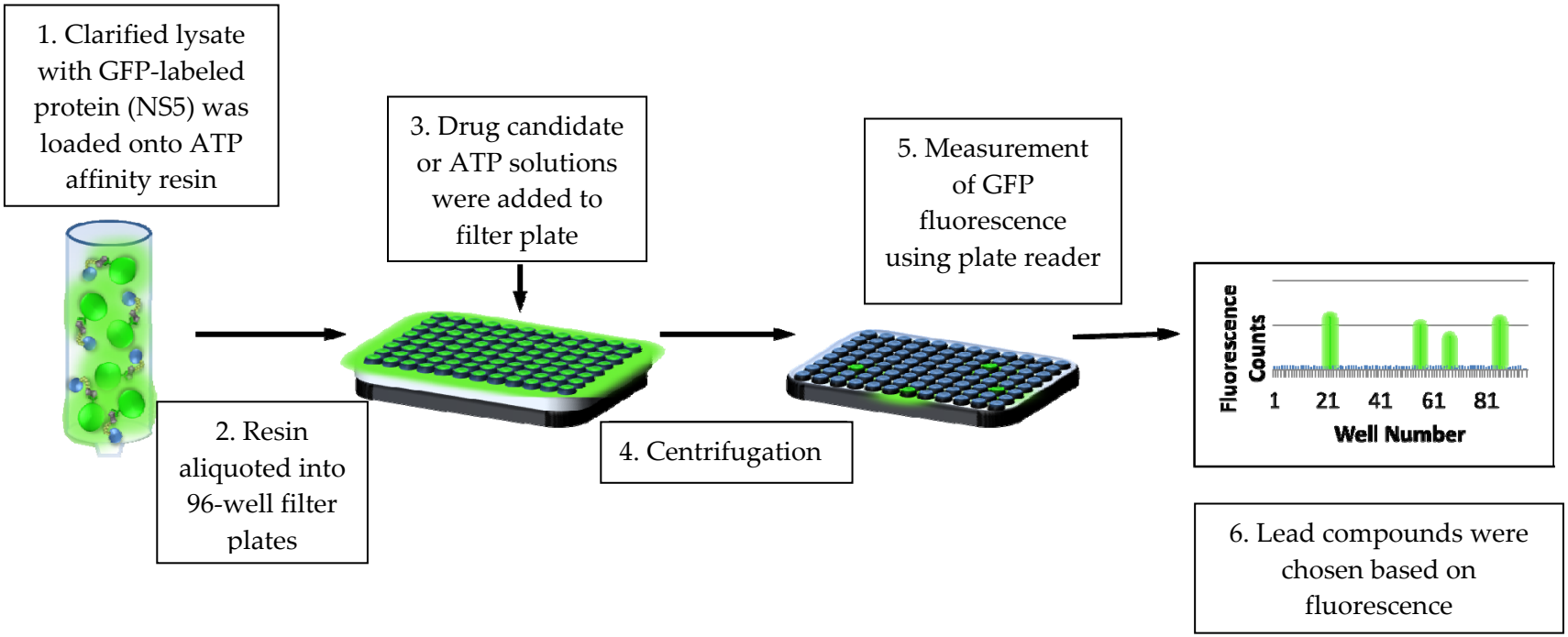

Figure 4: Overview of fluorescence-based small molecule drug screen. Crude cell lysate from HEK293 cells overexpressing GFP-NS5 was bound to ATP resin. Resin was aliquoted into 96-well plates and small-molecule solutions or soluble ATP was added. Fluorescence of eluted proteins was measured on a plate reader and compounds capable of yielding a fluorescence greater than 2.5-fold over background were flagged as lead compounds. Modified from (Carlson et al., 2013).

The ATP-sepharose resin was pre-washed with 60 mM $MgCl_2$ in 5 mM HEPES (3 resin-bed volumes). The clarified lysates containing recombinant full-length GFP-NS5 were combined with the pre-washed ATP-Sepharose resin (1:1 slurry, >50,000 fluorescence units per 50 μL of slurry as measured on a plate reader) and incubated for 15 minutes at room temperature. Following the incubation, the buffer (containing unbound proteins) was removed by gravity filtration through a sintered glass column. The resin was washed with 3 resin-bed volumes of low stringency wash buffer (LSWB) containing 50 mM Tris pH 7.5, 150mM NaCl, and 60 mM $MgCl_2$. LSWB (1 resin-bed volume) was then added to the resin to reestablish a 1:1 slurry. The slurry was aliquoted into 96-well PVDF filter plates (Corning 3504, Corning, NY) at 50 μL per well. On each 96-well plate, three wells were reserved for control samples. In these control-sample wells, 50 μL of ATP solution (0, 20, and 60 mM, respectively, in LSWB containing 10% DMSO) was added to 50 μL of slurry. The remainder of the plate wells were used to screen the candidate compounds.

Fifty microliters of each drug candidate (900 μM in LSWB containing 10% DMSO) was added to 50 μL of slurry. After a 15-minute incubation at room temperature, the eluates were collected by centrifugation (2000 rpm, 2 min) into a black 96-well collection plate (Costar 3915, Corning, NY). The GFP fluorescence in each well was measured using a 96-well plate reader (Perkin Elmer Victor *X*2 Multilabel Reader, lamp filter 485 nm, emission filter 535 nm). Samples exhibiting fluorescence greater than

2.5-fold over background were resolved by polyacrylamide gel electrophoresis on 4-15% SDS-PAGE gradient gels (Criterion Precast Gel; BioRad, Hercules, CA) and transferred to PVDF membranes.

Membranes were blocked with 5% milk in Tris-buffered saline (TBS; 50mM Tris pH 7.5, 150 mM NaCl), and probed with rabbit anti-GFP antibody at a 1:2000 dilution in TBS containing 0.05% Tween-20 (TBST) overnight at 4°C (Sigma Adrich G1544, St. Louis, MO). Membranes were washed three times (10 minutes each) in TBST, and the blots were incubated with HRP-conjugated anti-rabbit IgG antibody at a 1:1,000 dilution in TBS (Cell Signaling 7074, Beverly, MA). GFP-NS5 protein was then visualized using an ECL detection kit (Thermo Fisher, Waltham, MA) according to the manufacturer's instructions and analyzed on film.

2.2.6 Flow cytometry-based assay to measure percent DENV infection in a monocytic cell line

U937+DC-SIGN cells were seeded into a 96-well plate in 200 μL of cell culture media at a density of 5×10^4 cells/well then pre-treated with varying concentrations of the lead compounds. Cells were incubated in the compound-containing media for 1 hour at 37°C and 5% CO_2. Following the 1 hour incubation, the plate was centrifuged at 2000 rpm for 2 minutes to pellet the cells. The cell media was then decanted, and the cell pellets were re-suspended in DENV-NGC- containing media at a final MOI of 1 in a volume of 100 μL. The cells were returned to the incubator for 1 hour. After 1 hour, the cells were again centrifuged, and the viral culture media was aspirated. The pelleted

cells were re-suspended in 200 μL of compound-containing media at the same concentrations at which they were pre-treated. Cells were incubated for 48 hours post-infection.

Following the 48 hour infection, U937+DC-SIGN cells were transferred into a 96-well round bottom plate, washed twice with PBS, centrifuged at 2000 rpm for 2 min, and the wash was decanted. The cells were re-suspended in a 1:1000 dilution of Fixable viability 780nm stain (eBioscience) in PBS, and incubated on ice for 5 minutes. The dye was washed off with three consecutive washes with PBS. Cells were fixed with fresh 2% PFA for 10 minutes at room temperature and placed on the shaker for gentle agitation. The cells were centrifuged at 2,000 rpm for 2 minutes, and the supernatant was discarded by decanting. Pure 100% ice-cold methanol was added to the cells, and the cell solution was mixed thoroughly by pipetting up and down. Cells were incubated in the methanol for 20 minutes on ice to permeabilize the plasma membranes. Following centrifugation at 2,000 rpm for 2 minutes, the methanol was removed and replaced with blocking solution (PBS containing 0.5 % BSA). Cells were then washed three times consecutively with blocking solution. Primary antibody targeting the DENV envelope protein (4G2) was diluted 1:1000 in blocking solution and added to the cells. The cells were incubated in primary antibody solution overnight at 4°C.

The following day, the primary antibody solution was removed, and cells were washed three times with blocking solution. Secondary antibody, goat anti-mouse IgG

AlexaFluor 488, was prepared at a 1:1000 dilution in blocking solution and added to the cells. Cells then incubated for 45 minutes at room temperature protected from light. After removal of secondary antibody, cells were washed three times with blocking buffer and stored in 2% PFA no more than 3 days until flow cytometric analysis.

The immunofluorescently labeled cells were transferred to flow cytometry tubes (Corning) in a total volume of 200 μL of 2% PFA in PBS. The first sample injected into the flow cytometer (BD Cantos) was a control sample containing no virus. This control sample was used to optimize the forward light scatter and side light scatter (FSC and SSC, respectively) voltages by adjusting them until the majority of the cells appeared centered within the plot as opposed to sitting on the axes. A gate was drawn based on the uninfected control, which was a boundary between uninfected and infected cells as measured by fluorescence (high fluorescence indicates infection by immunofluorescence against DENV E protein). This gate was confirmed by analyzing the virus-infected control to ensure a part of that cell population registered as "infected." The voltage setting for 780 nm (the viability dye) was optimized using an uninfected control. After the settings had been applied, all sample data was collected and further analyzed using the FlowJo v.10 software (Tree Star) to determine percent infection and percent viability for each sample set of cells.

2.2.6.1 Optimization of DENV infection vs. MOI

Prior to any small molecule drug screening in the U937+DC-SIGN flow cytometric assay, an optimization study was performed to identify a reasonable range for MOI. This optimization identified an MOI of 2 to maximize the percent infection without adding additional virus. Above a MOI of 2, the MOI vs. percent infection is no longer a linear correlation as the percent infection reached its maximum. Figure 5 shows the correlation between the MOI of DENV2-NGC added vs. the measured percent infection by flow cytometry.

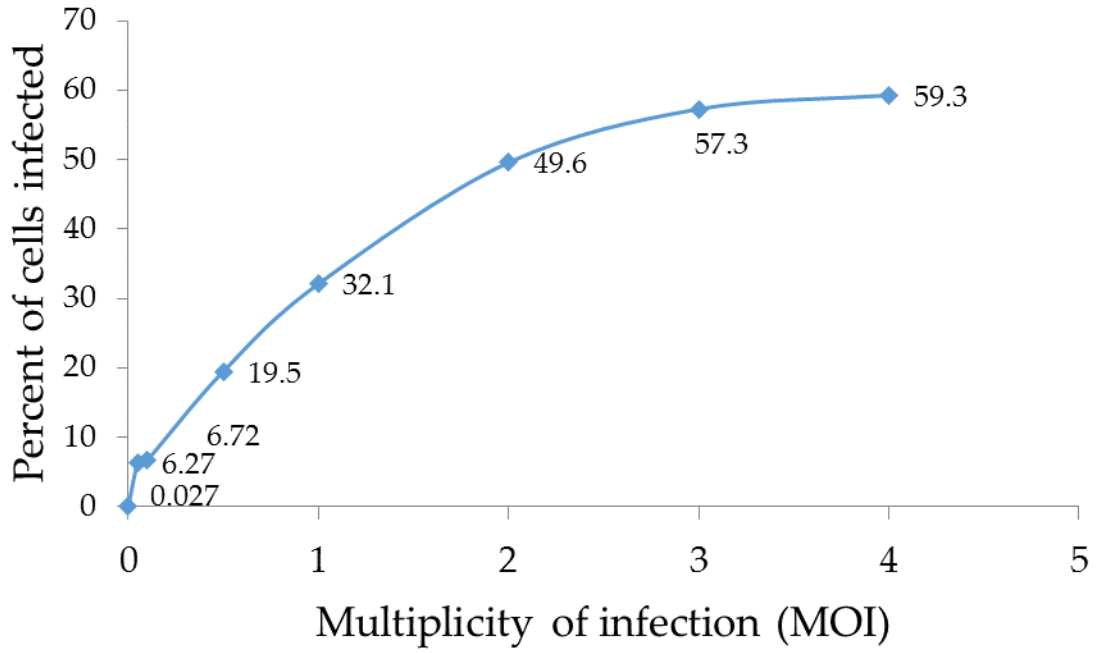

Figure 5: Optimization of DENV percent infection vs. multiplicity of infection in U937+DC-SIGN cells. A total of 2.5x10^4 cells were plated in each well of a 96-well plate in a total volume of 250uL of RPMI+/+. After 24 h, cells are re-suspended in DENV2-NGC virus to the indicated MOI. The next day, cells were subjected to immunofluorescence to determine the percent DENV infection.

Appendix B shows the flow cytometry 2D dot plots displaying positive and negative control cells (DENV-infected and mock-infected, respectively) with viability measurements. Additional flow cytometry plots corresponding to the optimization of DENV percent infection (Fig. 5) in side scatter (SSC) versus forward scatter (FSC), and the corresponding histograms that show population distribution as it pertains to fluorescence of the secondary antibody are found in Appendix D.

2.2.7 Focus-forming unit assay

African green monkey kidney Vero cells were plated into 24-well plates at a cell density of $1x10^5$ cells/well. Cells were allowed to incubate overnight. The following morning, the culture medium was removed by aspiration, and 100 μL of 10-fold serial dilutions of virus-containing media was added to Vero cell monolayers in triplicate. Cells were incubated for 1 hour at 37°C, with gentle agitation applied every 15-20 minutes. Following this 1 hour incubation, 500 μL of a 1:1 tragacanth gum/2x EMEM overlay supplemented with 2% FBS was added to each well. Cultures are incubated for 7 days at 37°C without agitation.

Following the 7-day incubation, the gum solution was removed by aspiration, and the cell monolayer was fixed with 4% paraformaldehyde (PFA) in phosphate-buffered saline (PBS; 137 mM NaCl, 2.7 mM KCl, 10 mM Na_2HPO_4, 1.8 mM KH_2PO_4, pH 7.4) for 15 minutes at room temperature. The PFA was then removed, and cells were

permeabilized with 0.5% Triton X-100 in PBS for 15 minutes at room temperature with gentle agitation. The permeabilization buffer was removed and replaced with blocking buffer (PBS containing 0.1% Tween-20 and 1% normal donkey serum). Cells remained in blocking buffer for 1 hour at room temperature. A primary antibody directed against DENV envelope protein, 4G2, was diluted in blocking buffer at 1:2000 and added to cells. Cells were kept at 4°C in the primary antibody overnight. The following day, the primary antibody solution was removed and cells were washed three times with PBS containing 0.1% Tween-20. Cells were then incubated in a secondary antibody solution of HRP-conjugated anti-mouse IgG antibody diluted in blocking buffer (1:2000 dilution) for 1 hour at room temperature. Cells were then washed three times with PBS containing 0.1% Tween-20.

The viral foci were stained at room temperature using 0.5 mL/well of VIP peroxidase-based substrate staining solution (Vector VIP Substrate Kit, Vector Labs, Burlingame, CA) in PBS, according to the manufacturer's instructions. Once a purple color became visible by eye, the substrate was removed by aspiration and the cell monolayers were rinsed once with water. The plates were air dried prior to counting the purple stained foci. The focus-forming units per milliliter (ffu/mL) were calculated based the number of foci divided by the product of the dilution factor and virus sample volume.

2.2.8 EC_{50} determination using cell-based flaviviral immunodetection (CFI) assay

A cell-based flaviviral immunodetection (CFI) assay was employed as previously described (Rathore et al., 2011) to determine antiviral activity of lead compounds and quantify the concentration of compound at which the percent of DENV infection was reduced by 50% (EC_{50}).

All of the compounds to be tested were initially dissolved in 95% DMSO as 20 mM stock solutions. The stock solutions were used in further dilutions with RMPI cell culture media to prepare the final compound concentrations needed in the CFI assay. All final compound dilutions resulted in a less than 1% DMSO concentration by volume.

Baby hamster kidney fibroblast (BHK-21) cells were selected for use in the CFI assay because they are highly permissive to DENV infection. BHK-21 cells were trypsinized and resuspended in RPMI 1640 cell culture media with 10% FBS. A total of 1.3×10^5 cells were plated into each well of a 96-well plate. The newly plated cells were incubated overnight at 37°C and 5% CO_2. The next day, cell culture media was aspirated and a mixture of DENV2-TSV01 at an MOI of 0.6 and the different concentrations of lead compounds in complete cell culture media was added to respective wells in the 96-well plate. The viral and compound cell culture media mixture remained in the presence of the cells for 1 hour in the incubator. Following the 1 hour incubation, the compound containing inoculums were removed and replaced with maintenance media comprised

of RPMI 1640, 2% FBS, and the same concentration of compound. Cells were incubated for 48 hours at 37°C and 5% CO_2.

After 48 hours, cells were washed once with PBS and fixed with ice cold 100% methanol for 15 minutes. Cell monolayers were washed two times with PBS+0.1% Tween-20. Cells were blocked in a blocking solution consisting of PBS+0.1% Tween supplemented with 1% FBS for 1 hour at room temperature. Blocking buffer was decanted and replaced with primary antibody solution containing the primary mouse monoclonal dengue anti-envelope (4G2) antibody at 0.05 mg/mL in blocking buffer. Cells were incubated overnight with the primary antibody solution at 4°C and then washed three times with PBS+0.1% Tween. Following the wash steps, cells were incubated in secondary antibody solution containing the goat anti-mouse IgG conjugated to an Alexa Fluor 488 nm probe for 1 hour at room temperature. Cells were then washed three times with PBS+0.1% Tween, and nuclei were stained with 4',6-diamidino-2-phenylindole (DAPI).

To quantify DENV-infected cells, the presence of the viral antigen, the DENV envelope protein, was detected using ImageXpress (Molecular Devices, Sunnyvale, CA). ImageXpress captured any fluorescence of cells at an emission of 488 nm, which correlated to the fluorescence of the secondary antibody. Only cells that contained the viral antigen would exhibit this fluorescence. Total cell number within each well of the

96-well plate was also determined using ImageXpress, which detected the nuclear dye, DAPI, which has an approximate emission wavelength of 450 nm.

Dose-response curves of percent DENV infection vs. the log of compound concentration for each lead compound. The concentration of compound at which the percent DENV infection was half of the maximum percent infection (EC_{50}), as measured by the presence of viral envelope protein was calculated using nonlinear regression analysis in the software program, Graphpad Prism 5.

2.2.9 Viability Assays

Two separate viability assays were used to determine cytotoxicity resulting from DENV-infection and treatments with lead compounds. Two different viability reagents were used, including a fixable viability stain and resazurin.

First, a fixable viability 780 nm stain was utilized during the flow cytometry-based percent infection assay as previously described in Section 2.2.6. The stain can only permeate cell membranes of necrotic cells, and once in the cytoplasm, the stain reacts with amine groups resulting in a fluorescent adduct at an emission of 780 nm. For the flow cytometry-based percent infection assay, the fixable viability 780 nm stain was chosen because it could be used prior to fixation with formaldehyde and could be used in a multiplex fluorescence assay with the fluorescence antibody complex of primary mouse anti-envelope antibody and secondary anti-mouse IgG Alexa Fluor 488 nm antibody.

Second, a chemical compound called resazurin (7-hydroxy-3H-phenoxazin-3-one 10-oxide), was used as an indicator of mitochondrial function in an additional viability assay. Resazurin is a nonfluorescent blue dye that when added to viable cells is reduced by the mitochondria to resorufin (7-Hydroxy-3*H*-phenoxazin-3-one), a fluorescent pink compound. In the resazurin viability assay, first U937+DC-SIGN cells were plated in a 96-well plate at a density of approximately 1 x 10^5 cells/well. Lead compounds were added to the cells, and cells were incubated at 37°C and 5% CO_2 for 24 hours. Following the 24 hour incubation, resazurin solution in PBS was added to each well at a concentration of 0.03 mg/mL. A negative control well contained culture media without U937+DC-SIGN cells or compound, but did contain the DMSO compound vehicle. The purpose of the negative control was to monitor for any chemical interference between the resazurin and cell culture media components. Additionally, a positive control well was comprised of cells that were treated with 100% methanol for 20 minutes to annihilate mitochondrial function and served as a nonviable cell sample. The plate of cells was returned to the incubator for 45 minutes to 1 hour.

After the incubation period, the 96-well plate was loaded into the plate reader and measurements were collected at an emission wavelength of 590 nm. The resazurin cell viability assay provided cytotoxicity results for the lead compounds in the absence of DENV.

2.2.10 RNA-dependent RNA polymerase (RdRp) assay

The RNA polymerase assay using DENV3 NS5 RdRp was performed as described previously (Niyomrattanakit et al., 2011). The RNA template, 3′UTR-U_{30} (5′-bio-U30-AACAGGUUCU*AGAACCUGUU*-3′), is a hairpin self-priming RNA containing a 30-nucleotide poly(U) incorporation region fused with the 3′UTR sequence (negative strand in italics, complementary positive strand underlined). Assays were performed using purified recombinant NS5, which were prepared as described previously (Yap et al., 2007). The recombinant protein was stored in 20 mM Tris-HCl (pH 7.0), 500 mM NaCl, 10% glycerol, and 10 mM 2-mercaptoethanol at -80^{0}C until use.

Prior to performing the assay, the RNA template was resuspended to 200 μM in a buffer consisting of 50 mM Tris-Cl (pH 8.0) and 150 mM NaCl in 0.1% diethyl pyrocarbonate (DEPC) water. The solution was then incubated at 55 °C to 60 °C for 5 min and placed at room temperature to allow the formation of the intramolecular hairpin. Polymerase reactions were performed in 96-well half-area black plates in final reaction volumes of 30 μL. RdRp activity was investigated using 100 nM DENV3 NS5 and 50 nM RNA template in a reaction containing 50 mM Tris-HCl (pH 7.0), 0.01% Triton X-100, 0.1 mM $MnCl_2$, 2 μM BBT-ATP, and test compound (HS-205020 or control compounds) added at eight final concentrations from 0 to 300 μM (0, 0.1, 0.3, 1, 3, 10, 30, 100 and 300 μM). Reactions were initiated by the addition of BBT-ATP and incubated for 60 minutes at 30^{0}C. The reactions were terminated by the addition of 20 μL of stop

buffer (200 mM NaCl, 25 mM $MgCl_2$, 1.5 M deoxyethanolamine) containing 25 nM calf-intestinal alkaline phosphatase (CIP). Reactions were further incubated for 30 minutes at 30^0C to allow the hydrolysis and release of BBT-PPi by the phosphatase.

Fluorescence emitted by BBT-PPi was monitored on a Tecan plate reader at excitation 422 nm and emission 566 nm. Percentage activity was calculated relative to the positive and negative controls. IC_{50} was calculated by plotting the data in Graphpad Prism software using non-linear regression-variable slope. IC_{50} value was extrapolated from $logIC_{50}$ according to the GraphPad algorithm (GraphPad version 5; GraphPad Software, San Diego, CA).

2.2.11 *In vitro* Hepatitis C virus assays

HuH7.5 cells were seeded into 24-well plates at 50,000 cells per well. The cells were incubated overnight at 37 °C and 5% CO_2. The following day, cells were infected with HCV JFH1 at an MOI of 0.1 for 2 hours in the incubator. After the 2 hour infection, virus was removed, and cell culture media plus compound (1 μM, 10 μM, 50 μM, 75 μM, or 100 μM) was added in triplicate, along with a DMSO control and a positive control consisting of 500 units/ml of interferon-α (IFN-α). The cells were maintained in the media plus compound for 72 h in the incubator at 37 °C and 5% CO_2.

After 72 h, the viral inoculums were removed and stored in the -80°C freezer. The cells were washed 1x with PBS. Cells were prepared for immunofluorescence analysis by fixing and permeabilizing the cells at room temperature for 20 minutes in

100% ice-cold methanol. After fixation and permeabilization, cell monolayers were washed 3 times with 1 mL of PBS followed by an overnight incubation at 4°C in blocking buffer (PBS, pH 7.4 + 1% BSA + 2.5mM EDTA). An overnight incubation in primary antibody solution (PBS, pH 7.4 + 1% BSA + 2.5mM EDTA + 1:300 dilution anti-core HCV antibody) was followed by an additional 3 washes with 1 mL of blocking buffer. After these washes, the cells were incubated at room temperature in secondary antibody solution (PBS, pH 7.4 + 1% BSA + 2.5mM EDTA + 1:1,000 anti-mouse Alexa Fluor 488 nm bound IgG). Following three more washes with 1 mL of blocking buffer, cells were briefly exposed to 4',6-diamidino-2-phenylindole (DAPI) for 60 seconds at 1 μg/mL. Excess DAPI was removed by three 5 minute washes with PBS. The sample wells were imaged using the Cellomics Array Scan VTI system (Cellomics). To determine the percentage of infection, the acquired images were analyzed using vHCS Scan software version 5.1.2.

A $TCID_{50}$ assay was used for virus titration of the frozen viral inoculums. First, HuH7.5 cells were plated in 96-well flat bottom plates. After an overnight incubation at 37°C and 5% CO_2, viral inoculums were added to the cell culture media in serial dilutions ranging from 10^0 to 10^{-2} in replicates of 8. The staining of the HuH7.5 cells was performed using a primary anti-HCV core antibody (Abcam), followed by a secondary Alexa Fluor 488 goat anti-mouse IgG (Invitrogen). The staining was analyzed by immunofluorescence microscopy. The number of wells that exhibited fluorescence

arising from the present of HCV core protein were labeled as "positive wells." Identification of both positive wells and total wells are required to calculate the $TCID_{50}$ using the Reed & Muench Calculator available from (Lindenbach, 2009).

2.2.12 Statistical Analyses

Statistical analyses were performed using GraphPad Prism 4.00 software (San Diego, CA). For percent infection, FFU values, $TCID_{50}$, titration data, and viable cell count data, the mean ± standard error of the mean is displayed. Statistical significance was determined using the Student's t-test. A p value less than 0.05 is denoted with an asterisk (*) and considered significant.

3. Identification of purine-utilizing proteins that are differentially expressed during DENV infection

By virtue of their purine binding pockets, purine-utilizing proteins (the "purinome") have proven a rich source of drug targets for many infectious diseases (Haystead, 2006). With this in mind, the aim of these experiments was to identify purine-binding proteins (both viral and host) targets that may serve as suitable targets to anti-DENV drug intervention. In order to identify such targets, a sulfur-35-labeled methionine/cysteine mixture was used to label actively translated proteins throughout a DENV2 infection life cycle in HuH7 human hepatoma cells or U937+DC-SIGN human monocytic cells. The protein targets would then be used in a small-molecule library

screening method (discussed in Chapter 4). Previous studies utilizing this small-molecule screen have helped to define early chemical starting points for other drug development strategies (Graves and Haystead, 2002, Duncan et al., 2012, Duncan et al., 2008, Fadden et al., 2010a, Carlson et al., 2013).

By specifically targeting purine-binding proteins that are actively translated in response to DENV-infection, it is possible to identify protein targets in the host and viral purinome. Proteins that are altered (up- or down-regulated) in response to DENV-infection can be identified by mass spectrometry and represent a more relevant protein target identification than most preliminary targets which were determined by measuring changes in mRNA quantities during DENV-infection (Liew and Chow, 2004, Warke et al., 2003, Ekkapongpisit et al., 2007).

This approach does not discriminate between identifying a virally-encoded protein target versus a host gene-encoded protein target. The advantages of inhibiting a viral protein with a drug is a decreased probability of side effects, assuming the drug is selective, and high certainty that inhibition of a viral protein will reduce virus propagation by a mechanism of action requiring that viral protein. On the other hand, host proteins are not under the genetic control of DENV, therefore host protein targets can evade virus-driven mutations that would otherwise cause drug resistance.

To identify purine-utilizing proteins that are actively translated during DENV infection, cells were first infected with DENV2 virus, and the infected cells were

cultured in medium containing radiolabeled amino acids (^{35}S-labeled methionine/cysteine) for specified periods of time throughout the course of infection (ranging between 0 to 24 hours) as described in Materials and Methods (Chapter 2). A schematic of the design of this time-course experiment is shown in Figure 6. This procedure allowed monitoring of both viral and host proteins that may be up-/down-regulated during the course of infection. In addition, mock-infected controls were used in order to exclude any changes that were unrelated to DENV2 infection. Following the metabolic labeling procedure, the infected cells were lysed, and purine-utilizing proteins were reversibly captured using immobilized ATP-Sepharose. Bound proteins were denatured from the resin by boiling the samples in 5x SDS running buffer and were separated by PAGE analysis and visualized by silver staining and autoradiography.

These metabolic labeling studies were performed in a human liver cell line, HuH7, and a human monocytic cell line, U937+DC-SIGN, to label translated proteins during DENV infection. These cell lines were chosen on the basis of their permissibility to DENV-infection and relevance as a target cell in human DENV-infections. HuH7 cells are a human hepatocellular carcinoma cell line that is permissive to DENV-infection and as a human cell line, it is a relevant target cell in human DENV-infections, specifically in the more severe manifestations including DHF and DSS where liver damage is observable (Alen and Schols, 2012). The U937+DC-SIGN cells are a human monocytic cell line constitutively expressing DC-SIGN (CD209) on the cell surface. Surface DC-

SIGN on U937 cells enhances virus infection in cell culture (Alen et al., 2012). Monocytes are indisputably recognized as a highly relevant DENV target cell in humans, and monocytes encounter the newly infected virus early on in infection along with dendritic cells, Langerhans cell, and macrophages.

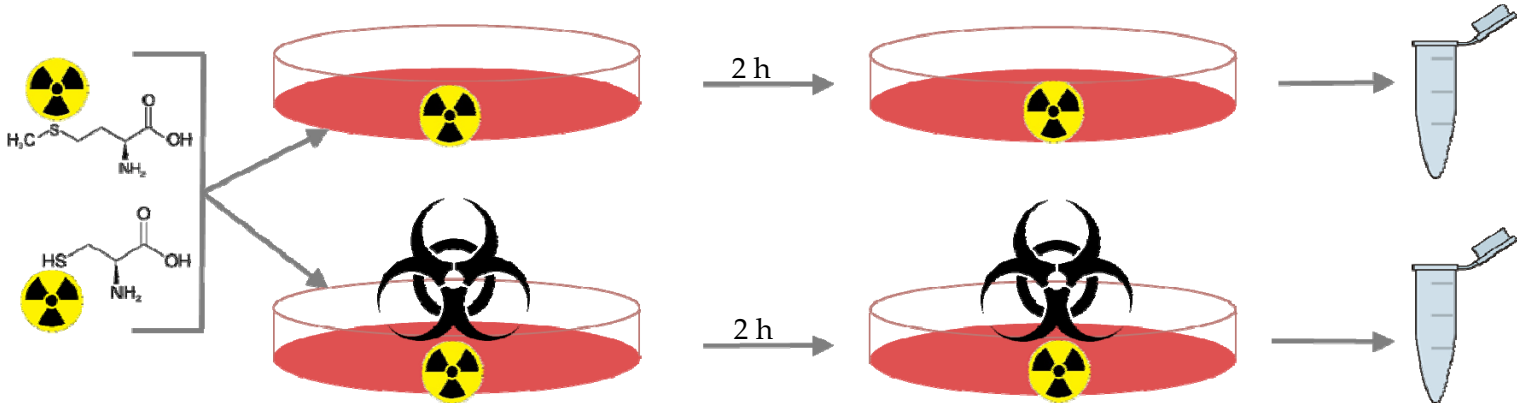

Figure 6: Schematic of [^{35}S]-metabolic labeling to identify purine-utilizing proteins that are up- or down-regulated in response to DENV infection. As described in Materials and Methods (Chapter 2), DENV2-NGC virus was added to HuH7 cells or U937+DC-SIGN cells. The radiolabeled amino acid mixture was added in equal quantities to either -infected HuH7 cells, mock-infected. After a 2 hour label, the cells in both samples are collected for analysis.

3.1 Twenty-four hour time course in DENV-infected human liver cells

A radioactive 24 h time course infection was performed in a human hepatocellular carcinoma cell line, HuH7 to probe for purine-binding protein expression level changes in response to DENV-infection.

As shown in the autoradiogram in Figure 7, there were marked increases in the translation of four proteins in the DENV-infected lysate (at 105 kDa, 70 kDa, 65 kDa and 8 kDa), compared to the mock-infected control lysate. For all four proteins, this increase occurred between 12 and 24 hours post-infection (p.i.). Mass spectrometry identified three of these proteins as virally encoded DENV NS5 (105 kDa), NS3 (68 kDa), and prM (21 kDa). The 70 kDa band could not be identified. No changes in protein levels were observed at the earlier time points between 0 and 8 hours post-infection (results shown in Appendix C).

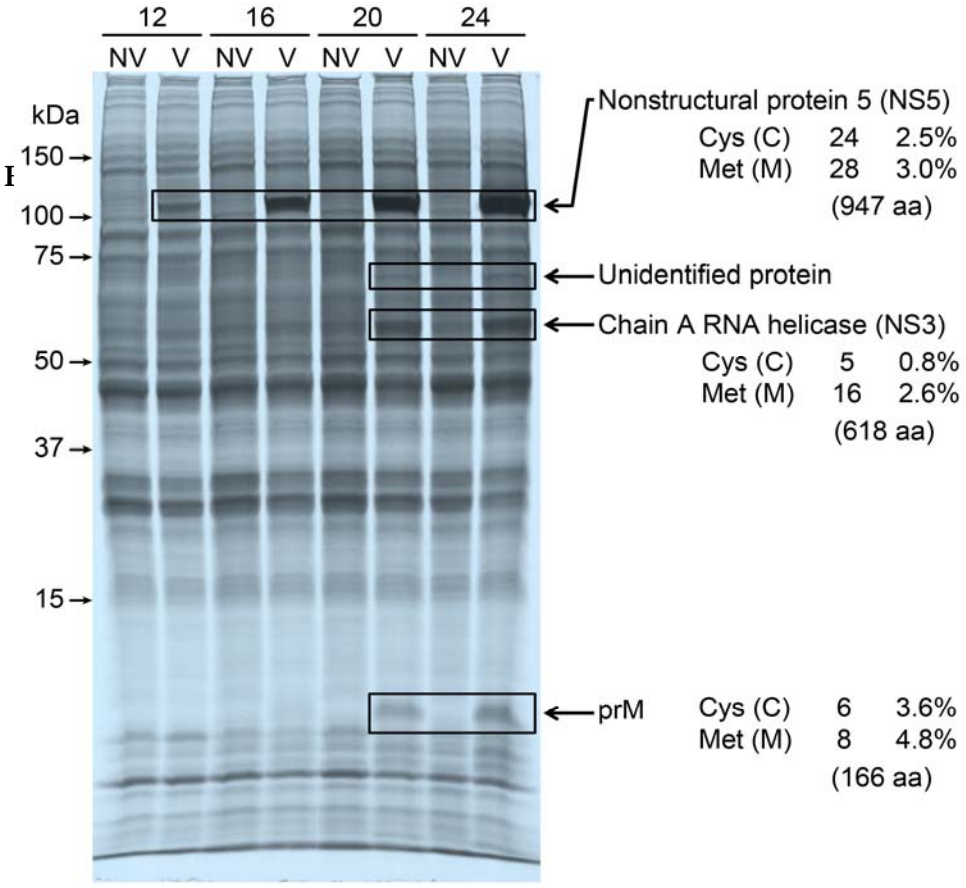

Figure 7: Late Time Points in DENV Infection (12 – 24 hours post-infection): [^{35}S] autoradiogram showing purine-binding proteins in DENV-infected cells (V) and uninfected control cells (NV), from 12 to 24 hours post-infection. Protein bands that showed increased expression levels in DENV-infected cells over time (and compared to controls) were excised, and proteins were and identified using mass spectrometry.

Of the three purine-binding proteins identified as being up-regulated during DENV infection, the detection of both NS5 and NS3 correspond well to what is known about these proteins' enzymatic activities and specific roles in the DENV viral life cycle. As described in the Introduction, NS5 contains two catalytic domains that utilize purines to carry out their enzymatic functions. The methyltransferase domain on the N-terminus of NS5 contains a GTP binding site that may be involved in cap recognition, and the polymerase domain on the C-terminus requires nucleotides to be positioned in the active site to carry out the RNA synthesis. Therefore, both catalytic domains of NS5 bind nucleotides in the course of their enzymatic activities, and therefore would be able to bind to the immobilized-ATP resin. The required role of NS5 in DENV propagation corresponds well to the observed increase in NS5 levels at approximately 8 hours to 24 hours post-infection in HuH7 cells.

Similarly to NS5, the NS3 protein contains two active sites capable of binding ATP. Specifically, NS3 contains both an NTPase and ATPase in the helicase domain on the C-terminus. The N-terminus contains a serine protease, but no expected purine-binding pocket exists there. As with NS5, the NS3 protein is required during viral RNA replication, which is consistent with the up-regulation detected during the mid- to late part of the viral life cycle. However, the mechanism by which prM was able to bind the ATP resin is unclear, since prM does not contain any known purine-binding domains. It

is possible that the retention of prM on the ATP resin was a result of allosteric or strong protein-protein interactions, rather than a direct binding interaction.

Interestingly, the majority of metabolically labeled proteins did not appear to be up-/down-regulated in response to DENV infection, as their levels remained unchanged throughout the course of infection. However, it is important to note that this method alone would not detect changes in levels of proteins that did not bind to the ATP resin. Mass spectrometry analysis identified the majority of these "unaffected" proteins as being host ATP-binding proteins (Appendix E).

Given the limited viral proteome, it is expected that the virus depends heavily of host proteins to propagate. Previous studies analyzing and quantifying the host mRNA levels in response to DENV-infection in several human cell lines identified tens to hundreds of different mRNAs that were altered (up- or down-regulated) in response to the infection (Liew and Chow, 2004, Warke et al., 2003, Ekkapongpisit et al., 2007). Some of these altered mRNAs encoded purine-binding proteins. However, we have shown that we do not observe a change at the protein level in the purinome of HuH7 or U937+DC-SIGN cells in response to DENV-infection. This suggests that the virus may be affecting the transcription of many host factors, but not any subsequent translation. This discrete host hijacking behavior of a virus is not uncommon. In fact, causing no significant changes in protein expression is one of the many ways in which a virus can evade the host innate immune response (Francica et al., 2010).

3.2 DENV-infection in human monocytic cells

To determine whether the results obtained from HuH7 cells would be similar in other DENV-relevant cell lines, a similar metabolic labeling experiment was performed in a human cell line, U937+DC-SIGN.

Figure 8 shows differences in [^{35}S] incorporation between virus-infected (V) and mock-infected control (C) samples. In this experiment, proteins bound to the resin were eluted using a boiling approach and using 100 mM soluble ATP. Boiling the ATP beads in SDS running buffer results in the denaturation of all proteins bound to the ATP resin, including proteins that were potentially non-specifically bound to the ATP-Sepharose. On the other hand, eluting bound proteins with the substrate, ATP, will release only proteins that have a nucleotide binding capacity (e.g., ATP active site, allosteric nucleotide binding). The major differences observed include the presence of NS3 and NS5, and three other bands. The first of the three bands is present right below the identified NS3 band. The MS analysis showed peptides mapping to NS3, HSP90, and ABC sub-family F. It is possible that the majority of the proteins present in the band is degraded NS3, which would explain the reduction in expected molecular weight. The second and third of the three bands are present below the 25 kDa marker. The MS report shows the presence of 40S ribosomal protein S9, IgG, and un-named proteins.

The identification of NS5 in both the protein sample from boiling and the protein sample from the addition of 100 mM ATP confirms that NS5 is both capable of binding the ATP resin and being eluted with soluble ATP.

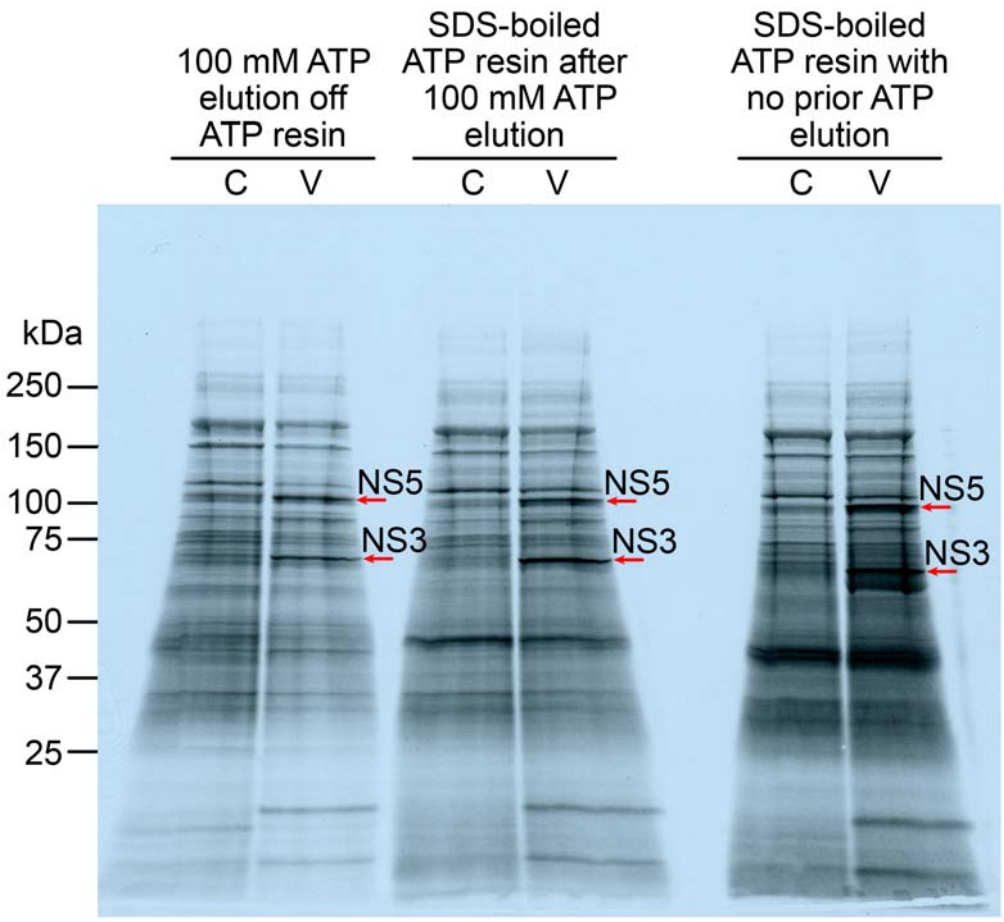

Figure 8: ATP-capture of DENV proteins NS5 and NS3 from DENV-infected (24 h p.i.) or control U937+DC-SIGN cells. Both NS proteins bind ATP-resin and eluted with 100 mM ATP. Control, or mock-infected protein samples are labeled as C and virus-infected samples as V. It is probable that the band directly beneath NS3 in the V lane is a degradation product of NS3. Additionally, the two bands present below the 25 kDa marker in the V lane were identified by MS as IgG, 40S ribosomal protein and unnamed proteins. The unnamed proteins may be degradation products of viral proteins that are present in low quantities and below the detection threshold. All other proteins identified were host ATP-binding proteins or unidentified based on copy number.

Two major differences observed between infected and control cells were the dense bands present in the virus-infected samples of all three conditions at 105 kDa and

approximately 68 kDa. Mass spectrometry analysis identified these proteins in as DENV NS5 and NS3, respectively. The presence of both NS5 and NS3 in all three conditions demonstrates ATP binding ability of the native viral proteins, ability to be eluted by soluble ATP (either by ATP interaction with a nucletotide binding site or an allosteric site), and that residual bound protein remains after ATP elution (which is typical for purine-utilizing proteins). The other bands on the autoradiogram were not identified as DENV originating, and were all host proteins or unidentified/null identifications.

Comparing the purine-binding proteins identified in these experiments to those identified in the HuH7 infection time course, there was an overlap in the identification of two of the three viral proteins, NS5 and NS3, (prM was only identified in the HuH7 infection time course), with the remainder of the proteins determined to human host proteins. The absence of vast protein expression level changes apart from the viral proteins suggest that DENV infection of HuH7 liver cells or U937+DC-SIGN monocytic cells has little effect on the expression of most of the abundant host ATP binding proteins.

3.3 Comparison of the DENV purinomics profile with published DENV proteomic studies

Previous studies have identified proteins whose expression levels are altered in response to DENV infection (Pattanakitsakul et al., 2007, Zhang et al., 2013, Mishra et al., 2012). It is important to note that these studies examined the whole proteome, in

contrast to our study specifically targeting only purine-utilizing proteins (purinome). In a human liver carcinoma cell line (HepG2), 17 differentially expressed host proteins were identified by 2-dimensional polyacrylamide gel electrophoresis (2D PAGE) and mass spectrometry (Pattanakitsakul et al., 2007). In another study using tissues from *Aedes* salivary glands, midgut, and C6/36 *Aedes albopictus* larva cells, using a similar 2D-PAGE technique, a total of 41 differentially expressed host proteins were identified (Zhang et al., 2013). A third study, also using a 2D-PAGE approach, demonstrated up-regulation of 2 host proteins in human monocytic THP1 cells (Mishra et al., 2012). A partial list of the proteins identified in these studies is shown in Table 1. As noted, the list of identified proteins includes a variety of purine-binding proteins, such as dehydrogenases, helicases, ATPases, and ATP synthase.

Table 1: Partial list of host proteins that have been shown to be up- or down-regulated in response to DENV infection in previous studies. As specified, ten of the identified proteins are capable of binding and utitlizing ATP.

Protein	NCBI ID	Up- or down-regulated	Purine binding?	Cell type	Reference
vinculin	gi|31543942	Down	No	HepG2	(Pattanakitsakul et al., 2007)
Succinate dehydrogenase, flavoprotein subunit	gi|1169337	Down	Yes	HepG2	(Pattanakitsakul et al., 2007)
ATP-dependent RNA helicase DDX17	gi|3122595	Up	Yes	HepG2	(Pattanakitsakul et al., 2007)
Calumenin	gi|2809324	Down	No	HepG2	(Pattanakitsakul et al., 2007)
ATP synthase, mitochondrial F1 complex	gi|24660110	Down	Yes	HepG2	(Pattanakitsakul et al., 2007)
Retinol dehydrogenase	gi|25141231	Up	Yes	HepG2	(Pattanakitsakul et al., 2007)
ATPase, V0 subunit d1	gi|19913432	Up	Yes	HepG2	(Pattanakitsakul et al., 2007)
Annexin 5	gi|4502107	Up	Yes	HepG2	(Pattanakitsakul et al., 2007)
Dehydrogenase/reductase SDR family	gi|3915733	Down	Yes	HeG2	(Pattanakitsakul et al., 2007)
Heterogenous nuclear ribonucleoprotein H	gi|5031753	Up	Yes	THP1	(Mishra et al., 2012)
Protein disulfide-isomerase A3	gi|21361657	Up	No	THP1	(Mishra et al., 2012)
Protein disulfide isomerase 1	gi|20068287	Down	No	*Aedes* midgut	(Zhang et al., 2013)
ATP synthase	gi|287945	Up	Yes	*Aedes* midgut	(Zhang et al., 2013)
Isocitrate dehydrogenase	gi|24660849	Up	Yes	C6/36	(Zhang et al., 2013)

Although previous whole-proteome studies have shown an up- or down-regulation of several purine-binding proteins, these proteins were not identified in our purinomic studies in HuH7 and U937+DC-SIGN cells.

The results of the studies using 2D PAGE to identify differentially expressed proteins varied significantly between studies while the resin capture of radiolabeled purine-binding proteins was consistent between the two cell lines used, HuH7 and U937+DC-SIGN. Of the 17 proteins identified in HepG2 cells (Pattanakitsakul et al., 2007), none of them were the 2 proteins reported in THP1 cells (Table 1) (Mishra et al., 2012), despite both studies utilizing a similar 2D PAGE approach.

The purinomic studies were enriching for purine-binding proteins, whereas the whole-proteome studies did not use any pre-selection criteria (e.g., affinity resin, fractionation, liquid chromatography). It would be more difficult to identify lower expression proteins with smaller or more modest changes in protein expression within the entire proteome because discrete changes may be hidden beneath protein bands arising from high expression proteins. Although each of the previous studies identified changes in protein expression, these changes were inconsistent across the cell lines used (HepG2, THP1, C6/36). In the purinomics studies, consistency between purine-binding proteins identified in the two cell lines (HuH7 and U937+DC-SIGN) was achieved. By exploiting the purinome an over 2,000 protein containing subset of the proteome, our

purinomic studies are tapping into a rich source of therapeutic targets while minimizing interference by the rest of the proteome.

3.4 ATP binding profile of GFP-NS5

The purine-binding proteins that were up-regulated in response to DENV infection in both a human liver and monocytic cell line were identified as DENV NS5, NS3, and prM (only in HuH7), as well as an unidentified proteins and ABC subfamily F (Fig. 7, 8). As discussed above, NS5 and NS3 both contain enzyme domains that utilize purines. Specifically, NS5 contains a methyltransferase domain and a polymerase domain, while NS3 contains a helicase domain with NTPase and ATPase activity. All of these enzymatic activities in both NS5 and NS3 are required for DENV infection and propagation.

In targeting a viral protein, ideally the viral protein would be unlike any host protein, which would reduce the probability of side effects. Additionally, targeting a viral protein that is well conserved across strains would provide the added advantage of having broad activity across strains. Targeting a DENV-required host protein to develop an antiviral would be advantageous in that host proteins are not under the direct control of the virus can evade mutations leading to reduced efficacy. However, a clear disadvantage to having an antiviral targeting a host protein would be the risk of severe side effects, especially when that host protein has an activity required for normal cellular function (e.g., required proteins involved in metabolism, cellular structure, and mitosis).

The rationale for the selection of NS5 as the target protein for further drug discovery efforts was two-fold. First, NS5 is the most highly conserved flaviviral protein. Thus, an inhibitor to DENV NS5 could have much broader anti-flaviviral applications. Secondly, NS5 contains two distinct enzymatic domains that are capable of binding ATP. Therefore, any candidate compounds identified in a screen using full-length NS5 protein, could be characterized further by determining which domain the compound is targeting. By using a GFP fusion truncated NS5 protein (such that is contains only the methyltransferase or only the polymerase) bound to ATP resin, elution studies with the candidate compound would elucidate the preferred target domain of NS5 by the candidate compound.

To evaluate NS5 as a suitable target protein to be used in our fluorescence-based small-molecule screen, it was necessary to perform preliminary testing to ensure that the purine-binding properties of NS5 were maintained when a GFP tag was added to the N-terminus of the protein (Appendix A). This was necessary because a fused GFP domain is required to produce the fluorescence read-out in the final step in our small-molecule library screening method. To evaluate and characterize an NS5/GFP fusion protein, a construct encoding full-length NS5 (DENV2-Townsville) fused to an N-terminal GFP domain (Rawlinson et al., 2009a) was expressed in human embryonic kidney (HEK293) cells. The HEK293 human-derived cells, were used to overexpress the recombinant proteins because of their ability to produce large quantities of proteins from transfected

plasmids. In the case of producing large quantities of the GFP-NS5 protein target, the identity of the mammalian cell that is producing it is unimportant because only the clarified lysate is used in subsequent experiments.

Clarified lysate containing overexpressed GFP-NS5 was incubated with ATP resin. The resin bound proteins are eluted with increasing concentrations of soluble ATP. The GFP fluorescence of the eluate resulting from the ATP elution was measured using a plate reader, and this fluorescence represented the relative quantity of GFP-NS5 within the sample. The measured GFP fluorescence was lowest at 0 mM ATP and with increasing concentrations of added ATP, the measured GFP fluorescence increased. This demonstrated that GFP-NS5 bound the resin, and was eluted in a concentration-dependent manner using soluble ATP.

Figure 9 shows the results of the ATP-elution studies. The results show that soluble ATP elutes GFP-NS5 from the resin in a concentration-dependent manner (Fig. 9A). The presence of GFP-NS5 was confirmed in the eluate by Western blot (Fig. 9B). These results also indicate a strong ATP-binding capacity of GFP-NS5, demonstrating that the fusion protein is suitable for further testing using our small-molecule drug screen.

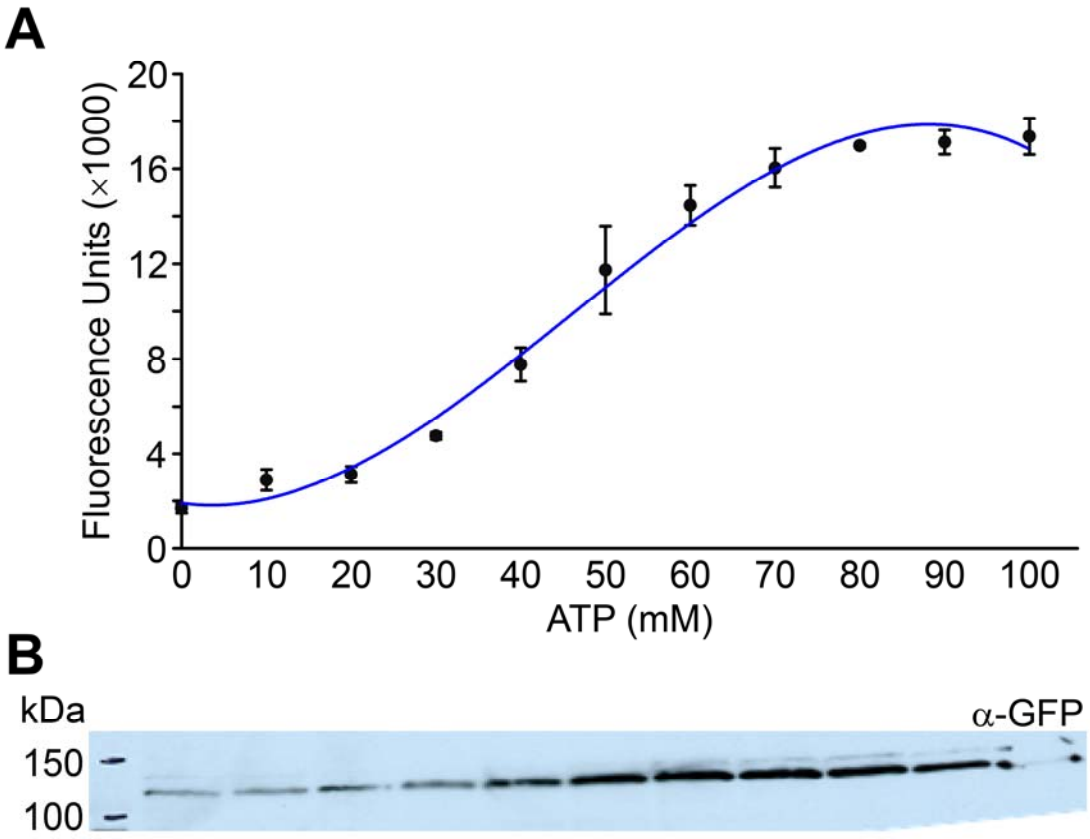

Figure 9: Elution profile of GFP-NS5. Crude HEK293 lysate containing GFP-NS5 was added to ATP resin to isolate purine-binding proteins. Soluble ATP was then added to elute proteins bound to the the resin. Levels of GFP-NS5 in the eluted samples were measured by fluorescence detection (A) and Western blot (B) with α-GFP antibody. The Western blot sample correlates to the fluorescence data point directly above it (0-100 mM ATP). Full length GFP-NS5 protein is approximately 130 kDa. (n=3, SEM)

NS5 is a multifunction viral protein that is required for DENV propagation and, as demonstrated here, is capable of binding immobilized-ATP with high affinity, both in its native form and as a GFP fusion protein. For these reasons, the fusion protein, GFP-NS5, was subsequently screened against a small-molecule library using a fluorescence-based chemoproteomic approach to identify lead compounds for further antiviral testing.

4. A fluorescence-based small-molecule screen identifies novel anti-DENV candidates

The 3,391 member small-molecule library was assembled using compounds purchased from several commercial vendors. The structural attributes of the small molecules were considered in order to avoid chemical liabilities. Chemical liabilities are substructures that have been implicated in a structure-toxicity relationship including moieties that are reactive towards glutathione or proteins, which often correlate with poor clinical outcomes (Park et al., 2011). Another goal in compound selection was to maximize structural diversity. The library screening method measured the ability of the small molecules to disrupt the interaction between GFP-NS5 and immobilized ATP in an ATP-Sepharose resin. To mimic the intracellular environment, ATP-Sepharose resin was added in sufficient quantities so as to mimic physiological concentrations of ATP. Complete details of the method are described in Materials and Methods (Chapter 2).

4.1 Identification of lead compounds that disrupt the binding of GFP-NS5 to immobilized ATP

Clarified lysate from HEK293 cells overexpressing GFP-NS5 was the source of NS5 enzyme used in the assay. The lysate was added to immobilized ATP-Sepharose resin, and small-molecule candidate compounds were tested for their ability to elute GFP-NS5 from the resin. Candidate compounds were tested at a concentration of 500 μM in 5% DMSO in LSWB. Each 96-well sample plate included three control wells: one negative control containing DMSO only, and two positive control samples containing only ATP as a competitor (20 mM ATP, and 60 mM ATP), in the absence of any candidate compound. The negative control provided a background reading, and the positive controls allowed confirmation of GFP-NS5 protein integrity, confirming that GFP-NS5 had bound to the immobilized ATP as anticipated, and that resin-bound GFP-NS5 was capable of being competitively eluted by the soluble substrate, ATP. The data from a given plate would not be considered if the positive control samples did not demonstrate a concentration-dependent increase in fluorescence with increasing concentrations of ATP (from 0 mM ATP to 60 mM ATP). The fluorescence values obtained from each plate were analyzed to identify samples with values greater than 2.5-fold over background (0 mM ATP).

Figure 10 is a heat map displaying the results of the screen. The library consisted of forty-seven 96-well plates containing candidate compounds and controls. In the heat map, each plate is labeled with a heading containing our unique plate identifier. Each

colored square corresponds to one compound in the library, or one control sample. Instead of listing raw fluorescence data, the heat map conveys relative fluorescence within a plate, with high levels of fluorescence being dark red, low levels being dark blue, and the median level being white. Hues within these three color confines represents a fluorescence value between the highest and median value or median value and lowest value. Each plate contained three ATP gradient positive controls (0 mM, 20 mM, and 60 mM) in the first column of each plate, occupying wells F1, G1, and H1, respectively. The remaining wells in the first column (filled in gray) represent wells that were left empty.

Of the 3,391 compounds in the library, 95 compounds (2.8% hit rate) were defined as "lead" compounds if they exhibited fluorescence levels greater than 2.5-fold above background. For example, well C8 in plate number THCB 001020 (top left corner of the heat map) produced a high level of fluorescence and represents a lead compound that was selected for further analysis. In this plate, the positive control well containing 60mM ATP appears a lighter shade of red, because the data from each plate was normalized relative to the most fluorescent well within the plate. The well outlined in black (plate THEN 018020, well E10) corresponds to the lead compound, HS-205020, which ultimately became our final lead anti-DENV compound (Chapter 6).

The 95 samples exhibiting a fluorescence exceeding the 2.5-fold threshold were analyzed by Western blotting using an anti-GFP antibody, as described in Materials and Methods (Chapter 2). Western blotting was performed to determine whether the fluorescence observed in the screening assay was due to the presence of GFP-NS5 protein in the eluate, as opposed to auto-fluorescence of the candidate compound. In the latter case, an auto-fluorescent compound would need to be excluded and not considered for further antiviral testing. Using the Western blot data detecting the presence or absence of eluted GFP-NS5, samples were classified according to their ability to elute GFP-NS5, as indicated by their band densities (absent, weak, or strong). The classification of absent, weak, or strong was made by visual examination of the Western blot film. Figure 11 shows a representative Western blot illustrating samples with absent, weak, and strong band densities. The lane designated as "EN009 F7" (from plate EN009, well F7) represents a typical example of a "strong" eluter. This eluate contains high levels of GFP-NS5, therefore the corresponding compound was considered a strong lead compound. Lane "EN008 G5" shows low levels of GFP-NS5, and is a typical example of "weak" lead compound. "EN008 G4" shows a typical "absent" eluter (absent of any detectable GFP-NS5). Of the 95 initial lead compounds, 50 compounds (53%) were categorized as strong hits, and 23 compounds (24%) were categorized as weak hits. The remaining 22 compounds (23%) were deemed false positives on the basis that, although they exhibited high levels of fluorescence in the small-molecule screen,

they failed to show detectable levels of GFP-NS5 by Western blot. Based on levels of GFP-NS5 detected in eluted samples, the corresponding candidate compounds were designated “strong”, “weak”, or “absent” . Samples absent of GFP-NS5 were not considered for further analysis.

We further narrowed the number of compounds of interest by identifying those that behaved promiscuously within our library. A compound in the library would be categorized as promiscuous if the compound were labeled as a strong eluter of GFP-NS5 in addition to being labeled a strong eluter of a previously screened human protein target As described previously, our library has been screened against a diverse array of purine-utilizing proteins, including several protein kinases (DAPKs and PIMKs), heat shock proteins (Hsp90, TRAP1, Hsp70), and several metabolic enzymes (Fatty acid synthase and Acetyl CoA carboxylase) (Carlson et al., 2013). Therefore, we utilized this information to determine whether any of the 50 strong hits in our GFP-NS5 experiments were also likely to target other purine-utilizing proteins. After eliminating the more promiscuous compounds that were strong eluters of GFP-NS5 and one or more other screened purine-utilizing proteins, we were able to narrow down the number of specific, unique hits to 18 compounds (<0.5% of the entire library). Unfortunately, upon reordering 10 mg of the compounds from the original vendors, only 16 of these compounds could be acquired.

To further prioritize our collection of 16 lead compounds we first sorted them based on their ability to elute GFP-NS5 from the immobilized-ATP resin in a dose-dependent manner. Similar to the experimental design for the small-molecule library screen as described in Materials and Methods (Chapter 2), clarified lysate containing GFP-NS5 was incubated with the immobilized-ATP resin. Following 3 resin-bed washes, the 1:1 (resin: LSWB) slurry was aliquoted into 96-well PVDF filter plates. The 16 lead compounds were added to the slurry at 10 μM, 100 μM, 500 μM, 1000 μM concentrations. Only six of the 16 compounds resulted in an increasing GFP fluorescence trend with increased compound concentration. Therefore, only six compounds were considered for *in vitro* anti-DENV assays.

Six of the compounds were then tested using *in vitro* anti-DENV assays, including the flow cytometry-based percent infection assay and focus-forming unit assay and viability assays, including fixable viability staining and resazurin cell viability assay. Based on the combined results of the anti-DENV assays and viability assays, one compound, HS-205020, showed high levels of antiviral activity as determined by reduction in both DENV percent infection and viral titer, and low cytotoxicity using two viability assays. We therefore selected HS-205020 to perform further studies. A summary outlining the progression from the initial 3,391 compounds, to the 6 compounds tested in anti-DENV assays, and ultimately to one single anti-DENV (NS5) compound, is shown in Figure 12.

The 6 lead compounds were subsequently tested in a variety of anti-DENV cell-based assays, virological tests, and anti-HCV assays to compare broad anti-*Flaviviridae* activity (as described in Chapter 5).

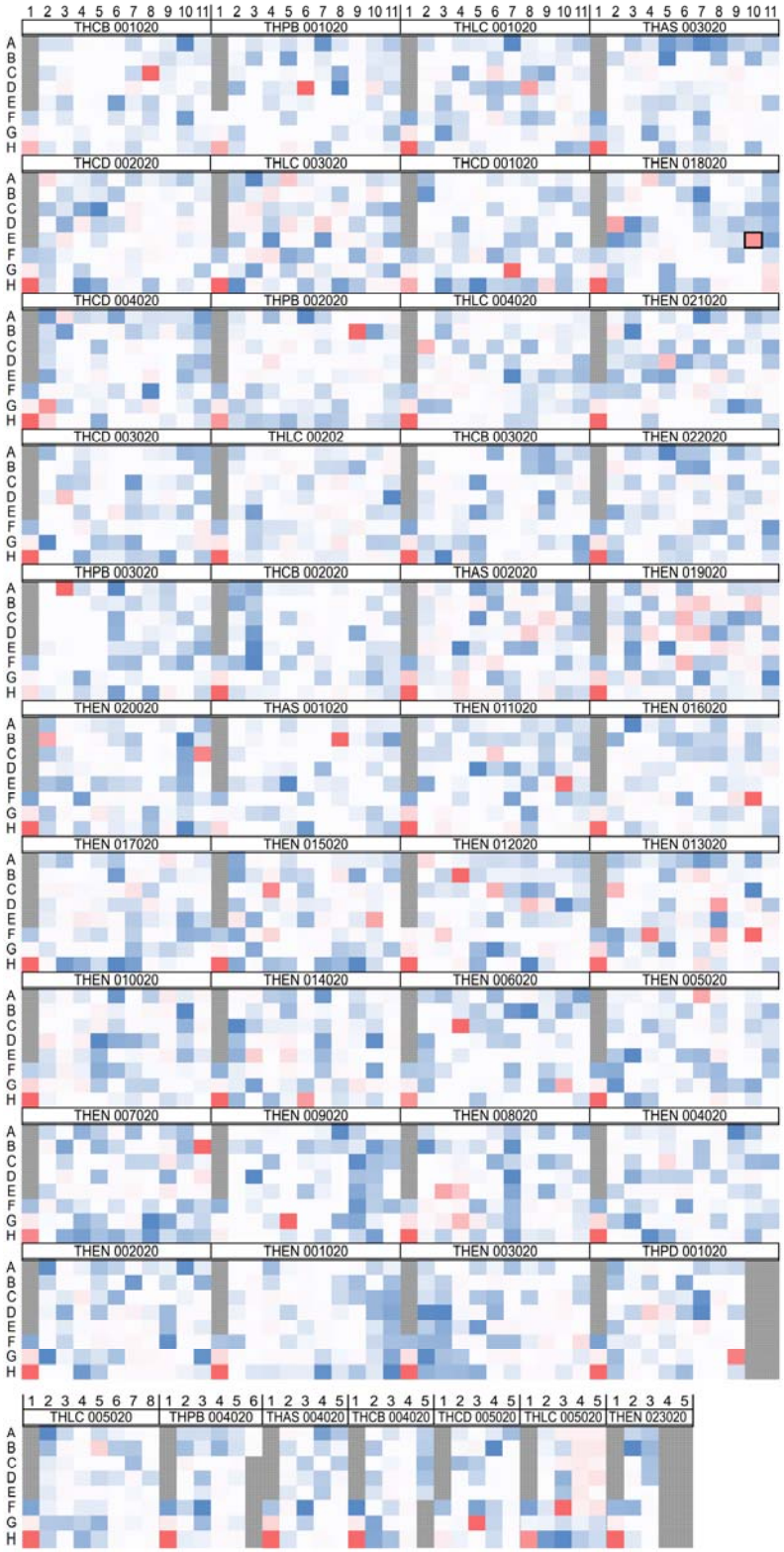
THCB 001020
THPB 001020
THLC 001020
THAS 003020
THCD 002020
THLC 003020
THCD 001020
THEN 018020
THCD 004020
THPB 002020
THLC 004020
THEN 021020
THCD 003020
THLC 00202
THCB 003020
THEN 022020
THPB 003020
THCB 002020
THAS 002020
THEN 019020
THEN 020020
THAS 001020
THEN 011020
THEN 016020
THEN 017020
THEN 015020
THEN 012020
THEN 013020
THEN 010020
THEN 014020
THEN 006020
THEN 005020
THEN 007020
THEN 009020
THEN 008020
THEN 004020
THEN 002020
THEN 001020
THEN 003020
THPD 001020
THLC 005020
THPB 004020
THAS 004020
THCB 004020
THCD 005020
THLC 005020
THEN 023020

Figure 10: Heat map displaying hits from the library screen against GFP-NS5. The library consisted of 47 96-well plates containing compounds. In the heat map, each plate is labeled with a heading containing our unique plate identifier. Instead of listing raw fluorescence data, the heat map conveys relative fluorescence within a plate, with high levels of fluorescence being dark red, low levels being dark blue, and the median level being white. Hues within these three color confines represent a fluorescence value between the highest and median value or median value and lowest value. Each plate had three positive control wells containing increased concentrations of soluble ATP (0 mM, 20 mM, and 60 mM) in the absence of test compound (wells F1, G1, and H1, respectively). The well shown with a black border corresponds to the lead compound, HS-205020. Wells shown in gray are empty.

Ladder (kDa)	EN 008 G5	EN 008 E4	EN 008 G4	EN 008 E3	EN 009 G5	EN 009 F8	EN 009 F7	EN 009 A10	LC 005 F3	SP 001 B5	EN 011 C6	EN 011 E10	EN 012 C6	EN 012 D8	EN 012 B4	EN 013 B7	60 mM ATP

Figure 11: Representative GFP-NS5 Western blot showing eluted samples from the small-molecule screen. The lane designated as "EN009 F7" (from plate EN009, well F7) represents a typical example of a "strong" eluter. This eluate contains high levels of GFP-NS5, therefore the corresponding compound was considered a strong lead compound. Lane "EN008 G5" shows lower levels of GFP-NS5, and is a typical example of "weak" lead compound. "EN008 G4" shows a typical "absent" eluter (no detectable GFP-NS5).

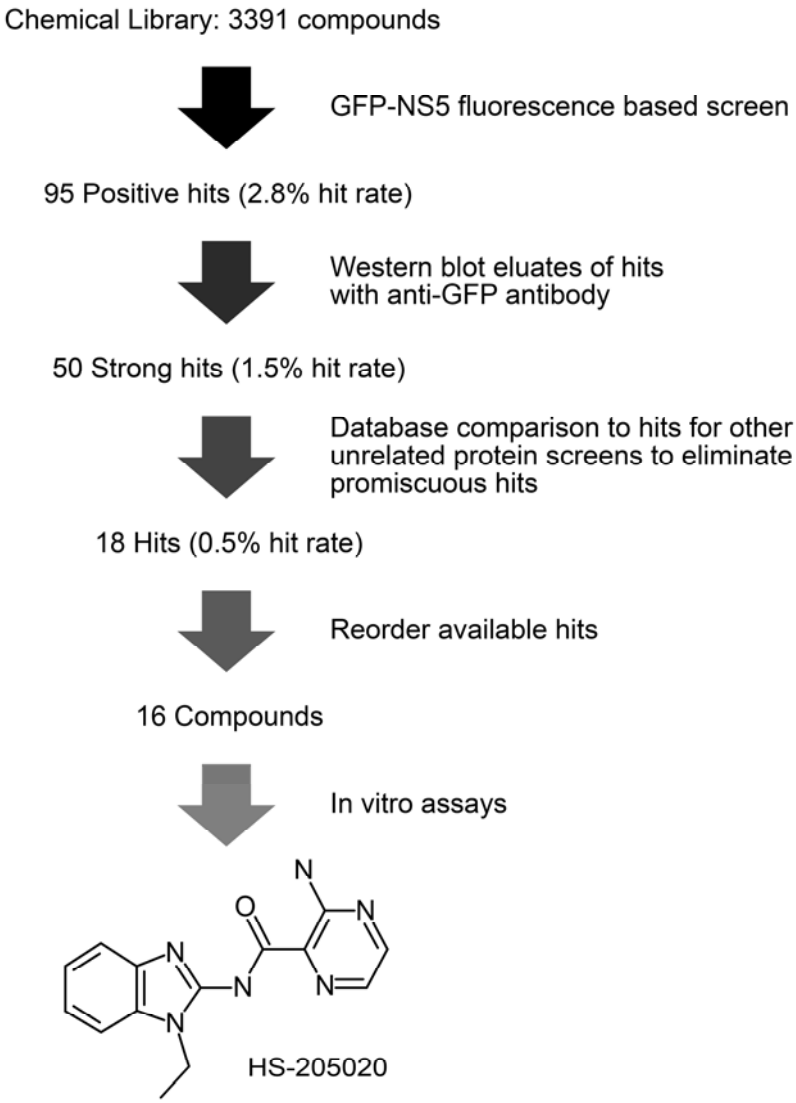

Figure 12: Flow chart summarizing the progression from 3,391 anti-DENV2 candidate compounds to one lead compound to be used in further analysis. The small-molecule library consisted of 3,391 candidate compounds, of which 95 were selected as lead compounds based on fluorescence signal in the small-molecule screening assay. Of those 95 lead compounds, only 50 were considered to be strong eluters of GFP-NS5, based on the Western-blot data showing high levels of GFP-NS5 protein in the corresponding eluates. A database search confirmed that 18 compounds were unique lead compounds for GFP-NS5 (showing no overlap with the unrelated proteins detected in previous screens). After subsequent anti-DENV assays measuring antiviral activity and cell toxicity, one lead compound (HS-205020) was chosen on the basis of its strong anti-DENV activity and minimal cell toxicity *in vitro*.

5. *In vitro* DENV antiviral assays

DENV antiviral assays were used to determine whether any of the six lead compounds we selected (as described in Chapter 4) exhibited anti-DENV activity. Figure 13 shows the molecular structure of the six lead compounds.

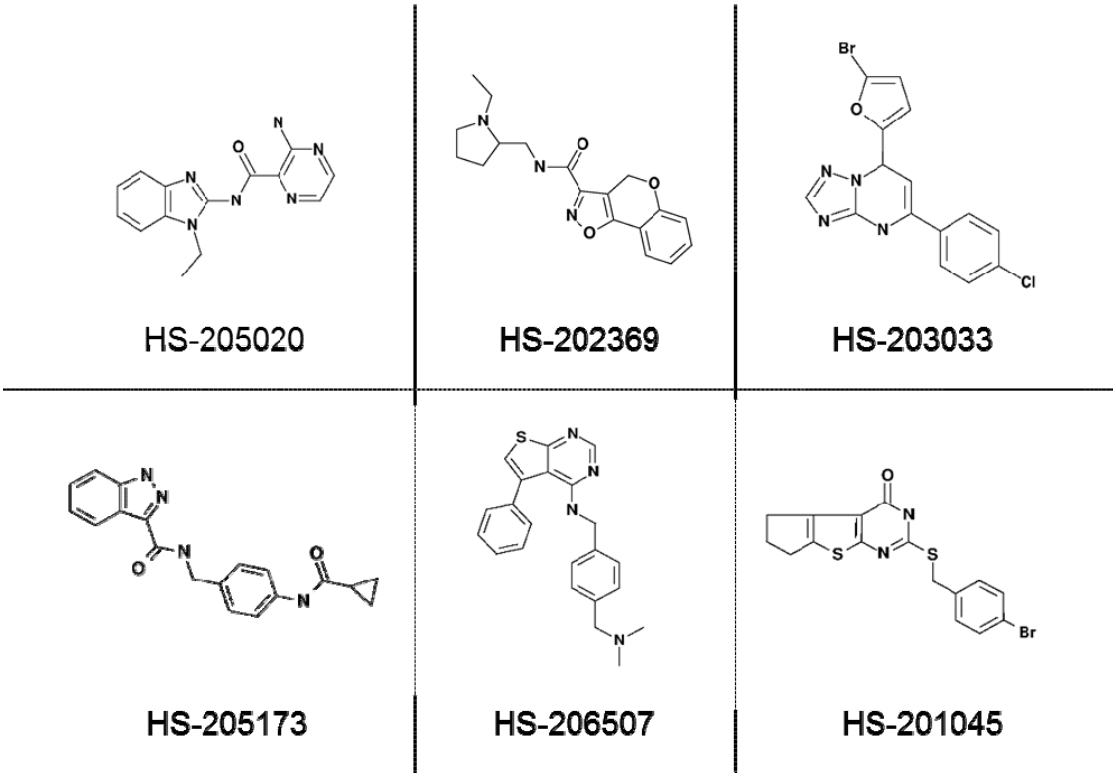

Figure 13: Molecular structures of the six lead compounds. These compounds were identified using a fluorescence-based small-molecule purinomics screen (Chapter 4) to identify drug candidates capable of interfering with the purine-binding activity of DENV NS5 protein. The progression from 3, 391 compounds to the six lead compounds was accomplished by screening against GFP-NS5 fusion protein reversibly bound to immobilized-ATP resin, followed by Western blot analysis confirming elution of GFP-NS5, and finally, concentration-dependent elutions of GFP-NS5 from immobilized-ATP resin using the candidate compounds.

The previous experiments (Chapter 4) utilized a small-molecule purinomic screening assay to identify potential candidates for anti-DENV drug therapies. Starting from a library of 3,391 compounds, the number of drug candidates was narrowed down to 6 lead compounds. This was accomplished by screening against GFP-NS5 fusion protein reversibly bound to immobilized-ATP resin, followed by Western blot analysis confirming elution of GFP-NS5, and finally, concentration-dependent elutions of GFP-NS5 from immobilized-ATP resin using the candidate compounds.

Next, it was necessary to determine which, if any, of the 6 lead compounds exhibited anti-DENV effects *in vitro* in cultured human cells, and whether any of the compounds exhibited cytotoxicity independent of viral infection. Thus, to further narrow the number of lead compounds and select a single lead compound to investigate further, we measured the effects of each compound on the reduction of percent DENV infection as well as infectious virus output. In addition, we evaluated any potential effects of the compounds on cell viability using an independent cytoxicity assay in non-infected cells. Based on the results of the anti-viral and cytotoxicity studies, we selected a single lead compound (HS-205020) for further investigation. This final lead compound was also tested against Hepatitis C virus (HCV) in a cell-based infection assay to observe for any broad anti-*Flaviviridae* activity.

5.1 Flow cytometric anti-DENV assay

To evaluate the anti-DENV properties of the 6 lead compounds, in vitro assays were performed utilizing flow cytometric analysis to measure percent DENV infection as well as cell viability. First, assay conditions were optimized as described in Section 2.2.6.1. Next, the assay was used to determine whether any of the lead compounds was able to reduce the percent infection of DENV-infected human monocytes (U937+DC-SIGN cells). The complete details of the assay are described in Materials and Methods (Chapter 2).

Briefly, cells were pre-treated for 1 hour with each of the 6 lead compounds at concentrations ranging from 0.5 μM to 100 μM. Each experiment included a negative control using DMSO alone, and a positive control using the compound C75. C75 is a FAS inhibitor that has been shown to inhibit DENV infection *in vitro* (Heaton et al., 2010). Following the pre-treatment, medium containing the compound was removed, and cells were then infected with DENV2-NGC at an MOI of 1. After a 1-hour incubation, the virus-containing medium was collected for subsequent analysis of viral titer (described in Section 5.2) and was replaced with medium containing the lead compounds at the same concentration as the pre-treatment, and incubation continued for 48 hours. Cells were then harvested and stained with a fixable cell viability stain (fixable 780 nm dye stain) to irreversibly label dead cells. After being fixed and permeabilized, cells were immunofluorescently labeled using a primary antibody targeting the DENV envelope

protein (E protein), followed by a secondary antibody tagged with Alexa Fluor 488. Cells were then subjected to flow cytometric analysis to simultaneously determine cell viability and percent DENV infection.

Figure 14 shows the DENV-infected and mock-infected cell controls within the gated flow cytometry plot and the percent DENV infection and cell viability results for each compound. The viability dye stains only those cells with a breach in membrane integrity, regardless of DENV-infection, and those cells were classified as nonviable. The immunofluorescent label targeted against the DENV envelope protein detects infected cells, regardless of cell viability. Therefore, cells fell into one of the following 4 categories (Fig. 15): uninfected viable (indicated in blue), infected viable (green), uninfected nonviable (red), and infected nonviable (black). Based on these endpoints, an "ideal" candidate compound, exhibiting high anti-viral properties and low cytotoxic effects, would produce an increase in the number of uninfected viable cells, along with a decrease in both infected cell types (viable/nonviable), and little or no increase in uninfected nonviable cells. In contrast, a non-ideal compound might show high anti-viral activity but also high cytotoxicity, resulting in a decrease the levels of infected cells but an increase in uninfected viable cells.

Only those compounds exhibiting significant antiviral properties and minimal cytotoxicity would be considered for further analysis. As shown in Figure 15, compounds HS-206507, HS-205020, and HS-203033 (Fig. 15B, E, and G), produced an

increase in uninfected viable cells (blue) as well as decrease in infected viable cells (green) from 0.5 μM to 100 μM compound concentration, indicating antiviral activity. Significant antiviral activity was defined as a greater than 50% reduction in infected viable cells without a concomitant increase of greater than 30% in the sum of the two nonviable subpopulations [uninfected nonviable cells (gray) and infected nonviable cells (red)] from 0.5 μM to 100 μM compound concentration.

In addition, these 3 antiviral compounds showed minimal cytotoxicity, in that they did not significantly increase, by 30% of greater, the percentage of the sum of both infected nonviable cells (red) and uninfected nonviable cells (black) compared to the DMSO vehicle control.

Compound HS-201045 (Fig. 15A) did not demonstrate antiviral activity, as shown by a minimal decrease in infected viable cells between 0.5 μM and 100 μM compound (19% decrease). In addition, HS-201045 showed significant cytotoxicity, as evidenced by the 46% increase in total nonviable cells. Two other lead compounds, HS-205173 and HS-202369 (Fig. 15C, F) did reduce the percent infection (96 % and 48%, respectively), but they did not do so without causing simultaneous significant increases in cytotoxicity (33% and 55%, respectively). The results of these studies showed that 3 compounds, HS-206507, HS-205020, and HS-203033 (Fig. 15B, E, and G), showed significant antiviral activity with percent infection reductions of 96%, 54%, and 73%, respectively, and exhibited minimal cytotoxicity of less than 30%. Therefore, these

compounds were studied in additional DENV assays to determine the best-performing hit.

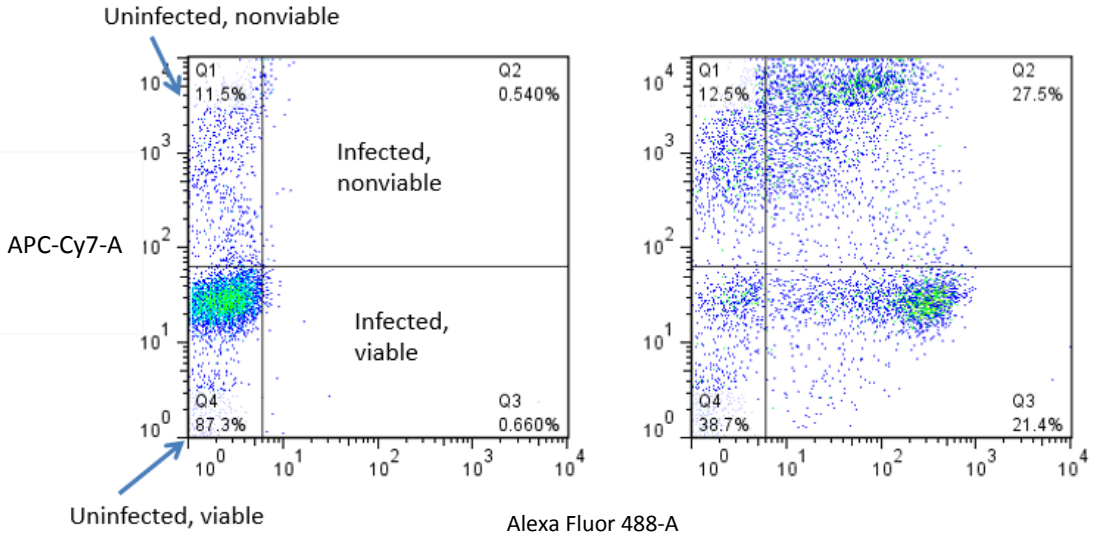

Figure 14: DENV- and mock-infected cell controls for the 48 h DENV compound screen. The four quandrants, or categories are confirmed by analyzing the DENV-infected cells and mock-infected cells. The mock-infected cells (left plot) shows a negligible cell population in the two infected quadrants and the DENV-infected cells (right plot) has a subpopulation of cells that are positive for the DENV stain.

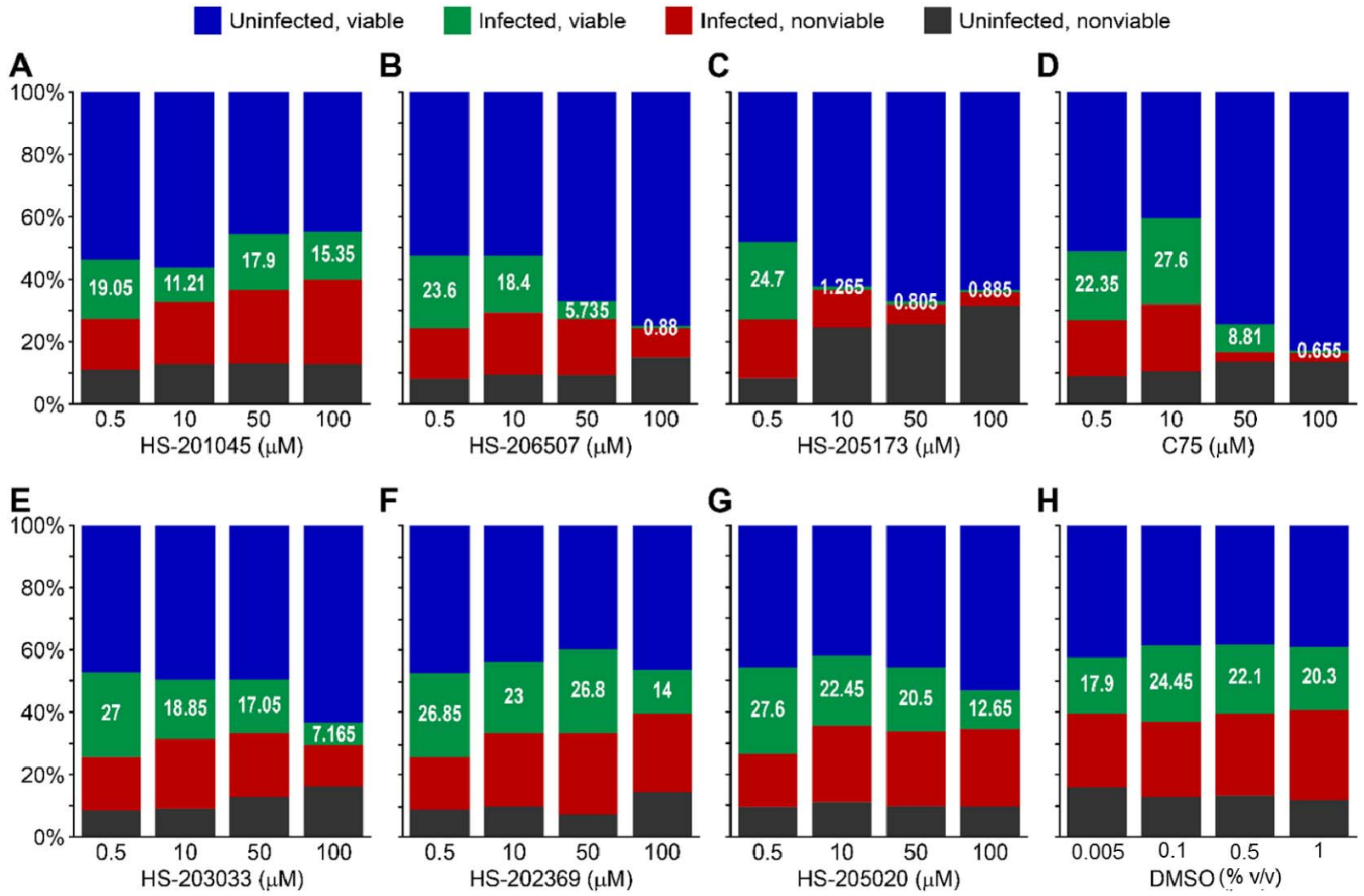
Uninfected, viable
Infected, viable
Infected, nonviable
Uninfected, nonviable
A
B
C
D
100%
80%
60%
40%
20%
0%
19.05
11.21
17.9
15.35
23.6
18.4
5.735
0.88
24.7
1.265
0.805
0.885
22.35
27.6
8.81
0.655
0.5
10
50
100
HS-201045 (μM)
HS-206507 (μM)
HS-205173 (μM)
C75 (μM)
E
F
G
H
27
18.85
17.05
7.165
26.85
23
26.8
14
27.6
22.45
20.5
12.65
17.9
24.45
22.1
20.3
HS-203033 (μM)
HS-202369 (μM)
HS-205020 (μM)
0.005
0.1
0.5
1
DMSO (% v/v)

Figure 15: Flow cytometric analysis of reduction in percent infection with lead compounds. Cells were pre-treated with lead compounds at 0.5 μM, 10 μM, 50 μM, and 100 μM, or comparable volumes of DMSO vehicle (negative control). The positive control was the compound C75, which is a FAS inhibitor that has been shown to inhibit DENV. Antibody targeted against DENV E protein was used to monitor percent infection, and fixable viability stain was used to simultaneously monitor cell viability. Only HS-206507, HS-203033, and HS-205020 significantly decreased the percent infection without increasing the nonviable cells by 50% or greater.

5.2 Quantifying the titer of infectious DENV using a focus-forming unit assay

In the previous experiments, anti-DENV properties of the six lead compounds were evaluated using flow cytometric analysis (Fig. 15) to evaluate DENV antiviral activity, as well as cytotoxicity. Three of the compounds, HS-206507, HS-205020, and HS-203033 (Fig. 15B, E, and G), showed significant antiviral activity and minimal cytotoxicity. These compounds were chosen for further analysis to quantify their DENV anti-viral properties, including their effect on levels of infectious DENV virus produced and released by infected cells.

Two of the most powerful assays in the virology field are the plaque assay and the focus-forming unit assay (FFA), both of which are used to determine viral titer. Both of these assays are used to quantify the titer of infectious virus per milliliter by infecting host-cell monolayers with various dilutions of a virus sample and incubating the cells under a semisolid overlay medium, which restricts the spread of infectious virus between host cells in the monolayer. The plaque assay depends on the ability of the virus to lyse the host cells in order to form visible plaques. However, cell lysis does not occur with all classes of viruses, as is the case with some strains of DENV (Lambeth et al., 2005). The focus-forming unit assay (FFA) addresses this limitation of the plaque assay, as it does not depend on cell lysis in order to quantify viral titers. Instead, the FFA utilizes fluorescently labeled antibodies directed against a viral antigen to detect the viral antigen within cells exposed to viral inoculum. Due to the semisolid overlay

medium (typically tragacanth gum), infectious virus is unable to spread throughout the culture to re-infect cells across the entire monolayer. This results in the formation of discrete foci, or clusters formed by infectious virus and locally infected cells. Following an incubation period to allow infection and formation of foci, the overlay medium is removed, and the cell monolayers are subsequently probed with fluorescently labeled antibodies against a viral antigen. Fluorescence microscopy is then used to count and quantify the number of foci within the monolayer. The results of the FFA are expressed as focus-forming units per milliliter of inoculum (FFU/mL).

An advantage of the FFA over the percent infection assay is that the FFA exclusively identifies the titer of infectious virus. Although both the FFA and percent infection assays use immunofluorescence directed against a viral antigen, the FFA measures the viral antigen output only after using the cell culture media to re-infect newly seeded DENV-permissive cells. Therefore, only virus capable of infecting these cells will be detected. In the percent infection assay, the viral antigen can be present in a cell and never be incorporated in a released, infectious mature virion. Examples include viral binding or entry without uncoating and an inability of the cell to assemble progeny virions. Both of these scenarios would result in a positive immunofluorescence signal corresponding to the presence of the viral antigen, despite the cell not producing infectious virus.

To determine the effect of each compound on the release of infectious virus from cells, the virus-containing medium (inoculum) from the previous flow cytometry experiments (Section 5.1) was collected and reserved for subsequent analysis by focus-forming unit assay. The inocula from samples treated with the three lead compounds, HS-206507, HS-205020, and HS-203033, were serially diluted and used to quantify infectious virus released from the U937+DC-SIGN cells after treatment with each concentration of the experimental compounds. Experimental details for the focus-forming assay are described in detail in Materials and Methods (Chapter 2). After immunostaining for the presence of DENV envelope protein (E protein), the foci were counted, and viral titers were calculated. Viral titers in units of FFU/mL are determined by dividing the number of foci counted by the volume of the starting or original inoculum, accounting for any dilutions of the inoculum if performed.

Figure 16 shows the results of the focus-forming unit assay. The cell culture media from each compound treated monocytic cell sample in the flow cytometry-based percent infection assay was collected and analyzed in the FFA. In the flow cytometry-based percent infection assay, monocytic cells were incubated in antibodies directed against the viral antigen, DENV envelope protein, followed by a secondary antibody conjugated to the fluorescent tag, Alexa Fluor 488. Analysis of the immunostained monocytic cells using flow cytometry determined the percent infection and viability of each compound-treated sample. Three compounds, HS-206507, HS-205020, and HS-

203033 (Fig. 15B, E, and G), showed significant antiviral activity at a concentration of 100 μM with percent infection reductions of 96%, 54%, and 73%, respectively, and exhibited minimal cytotoxicity of less than 30% in the flow cytometry-based percent infection assay. The cell culture media from the sample wells corresponding to treatment with high concentrations (50 μM and 100 μM) of the three compounds of interest, HS-206507, HS-205020, and HS-203033. One negative, untreated control was the cell culture media from monocytic cells that were not treated with any compound, but were infected in an identical manner to the compound treated monocytic cells with DENV2-NGC. A second negative control consisted of DENV-infected monocytic cells treated only with the DMSO vehicle. Two compounds, ribavirin and C75, a GTP analog and FAS inhibitor, have both been shown in previous studies to reduce DENV infection *in vitro* (McDowell et al., 2010, Heaton et al., 2010). Cell culture media collected from DENV-infected monocytic cells treated with 50 μM and 100 μM of ribavirin and C75.

Of all the compounds tested, HS-206507 yielded the lowest reduction in viral titer (1.7 fold at 50 μM, and 2 fold at 100 μM; $p < 0.05$), even though it had produced a significant reduction in the percent infection (96% at 100 μM; $p < 0.03$) in the previous experiment (Fig. 15B). On the other hand, HS-205020 demonstrated the greatest reduction in infectious virus (FFU/mL) compared to the DMSO negative control (47 fold at 50 μM, and 121 fold at 100 μM; $p < 0.03$). Notably, these reductions in viral titer were

also greater than those observed for either of the two positive controls, C75 and ribavirin (Fig. 16).

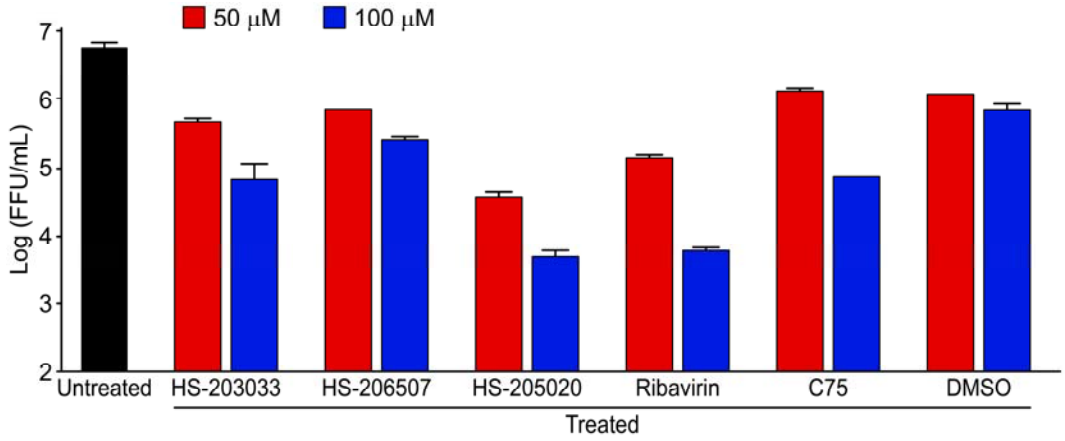

Figure 16: Focus-forming assay to determine production of infectious virus in the presence of candidate compounds. The compound-containing media from the previous DENV percent infection flow cytometry based assay (Fig. 15) were used in the FFA in triplicate. HS-205020 demonstrated a significant reduction in FFU/mL compared with the DMSO negative control (47- fold and 121- fold at 50 μM and 100 μM, respectively), and also resulted in a lower viral titer than the positive controls, ribavirin and C75. (n=3, SEM)

5.3 Independent viability assay to determine cytotoxicity of lead compounds in the absence of DENV

To further evaluate whether any of the lead compounds exhibited cytotoxic properties, their effect on cell viability was analyzed using the "resazurin assay" in the absence of DENV infection. Resazurin is a blue nonfluorescent reagent that is reduced by metabolic processes in viable cells to produce resorufin, which is highly fluorescent. The conversion only occurs in viable cells; therefore the amount of resorufin produced is proportional to the number of viable cells in the culture.

The resazurin assay was performed using the three lead compounds that had significantly reduced the percent DENV infection in U937+DC-SIGN cells in previous experiments (Fig. 15B, E, G): HS-203033, HS-205020, and HS-206507. Non-infected U937+DC-SIGN cells were exposed to multiple concentrations each of each compound for 24 hours. DMSO was used as a negative control, and a marketed antiviral drug, ribavirin, was used as a positive control. Ribavirin is an FDA approved therapeutic for Hepatitis C Virus (HCV), and has therefore been evaluated extensively for potential cytotoxic effects. After the 24-hour incubation with candidate compounds or controls, resazurin compound was added, and the resulting fluorescence was used to calculate the percent of viable cells relative to DMSO controls (Fig. 17). As shown, HS-203033 exhibited the smallest effect on cell viability, indicating minimal cytotoxicity. HS-205020 also showed comparatively low levels of cytotoxicity. At the highest concentration (100

μM), HS-205020 produced a reduction in viability of no more than 20% relative to control. In contrast, HS-206507 showed significant reductions in cell viability, and was determined to be cytotoxic in the resazurin assay At all concentrations tested, the effect on cell viability of both HS-203033 and HS-205020 were comparable to (within 5-10%), if not lower than, that observed with ribavirin.

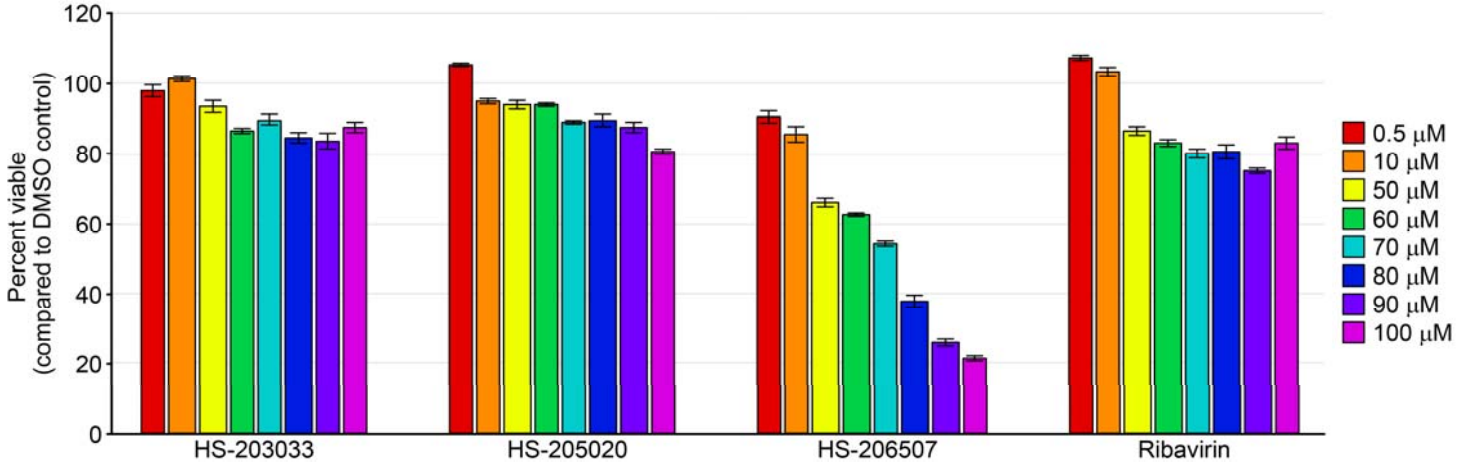

Figure 17: Resazurin viability assay. Non-infected U937+DC-SIGN cells were plated in 96-well plates and treated with compounds at the concentrations indicated. After a 24-hour exposure to the compound, resazurin was added to each well. The resulting fluorescence was measured and used to determine the percentage of viable cells relative to DMSO controls. The results show that the viability of cells treated with HS-203033 or HS-205020 was comparable to those treated with the drug ribavirin. (n=3, SEM)

5.4 Determination of EC_{50} for top 3 lead compounds in a cell-based flaviviral immunodetection (CFI) assay

Each of the three lead compounds resulted in a reduction in the percentage of U937+ DC-SIGN cells infected with DENV2-NGC (Fig. 15). Therefore, to further distinguish between their anti-viral properties, the compounds were evaluated using another established antiviral assay, the cell-based flaviviral immunodetection (CFI) assay. The CFI assay is very similar in set-up to the percent infection assay (Chapter 5.1). A highly DENV permissive cell line, BHK-21, was used to measure antiviral effects upon concomitant compound treatment and viral infection. Following a 1 hour incubation in both compound and DENV, the cells were washed to remove excess extracellular virus, and compound-containing media at identical concentrations was re-added. After a 48 hour incubation post-infection, the cells were subjected to immunofluorescence staining to detect the viral antigen, envelope protein as described in Methods and Materials (Chapter 2).

From the CFI assay, a plot was derived displaying the percent infection or cell number versus the log of the compound concentration. The cell number provides a readout as to approximate cell viability because BHK-21 cells, when healthy, are adherent while nonviable cells will likely detach from the plate. To determine the EC_{50}, nonlinear regression was fitted to the plot of percent infection vs. log of compound concentration and an EC_{50} for each compound was calculated using GraphPad software as previously described (Rathore et al., 2011). The EC_{50} is effective concentration of a

compound where 50% of its maximum effect is observed. The lower the EC_{50} value, the more potent the compound is in lowering the percent infection of DENV in BHK-21 cells. However, it is imperative to also consider viability measurements in coordination with EC_{50} determinations to avoid a viability issue (dead cell with lack of viral antigen) from being mistakenly labeled as an uninfected cell that would contribute to a lower EC_{50} evaluation.

A desired outcome would look similar to that plot for the positive control, celgosivir (Fig.18B). There you see a decrease in the percent infection with increasing compound concentration (black line). Interpolating the EC_{50}, point at which the percent infection is half maximal, or half of the percent infection at 0 μM or lowest micromolar concentration tested will approximate relative potencies of the lead compounds. HS-203033 did not cause a significant effect on percent infection. The calculated EC_{50} values for celgosivir, HS-206507, and HS-205020 were 0.1304 μM, 10.27 μM, and 55.65 μM, respectively. Although, HS-206507 treatment exhibited a lower EC_{50} value in BHK-21 cells, there was concern over viability of the cells.

As an example, consider the compound concentration of 100 μM (2.0 on the log scale). At 100 μM of HS-206507, the percent infection of cells was negligible, which would be promising if the cell number had not reduced significantly as well (3,500 cells). On the other hand, at 100 μM of HS-205020, the percent infection of cells was less than 5%, and the cell number remained high (11,000 cells).

HS-203033 failed to show any reduction in percent infection that could be differentiated from a cytotoxic effect, given that the curves nearly mirror each other (Fig. 18C). Although HS-206507 had the most potent EC_{50} (10.27 μM), the cell number curve overlapped with the percent reduction in infected cells, suggesting a cytotoxic effect (Fig. 18E). HS-205020, exhibited a calculated EC_{50} of 55.65 μM, with a decent separation between the percent infection curve and the cell number curve, indicating minimal cytotoxicity (Fig. 18D).

In these experiments, HS-205020 showed an anti-DENV effect as measured by percent DENV infection in BHK-21 cells. Importantly, in the previous experiments (Chapter 5.2) using U937+DC-SIGN cells, the HS-205020 compound had also demonstrated the greatest inhibition in production of infectious virus compared with the DMSO control (121 fold; $p < 0.03$) (Fig. 16). In all experiments evaluating cytotoxicity of the lead compounds (Fig 15, 17, and 18), HS-205020 showed minimal cytotoxicity, equal to or less than that of an existing FDA approved antiviral (Fig 17). Based on the combined results of these studies, we selected HS-205020 as the lead compound to be evaluated in subsequent experiments.

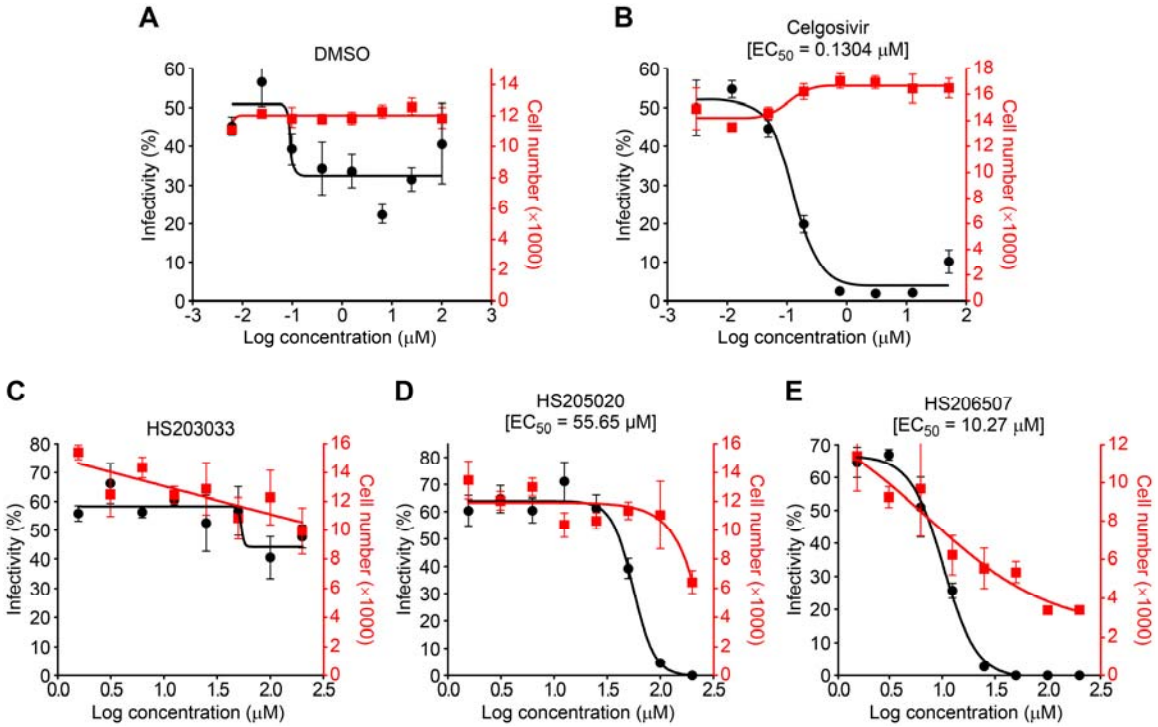

Figure 18: Cell-based *Flavivirus* immunodetection assay. BHK-21 cells were infected with DENV2-TSV01 in the presence of the screen hits. After infection, the compounds remained in the culture media. The viability was measured by cell number (red line) and percent infection (black line) by immunofluorescence as described (E-protein antibody, 4G2). (A) DMSO control. (B) The positive control, celgosivir, strongly inhibited DENV propagation. (C) HS-203033 was ineffective at reducing the percent infection in these cells. (D-E) The close proximity between the viability curve and percent infection for HS-206507 made this compound a lower priority than HS-205020 (EC_{50} = 55.65 μM) (n=3, SEM) Courtesy of Subhash Vasudevan, Duke-NUS

6. HS-205020 preferentially binds the RNA-dependent RNA polymerase (RdRp) of DENV and reduces enzymatic activity *in vitro*

HS-205020 was identified in the small-molecule screen because of its ability to elute GFP-NS5 from an immobilized-ATP resin (Chapter 4). Additionally, we have shown that HS-205020 is an anti-DENV agent. Treatment of DENV-infected U937+DC-SIGN cells with 100 μM HS-205020 resulted in a 50% reduction in the percent infection and a 2-fold log decrease in levels of infectious virus (Chapter 5). However, this data does not shed light onto the precise mechanism of action of this compound.

NS5 has two distinct purine-dependent enzymatic domains: a methyltransferase domain (AA 1-319) and a polymerase domain (AA 406-900). HS-205020 could be directly binding to and inhibiting the methyltransferase domain, the polymerase domain, or both domains simultaneously. Alternatively, the compound could be interacting allosterically with NS5, resulting in a conformational change in the protein, thereby disrupting enzymatic activity indirectly. It is also possible that HS-205020 could be acting independently of NS5 altogether, and that the observed elution of GFP-NS5 by the compound may have been coincidental. In order to explore the precise mechanism(s) of the antiviral activity of HS-205020 produces its antiviral effects, two truncated forms of the protein were generated, each containing only one of the enzymatic domains. The truncated enzymes, along with full-length NS5, were then evaluated in the presence of HS-205020.

6.1 Elution profiles of NS5 methyltransferase and polymerase domains

NS5 has two distinct domains that utilize purines to carry out their enzymatic functions. The methyltransferase domain of DENV (AA 1-319) contains a GTP-binding site that may be involved in formation of the methyl cap of viral RNA, and the polymerase domain of DENV (AA 406-900) requires nucleotides to be positioned in the active site to carry out viral RNA synthesis. Because both domains contain nucleotide-binding pockets, we sought to determine which domain (or domains) HS-205020 might be targeting. Two truncated GFP-NS5 constructs were generated, AA 1-319 and AA 406-900, each containing only one of the NS5 enzymatic domains (methyltransferase domain and polymerase domain, respectively). The truncated GFP fusion proteins were overexpressed in HEK293 cells, and equal levels of protein were bound to immobilized-ATP resin using the same method described in earlier experiments. Each fusion protein, as well as full-length GFP-NS5, was then tested for its ability to be eluted by the HS-205020 compound or soluble ATP. The ATP and HS-205020 elution profiles for both domains were compared to full-length GFP-NS5 (Fig. 19)

Figure 19A (left graph) shows that the two truncated GFP-NS5 proteins (AA 1-319 and AA 406-900) were eluted by soluble ATP in a concentration-dependent manner, with both proteins showing comparable elution profiles. At 100 μM ATP, levels of either eluted protein were significantly increased, nearly 3-fold greater than the control (LSWB). ATP was able to elute full-length GFP-NS5 protein with the greatest efficiency,

at nearly twice the level (6-fold greater than the control) of that observed with either of the fusion proteins at 100 μM ATP.

The elution profiles of the truncated and full-length proteins were then evaluated using increasing concentrations of HS-205020 (Fig. 19A, right graph). Interestingly, out of the three proteins, the truncated protein containing the polymerase domain, GFP-NS5 (AA 406-900), was the most sensitive to elution by HS-205020. Approximately 3-fold more GFP-NS5 (AA 406-900) protein was eluted with 500 μM of compound, relative to the control. At the same concentration of HS-205020, levels of eluted full-length GFP-NS5 and truncated GFP-NS5 (AA 1-319) were only 2-fold over the control. For all three proteins, the increase in fluorescence from 0 μM to 500 μM HS-205020 was statistically significant ($p < 0.02$). These results strongly suggest that HS-205020 preferentially binds to the polymerase domain of NS5.

The eluted fractions were analyzed by Western blot to confirm that the fluorescence data used to generate the elution profiles was indeed due to the presence of the GFP fusion protein in the eluate (Fig. 19B; left and right blots). The control samples (LSWB vehicle alone) are shown in lane 1 of each blot. The remaining lanes in each blot correspond to concentrations of ATP or HS-205020 indicated in the graphs. The data confirmed that increasing levels of fluorescence units corresponded to increasing levels of GFP protein at the appropriate expected molecular weight.

The samples from the elution studies (Fig. 19C) were further analyzed to quantify of the levels of protein that did not bind to the immobilized-ATP resin initially (non-binding) or was retained on the resin after elution with the highest concentration of compound (100 mM for ATP, and 500 μM for HS-205020), track the "fate" of the entire sample added the resin. Data was expressed as a percentage of the total amount of protein added to the resin. Full-length GFP-NS5 showed the highest affinity for soluble ATP and immobilized ATP as well. Nearly 81% of full-length protein was eluted with 100 mM soluble ATP, compared to 43% and 40% of the AA 1-319 and AA 406-900 truncated proteins, respectively. Only 9-12% of the full-length protein failed to bind immobilized ATP (non-binding) when samples were initially added to the resin, compared to 20% to 26% of the AA 1-319 and AA 406-900 truncated protein samples. The results also confirm that both of the truncated proteins showed similar affinity to the immobilized-ATP resin itself, as evidenced by comparable levels of non-binding protein (Fig. 19C).

The data from Fig. 19A (right graph) had also shown that, of all the three proteins, GFP-NS5 (AA 406-900) was the most sensitive to elution by HS-205020. When expressed as a percentage of total protein as (Fig. 19C), 500 μM HS-205020 was able to elute approximately 48% of GFP-NS5 (AA 406-900) bound on the ATP resin, whereas only approximately 20% of the other two proteins (full-length protein and AA

1-319) was eluted. This further supports the idea that HS-205020 may selectively target the polymerase domain of NS5.

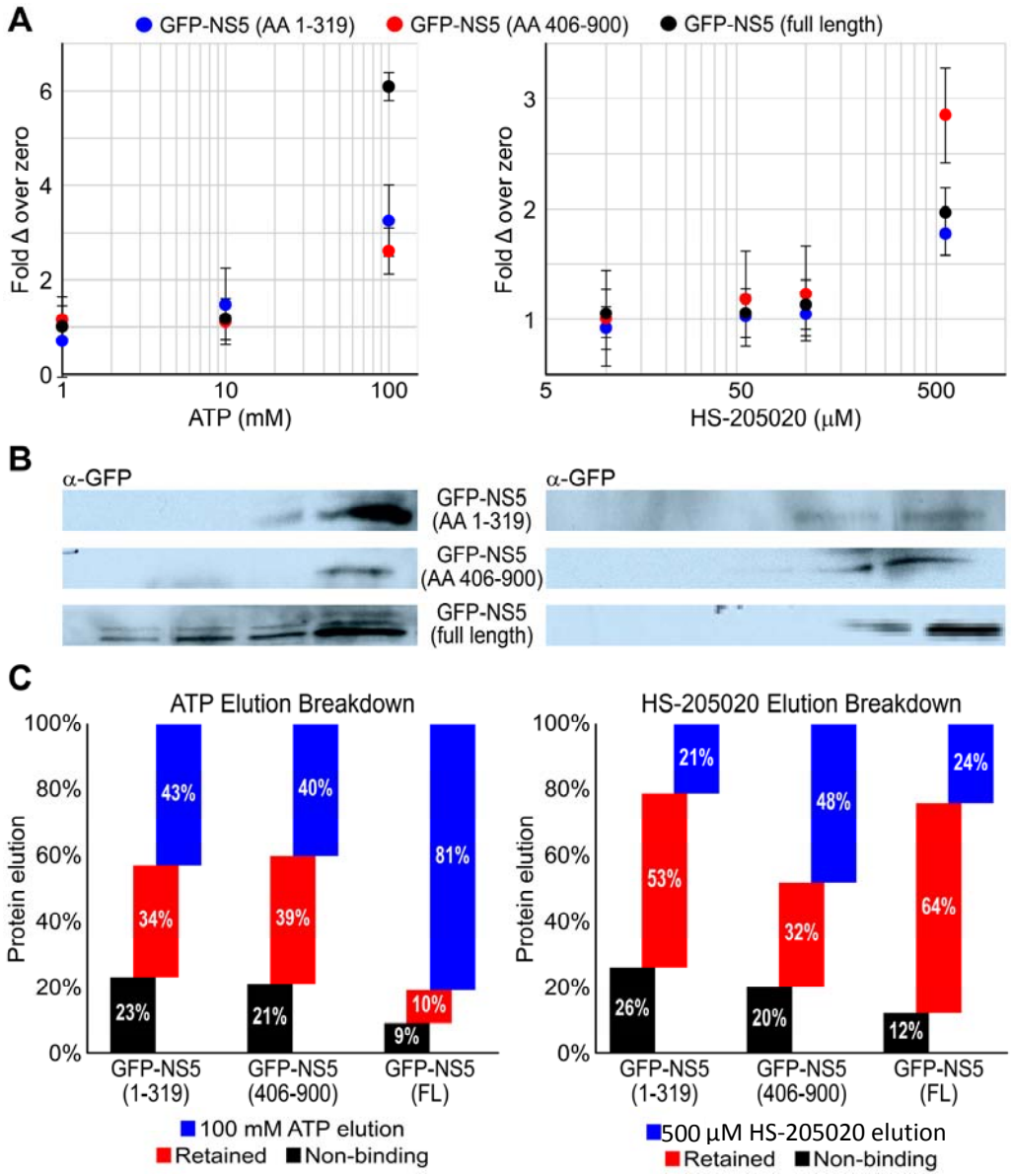
A
GFP-NS5 (AA 1-319)
GFP-NS5 (AA 406-900)
GFP-NS5 (full length)
Fold Δ over zero
ATP (mM)
HS-205020 (μM)
B
α-GFP
GFP-NS5 (AA 1-319)
GFP-NS5 (AA 406-900)
GFP-NS5 (full length)
C
ATP Elution Breakdown
HS-205020 Elution Breakdown
Protein elution
GFP-NS5 (1-319)
GFP-NS5 (406-900)
GFP-NS5 (FL)
100 mM ATP elution
500 μM HS-205020 elution
Retained
Non-binding

Figure 19: Relative ATP and HS-205020 elution profiles of truncated, domain-based, GFP-NS5 proteins. (A) The methyltransferase domain (blue), polymerase domain (red), and full-length GFP (black) proteins were eluted from immobilized-ATP resin with increasing concentrations of soluble ATP or HS-205020, and all three proteins showed a concentration-dependent elution profile. HS-205020 eluted the polymerase domain, GFP-NSF (406-900), to the greatest extent, exhibiting the largest increase in elution at 500 μM HS-205020. (B) Western blot analysis to confirm the presence of GFP fusion proteins in the eluate. Control samples (LSWB) are shown in lane 1 of each blot. Lanes 2, 3, and 4 in each blot correspond to concentrations of ATP or HS-205020 indicated in the graphs. The results corresponded to the elution profiles for each truncated GFP-NS5 protein and full-length GFP-NS5. (C) Quantification of the percent of total protein that was either eluted with 100 mM ATP (blue), did not bind the immobilized-ATP resin initially (black), or was retained on the resin after the addition of 100 mM ATP (red).

6.2 Determination of IC_{50} of HS-205020 against the DENV NS5 polymerase

A standard measurement used to evaluate a drug candidate is the IC_{50} value, which is defined as the concentration of a test compound required to achieve half maximal (50%) inhibition of an enzymatic reaction, such as the replication of viral RNA. The IC_{50} value is commonly used as parameter in evaluating anti-viral potency.

To determine the IC_{50} of the test compound HS-205020, an *in vitro* polymerase assay utilizing purified DENV2 NS5 was used to test the ability of the candidate compound, HS-205020, to inhibit RdRp activity. We used a fluorescence-based polymerase assay that was previously developed and validated for high-throughput screening of RdRp inhibitors (Yap et al., 2007).This assay utilizes a modified ATP analogue (BBT-ATP) and a self-priming 3′UTR-U_{30} RNA template as reaction substrates. BBT-ATP is an adenosine nucleotide that has been modified by conjugating a BBT (2′-[2-benzothiazoyl]-6′-hydroxybenzothiazole) fluorophore group to the γ-phosphate of ATP, resulting in a nonfluorescent substrate named BBT-ATP. During the polymerization reaction, BBT-ATP is incorporated into the nascent RNA, and free BBT-diphosphate (BBT_{PPi}) is released as a product of the reaction. The reaction with calf intestinal phosphatase (CIP) in a high pH buffer terminates the polymerase reaction, and CIP converts nonfluorescent BBT_{PPi} to the highly fluorescent BBT molecule. Measurement of this final reaction product serves as an indirect measure of RdRp enzymatic activity.

Figure 20 shows the results of the RdRp polymerase assay using DENV NS5. Polymerase activity was monitored in the presence of eight concentrations of HS-205020 ranging between 0 and 300 μM (0.1, 0.3, 1, 3, 10, 30, 100, and 300 μM). A reaction containing all assay components except HS-205020 was used as a positive control and was designated as 100% activity. A reaction continuing all assay components except the NS5 enzyme was used as a negative control, designated as 0% activity. For the reactions containing HS-205020, enzymatic activity was expressed as a percentage normalized to the positive and negative control reactions. The normalized data was plotted on a semi-log curve (using $\log_{10}$ of μM concentration) to calculate the IC_{50} for HS-205020.

In the presence of HS-205020, RdRp activity was reduced compared to the positive control reactions (Fig. 20). Starting at approximately 30 μM (of HS-205020), a reduction in polymerase activity was noted, with a drastic decrease in activity observed between 100 μM and 300 μM ($\log_{10}2.0$ and $\log_{10}2.48$ on the graph, respectively). The calculated IC_{50} of HS-205020 in this assay was 102 μM. This observed inhibition of polymerase activity by HS-205020 supports the truncation studies, suggesting that the polymerase domain is the primary binding site on NS5 for HS-205020.

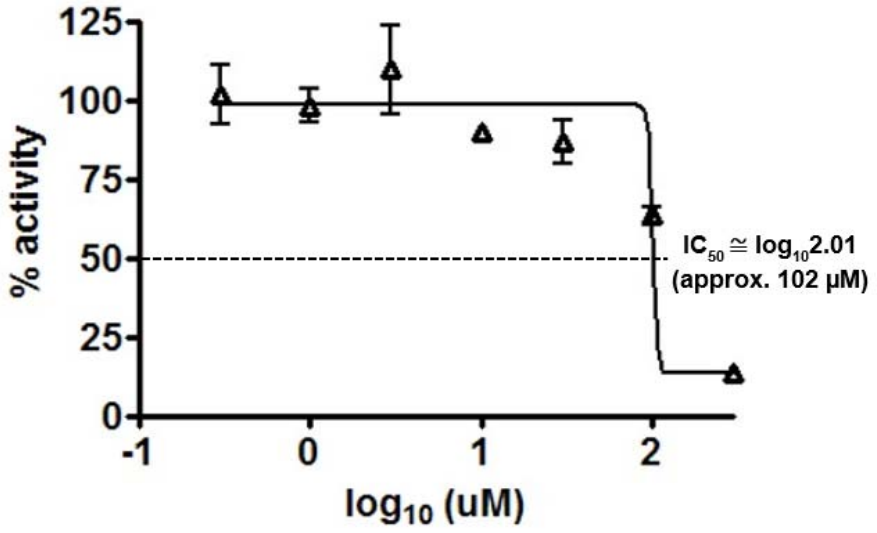

Figure 20: Inhibition of DENV RdRp activity by HS-205020. The *in vitro* activity of DENV RdRp was monitored in the presence of 8 concentrations of HS-205020 ranging from 0 to 300 µM (0,0.1, 0.3, 1, 3, 10, 30, 100, and 300 µM). Results were plotted on a semi-log curve to determine the IC_{50} for HS-205020. Starting at approximately 30 µM of test compound, a reduction in polymerase activity was noted, with a drastic decrease observed between 100 µM and 300 µM HS-205020. The calculated IC_{50} of HS-205020 in this assay is $\log_{10}2.01 = 102$ µM. Courtesy of Subhash Vasudevan, Duke-NUS.

7. HS-205020 activity in a cell culture model of Hepatitis C virus

To explore possible broad spectrum anti-*Flaviviridae* activity, HS-205020 was tested in a model of Hepatitis C virus, a member of the *Flaviviridae* family, but not in the genus *Flavivirus*.

7.2 A Flaviviridae member: Hepatitis C Virus

Hepatitis C virus (HCV) is a (+)ssRNA virus that is the only virus in the *Hepacivirus* genus. HCV is related to DENV, in that both are classified as members within the *Flaviviridae* family. The HCV genome encodes for one polyprotein that consists of structural core and envelope proteins, in addition to five nonstructural proteins including NS2, NS3, NS4b, NS5a, and NS5b. Similar to the DENV NS3 protein, HCV NS3 contains a serine protease and helicase domain. HCV NS5b is an RNA-dependent RNA polymerase (RdRp), whose active site is highly conserved across HCV genotypes. The equivalent enzyme in DENV is the C-terminal domain of NS5 which contains the RdRp. The N-terminus of DENV NS5 contains a methyltransferase domain. Unlike DENV, HCV does not encode a methyltransferase. Thus, the utility of evaluating the antiviral properties of HS-205020 against HCV are twofold. First, it may help to confirm our previous observations suggesting that HS-205020 selectively targets the polymerase domain of NS5, rather than the methyltransferase domain. Second, and most importantly, it will help us determine whether HS-205020 may have broad spectrum activity within the *Flaviviridae* family of viruses.

7.3 HS-205020 reduces production of infectious virus but not percent infection for HCV

To address the anti-viral activity of HS-205020 on related *Flaviviridae* viruses we tested its activity against Hepatitis C virus (HCV). Despite DENV and HCV belonging to different genera, HCV NS5b (the viral polymerase) and DENV NS5 have similar active site structures (Yap et al., 2007). We therefore tested the effects of HS-205020 treatment on HCV-infected HuH7.5 cells. Two different assays were used to measure different endpoints: an infection assay to measure the effect of HS-205020 on the percentage of HCV-infected cells, and a $TCID_{50}$ (50% tissue culture infectious dose) assay to measure the effect of the compound on the release of infectious HCV.

As shown in Figure 21A, we observed slight reductions in the percent infection with HS-205020 treatment at the higher concentrations (15% reduction at 50 μM; 21% at 75 μM; and 9% at 100 μM) compared with the DMSO control. However, these reductions were not statistically significant ($p < 0.09$, 0.20, and 0.50, respectively). In contrast, the positive control containing 500 U/mL of interferon (IFN) abolished HCV percent infection below the detection threshold. However, when the supernatants from the infected and compound-treated HuH7.5 cells were used in a $TCID_{50}$ assay, HS-205020 reduced the production of infectious HCV at concentrations of 50 μM, 75 μM, and 100 μM, with fold reductions of 19.9, 25.1, and 39.8, respectively (Fig. 21B). These initial findings indicate that HS-205020 may have a broad spectrum activity within *Flaviviridae*.

Although treatment of HCV-infected cells with HS-205020 resulted in a minimal decrease in percent infection, the significant decrease in the release of infectious virus indicates that HS-205020 exhibits anti-HCV activity. In an infection assay, a viral antigen is used as an indicator of cellular infection. In the case of HCV infection assays, this antigen is HCV core protein. Although the core protein may be present within an HCV-infected cell, this does not necessarily mean that the cell is actively producing progeny virus. If HS-205020 does in fact reduce RdRp polymerase activity as we hypothesize, an HCV virion would still be able to enter the host cell, uncoat, and release its viral RNA genome. The uncoating process would result in the presence of detectable HCV core protein in the host cell cytoplasm. It is this original, incoming virus that is responsible for the introduction of the core protein, which is then detected using immunofluorescence as described in Materials and Methods (Chapter 2).

The viral RNA genome of HCV is similar to that of DENV in that it has a positive-sense single stranded RNA genome that acts as a messenger RNA, which is initially translated to produce viral proteins. This initial translation yields additional detectable core protein. However, in the presence of an RNA polymerase inhibitor, the production of infectious progeny virus would be reduced, as there would be limited viral RNA available to incorporate in new infectious progeny virus. In this case, a measurement of released infectious progeny virus (using the $TCID_{50}$ assay) might be more informative than the infection assay in determining the antiviral effects of HS-

205020. Assays utilizing viral titer determinations, including FFA and $TCID_{50}$ assays, are considered somewhat of a gold standard in determining anti-viral activity, compared with assays measuring viral antigens alone. Thus, although the infection assays did not show dramatic effects on percent infection, the $TCID_{50}$ findings suggest that HS-205020 may have a broad anti-viral activity within *Flaviviridae*.

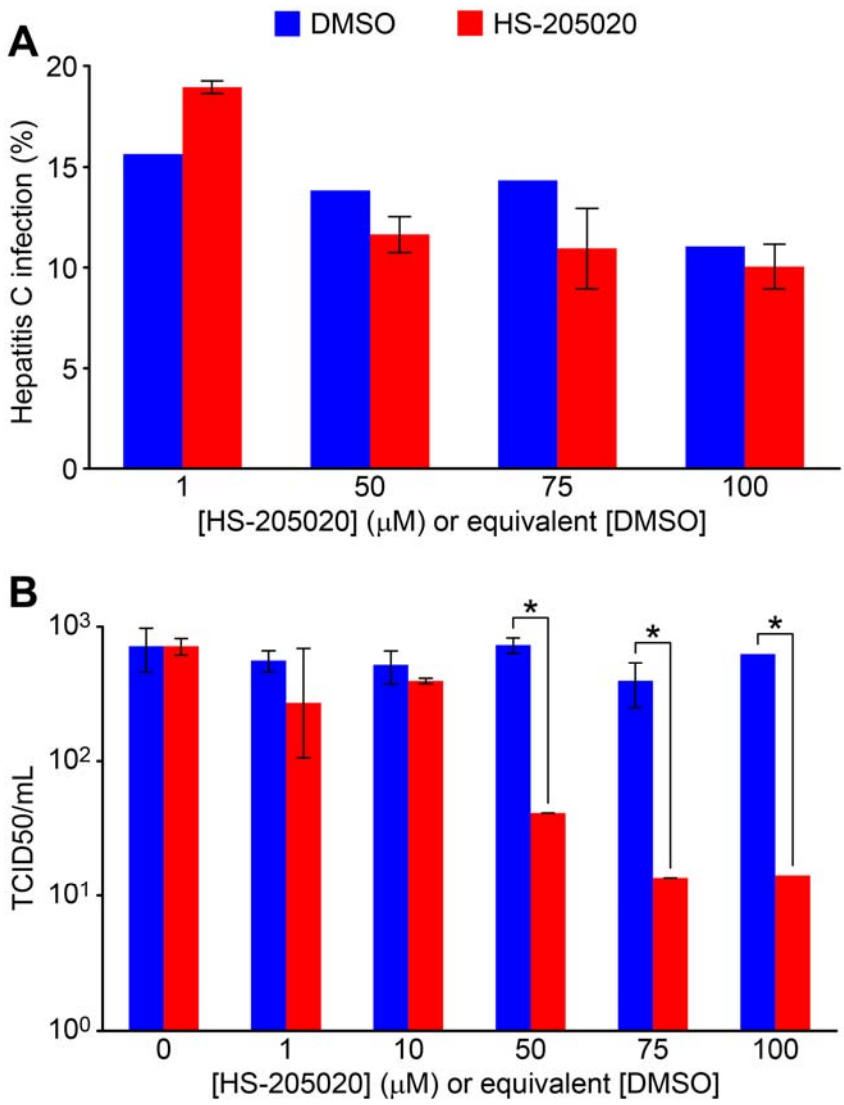

Figure 21: HS-205020 activity in HCV-infected HuH7.5 cells (A) Assay measuring percent infection in HuH7.5 cells treated with HS-205020. The results demonstrated no significant reduction in the percent infection with treatment compared with DMSO control. (n=3, SEM) (B) The $TCID_{50}$ assay using the supernatants from the experiment in (A) did show a significant reduction in infectious virus compared with the DMSO control, at 50 μM, 75 μM, and 100 μM HS-205020 (19.9-, 25.1-, and 39.8-fold reduction in $TCID_{50}$ values, respectively) (* $p < 0.5$). The $TCID_{50}$ findings suggest that HS-205020 may have a broad spectrum activity within *Flaviviridae.* (n=3, SEM)

8. Conclusions

The aim of this study was to identify a dengue virus-required purine-binding protein target against which to screen drug-candidate compounds. The goal was to identify a drug-candidate compound capable of inhibiting dengue virus while exhibiting minimal toxicity *in vitro*.

Herein, we used an ATP-Sepharose resin to isolate the purinome (purine-binding proteins) of DENV-infected and mock-infected cells using two human cell types: HuH7, a liver-derived cell line, and U937+DC-SIGN, a monocytic cell line. Analysis of metabolically labeled proteins (^{35}S-methionine/cysteine) showed few changes in purine-binding protein levels between DENV-infected and mock-infected cells (Figure 7, 8). These results suggest that DENV infection of HuH7 or U937+DC-SIGN cells had little effect on the expression of host ATP-binding proteins detectable using this method. Not surprisingly, the DENV viral encoded purine-binding proteins were up-regulated in response to infection (Figure 7, 8). Most notable were non-structural protein 5 (NS5) and non-structural protein 3 (NS3). Ultimately, NS5 was selected as the target for drug-candidate screening because it is the most highly conserved flaviviral protein. Thus, a compound that is capable of inhibiting NS5 enzymatic functions may also serve as a broad anti-flaviviral agent.

A 3,391 compound library was screened against a GFP-NS5 fusion protein, with the goal of identifying one or more lead compounds that would interact with GFP-NS5

and show anti-DENV activity. First, all 3,391 compounds were tested for their ability to elute GFP-NS5 from an immobilized-ATP resin, as measured by GFP fluorescence using a 96-well plate assay. Ninety-five compounds generated eluates showing a measured GFP fluorescence greater than or equal to a threshold of at least 2.5-fold greater than background (negative control sample). To further narrow the selection of the drug-candidate compounds, we performed GFP-NS5 Western blot analysis of the eluates from the 95 compounds that had met or exceeded the fluorescence threshold in the screening assay. Only the 50 compounds that strongly eluted GFP-NS5, as confirmed by Western blot, were compared to the database containing lead compounds for unrelated proteins in previous screens. The database search confirmed that 18 compounds were unique lead compounds for GFP-NS5, showing no overlap with the unrelated proteins detected in previous screens. The 18 unique lead compounds were then tested for their ability to elute GFP-NS5 from immobilized-ATP in a concentration-dependent manner. Six compounds displayed a concentration-dependent elution profile, confirming a specific interaction with GFP-NS5. These compounds were then evaluated for anti-DENV activity using two separate *in vitro* assays with distinct endpoints: percent infected cells, and release of infectious DENV virus.

The performance of the candidate compounds in the anti-DENV assays allowed us to narrow our selection to one chemical scaffold (compound) of interest for further drug development. The drug-candidate compound, HS-205020, was shown to have

significant anti-DENV activity in both U937+DC-SIGN and BHK-21cells. A likely mechanism of action was determined, as HS-205020 was shown to preferentially bind to the RNA polymerase domain of NS5, and also inhibited the polymerase activity of NS5 in an *in vitro* RdRp assay. Cytotoxicity of the compound was evaluated using two assays: a live/dead viability stain to measure cell membrane integrity, and a resazurin assay to detect metabolically active cells. The cytotoxicity profile of HS-205020 was shown to be comparable to that of ribavirin, an FDA-approved anti-HCV drug. Finally, to explore potential broad spectrum anti-*Flaviviridae* activity, HS-205020 was tested in a model of Hepatitis C virus. Although infection assays did not show dramatic effects on percent infection, there was a significant decrease in the level of infectious HCV virus suggesting that HS-205020 may have a broad anti-viral activity within *Flaviviridae*.

Previously reported inhibitors of NS5 have fallen short in terms of their clinical usefulness due to toxicity (likely due to purine-structure similarity) or lack of transference of antiviral effects from pre-clinical studies to humans (Stevens et al., 2009, Stahla-Beek et al., 2012, Lim et al., 2011, Niyomrattanakit et al., 2010, Yin et al., 2009). The HS-205020 molecular scaffold differs from traditional nucleoside analogues because of its modified indole functionality and lack of two additional nitrogens that are required to be classified as a purine (Figure 13). Additionally, whereas most published nucleotide-based inhibitors of DENV and HCV contain a ribosyl group, HS-205020 does not have a sugar backbone.

The results of our binding studies using truncated recombinant forms of NS5, along with an *in vitro* RNA-dependent RNA polymerase assay measuring NS5 RdRp activity, suggest that the anti-DENV activity of HS-205020 involves direct inhibition of the NS5 polymerase activity. However, in the absence of a crystal structure of DENV NS5 in complex with HS-205020, the precise molecular mechanisms by which the compound inhibits polymerase activity are yet to be determined. One possibility is that the compound interacts directly with the NS5 polymerase domain and displaces ATP from its binding site. Alternatively, it may act allosterically, resulting in a conformational change in the protein, thereby disrupting the ATP binding site indirectly.

In this study, proteome mining technology was utilized to discover a novel inhibitor of DENV NS5, HS-205020. This approach was previously utilized to discover SNX5422, an inhibitor of Hsp90, and more recently, HS-38, a selective inhibitor of the DAPKs (Fadden et al., 2010, Carlson et al., 2013, Rajan et al., 2011). The advantage of the proteome mining approach is its innovative yet uncomplicated design. It is a binding assay that uses ATP to capture proteins that can then be readily screened against a library of small-molecule scaffolds that are structurally divergent from the purine backbone. This structural divergence reduces the probability of defining compounds that will broadly bind to multiple targets within the host purinome, possibly resulting in toxicity. This approach also does not require radiolabeled substrates or even a crystal

structure of the targeted protein. For these reasons, we would advocate using this purinome screening approach for rapidly and efficiently defining novel molecular scaffolds for other antiviral targets that are known to bind nucleotides, including DENV NS3, reverse transcriptases, and DNA helicases.

In summation, HS-205020, was able to competitively elute GFP-NS5 from the ATP resin and also exhibited antiviral activity in both the U937+DC-SIGN human monocyte cell line and BHK-21 cells. Additionally, HS-205020 was able to inhibit DENV NS5 RNA polymerase activity *in vitro*. HS-205020 is chemically distinct from the majority of previously reported NS5 inhibitors, which are nucleoside analogs that can cause severe toxicity in animal studies. In contrast, over the concentration range that produced anti-DENV effects, HS-205020 showed comparable viabilities to ribavirin, an FDA approved hepatitis C virus (HCV) therapeutic. These findings support HS-205020 as a potential dengue antiviral candidate, and its chemical scaffold represents as an ideal starting compound for future structure-activity relationship studies.

9. Future Directions

Optimization of a drug-candidate compound to generate a more refined, potent, and extensively tested lead compound involves many steps (Hughes et al., 2011). These generally include the following six components: target identification and validation,

assay development, high throughput screening, hit identification, lead optimization and finally the selection of a candidate molecule for clinical development.

The first four preclinical steps were completed during the course of the aforementioned research (target identification and validation, assay development, high throughput screening, and hit identification). Assay development of the fluorescence-based small-molecule screen for purinomic proteins had been completed and validated prior to the initiation of this project, and this assay had been utilized in other drug-candidate screening studies (Fadden et al., 2010, Carlson et al., 2013). To apply this assay to an anti-DENV drug-candidate screen, target identification was required in order to select an appropriate protein to be used in the small-molecule screen. Analysis of metabolically labeled proteins showed few changes in levels of host-derived purine-binding proteins between DENV-infected and mock-infected cells, excluding the possibility of using a host-encoded protein as a target for our screen. Not surprisingly, DENV viral encoded purine-binding proteins were up-regulated in response to infection (Fig. 7 and 8), notably non-structural protein 5 (NS5) and non-structural protein 3 (NS3). Ultimately, NS5 was selected as the target for drug-candidate screening because it is a highly conserved flaviviral protein.

Typically, after the selection of an antiviral drug target (in this case DENV NS5), target validation is required to confirm the protein is expressed in virus-infected cells or tissues, and that knock-out or inhibition of the gene encoding the target protein results

in an observed or measured antiviral effect. As expected, dengue virus non-structural protein 5 (NS5) was only expressed in virus-infected cells, which confirms its presence in virus-infected cells or tissues. Others have shown that deletions or mutations in the NS5 conserved motif (glycine- aspartic acid- aspartic acid), characteristic of RNA-dependent RNA polymerases, inactivate the polymerase. This results in a reduction in DENV infection (Hanley et al., 2002) thus addressing the second component of target validation.

As stated earlier, the development of the assay (step two in preclinical development) that was utilized to screen for promising drug-candidates was completed and validated prior to the inception of this research project. Figure 4 and Section 2.2.5 summarize the fluorescence-based small-molecule library screening protocol used in the identification of this novel NS5-targeted chemical scaffold, as well as in previous drug-development studies targeting ZIPK, DAPK, and Hsp90 (with minor modifications to protocol design)(Fadden et al., 2010, Carlson et al., 2013). NS5 was modified to be screening-ready by the development of a GFP-fusion NS5 construct that could be used to express large quantities of recombinant GFP-NS5 in mammalian cells (Rawlinson et al., 2009). Once the GFP-NS5 protein was shown to bind to the ATP-Sepharose resin in the assay, and be eluted by the addition of soluble ATP, the NS5 target protein was ready to be subjected to the high throughput screen.

The third step in the lead optimization pathway was the application of the high throughput fluorescence-based small molecule assay screen, using GFP-tagged NS5 protein (GFP-NS5), as described above. Figure 12 shows how the compound pool was narrowed down from 3,391 compounds to 6 compounds. This process entailed analyzing the compounds based on their ability to elute recombinant GFP-NS5 from an immobilized-ATP resin using a 96-well high throughput assay. Further narrowing of the drug-candidate compounds involved Western blot analysis of the eluates from the 95 compounds that were had been able to elute GFP fluorescence (assumed to be GFP-NS5). Only the compounds that were confirmed as having eluted significant levels of GFP-NS5 (confirmed by Western blot) were then tested for their ability to elute bound GFP from the ATP resin in a concentration-dependent manner. Six compounds displayed a concentration-dependent GFP-NS5 elution profile and were subsequently evaluated using *in vitro* anti-DENV assays.

The performance of the compounds in the anti-DENV assays allowed us to hone in on one chemical scaffold (compound) of interest for further drug development, thus completing the fourth step in preclinical development. The drug-candidate compound, HS-205020, was identified and confirmed to exhibit anti-DENV activity, and was subsequently determined to inhibit the RNA polymerase activity of NS5 (RdRp). The cytotoxicity profile, as measured using both a live/dead viability stain and the

metabolism-dependent resazurin assay, was comparable to that of ribavirin (an FDA-approved anti-HCV drug).

What has yet to be determined for this compound is whether or not it can be structurally optimized to improve its anti-viral qualities (IC_{50}, EC_{50}, infectious virus titers, and percent cell infection) and cytotoxicity profile. The optimization of the lead compound is the fifth step in preclinical drug discovery and development. In the anti-DENV studies, HS-205020 did demonstrate significant antiviral activity as determined using multiple endpoints, and these effects were demonstrated in two DENV-relevant human cell types (hepatic and monocytic). However, the lead optimization process could potentially result in an even more robust antiviral compound. Additionally, although HS-205020 exhibited minimal toxicity in the cell-based assays, any observable cytotoxicity could potentially be reduced further by optimization of the lead compound.

Lead optimization typically involves structure-activity relationship (SAR) studies. SAR involves studying the chemical scaffold of the lead drug-candidate compound and modifying, removing, or adding moieties to the general scaffold. Hundreds-to-thousands of iterations of HS-205020 could be designed, and five examples of such structural analogs are summarized below in Figure 22. These five analogs represent a starting point for further drug development targeting the DENV NS5 protein.

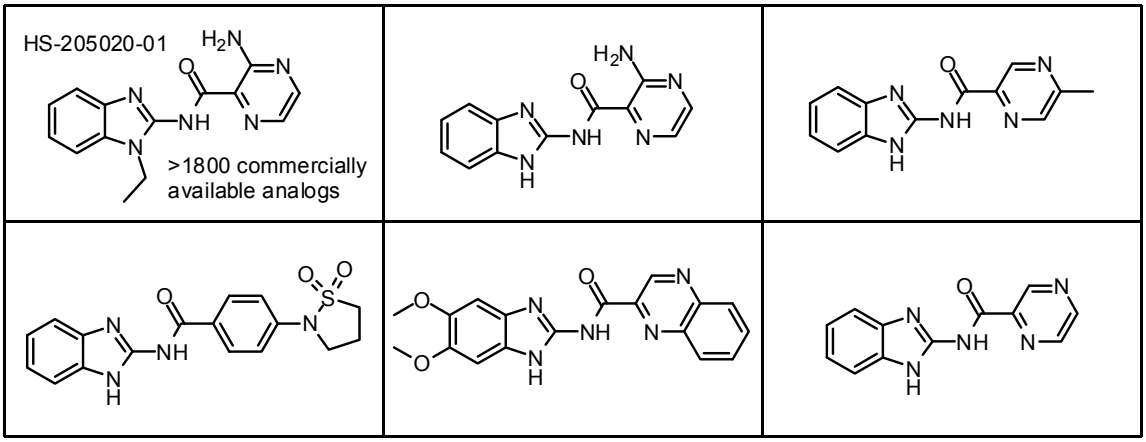

Figure 22: Five SAR-based analogs to HS-205020

To date, HS-205020 has only been tested for efficacy in two members of the *Flaviviridae* family (DENV and HCV). Within the *Flavivirus* genus, NS5 is the most highly conserved flaviviral protein. Therefore, there is great opportunity to test this drug-candidate compound against a variety of other flaviviruses, including yellow fever virus, West Nile virus, and tick-borne encephalitis. Many human diseases that are caused by flaviviruses, particularly neglected tropical diseases, lack any effective means of pharmacological prevention or intervention. The development of an anti-DENV drug that also has broader applications across *Flaviviridae* could potentially offer a viable means of intervention against these continued threats to global public health.

Appendix A

DNA Sequence of pEPI-eGFP-NS5 (1-900) (Rawlinson et al., 2009a)

ATTGTGAAGGTATACTTTCTTTTCACATAAATTTGTAGTCAATATGTTCACCCCAAAAAAGCTGTTTGTT

AACTTGTCAACCTCATTTCAAAATGTATATAGAAAGCCCAAAGACAATAACAAAAATATTCTTGTAGAACAAAA

TGGGAAAGAATGTTCCACTAAATATCAAGATTTAGAGCAAAGCATGAGATGTGTGGGGATAGACAGTGAGGCTG

ATAAAATAGAGTAGAGCTCAGAAACAGACCCATTGATATATGTAAGTGACCTATGAAAAAAATATGGCATTTTA

CAATGGGAAAATGATGATCTTTTTCTTTTTTAGAAAAACAGGGAAATATATTTATATGTAAAAAATAAAAGGGAA

CCCATATGTCATACCATACACACAAAAAAATTCCAGTGAATTATAAGTCTAAATGGAGAAGGCAAAACTTTAAA

TCTTTTAGAAAATAATATAGAAGCATGCCATCATGACTTCAGTGTAGAGAAAAATTTCTTATGACTCAAAGTCCT

AACCACAAAGAAAAGATTGTTAATTAGATTGCATGAATATTAAGACTTATTTTTAAAATTAAAAAACCATTAAGA

AAAGTCAGGCCATAGAATGACAGAAAATATTTGCAACACCCCAGTAAAGAGAATTGTAATATGCAGATTATAAA

AAGAAGTCTTACAAATCAGTAAAAAATAAAACTAGACAAAAATTTGAACAGATGAAAGAGAAACTCTAAATAA

TCATTACACATGAGAAACTCAATCTCAGAAATCAGAGAACTATCATTGCATATACACTAAATTAGAGAAATATT

AAAAGGCTAAGTAACATCTGTGGCAATATTGATGGTATATAACCTTGATATGATGTGATGAGAACAGTACTTTAC

CCCATGGGCTTCCTCCCCAAACCCTTACCCCAGTATAAATCATGACAAATATACTTTAAAAACCATTACCCTATA

TCTAACCAGTACTCCTCAAAACTGTCAAGGTCATCAAAAATAAGAAAAGTCTGAGGAACTGTCAAAACTAAGAG

GAACCCAAGGAGACATGAGAATTATATGTAATGTGGCATTCTGAATGAGATCCCAGAACAGAAAAAGAACAGT

AGCTAAAAAAACTAATGAAATATAAATAAAGTTTGAACTTTAGTTTTTTTTAAAAAAGAGTAGCATTAACACGGCA

AAGTCATTTTCATATTTTTCTTGAACATTAAGTACAAGTCTATAATTAAAAATTTTTTAAATGTAGTCTGGAACATT

GCCAGAAACAGAAGTACAGCAGCTATCTGTGCTGTCGCCTAACTATCCATAGCTGATTGGTCTAAAATGAGATAC

ATCAACGCTCCTCCATGTTTTTTGTTTTCTTTTTAAATGAAAAACTTTATTTTTTAAGAGGAGTTTCAGGTTCATAGC

AAAATTGAGAGGAAGGTACATTCAAGCTGAGGAAGTTTTCCTCTATTCCTAGTTTACTGAGAGATTGCATCATGA

ATGGGTGTTAAATTTTGTCAAATGCTTTTTCTGTGTCTATCAATATGACCATGTGATTTTCTTCTTTAACCTGTTGAT

GGGACAAATTACGTTAATTGATTTTCAAACGTTGAACCACCCTTACATATCTGGAATAAATTCTACTTGGTTGTGG

TGTATATTTTTTGATACATTCTTGGATTCTTTTTGCTAATATTTTGTTGAAAATGTTTGTATCTTTGTTCATGAGAGAT

ATTGGTCTGTTGTTTTCTTTTCTTGTAATGTCATTTTCTAGTTCCGGTATTAAGGTAATGCTGGCCTAGTTGAATGAT

TTAGGAAGTATTCCCTCTGCTTCTGTCTTCTGAAAGAGATTGTAGAAAGTTGATACAATTTTTTTTTCTTTAAATAT

CTTGATAgaattctgcagtcgacggtaccgcgggcccgggatccaccggatctagataactgatcataatcagccataccacatttgtagaggttttacttgctttaaaaaacct

cccacacctccccctgaacctgaaacataaaatgaatgcaattgttgttgttaacttgtttattgcagcttataatggttacaaataaagcaatagcatcacaaatttcacaaataaagca

ttttttttcactgcattctagttgtggtttgtccaaactcatcaatgtatcttaacgcgtaaattgtaagcgttaatattttgttaaaattcgcgttaaatttttgttaaatcagctcatttttttaacc

aataggccgaaatcggcaaaatcccttataaatcaaaagaatagaccgagatagggttgagtgttgttccagtttggaacaagagtccactattaaagaacgtggactccaacgtc

aaagggcgaaaaaccgtctatcagggcgatggcccactacgtgaaccatcaccctaatcaagtttttggggtcgaggtgccgtaaagcactaaatcggaaccctaaagggagcc

cccgatttagagcttgacggggaaagccggcgaacgtggcgagaaaggaagggaagaaagcgaaaggagcgggcgctagggcgctggcaagtgtagcggtcacgctgcg

cgtaaccaccacacccgccgcgcttaatgcgccgctacagggcgcgtcaggtggcacttttcggggaaatgtgcgcggaacccctatttgtttatttttctaaatacattcaaatatgt

atccgctcatgagacaataaccctgataaatgcttcaataatattgaaaaaggaagagtcctgaggcggaaagaaccagctgtggaatgtgtgtcagttagggtgtggaaagtcc

ccaggctccccagcaggcagaagtatgcaaagcatgcatctcaattagtcagcaaccaggtgtggaaagtccccaggctccccagcaggcagaagtatgcaaagcatgcatctc

aattagtcagcaaccatagtcccgcccctaactccgcccatcccgcccctaactccgcccagttccgcccattctccgccccatggctgactaatttttttttatttatgcagaggccgagg

ccgcctcggcctctgagctattccagaagtagtgaggaggctttttggaggcctaggcttttgcaaagatcgatcaagagacaggatgaggatcgtttcgcatgattgaacaagat

ggattgcacgcaggttctccggccgcttgggtggagaggctattcggctatgactgggcacaacagacaatcggctgctctgatgccgccgtgttccggctgtcagcgcaggggc

gcccggttctttttgtcaagaccgacctgtccggtgccctgaatgaactgcaagacgaggcagcgcggctatcgtggctggccacgacgggcgttccttgcgcagctgtgctcgac

gttgtcactgaagcgggaagggactggctgctattgggcgaagtgccggggcaggatctcctgtcatctcaccttgctcctgccgagaaagtatccatcatggctgatgcaatgcg

gcggctgcatacgcttgatccggctacctgcccattcgaccaccaagcgaaacatcgcatcgagcgagcacgtactcggatggaagccggtcttgtcgatcaggatgatctggac

gaagagcatcaggggctcgcgccagccgaactgttcgccaggctcaaggcgagcatgcccgacggcgaggatctcgtcgtgacccatggcgatgcctgcttgccgaatatcatg

gtggaaaatggccgcttttctggattcatcgactgtggccggctgggtgtggcggaccgctatcaggacatagcgttggctacccgtgatattgctgaagagcttggcggcgaatg

ggctgaccgcttcctcgtgctttacggtatcgccgctcccgattcgcagcgcatcgccttctatcgccttcttgacgagttcttctgagcgggactctggggttcgaaatgaccgaccaa

gcgacgcccaacctgccatcacgagatttcgattccaccgccgccttctatgaaaggttgggcttcggaatcgttttccgggacgccggctggatgatcctccagcgcggggatctc

atgctggagttcttcgcccaccctagggggaggctaactgaaacacggaaggagacaataccggaaggaacccgcgctatgacggcaataaaaagacagaataaaacgcacg

gtgttgggtcgtttgttcataaacgcggggttcggtcccagggctggcactctgtcgataccccaccgagaccccattggggccaatacgcccgcgtttcttccttttccccacccac

cccccaagttcgggtgaaggcccagggctcgcagccaacgtcggggcggcaggccctgccatagcctcaggttactcatatatactttagattgatttaaaacttcatttttaatttaa

aaggatctaggtgaagatccttttttgataatctcatgaccaaaatcccttaacgtgagttttcgttccactgagcgtcagaccccgtagaaaagatcaaaggatcttcttgagatccttttt

tttctgcgcgtaatctgctgcttgcaaacaaaaaaaccaccgctaccagcggtggtttgtttgccggatcaagagctaccaactctttttccgaaggtaactggcttcagcagagcgc

agataccaaatactgtccttctagtgtagccgtagttaggccaccacttcaagaactctgtagcaccgcctacatacctcgctctgctaatcctgttaccagtggctgctgccagtggcg

ataagtcgtgtcttaccgggttggactcaagacgatagttaccggataaggcgcagcggtcgggctgaacgggggttcgtgcacacagcccagcttggagcgaacgacctaca

ccgaactgagatacctacagcgtgagctatgagaaagcgccacgcttcccgaagggagaaaggcggacaggtatccggtaagcggcagggtcggaacaggagagcgcacg

agggagcttccagggggaaacgcctggtatctttatagtcctgtcgggtttcgccacctctgacttgagcgtcgatttttgtgatgctcgtcaggggggcggagcctatggaaaaac

gccagcaacgcggccttttacggttcctggccttttgctggccttttgctcacatgttctttcctgcgttatcccctgattctgtggataaccgtattaccgccatgcattagttattaatagt

aatcaattacggggtcattagttcatagcccatatatggagttccgcgttacataacttacggtaaatggcccgcctggctgaccgcccaacgacccccgcccattgacgtcaataat

gacgtatgttcccatagtaacgccaatagggactttccattgacgtcaatgggtggagtatttacggtaaactgcccacttggcagtacatcaagtgtatcatatgccaagtacgcccc

ctattgacgtcaatgacggtaaatggcccgcctggcattatgcccagtacatgaccttatgggactttcctacttggcagtacatctacgtattagtcatcgctattaccatggtgatgc

ggttttggcagtacatcaatgggcgtggatagcggtttgactcacggggatttccaagtctccaccccattgacgtcaatgggagtttgttttggcaccaaaatcaacgggactttcc

aaaatgtcgtaacaactccgccccattgacgcaaatgggcggtaggcgtgtacggtgggaggtctatataagcagagctggtttagtgaaccgtcagatccgctagcGCTAC

CGGTCGCCACCATGGTGAGCAAGGGCGAGGAGCTGTTCACCGGGGTGGTGCCCATCCTGGTCGAGCTGGACGGC

GACGTAAACGGCCACAAGTTCAGCGTGTCCGGCGAGGGCGAGGGCGATGCCACCTACGGCAAGCTGACCCTGA

AGTTCATCTGCACCACCGGCAAGCTGCCCGTGCCCTGGCCCACCCTCGTGACCACCCTGACCTACGGCGTGCAGT

GCTTCAGCCGCTACCCCGACCACATGAAGCAGCACGACTTCTTCAAGTCCGCCATGCCCGAAGGCTACGTCCAG

GAGCGCACCATCTTCTTCAAGGACGACGGCAACTACAAGACCCGCGCCGAGGTGAAGTTCGAGGGCGACACCCT

GGTGAACCGCATCGAGCTGAAGGGCATCGACTTCAAGGAGGACGGCAACATCCTGGGGCACAAGCTGGAGTAC

AACTACAACAGCCACAACGTCTATATCATGGCCGACAAGCAGAAGAACGGCATCAAGGTGAACTTCAAGATCC

GCCACAACATCGAGGACGGCAGCGTGCAGCTCGCCGACCACTACCAGCAGAACACCCCCATCGGCGACGGCCC

CGTGCTGCTGCCCGACAACCACTACCTGAGCACCCAGTCCGCCCTGAGCAAAGACCCCAACGAGAAGCGCGATC

ACATGGTCCTGCTGGAGTTCGTGACCGCCGCCGGGATCACTCTCGGCATGGACGAGCTGTACAAGTCCGGACTCA

gatATCAAACAAGTTTGTACAAAAAAGCAGGCTctGGAACTGGCAACATAGGAGAGACGCTTGGAGAGAAATGGA

AAAACCGGTTGAATGCATTGGGGAAGAGTGAATTCCagatctATAAGAAAAGTGGAATCCAGGAAGTGGATAGAA

CCTTAGCAAAAGAAGGCATCAAAAGAGGAGAAACGGACCATCACGCTGTGTCGCGAGGCTCGGCGAAACTGAG

ATGGTTCGTCGAGAGAAACCTGGTCACACCAGAAGGGAAAGTAGTGGACCTTGGCTGCGGCAGGGGgGGCTGGT

CATACTATTGTGGGGGACTAAAGAATGTAAAAGAAGTCAAAGGCCTAACAAAAGGAGGACCAGGACACGAAG

AACCCATTCCCATGTCAACATATGGTTGGAATCTGGTGCGTCTTCAAAGTGGAGTTGATGTTTTTTTTACTCCGCC

AGAAAAGTGTGACACATTACTGTGTGACATAGGGGAGTCGTCACCAAACCCCACGGTTGAGGCAGGACGAACA

CTCAGAGTTCTAAACTTAGTGGAAAATTGGCTGAACAACAACACCCAATTTTGCATAAAGGTTCTCAACCCATAT

ATGCCCTCAGTTATAGAAAAAATGGAAGCGCTACAAAGGAAATACGGAGGAGCTTTGGTGAGGAATCCACTCTC

ACGAAATTCCACACACGAGATGTACTGGGTATCCAATGCtTCCGGGAACATAGTGTCATCAGTGAACATGATTTC

AAGaATGTTGATtAACAGATTCACAATGAGACATAAGAAGGCCACaTACGAGCCAGATGTTGACCTCGGAAGCGG

AACCCGCAACATCGGAATTGAAAGTGAGACACCAAATTTAGACATAATTGGGAAAAGAATAGAGAAAATAAAA

CAAGAGCATGAAACATCATGGCACTATGACCAAGACCACCCATACAAAACGTGGGCCTACCATGGCAGCTACG

AAACAAAACAGACTGGATCAGCATCAtccatggtgaacggagtggttaggcTGCTAACAAAACCTTGGGACATCATCCCTATG

GTGACACAGATGGCAATGACAGACACGACTCCATTTGGGCAACAGCGCGTTTTCAAAGAGAAAGTGGACACGA

GAACCCAAGAACCGAAAGAAggcacGaaAaaactaatgAAAATCACGGCAGAATGGCTcTGGAAAGAACTAGGaAAGA

AAAAGACACCTAGGATGTGCACCAGAGAAGAATTcacaagaaaggtgagaagcAATGCAGCCTTAGGTGCCATATTCACT

GATGAGAACAAGTGGAAGTCGGCACGTGAGGCTGTTGAAGATAGTGGATTTTGGGAATTGGTTGACAAGGAAAG

GAATCTCCATCTTGAAGGAAAGTGTGAGACATGTGTGTATAACATGATGGGAAAGAGAGAGAAGAAGCTAGGG

GAGTTCGGCAAAGCAAAAGGCAGCAGAGCCATATGGTACATGTGGCTTGGAGCACGCTTCTTAGAGTTTGAAGC

CCTAGGATTCTTGAATGAAGATCACTGGTTTTCCAGAGAGAACTCCCTGAGTGGAGTGGAAGGAGAAGGGCTGC

ACAAACTAGGCTACATTTTAAGAGACGTGAGTAAGAAAGAAGGAGGAGCAATGTACGCCGATGACACCGCAGG

ATGGGACACAAGAATCACACTAGAGGACTTAAAAAATGAAGAAATGGTGACAAACCACATGGAAGGAGAACA

CAAGAAACTTGCTGAAGCCATTTTCAAATTAACGTACCAAAACAAGGTGGTGCGTGTGCAAAGACCAACACCAA

GAGGCACAGTAATGGACATTATATCGAGAAGAGACCAAAGAGGTAGTGGACAAGTTGTCACCTACGGCCTCAAT

ACTTTCACCAACATGGAAGCCCAACTGATCAGACAGATGGAGGGAGAAGGAGTCTTCAAAAGCATCCAGCACC

TGACAGTCACAGAAGAAATTGCAGTGAAAAACTGGTTAGTAAGAGTGGGGCGTGAGAGGTTATCAAGAATGGC

CATCAGTGGAGATGATTGTGTTGTGAAACCcTTAGATGACAGGTTTGCAAGCGCTCTAACAGCTCTAAATGACAT

GGGAAAGGTTAGGAAAGACATACAACAATGGGAACCTTCAAGAGGATGGAACGATTGGACACAAGTGCCCTTT

TGTTCACACCATTTCCATGAGTTAATCATGAAGGACGGTCGTGTACTCGTAGTTCCATGTAGAAACCAAGATGAA

CTGATTGGTAGGGCCCGAATTTCCCAGGGAGCCGGGTGGTCCTTGCGGGAAACAGCCTGTTTGGGGAAGTCTTAC

GCCCAAATGTGGAGCCTGATGTACTTCCACAGACGTGACCTTAGGCTGGCGGCAAATGCCATTTGCTCGGCAGTC

CCATCACATTGGGTTCCAACAAGTCGAACAACCTGGTCCATACACGCCACACATGAGTGGATGACAACAGAAGA

CATGCTGACAGTCTGGAACAGGGTGTGGATTCAAGAAAACCCATGGATGGAAGACAAAACTCCAGTAGAATCA

TGGGAGGAAATCCCATATTTGGGGAAAAGAGAAGACCAATGGTGCGGCTCATTGATTGGGCTAACAAGCAGGG

CCACCTGGGCAAAGAACATCCAAACAGCAATAAATCAAGTTAGATCCCTAATAGGCAATGAGGAATACACAGA

CTACATGCCATCCATGAAAAGATTCAGAAGAGAAGAGGAAGAGGCAGGAGTCCTGTGGtgACCCAGCTTTCTTGT

ACAAAGTGGTTCGATatcAATAAACTTATAAATTGTGAGAGAAATTAATGAATGTCTAAGTTAATGCAGAAACGG

AGAGACATACTATATTCATGAACTAAAAGACTTAAT

Appendix B

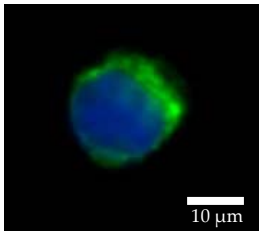
10 µm

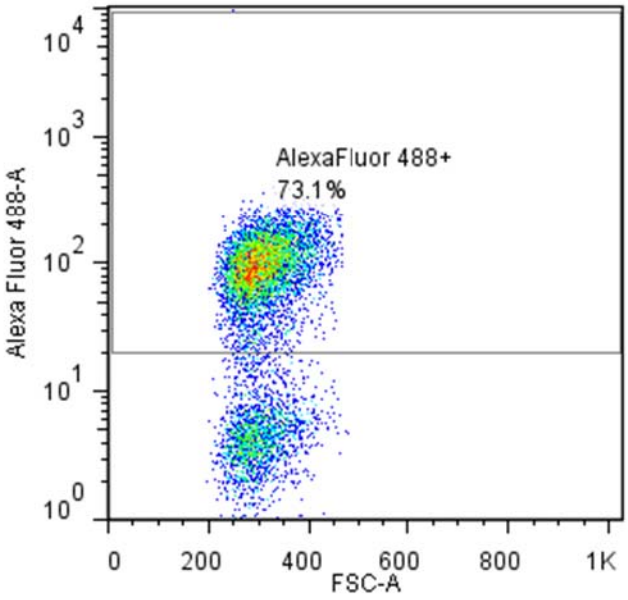
AlexaFluor 488+
73.1%
Alexa Fluor 488-A
FSC-A
0
200
400
600
800
1K

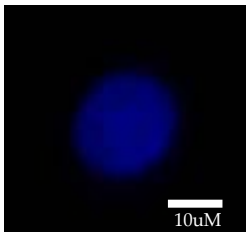
10uM

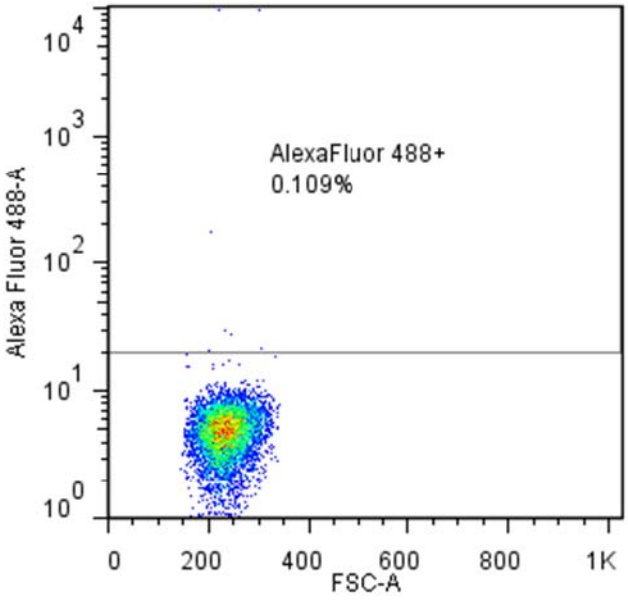
AlexaFluor 488+
0.109%
Alexa Fluor 488-A
FSC-A
0
200
400
600
800
1K

Appendix B: Flow cytometric analysis of DENV-infected and mock-infected U937+DC-SIGN cells. DENV-infected cell sample (top panel) shows a greater than 70% percent infection as measured by the immunofluorescence using a primary antibody directed against DENV E protein. Mock-infection produced negligible infection. An immunofluorescence image of a DENV-infected and mock-infected U937+DC-SIGN cell is included adjacent to the plot with the white marker representing 10 μm in length.

Appendix C

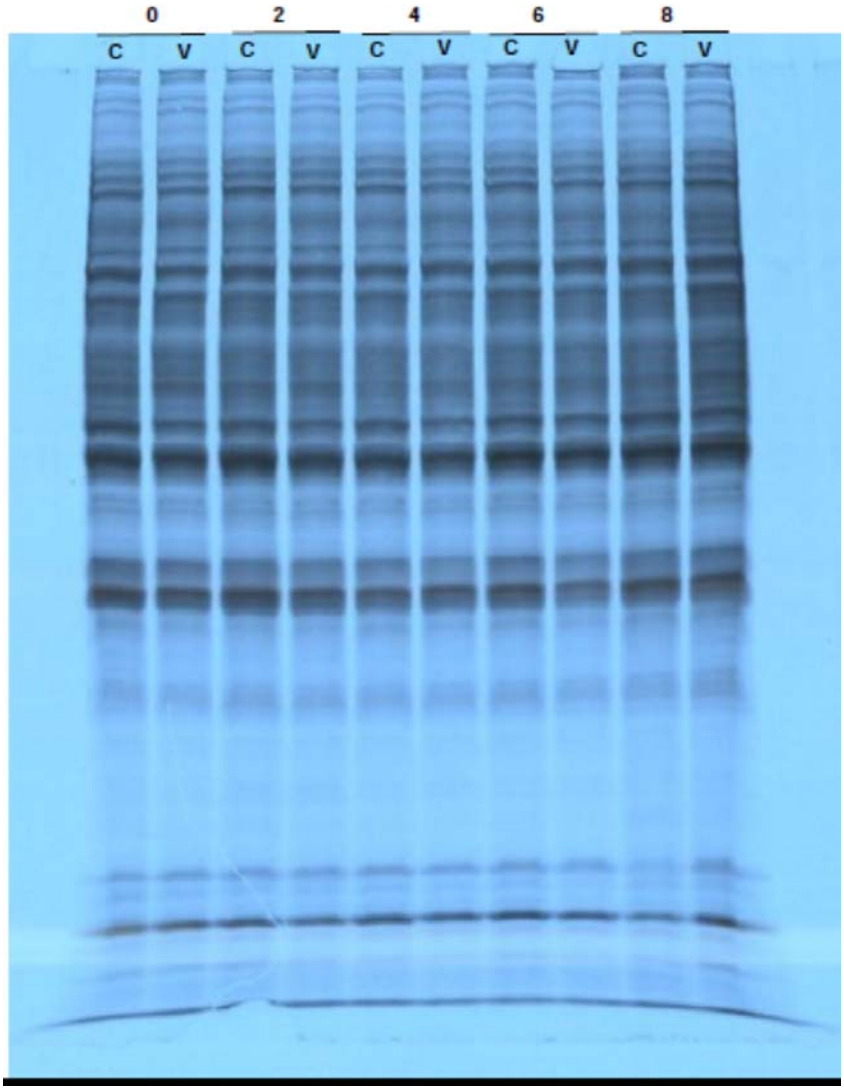

Appendix C1: Early Time Points (0 – 8 h post-infection): [^{35}S] autoradiogram of purine binding proteins in both control, uninfected cells (C) and DENV-infected cells (V) from hour zero to eight post-infection. No observable protein differences are noted between the C and V samples at these early time points in infection.

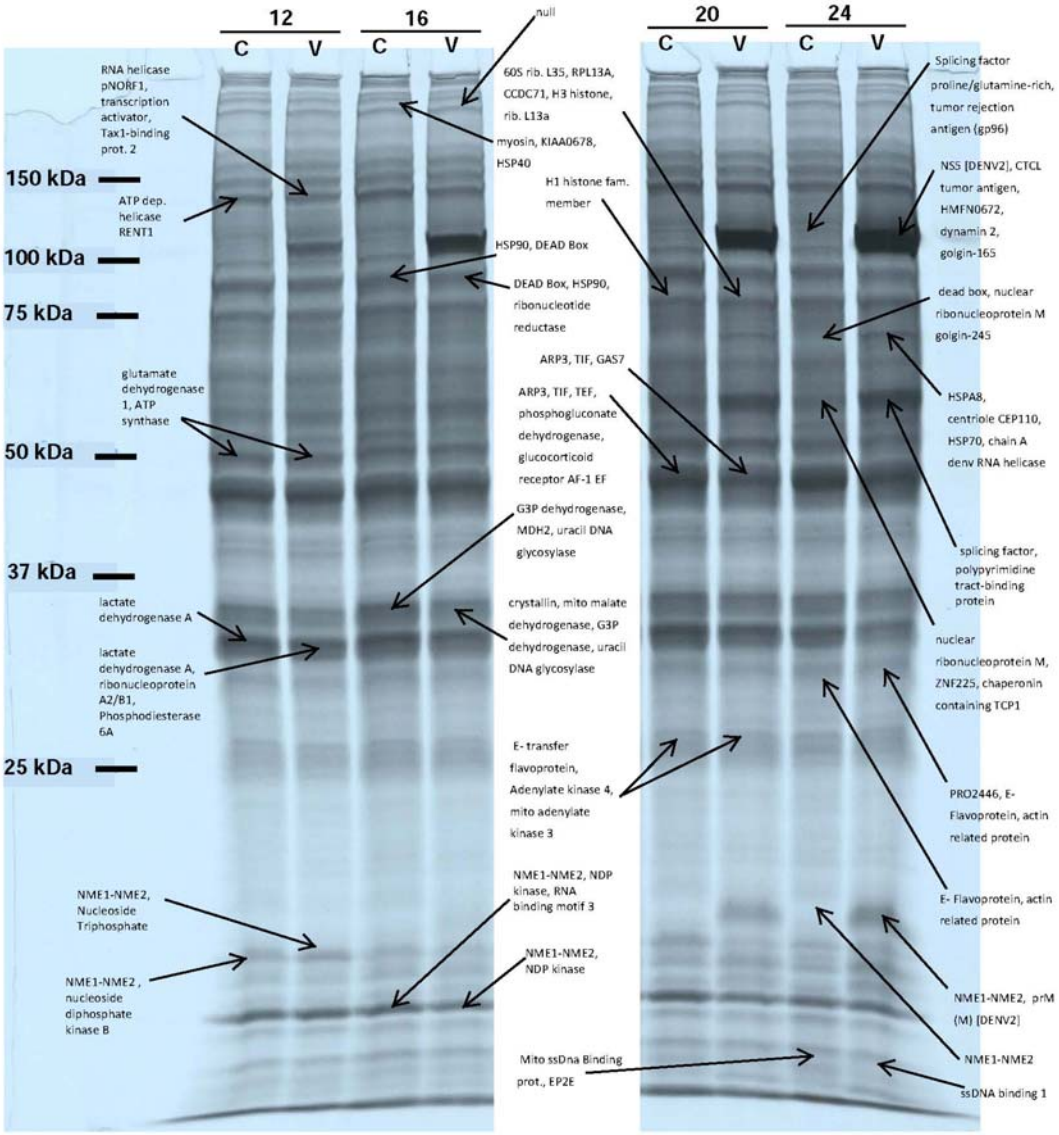

Appendix C2: The same ^{35}S autoradiogram as in Figure 7 showing the proteins identified in the indicated bands.

Appendix D

Virus: MOI = 0
Antibodies: 4G2, No Alexa Fluor 488 (AF488)

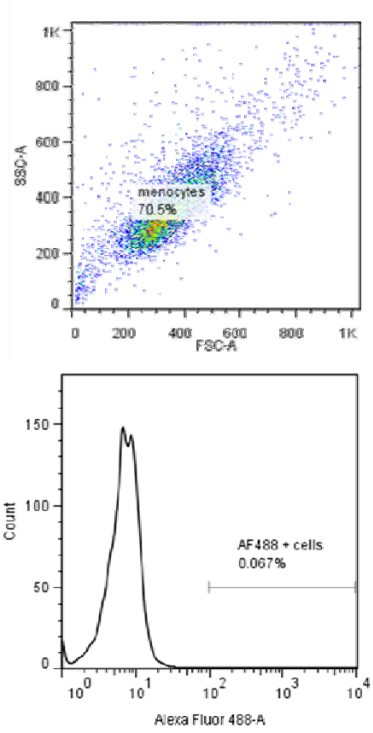

Virus: MOI = 0
Antibodies: 4G2, AF488

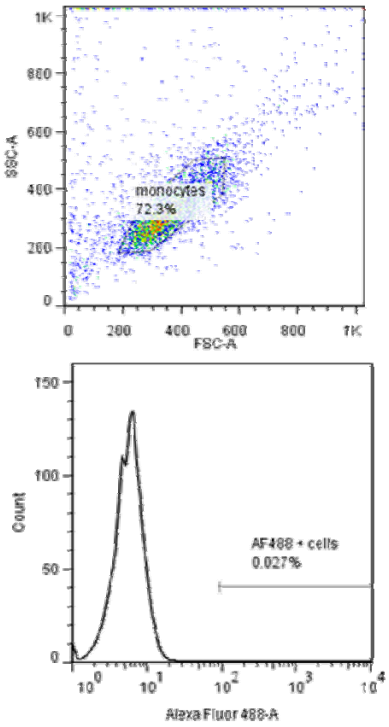

Virus: MOI = 0.05
Antibodies: 4G2, AF488

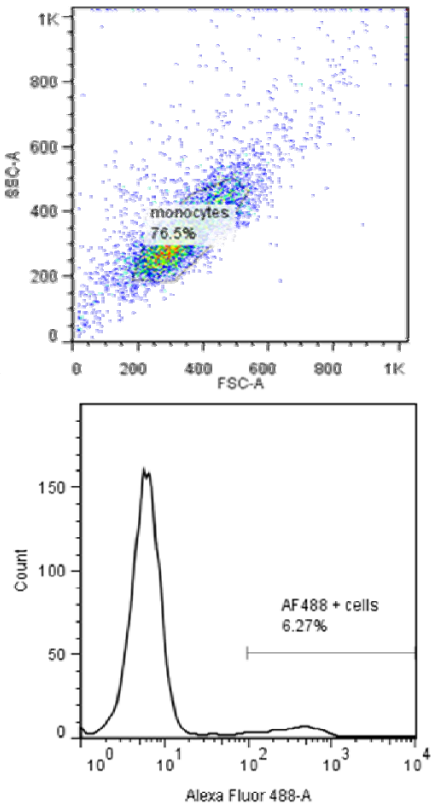

Virus: MOI = 0.1
Antibodies: 4G2, AF488

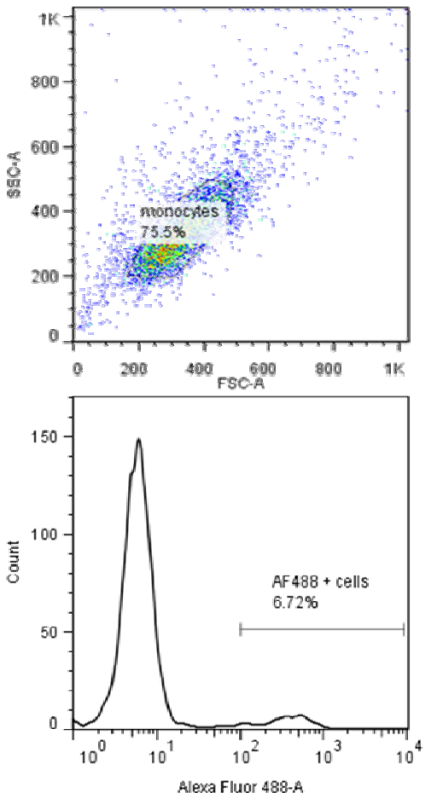

Virus: MOI = 2
Antibodies: 4G2, AF488

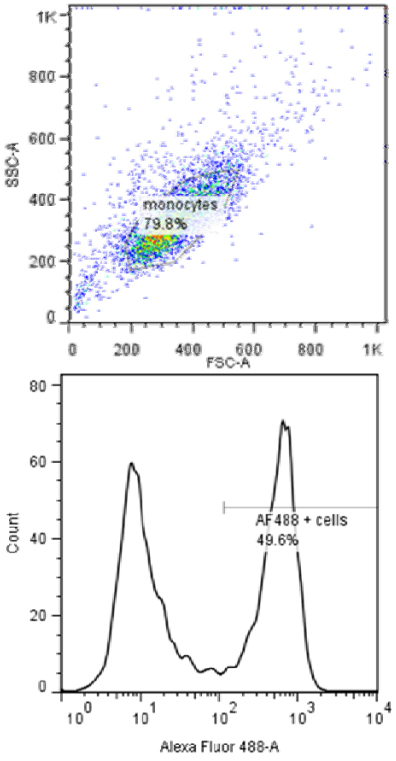

Virus: MOI = 3
Antibodies: 4G2, AF488

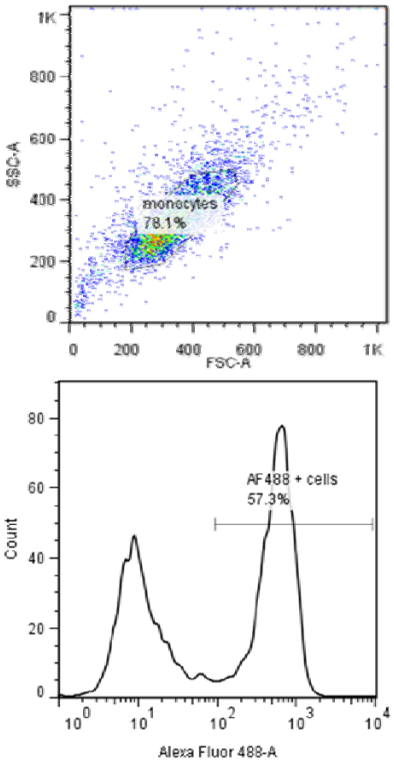

Appendix E

Spot Idx/Pos	181/H17	1	Instr./Spot Origin	ab4700/042810	Process Status	Analysis Succeeded
Plate [#] Name	[1] 042810		4700 Sample Name		Spectra	13

Rank	Protein Name	Accession No.	Protein MW	Protein Score	Protein C. I. %	Total Ion Score	Total Ion C. I. %
1	CTCL tumor antigen se20-7 [Homo sapiens]	gi|11385652	73769.5	56	98.434		

Peptide Information

Calc. Mass	Obsrv. Mass	± da	± ppm	Start Seq.	End Seq.	Sequence	Ion Score	C. I. %	Modification
1302.7449	1302.7048	-0.0401	-31	125	135	VKQEVVDVMKK			
1332.7191	1332.7322	0.0131	10	95	105	KLKAEMDEQIK			
1635.8588	1635.8796	0.0208	13	74	88	AAFEELEKALSTAQK			
1638.9788	1638.9512	-0.0276	-17	416	429	ALKDQINQLELLLK			
1722.8591	1722.9172	0.0581	34	163	175	LQTREREFQEQMK			
1764.8948	1764.9423	0.0475	27	167	180	EREFQEQMKVALEK			
1765.9153	1765.9631	0.0478	27	294	307	LQVLKQQYQTEMEK			
1767.9598	1767.9252	-0.0346	-20	136	150	SSEEQIAKLQKLHEK			
1980.0647	1980.1284	0.0637	32	176	192	VALEKSQSEYLKISQEK			
1980.0647	1980.1284	0.0637	32	176	192	VALEKSQSEYLKISQEK			
2008.0344	2008.0818	0.0474	24	71	88	SERAAFEELEKALSTAQK			
2011.0355	2011.0939	0.0584	29	434	450	HLKEHQAHVENLEADIK			
2202.1111	2202.1943	0.0832	38	324	341	EIIFQAHIEEMNEKTLEK			
2215.175	2215.208	0.033	15	16	34	NLIEQLEQDKGMVIAETKR			
2229.2271	2229.2144	-0.0127	-6	116	134	ISLQQELSRVKQEVVDVMK			
2373.2329	2373.291	0.0581	24	13	33	DAKNLIEQLEQDKGMVIAETK			
2651.3523	2651.4546	0.1023	39	220	241	DLQQEAETYRTRILELESSLEK			
2783.4182	2783.4326	0.0144	5	393	415	NHHQQQVDSIIKEHEVSIQRTEK			
2783.4182	2783.4326	0.0144	5	393	415	NHHQQQVDSIIKEHEVSIQRTEK			

20	putative protein product of HMFN0672 [Homo sapiens]	gi|51555	92622.3	40	28.403			

Peptide Information

Calc. Mass	Obsrv. Mass	± da	± ppm	Start Seq.	End Seq.	Sequence	Ion Score	C. I. %	Modification
1108.6108	1108.6534	0.0426	38	59	67	RVLSNTYQK			
1221.6698	1221.7092	0.0394	32	556	566	NGIYASRTLAR			
1221.6698	1221.7092	0.0394	32	556	566	NGIYASRTLAR			
1253.696	1253.7197	0.0237	19	172	181	LLHRTEELSR			
1264.726	1264.7104	-0.0156	-12	444	453	EYIRKSLLDK			
1288.7153	1288.7308	0.0155	12	386	395	NEMIKLQRTR			
1298.6997	1298.7285	0.0288	22	756	765	EMEKLHRSLR			
1334.7201	1334.7512	0.0311	23	494	504	FAEEKVELLEK			
1735.9635	1735.9049	-0.0586	-34	551	566	AVCLKNGIYASRTLAR			
1765.9199	1765.9631	0.0432	24	340	355	ACQRGFCRDVALVVTK			
1875.9745	1875.9874	0.0129	7	312	328	CSVIWVISDIERVSGGR			
2033.996	2034.0406	0.0446	22	746	762	ELADVGSEYKEMEKLHR			
2227.2544	2227.2356	-0.0188	-8	225	244	IPTSRVITLKAEEAEELSIK			
2240.2471	2240.2817	0.0346	15	348	366	DVALVVTKMDKLHLPEYLR			
2261.177	2261.1936	0.0166	7	235	253	AEEAEELSIKLDPYIRTQR			
2299.1975	2299.1907	-0.0068	-3	706	724	AQERMQHQFQQLKTGIVEK			
2379.3394	2379.2786	-0.0608	-26	630	650	KNFLIQEISAILGGLEDHILR			
2800.3423	2800.4329	0.0906	32	2	25	AETKDVFGQEPHPVEDDLYKEPTR			

28	dynamin 2 isoform 3 [Homo sapiens]	gi|56549	97590.9	38	1.168			

Peptide Information

Calc. Mass	Obsrv. Mass	± da	± ppm	Start Seq.	End Seq.	Sequence	Ion Score	C. I. %	Modification
991.5683	991.6061	0.0378	38	446	453	LSSYPRLR			
1106.5914	1106.6289	0.0375	34	559	567	YMLPLDNLK			
1158.6729	1158.6517	-0.0212	-18	300	309	LQSQLLSLEK			
1348.7471	1348.7173	-0.0298	-22	654	665	NLVDSYVAIINK			
1474.776	1474.8234	0.0474	32	316	327	NFRPDDPTRKTK			
1621.8835	1621.936	0.0525	32	400	414	TGLFTPDLAFEAIVK			
1635.8448	1635.8796	0.0348	21	446	458	LSSYPRLREETER			
1735.9125	1735.9049	-0.0076	-4	45	59	SSVLENFVGRDFLPR			
1762.9445	1762.884	-0.0605	-34	230	245	GYIGVVNRSQKDIEGK			
1875.9435	1875.9874	0.0439	23	257	271	KFFLSHPAYRHMADR			
1899.9854	1899.9282	-0.0572	-30	669	684	DLMPKTIMHLMINNTK			
2254.2666	2254.2515	-0.0151	-7	846	866	RPPAAPSRPTIIRPAEPSLLD			
2273.1692	2273.1973	0.0281	12	167	188	ESSLILAVTPANMDLANSDALK			
2289.2634	2289.1868	-0.0766	-33	654	673	NLVDSYVAIINKSIRDLMPK			
2341.1685	2341.2292	0.0607	26	365	382	IFHERFPFELVKMEFDEK			
2497.2292	2497.2791	0.0499	20	570	590	DVEKGFMSNKHVFAIFNTEQR			
3139.824	3139.7295	-0.0945	-30	114	142	GISPVPINLRVYSPHVLNLTLIDLPGITK			

32	golgin-165	gi|55330	66309.7	38	0			

Peptide Information

Calc. Mass	Obsrv. Mass	± da	± ppm	Start Seq.	End Seq.	Sequence	Ion Score	C. I. %	Modification
1074.6152	1074.6427	0.0275	26	415	423	EKEKVNSLK			
1074.6152	1074.6427	0.0275	26	415	423	EKEKVNSLK			
1081.5887	1081.6182	0.0295	27	341	349	LALELEHEK			
1266.7052	1266.7295	0.0243	19	341	351	LALELEHEKGK			
1266.7052	1266.7295	0.0243	19	341	351	LALELEHEKGK			
1282.6862	1282.7196	0.0334	26	127	137	TAEAELSRLHR			
1332.7117	1332.7322	0.0205	15	7	20	TGDSAALQAVKSGK			
1348.733	1348.7173	-0.0157	-12	229	240	AYENAVGILSRR			
1596.8162	1596.829	0.0128	8	113	125	ELRQELMQVHGEK			
1635.8812	1635.8796	-0.0016	-1	5	20	FRTGDSAALQAVKSGK			
1716.865	1716.8021	-0.0629	-37	312	325	EKVLELEDELQESR			
1965.0624	1965.0811	0.0187	10	127	143	TAEAELSRLHREVAQVR			
2014.0563	2014.1117	0.0554	28	530	546	EIQSLKQQLDLTEQQGR			
2208.2234	2208.2935	0.0701	32	275	294	IQALEAELQAVSHSKTLLEK			
2208.2234	2208.2935	0.0701	32	275	294	IQALEAELQAVSHSKTLLEK			
2221.2773	2221.239	-0.0383	-17	376	394	READLVQLNLQVQAVLQRK			
2299.2	2299.1907	-0.0093	-4	528	546	EREIQSLKQQLDLTEQQGR			

Spot Idx/Pos	182/H19	2	Instr./Spot Origin	ab4700/042810	Process Status	Analysis Succeeded
Plate [#] Name	[1] 042810		4700 Sample Name		Spectra	13

Rank	Protein Name	Accession No.	Protein MW	Protein Score	Protein C. I. %	Total Ion Score	Total Ion C. I. %
1	Splicing factor proline/glutamine-rich (polypyrimidine tract binding protein associated) [Homo sapi	gi|29881667	76140.7	57	98.636		

Peptide Information

Calc. Mass	Obsrv. Mass	± da	± ppm	Start	End	Sequence	Ion	C. I. %	Modification

				Seq.	Seq.		Score
1120.5204	1120.5302	0.0098	9	682	693	GMGPGTPAGYGR	
1143.6268	1143.6382	0.0114	10	366	376	FATHAAALSVR	
1143.6268	1143.6382	0.0114	10	366	376	FATHAAALSVR	
1153.6364	1153.6501	0.0137	12	333	342	GFGFIKLESR	
1267.6211	1267.6398	0.0187	15	33	44	SPPPGMGLNQNR	
1341.6656	1341.6849	0.0193	14	667	681	FGQGGAGPVGGQGPR	
1341.6656	1341.6849	0.0193	14	667	681	FGQGGAGPVGGQGPR	
1347.6776	1347.6803	0.0027	2	6	18	FRSRGGGGGGFHR	
1398.7964	1398.801	0.0046	3	364	376	VRFATHAAALSVR	
1649.8856	1649.9034	0.0178	11	272	286	ISDSEGFKANLSLLR	
1743.8945	1743.8977	0.0032	2	343	358	ALAEIAKAELDDTPMR	
1762.7819	1762.7941	0.0122	7	480	493	FAQHGTFEYEYSQR	
1762.7819	1762.7941	0.0122	7	480	493	FAQHGTFEYEYSQR	
1964.0123	1964.0171	0.0048	2	299	315	LFVGNLPADITEDEFKR	
1964.0123	1964.0171	0.0048	2	299	315	LFVGNLPADITEDEFKR	
2428.1196	2428.1335	0.0139	6	517	536	DKLESEMEDAYHEHQANLLR	
2639.2986	2639.3003	0.0017	1	377	399	NLSPYVSNELLEEAFSQFGPIER	
2639.2986	2639.3003	0.0017	1	377	399	NLSPYVSNELLEEAFSQFGPIER	
2673.2791	2673.2612	-0.0179	-7	243	267	GGRQHHPPYHQQHHQGPPPGGPGGR	

Rank	Protein Name	Accession No.	Protein MW	Protein Score	Protein C. I. %	Total Ion Score	Total Ion C. I. %
4	tumor rejection antigen (gp96) 1 [Homo sapiens]	gi|4507677	92411.3	44	73.399		

Peptide Information

Calc. Mass	Obsrv. Mass	± da	± ppm	Start Seq.	End Seq.	Sequence	Ion Score	C. I. %	Modification
1015.473	1015.4883	0.0153	15	396	404	GLFDEYGSK			
1485.7543	1485.766	0.0117	8	435	448	GVVDSDDLPLNVSR			
1544.8278	1544.8228	-0.005	-3	103	116	ELISNASDALDKIR			
1751.8243	1751.8429	0.0186	11	415	428	RVFITDDFHDMMPK			
1751.8243	1751.8429	0.0186	11	415	428	RVFITDDFHDMMPK			
2112.1116	2112.1108	-0.0008	0	143	161	NLLHVTDTGVGMTREELVK			
2260.0627	2260.0723	0.0096	4	512	530	FQSSHHPTDITSLDQYVER			
2260.0627	2260.0723	0.0096	4	512	530	FQSSHHPTDITSLDQYVER			
2265.1145	2265.1028	-0.0117	-5	664	683	AQAYQTGKDISTNYYASQKK			
2283.1414	2283.1443	0.0029	1	411	428	LYVRRVFITDDFHDMMPK			
2299.0481	2299.0669	0.0188	8	640	660	LTESPCALVASQYGWSGNMER			
2728.3384	2728.3604	0.022	8	44	67	TDDEVVQREEEAIQLDGLNASQIR			
2733.4556	2733.4648	0.0092	3	701	724	IKEDEDDKTVLDLAVVLFETATLR			
3157.5354	3157.5505	0.0151	5	40	67	EGSRTDDEVVQREEEAIQLDGLNASQIR			

Spot Idx/Pos	183/H21	3		**Instr./Spot Origin**	ab4700/042810	**Process Status**	Analysis Succeeded
Plate [#] Name	[1] 042810			**4700 Sample Name**		**Spectra**	13

Rank	Protein Name	Accession No.	Protein MW	Protein Score	Protein C. I. %	Total Ion Score	Total Ion C. I. %
1	premembrane [Dengue virus type 2]	gi|18308050	13563.5	45	0	4	0

Peptide Information

Calc. Mass	Obsrv. Mass	± da	± ppm	Start Seq.	End Seq.	Sequence	Ion Score	C. I. %	Modification
1139.5625	1139.5715	0.009	8	7	16	NGEPHMIVSR	4	0	
1139.5625	1139.5715	0.009	8	7	16	NGEPHMIVSR			
1412.6151	1412.6093	-0.0058	-4	107	118	TETWMSSEGAWK			
1524.7587	1524.7587	0	0	7	19	NGEPHMIVSRQEK			
1565.8468	1565.8579	0.0111	7	92	106	SVALVPHVGMGLETR			
1565.8468	1565.8579	0.0111	7	92	106	SVALVPHVGMGLETR			

2	prM (M) protein [Dengue virus type 2]	gi|25059129	18859.3	40	0	4	0		

Peptide Information

Calc. Mass	Obsrv. Mass	± da	± ppm	Start Seq.	End Seq.	Sequence	Ion Score	C. I. %	Modification
1139.5625	1139.5715	0.009	8	7	16	NGEPHMIVSR	4	0	
1139.5625	1139.5715	0.009	8	7	16	NGEPHMIVSR			
1412.6151	1412.6093	-0.0058	-4	107	118	TETWMSSEGAWK			
1524.7587	1524.7587	0	0	7	19	NGEPHMIVSRQEK			
1565.8468	1565.8579	0.0111	7	92	106	SVALVPHVGMGLETR			
1565.8468	1565.8579	0.0111	7	92	106	SVALVPHVGMGLETR			

15	polyprotein [Dengue virus type 2]	gi|58234	17119.3	33	0	4	0		

Peptide Information

Calc. Mass	Obsrv. Mass	± da	± ppm	Start Seq.	End Seq.	Sequence	Ion Score	C. I. %	Modification
1139.5625	1139.5715	0.009	8	99	108	NGEPHMIVSR	4	0	
1139.5625	1139.5715	0.009	8	99	108	NGEPHMIVSR			
1524.7587	1524.7587	0	0	99	111	NGEPHMIVSRQEK			
3337.7402	3337.7163	-0.0239	-7	79	108	TAGMIIMLIPTVMAFHLTTRNGEPHMIVSR			

16	polyprotein [Dengue virus type 2]	gi|52219	17111.2	33	0	4	0		

Peptide Information

Calc. Mass	Obsrv. Mass	± da	± ppm	Start Seq.	End Seq.	Sequence	Ion Score	C. I. %	Modification
1139.5625	1139.5715	0.009	8	99	108	NGEPHMIVSR	4	0	
1139.5625	1139.5715	0.009	8	99	108	NGEPHMIVSR			
1524.7587	1524.7587	0	0	99	111	NGEPHMIVSRQEK			
3337.7402	3337.7163	-0.0239	-7	79	108	TVGMIIMLIPTAMAFHLTTRNGEPHMIVSR			

2	NME1-NME2 protein [Homo sapiens]	gi|66392203	30117.6	29	0		

Peptide Information

Calc. Mass	Obsrv. Mass	± da	± ppm	Start Seq.	End Seq.	Sequence	Ion Score	C. I. %	Modification
1344.7633	1344.7715	0.0082	6	7	18	TFIAIKPDGVQR			
1344.7633	1344.7715	0.0082	6	122	133	TFIAIKPDGVQR			
1785.9163	1785.9147	-0.0016	-1	204	220	VMLGETNPADSKPGTIR			
1785.9163	1785.9147	-0.0016	-1	89	105	VMLGETNPADSKPGTIR			

Spot Idx/Pos	184/H23	4	**Instr./Spot Origin**	ab4700/042810	**Process Status**	Analysis Succeeded
Plate [#] Name	[1] 042810		**4700 Sample Name**		**Spectra**	13

Rank	Protein Name	Accession No.	Protein MW	Protein Score	Protein C. I. %	Total Ion Score	Total Ion C. I. %
4	NME1-NME2 protein [Homo sapiens]	gi|66392203	30117.6	23	0		

Peptide Information

Calc. Mass	Obsrv. Mass	± da	± ppm	Start Seq.	End Seq.	Sequence	Ion Score	C. I. %	Modification
1344.7633	1344.7639	0.0006	0	122	133	TFIAIKPDGVQR			
1344.7633	1344.7639	0.0006	0	7	18	TFIAIKPDGVQR			
1785.9163	1785.9246	0.0083	5	89	105	VMLGETNPADSKPGTIR			
1785.9163	1785.9246	0.0083	5	204	220	VMLGETNPADSKPGTIR			

Spot Idx/Pos	193/H14	5	**Instr./Spot Origin**	ab4700/042810	**Process Status**	Analysis Succeeded
Plate [#] Name	[1] 042810		**4700 Sample Name**		**Spectra**	13

Rank	Protein Name	Accession No.	Protein MW	Protein Score	Protein C. I. %	Total Ion Score	Total Ion C. I. %
1	splicing factor homolog - human	gi|543010	54233.3	65	99.794		

Peptide Information

Calc. Mass	Obsrv. Mass	± da	± ppm	Start Seq.	End Seq.	Sequence	Ion Score	C. I. %	Modification
1147.6179	1147.6321	0.0142	12	271	279	WKALIEMEK			
1195.6581	1195.6519	-0.0062	-5	110	119	GFGFIRLETR			
1231.6792	1231.6819	0.0027	2	191	202	GIVEFSGKPAAR			
1248.6735	1248.6707	-0.0028	-2	97	107	YGKAGEVFIHK			
1457.7706	1457.7668	-0.0038	-3	338	348	KQLELRQEEER			
1538.6694	1538.6843	0.0149	10	384	398	MGQMAMGGAMGINNR			
1695.7471	1695.7589	0.0118	7	257	270	FAQPGSFEYEYAMR			
1695.7471	1695.7589	0.0118	7	257	270	FAQPGSFEYEYAMR			
1812.9888	1812.989	0.0002	0	120	135	TLAEIAKVELDNMPLR			
1814.0031	1813.995	-0.0081	-4	185	202	GRPSGKGIVEFSGKPAAR			
1859.9207	1859.9332	0.0125	7	76	91	LFVGNLPPDITEEEMR			
1859.9207	1859.9332	0.0125	7	76	91	LFVGNLPPDITEEEMR			
1880.0183	1879.993	-0.0253	-13	138	153	QLRVRFACHSASLHVR			
1988.0156	1988.0286	0.013	7	76	92	LFVGNLPPDITEEEMRK			
2163.0649	2163.074	0.0091	4	435	456	FGQAATMEGIGAIGGTPPAFNR			
2163.0649	2163.074	0.0091	4	435	456	FGQAATMEGIGAIGGTPPAFNR			
2231.1487	2231.1167	-0.032	-14	74	92	SRLFVGNLPPDITEEEMRK			
2498.177	2498.1924	0.0154	6	294	313	EKLEMEMEAARHEHQVMLMR			
2668.3252	2668.3274	0.0022	1	154	176	NLPQYVSNELLEEAFSVFGQVER			
2668.3252	2668.3274	0.0022	1	154	176	NLPQYVSNELLEEAFSVFGQVER			
3451.7058	3451.7124	0.0066	2	399	434	GAMPPAPVPAGTPAPPGPATMMPDGTLGLTPPTTER			

12	polypyrimidine tract-binding protein 1 isoform c [Homo sapiens]	gi|14165466	57185.6	24	0	

Peptide Information

Calc. Mass	Obsrv. Mass	± da	± ppm	Start Seq.	End Seq.	Sequence	Ion Score	C. I. %	Modification
1184.6521	1184.6644	0.0123	10	2	13	DGIVPDIAVGTK			
1431.7379	1431.7369	-0.001	-1	123	134	GQPIYIQFSNHK			
2039.0959	2039.0962	0.0003	0	349	366	VTPQSLFILFGVYGDVQR			
2039.0959	2039.0962	0.0003	0	349	366	VTPQSLFILFGVYGDVQR			
2144.0002	2144.0244	0.0242	11	419	437	EGQEDQGLTKDYGNSPLHR			
2275.2766	2275.2791	0.0025	1	326	348	IAIPGLAGAGNSVLLVSNLNPER			
2275.2766	2275.2791	0.0025	1	326	348	IAIPGLAGAGNSVLLVSNLNPER			
3206.5132	3206.5435	0.0303	9	95	122	NQAFIEMNTEEAANTMVNYYTSVTPVLR			
3391.6296	3391.6753	0.0457	13	93	122	GKNQAFIEMNTEEAANTMVNYYTSVTPVLR			
3680.8845	3680.8735	-0.011	-3	147	185	AQAALQAVNSVQSGNLALAASAAAVDAGMAMAGQSPVLR			

Spot Idx/Pos	138/F4	6	**Instr./Spot Origin**	ab4700/042810	**Process Status**	Analysis Succeeded
Plate [#] Name	[1] 042810		**4700 Sample Name**		**Spectra**	13

Rank	Protein Name	Accession No.	Protein MW	Protein Score	Protein C. I. %	Total Ion Score	Total Ion C. I. %
1	non-POU domain containing, octamer-binding [Homo sapiens]	gi|34932414	54197.3	87	99.999		

Protein Group

splicing factor homolog - human	gi|543010	54233.3

Peptide Information

Calc. Mass	Obsrv. Mass	± da	± ppm	Start Seq.	End Seq.	Sequence	Ion Score	C. I. %	Modification
1147.6179	1147.5594	-0.0585	-51	271	279	WKALIEMEK			
1180.5714	1180.5752	0.0038	3	305	313	HEHQVMLMR			
1195.6581	1195.5901	-0.068	-57	110	119	GFGFIRLETR			
1336.6235	1336.6051	-0.0184	-14	294	304	EKLEMEMEAAR			
1480.7179	1480.6635	-0.0544	-37	366	378	QQEGFKGTFPDAR			
1538.6694	1538.6031	-0.0663	-43	384	398	MGQMAMGGAMGINNR			
1538.6694	1538.6031	-0.0663	-43	384	398	MGQMAMGGAMGINNR			
1636.819	1636.7764	-0.0426	-26	365	378	RQQEGFKGTFPDAR			
1695.7471	1695.6763	-0.0708	-42	257	270	FAQPGSFEYEYAMR			
1695.7471	1695.6763	-0.0708	-42	257	270	FAQPGSFEYEYAMR			
1812.9888	1812.8975	-0.0913	-50	120	135	TLAEIAKVELDNMPLR			
1824.8479	1824.8483	0.0004	0	358	371	QQEEMMRRQQEGFK			
1859.9207	1859.8271	-0.0936	-50	76	91	LFVGNLPPDITEEEMR			
1859.9207	1859.8271	-0.0936	-50	76	91	LFVGNLPPDITEEEMR			
2163.0649	2162.9634	-0.1015	-47	435	456	FGQAATMEGIGAIGGTPPAFNR			
2163.0649	2162.9634	-0.1015	-47	435	456	FGQAATMEGIGAIGGTPPAFNR			
2231.1487	2231.0532	-0.0955	-43	74	92	SRLFVGNLPPDITEEEMRK			
2303.0549	2303.0408	-0.0141	-6	252	270	EQPPRFAQPGSFEYEYAMR			
2498.177	2498.0669	-0.1101	-44	294	313	EKLEMEMEAARHEHQVMLMR			
2668.3252	2668.187	-0.1382	-52	154	176	NLPQYVSNELLEEAFSVFGQVER			
2668.3252	2668.187	-0.1382	-52	154	176	NLPQYVSNELLEEAFSVFGQVER			
3451.7058	3451.4951	-0.2107	-61	399	434	GAMPPAPVPAGTPAPPGPATMMPDGTLGLTPPTTER			

3	heterogeneous nuclear ribonucleoprotein M isoform b [Homo sapiens]	gi|14141154	73512.3	65	99.774	

Peptide Information

Calc. Mass	Obsrv. Mass	± da	± ppm	Start Seq.	End Seq.	Sequence	Ion Score	C. I. %	Modification
1167.5833	1167.5872	0.0039	3	620	628	NLPFDFTWK			
1214.5759	1214.6051	0.0292	24	38	48	GEGERPAQNEK			
1336.671	1336.6051	-0.0659	-49	647	659	MENGKSKGCGVVK			
1383.6143	1383.5405	-0.0738	-53	568	582	MGLAMGGGGGASFDR			
1480.7069	1480.6635	-0.0434	-29	398	410	MGLVMDRMGSVER			
1550.7413	1550.8208	0.0795	51	433	446	MGQTMERIGSGVER			
1550.7413	1550.8208	0.0795	51	433	446	MGQTMERIGSGVER			
1715.8164	1715.8145	-0.0019	-1	113	127	GCAVVEFKMEESMKK			
1739.9591	1739.87	-0.0891	-51	70	83	RYRAFITNIPFDVK			
1821.9163	1821.8356	-0.0807	-44	652	668	SKGCGVVKFESPEVAER			
2163.0476	2162.9634	-0.0842	-39	589	612	GNFGGSFAGSFGGAGGHAPGVARK			
2163.0476	2162.9634	-0.0842	-39	589	612	GNFGGSFAGSFGGAGGHAPGVARK			
2211.05	2210.9856	-0.0644	-29	398	417	MGLVMDRMGSVERMGS			

							GIER
	2249.0947	2248.9844	-0.1103	-49	512	531	MATGLERMGANNLERM GLER
	2273.1487	2273.0679	-0.0808	-36	465	485	VGQTIERMGSGVERMGP AIER
	2283.0896	2283.0515	-0.0381	-17	634	653	FNECGHVLYADIKMENG KSK
	2599.2107	2599.2087	-0.002	-1	365	390	MGPGIDRLGGAGMERM GAGLGHGMDR
	2733.3125	2733.1404	-0.1721	-63	493	518	MVPAGMGAGLERMGPV MDRMATGLER
	2829.416	2829.2468	-0.1692	-60	95	120	VGEVTYVELLMDAEGKS RGCAVVEFK

12 ZNF225 [amino acids 79-706] [Homo sapiens] gi|9502402 73081.2 56 98.283

Peptide Information

Calc. Mass	Obsrv. Mass	± da	± ppm	Start Seq.	End Seq.	Sequence	Ion Score	C. I. %	Modification
1044.5221	1044.4824	-0.0397	-38	343	351	AHSGEKPYR			
1380.6654	1380.621	-0.0444	-32	443	453	FTQNSQLYSHR			
1403.6558	1403.5857	-0.0701	-50	268	278	CEECGKRFIYR			
1550.7822	1550.8208	0.0386	25	415	426	FTQNSQLYTHRR			
1550.7822	1550.8208	0.0386	25	414	425	RFTQNSQLYTHR			
1566.7805	1566.735	-0.0455	-29	251	264	SALNSHRMVHTGEK			
1695.765	1695.6763	-0.0887	-52	119	133	VHMGEKLYNCDVCGK			
1695.765	1695.6763	-0.0887	-52	119	133	VHMGEKLYNCDVCGK			
1715.8361	1715.8145	-0.0216	-13	338	351	YSHQRAHSGEKPYR			
1729.8993	1729.8163	-0.083	-48	557	570	WASTHLTHQRLHSR			
1815.8879	1815.8359	-0.052	-29	235	250	EKPFRCDTCGKSFGLK			
1875.8839	1875.8468	-0.0371	-20	511	526	LHGDEKPFKCEECGKR			
1923.9163	1923.8796	-0.0367	-19	240	257	CDTCGKSFGLKSALNSH R			
2077.1301	2077.051	-0.0791	-38	502	519	ASSILNHKRLHGDEKPFK			
2211.0684	2210.9856	-0.0828	-37	455	474	VHTGVKPYKCEECGKGF NSK			
2242.979	2243.0322	0.0532	24	464	482	CEECGKGFNSKFNLDMH QR			
2249.1064	2248.9844	-0.122	-54	106	124	SFCYSSALRIHQRVHMG EK			

Spot Idx/Pos	194/H16	7	**Instr./Spot Origin**	ab4700/042810	**Process Status** Analysis Succeeded
Plate [#] Name	[1] 042810		**4700 Sample Name**		**Spectra** 13

Rank	Protein Name	Accession No.	Protein MW	Protein Score	Protein C. I. %	Total Ion Score	Total Ion C. I. %
5	hypothetical protein [Homo sapiens]	gi|34365255	56551.9	32	0		

Peptide Information

Calc. Mass	Obsrv. Mass	± da	± ppm	Start Seq.	End Seq.	Sequence	Ion Score	C. I. %	Modification
975.5105	975.512	0.0015	2	319	326	SEVKDEIR			
1360.7001	1360.6941	-0.006	-4	295	305	KQMANQKDLER			
1491.7537	1491.7567	0.003	2	140	152	ESEESKLDQVLSK			
1647.837	1647.8448	0.0078	5	195	209	SGELLALQKEADSMR			
1678.8767	1678.8824	0.0057	3	125	137	LVQQEMMFQRLQK			
1708.8687	1708.8544	-0.0143	-8	169	182	WCESLEKTLSQTKR			
1837.9918	1838.0012	0.0094	5	210	224	ADFSLLRNQFLTERK			
1840.9398	1840.9482	0.0084	5	108	122	QQQLQVLQNEIEENK			
2034.9912	2034.9933	0.0021	1	160	175	VRTLQEEERWCESLEK			
2217.1042	2217.1138	0.0096	4	278	294	RLMKELNQMQYEYTELK			
2226.1182	2226.1306	0.0124	6	26	44	DKLSLHNDISAMQQQLQ EK			
2262.1836	2262.1836	0	0	67	85	QDLLHTTKHQDVLLSEQT R			
2338.1509	2338.1682	0.0173	7	377	395	LNFSQVHIMDEHWRGEA LR			

14	HSPA8 protein [Homo sapiens]	gi|48257068	64633.1	27	0	

Peptide Information

Calc. Mass	Obsrv. Mass	± da	± ppm	Start Seq.	End Seq.	Sequence	Ion Score	C. I. %	Modification
1199.6742	1199.6604	-0.0138	-12	101	112	DAGTIAGLNVLR			
1235.624	1235.632	0.008	6	178	187	MVNHFIAEFK			
1252.6605	1252.6497	-0.0108	-9	68	78	MKEIAEAYLGK			
1253.616	1253.6311	0.0151	12	243	252	FEELNADLFR			
1391.7252	1391.7244	-0.0008	-1	178	188	MVNHFIAEFKR			
1480.7543	1480.7609	0.0066	4	241	252	ARFEELNADLFR			
1480.7543	1480.7609	0.0066	4	241	252	ARFEELNADLFR			
1653.8318	1653.8531	0.0213	13	30	43	HWPFMVVNDAGRPK			
1745.8088	1745.7985	-0.0103	-6	525	538	NQTAEKEEFEHQQK			
1838.0129	1838.0012	-0.0117	-6	267	283	LDKSQIHDIVLVGGSTR			
1952.0599	1952.035	-0.0249	-13	393	410	DNNLLGKFELTGIPPAPR			
1981.9977	1981.9973	-0.0004	0	79	96	TVTNAVVTVPAYFNDSQ R			
1981.9977	1981.9973	-0.0004	0	79	96	TVTNAVVTVPAYFNDSQ R			
2774.3267	2774.3303	0.0036	1	365	388	QTQTFTTYSDNQPGVLIQ VYEGER			
2997.4575	2997.4656	0.0081	3	214	240	TLSSSTQASIEIDSLYEGI DFYTSITR			

29	centriole associated protein CEP110 [Homo sapiens]	gi|3435244	116741.2	24	0	

Peptide Information

Calc. Mass	Obsrv. Mass	± da	± ppm	Start Seq.	End Seq.	Sequence	Ion Score	C. I. %	Modification
975.5105	975.512	0.0015	2	831	838	SEVKDEIR			
1187.6378	1187.6272	-0.0106	-9	477	487	RVLAAAEENSK			
1360.7001	1360.6941	-0.006	-4	807	817	KQMANQKDLER			
1443.755	1443.7632	0.0082	6	163	175	ADQQLRSLQADAK			
1524.7726	1524.7831	0.0105	7	194	207	IVAAKDSDFQCLSK			
1524.7726	1524.7831	0.0105	7	194	207	IVAAKDSDFQCLSK			
1551.7496	1551.7626	0.013	8	625	637	ERESEESKLETSK			
1647.837	1647.8448	0.0078	5	707	721	SGELLALQKEADSMR			
1678.8767	1678.8824	0.0057	3	612	624	LVQQEMMFQRLQK			
1708.8687	1708.8544	-0.0143	-8	681	694	WCESLEKTLSQTKR			
1799.8955	1799.9078	0.0123	7	41	55	SLECEVEELHRTVQK			
1837.9918	1838.0012	0.0094	5	722	736	ADFSLLRNQFLTERK			
1840.9398	1840.9482	0.0084	5	595	609	QQQLQVLQNEIEENK			
2034.9912	2034.9933	0.0021	1	672	687	VRTLQEEERWCESLEK			
2217.1042	2217.1138	0.0096	4	790	806	RLMKELNQMQYEYTELK			
2226.1182	2226.1306	0.0124	6	513	531	DKLSLHNDISAMQQQLQ EK			
2262.1836	2262.1836	0	0	554	572	QDLLHTTKHQDVLLSEQT R			
2283.1509	2283.1655	0.0146	6	256	275	SQVTSQQQEMAVLDRQL GHK			
2338.1521	2338.1682	0.0161	7	132	151	FTDAKRSLLQTESDAEEL ER			

33	heat shock 70kDa protein 8 isoform 2 variant [Homo sapiens]	gi|62896815	53466.4	24	0	

Peptide Information

Calc. Mass	Obsrv. Mass	± da	± ppm	Start Seq.	End Seq.	Sequence	Ion Score	C. I. %	Modification
1199.6742	1199.6604	-0.0138	-12	160	171	DAGTIAGLNVLR			

1235.624	1235.632	0.008	6	237	246	MVNHFIAEFK	
1252.6605	1252.6497	-0.0108	-9	127	137	MKEIAEAYLGK	
1253.616	1253.6311	0.0151	12	302	311	FEELNADLFR	
1391.7252	1391.7244	-0.0008	-1	237	247	MVNHFIAEFKR	
1480.7543	1480.7609	0.0066	4	300	311	ARFEELNADLFR	
1480.7543	1480.7609	0.0066	4	300	311	ARFEELNADLFR	
1653.8318	1653.8531	0.0213	13	89	102	HWPFMVVNDAGRPK	
1838.0129	1838.0012	-0.0117	-6	326	342	LDKSQIHDIVLVGGSTR	
1981.9977	1981.9973	-0.0004	0	138	155	TVTNAVVTVPAYFNDSQR	
1981.9977	1981.9973	-0.0004	0	138	155	TVTNAVVTVPAYFNDSQR	
2774.3267	2774.3303	0.0036	1	424	447	QTQTFTTYSDNQPGVLIQVYEGER	
2997.4575	2997.4656	0.0081	3	273	299	TLSSSTQASIEIDSLYEGIDFYTSITR	

Spot Idx/Pos	140/F8	8	**Instr./Spot Origin**	ab4700/042810	**Process Status** Analysis Succeeded
Plate [#] Name	[1] 042810		**4700 Sample Name**		**Spectra** 13

Rank	Protein Name	Accession No.	Protein MW	Protein Score	Protein C. I. %	Total Ion Score	Total Ion C. I. %
2	dead box, X isoform [Homo sapiens]	gi|25805	73226	44	74.005		

Peptide Information

Calc. Mass	Obsrv. Mass	± da	± ppm	Start Seq.	End Seq.	Sequence	Ion Score	C. I. %	Modification
895.5148	895.5149	0.0001	0	38	44	YIPPHLR			
1182.5497	1182.5872	0.0375	32	100	110	GRSDYDGIGSR			
1182.5497	1182.5872	0.0375	32	100	110	GRSDYDGIGSR			
1300.6392	1300.6202	-0.019	-15	479	488	DREEALHQFR			
1300.6392	1300.6202	-0.019	-15	479	488	DREEALHQFR			
1320.6793	1320.6575	-0.0218	-17	277	287	ELAVQIYEEAR			
1320.6793	1320.6575	-0.0218	-17	277	287	ELAVQIYEEAR			
1336.6388	1336.625	-0.0138	-10	352	362	MLDMGFEPQIR			
1336.6388	1336.625	-0.0138	-10	352	362	MLDMGFEPQIR			
1485.8787	1485.8275	-0.0512	-34	264	276	KQYPISLVLAPTR			
1502.7094	1502.7466	0.0372	25	82	95	SSFFSDRGSGSRGR			
1524.7804	1524.756	-0.0244	-16	535	548	VGNLGLATSFFNER			
1524.7804	1524.756	-0.0244	-16	535	548	VGNLGLATSFFNER			
1557.7947	1557.7716	-0.0231	-15	395	407	DFLDEYIFLAVGR			
1557.7947	1557.7716	-0.0231	-15	395	407	DFLDEYIFLAVGR			
2083.0242	2082.9902	-0.034	-16	512	528	HVINFDLPSDIEEYVHR			
2332.2546	2332.1785	-0.0761	-33	231	252	TAAFLLPILSQIYSDGPGEALR			

8	heterogeneous nuclear ribonucleoprotein M isoform a variant [Homo sapiens]	gi|62089046		65211.2	21	0	

Peptide Information

Calc. Mass	Obsrv. Mass	± da	± ppm	Start Seq.	End Seq.	Sequence	Ion Score	C. I. %	Modification
1427.7133	1427.7297	0.0164	11	477	491	MGPAMGPALGAGIER			
1613.7773	1613.7665	-0.0108	-7	342	356	MGPLGLDHMASSIER			
2034.9528	2034.9397	-0.0131	-6	513	535	GNFGGSFAGSFGGAGGHAPGVAR			
2034.9528	2034.9397	-0.0131	-6	513	535	GNFGGSFAGSFGGAGGHAPGVAR			
2211.05	2211.05	0	0	322	341	MGLVMDRMGSVERMGSGIER			
2283.0896	2283.1208	0.0312	14	558	577	FNECGHVLYADIKMENGKSK			
2286.115	2286.1216	0.0066	3	469	491	MGANSLERMGPAMGPALGAGIER			

9	golgin-245 [Homo sapiens]	gi|1173565		244378.2	48	88.388	

Peptide Information

Calc. Mass	Obsrv. Mass	± da	± ppm	Start Seq.	End Seq.	Sequence	Ion Score	C. I. %	Modification
895.5359	895.5149	-0.021	-23	336	342	LQKLHEK			
1104.5782	1104.569	-0.0092	-8	1166	1175	ADIESLVTEK			
1104.5782	1104.569	-0.0092	-8	1166	1175	ADIESLVTEK			
1182.6224	1182.5872	-0.0352	-30	2	11	ERSLSSYRGK			
1182.6224	1182.5872	-0.0352	-30	2	11	ERSLSSYRGK			
1233.6508	1233.6006	-0.0502	-41	1508	1517	KQLLSQMEEK			
1233.6508	1233.6006	-0.0502	-41	1508	1517	KQLLSQMEEK			
1439.7375	1439.7792	0.0417	29	373	384	SQSEYLKISQEK			
1439.7375	1439.7792	0.0417	29	373	384	SQSEYLKISQEK			
1502.806	1502.7466	-0.0594	-40	838	850	KELENTALELSQK			
1524.7903	1524.756	-0.0343	-22	1050	1062	SNKSLEDKSLEFK			
1524.7903	1524.756	-0.0343	-22	1050	1062	SNKSLEDKSLEFK			
1592.8577	1592.905	0.0473	30	456	468	HNKEITVMVEKHK			
1635.8588	1635.8716	0.0128	8	266	280	AAFEELEKALSTAQK			
1778.9143	1778.8341	-0.0802	-45	410	423	LRDLQQEAETYRTR			
1833.9812	1833.9382	-0.043	-23	1063	1078	KLSEELAIQLDICCKK			
1910.9528	1910.9139	-0.0389	-20	1509	1523	QLLSQMEEKEEQYKK			
1930.0062	1929.9452	-0.061	-32	44	59	IAELREELQMDQQAKK			
1951.0494	1950.9677	-0.0817	-42	1588	1603	TYEEKISVLQRNLTEK			
1971.0028	1970.9785	-0.0243	-12	172	187	EALQEQLDERLQELEK			
1982.9487	1982.9662	0.0175	9	1913	1928	RYEEILDAREEEMTAK			
2078.0083	2077.9739	-0.0344	-17	580	596	MDEQKNHHQQQVDSIIK			
2082.0171	2082.0344	0.0173	8	1914	1930	YEEILDAREEEMTAKVR			
2084.0518	2083.9934	-0.0584	-28	1981	1996	EQEFREQIHNLEDRLK			
2233.1445	2233.0481	-0.0964	-43	534	553	LDVNQTELESLSSELSEVLK			
2256.1177	2256.0205	-0.0972	-43	728	746	QNSEMEQKVKSLTQVYESK			

Spot Idx/Pos	141/F10	9	**Instr./Spot Origin**	ab4700/042810	**Process Status** Analysis Succeeded
Plate [#] Name	[1] 042810		**4700 Sample Name**		**Spectra** 13

Rank	Protein Name	Accession No.	Protein MW	Protein Score	Protein C. I. %	Total Ion Score	Total Ion C. I. %
1	PRO2446 [Homo sapiens]	gi|7959903	27175.8	77	99.988		

Peptide Information

Calc. Mass	Obsrv. Mass	± da	± ppm	Start Seq.	End Seq.	Sequence	Ion Score	C. I. %	Modification
1343.7065	1343.7135	0.007	5	183	193	DNTINLIHTFR			
1354.726	1354.7419	0.0159	12	52	63	DSIVHQAGMLKR			
1450.7549	1450.7675	0.0126	9	136	148	ASHTAPQVLFSHR			
1450.7549	1450.7675	0.0126	9	136	148	ASHTAPQVLFSHR			
1606.8561	1606.8541	-0.002	-1	135	148	RASHTAPQVLFSHR			
1760.7874	1760.7946	0.0072	4	73	86	YFQFQEEGKEGENR			
1760.7874	1760.7946	0.0072	4	73	86	YFQFQEEGKEGENR			
1918.0181	1918.0171	-0.001	-1	8	23	FYKELQAHGADELLKR			
1955.9167	1955.9307	0.014	7	87	102	AVIHYRDDETMYVESK			
2083.0957	2083.0916	-0.0041	-2	106	124	VTVVFSTVFKDDDDVVIGK			
2257.2087	2257.2166	0.0079	3	136	155	ASHTAPQVLFSHREPPLELK			
2257.2087	2257.2166	0.0079	3	136	155	ASHTAPQVLFSHREPPLELK			
2413.241	2413.2661	0.0251	10	183	201	DNTINLIHTFRDYLHYHIK			
2992.5376	2992.5549	0.0173	6	106	131	VTVVFSTVFKDDDDVVIGKVFMQEFK			
3088.5513	3088.5608	0.0095	3	24	51	VYGSFLVNPESGYNVSLLYDLENLPASK			

2	Chain A, Three-Dimensional Structure Of Human Electron Transfer Flavoprotein To 2.1 A Resolution	gi|2781202	33075.4	77	99.987	13	85.488		

Peptide Information

Calc. Mass	Obsrv. Mass	± da	± ppm	Start Seq.	End Seq.	Sequence	Ion Score	C. I. %	Modification
1714.8005	1714.8143	0.0138	8	84	99	QFNYTHICAGASAFGK			
1736.0204	1736.0052	-0.0152	-9	68	83	GLLPEELTPLILATQK			
1736.0204	1736.0052	-0.0152	-9	68	83	GLLPEELTPLILATQK			
1751.0676	1751.066	-0.0016	-1	105	121	VAAKLEVAPISDIIAIK			
1812.9602	1812.9628	0.0026	1	215	231	LLYDLADQLHAAVGASR			
1812.9602	1812.9628	0.0026	1	215	231	LLYDLADQLHAAVGASR	13	85.488	
1904.917	1904.9191	0.0021	1	232	250	AAVDAGFVPNDMQVGQTGK			
2351.3154	2351.3098	-0.0056	-2	251	273	IVAPELYIAVGISGAIQHLAGMK			
2475.2625	2475.2732	0.0107	4	209	231	SGENFKLLYDLADQLHAAVGASR			
2475.2625	2475.2732	0.0107	4	209	231	SGENFKLLYDLADQLHAAVGASR			
2553.4648	2553.4614	-0.0034	-1	105	128	VAAKLEVAPISDIIAIKSPDTFVR			
2553.4648	2553.4614	-0.0034	-1	105	128	VAAKLEVAPISDIIAIKSPDTFVR			
2821.5054	2821.5051	-0.0003	0	2	28	QSTLVIAEHANDSLAPITLNTITAATR			
2821.5054	2821.5051	-0.0003	0	2	28	QSTLVIAEHANDSLAPITLNTITAATR			
2888.6494	2888.6521	0.0027	1	58	83	VLVAQHDVYKGLLPEELTPLILATQK			
2947.5813	2947.5933	0.012	4	277	303	TIVAINKDPEAPIFQVADYGIVADLFK			

3	actin related protein 2/3 complex subunit 2 [Homo sapiens]	gi|5031599	34311.5	74	99.975				

Peptide Information

Calc. Mass	Obsrv. Mass	± da	± ppm	Start Seq.	End Seq.	Sequence	Ion Score	C. I. %	Modification
1101.6084	1101.6196	0.0112	10	1	9	MILLEVNNR			
1101.6084	1101.6196	0.0112	10	1	9	MILLEVNNR			
1343.7065	1343.7135	0.007	5	238	248	DNTINLIHTFR			
1354.726	1354.7419	0.0159	12	107	118	DSIVHQAGMLKR			
1450.7549	1450.7675	0.0126	9	191	203	ASHTAPQVLFSHR			
1450.7549	1450.7675	0.0126	9	191	203	ASHTAPQVLFSHR			
1606.8561	1606.8541	-0.002	-1	190	203	RASHTAPQVLFSHR			
1760.7874	1760.7946	0.0072	4	128	141	YFQFQEEGKEGENR			
1760.7874	1760.7946	0.0072	4	128	141	YFQFQEEGKEGENR			
1918.0181	1918.0171	-0.001	-1	63	78	FYKELQAHGADELLKR			
1955.9167	1955.9307	0.014	7	142	157	AVIHYRDDETMYVESK			
2083.0957	2083.0916	-0.0041	-2	161	179	VTVVFSTVFKDDDDVVIGK			
2257.2087	2257.2166	0.0079	3	191	210	ASHTAPQVLFSHREPPLELK			
2257.2087	2257.2166	0.0079	3	191	210	ASHTAPQVLFSHREPPLELK			
2413.241	2413.2661	0.0251	10	238	256	DNTINLIHTFRDYLHYHIK			
2992.5376	2992.5549	0.0173	6	161	186	VTVVFSTVFKDDDDVVIGKVFMQEFK			
3088.5513	3088.5608	0.0095	3	79	106	VYGSFLVNPESGYNVSLLYDLENLPASK			

Spot Idx/Pos	142/F12	10	**Instr./Spot Origin**	ab4700/042810	**Process Status**	Analysis Succeeded
Plate [#] Name	[1] 042810		**4700 Sample Name**		**Spectra**	13

Rank	Protein Name	Accession No.	Protein MW	Protein Score	Protein C. I. %	Total Ion Score	Total Ion C. I. %
1	actin related protein 2/3 complex subunit 2 [Homo sapiens]	gi|5031599	34311.5	113	100	10	72.814

Peptide Information

Calc. Mass	Obsrv. Mass	± da	± ppm	Start Seq.	End Seq.	Sequence	Ion Score	C. I. %	Modification
1101.6084	1101.605	-0.0034	-3	1	9	MILLEVNNR			
1101.6084	1101.605	-0.0034	-3	1	9	MILLEVNNR	8	50.643	
1270.6248	1270.6273	0.0025	2	180	189	VFMQEFKEGR			
1314.7489	1314.7307	-0.0182	-14	55	65	VMVSISLKFYK			
1343.7065	1343.7064	-0.0001	0	238	248	DNTINLIHTFR			
1354.726	1354.7288	0.0028	2	107	118	DSIVHQAGMLKR			
1450.7549	1450.7538	-0.0011	-1	191	203	ASHTAPQVLFSHR			
1450.7549	1450.7538	-0.0011	-1	191	203	ASHTAPQVLFSHR			
1479.7914	1479.8063	0.0149	10	66	78	ELQAHGADELLKR			
1606.8561	1606.8483	-0.0078	-5	190	203	RASHTAPQVLFSHR			
1760.7874	1760.7944	0.007	4	128	141	YFQFQEEGKEGENR			
1760.7874	1760.7944	0.007	4	128	141	YFQFQEEGKEGENR	3	0	
1918.0181	1918.0205	0.0024	1	63	78	FYKELQAHGADELLKR			
1955.9167	1955.9294	0.0127	6	142	157	AVIHYRDDETMYVESK			
1955.9167	1955.9294	0.0127	6	142	157	AVIHYRDDETMYVESK			
2083.0957	2083.0823	-0.0134	-6	161	179	VTVVFSTVFKDDDDVVIGK			
2257.2087	2257.2156	0.0069	3	191	210	ASHTAPQVLFSHREPPLELK			
2257.2087	2257.2156	0.0069	3	191	210	ASHTAPQVLFSHREPPLELK			
2413.241	2413.2507	0.0097	4	238	256	DNTINLIHTFRDYLHYHIK			
2990.5508	2990.5901	0.0393	13	204	230	EPPLELKDTDAAVGDNIGYITFVLFPR			
3088.5513	3088.5667	0.0154	5	79	106	VYGSFLVNPESGYNVSLLYDLENLPASK			

3	Chain A, Three-Dimensional Structure Of Human Electron Transfer Flavoprotein To 2.1 A Resolution	gi|2781202	33075.4	92	100	2	0		

Peptide Information

Calc. Mass	Obsrv. Mass	± da	± ppm	Start Seq.	End Seq.	Sequence	Ion Score	C. I. %	Modification
1171.647	1171.6427	-0.0043	-4	58	67	VLVAQHDVYK			
1714.8005	1714.8076	0.0071	4	84	99	QFNYTHICAGASAFGK			
1736.0204	1736.0026	-0.0178	-10	68	83	GLLPEELTPLILATQK			
1751.0676	1751.057	-0.0106	-6	105	121	VAAKLEVAPISDIIAIK			
1776.865	1776.8628	-0.0022	-1	170	185	ASSTSPVEISEWLDQK			
1776.865	1776.8628	-0.0022	-1	170	185	ASSTSPVEISEWLDQK	2	0	
1812.9602	1812.9636	0.0034	2	215	231	LLYDLADQLHAAVGASR			
1812.9602	1812.9636	0.0034	2	215	231	LLYDLADQLHAAVGASR			
1904.917	1904.9043	-0.0127	-7	232	250	AAVDAGFVPNDMQVGQTGK			
1904.917	1904.9043	-0.0127	-7	232	250	AAVDAGFVPNDMQVGQTGK			
2119.0918	2119.093	0.0012	1	170	188	ASSTSPVEISEWLDQKLTK			
2351.3154	2351.2976	-0.0178	-8	251	273	IVAPELYIAVGISGAIQHLAGMK			
2475.2625	2475.272	0.0095	4	209	231	SGENFKLLYDLADQLHAAVGASR			
2553.4648	2553.4648	0	0	105	128	VAAKLEVAPISDIIAIKSPD			

							TFVR
	2553.4648	2553.4648	0	0	105	128	VAAKLEVAPISDIIAIKSPD TFVR
	2821.5054	2821.5046	-0.0008	0	2	28	QSTLVIAEHANDSLAPITL NTITAATR
	2821.5054	2821.5046	-0.0008	0	2	28	QSTLVIAEHANDSLAPITL NTITAATR
	2888.6494	2888.6392	-0.0102	-4	58	83	VLVAQHDVYKGLLPEELT PLILATQK
	2947.5813	2947.5796	-0.0017	-1	277	303	TIVAINKDPEAPIFQVADY GIVADLFK

Spot Idx/Pos	143/F14	11	**Instr./Spot Origin**	ab4700/042810	**Process Status**	Analysis Succeeded
Plate [#] Name	[1] 042810		**4700 Sample Name**		**Spectra**	3

Rank	Protein Name	Accession No.	Protein MW	Protein Score	Protein C. I. %	Total Ion Score	Total Ion C. I. %
17	Single-stranded DNA binding protein 1 [Homo sapiens]	gi|62205329	17348.1	15	0		

Peptide Information

Calc. Mass	Obsrv. Mass	± da	± ppm	Start Seq.	End Seq.	Sequence	Ion Score	C. I. %	Modification
883.4995	883.493	-0.0065	-7	39	46	VGQDPVLR			
1044.6312	1044.6343	0.0031	3	87	95	ISVFRPGLR			

Spot Idx/Pos	144/F16	12	**Instr./Spot Origin**	ab4700/042810	**Process Status**	Analysis Succeeded
Plate [#] Name	[1] 042810		**4700 Sample Name**		**Spectra**	13

Rank	Protein Name	Accession No.	Protein MW	Protein Score	Protein C. I. %	Total Ion Score	Total Ion C. I. %
1	Chain A, Human Mitochondrial Single-Stranded Dna Binding Protein	gi|2624694	15185.8	99	100		

Peptide Information

Calc. Mass	Obsrv. Mass	± da	± ppm	Start Seq.	End Seq.	Sequence	Ion Score	C. I. %	Modification
883.4995	883.4959	-0.0036	-4	23	30	VGQDPVLR			
1044.6312	1044.6274	-0.0038	-4	71	79	ISVFRPGLR			
1164.6959	1164.6891	-0.0068	-6	13	22	SLNRVHLLGR			
1616.7373	1616.7599	0.0226	14	98	110	IDYGEYMDKNNVR			
1778.8894	1778.9095	0.0201	11	36	50	NPVTIFSLATNEMWR			
1992.0647	1992.066	0.0013	1	112	129	QATTIIADNIIFLSDQTK			
2148.1658	2148.1343	-0.0315	-15	111	129	RQATTIIADNIIFLSDQTK			
2293.0842	2293.0598	-0.0244	-11	51	70	SGDSEVYQLGDVSQKTT WHR			
2320.1753	2320.1577	-0.0176	-8	31	50	QVEGKNPVTIFSLATNEM WR			
2378.2449	2378.2454	0.0005	0	112	132	QATTIIADNIIFLSDQTKEK E			

4	EP2E [Homo sapiens]	gi|10799277	9085.3	29	0	

Peptide Information

Calc. Mass	Obsrv. Mass	± da	± ppm	Start Seq.	End Seq.	Sequence	Ion Score	C. I. %	Modification
1422.6763	1422.6794	0.0031	2	27	38	NTICRMQQGICR			
1422.6763	1422.6794	0.0031	2	27	38	NTICRMQQGICR			
2384.0161	2384.0339	0.0178	7	59	80	CCVSNTDEEGKEKPEMD GRSGI			
3354.7852	3354.7366	-0.0486	-14	2	31	KVFFLFAVLFCLVQTNSG DVPPGIRNTICR			

Spot Idx/Pos	195/H18	13	**Instr./Spot Origin**	ab4700/042810	**Process Status**	Analysis Succeeded
Plate [#] Name	[1] 042810		**4700 Sample Name**		**Spectra**	13

Rank	Protein Name	Accession No.	Protein MW	Protein Score	Protein C. I. %	Total Ion Score	Total Ion C. I. %
1	PREDICTED: similar to 60S ribosomal protein L35 [Homo sapiens]	gi|51459132	14555.4	48	88.388		

Peptide Information

Calc. Mass	Obsrv. Mass	± da	± ppm	Start Seq.	End Seq.	Sequence	Ion Score	C. I. %	Modification
817.5076	817.5087	0.0011	1	1	7	MAKIKAR			
823.5009	823.4944	-0.0065	-8	93	98	HRLNKR			
825.4941	825.4947	0.0006	1	8	14	DLHGKKK			
902.524	902.5374	0.0134	15	111	117	ERLCLLR			
924.5373	924.5402	0.0029	3	6	13	ARDLHGKK			
946.5468	946.5562	0.0094	10	104	110	TKKQQWK			
988.5785	988.5778	-0.0007	-1	33	43	VAKVTGGAASK			
995.5857	995.5863	0.0006	1	90	97	ATRHRLNK			
1012.5785	1012.5893	0.0108	11	99	106	EEHLKTKK			
1018.5891	1018.5967	0.0076	7	36	46	VTGGAASKLSK			
1030.6189	1030.6138	-0.0051	-5	111	118	ERLCLLRK			
1037.6213	1037.6206	-0.0007	-1	4	12	IKARDLHGK			

2	RPL13A protein [Homo sapiens]	gi|111494155	16706.4	39	19.667	

Peptide Information

Calc. Mass	Obsrv. Mass	± da	± ppm	Start Seq.	End Seq.	Sequence	Ion Score	C. I. %	Modification
828.5011	828.4939	-0.0072	-9	57	64	MVVPAALK			
844.5151	844.514	-0.0011	-1	105	110	IHYRKK			
872.5312	872.5234	-0.0078	-9	116	122	LRKQAEK			
915.5522	915.5591	0.0069	8	103	109	AKIHYRK			
915.5522	915.5591	0.0069	8	103	109	AKIHYRK			
971.5632	971.5668	0.0036	4	34	42	GQAALDRLK			
973.5676	973.571	0.0034	3	123	130	NVEKKIDK			
977.5679	977.5819	0.014	14	18	24	IFWRTVR			
977.5679	977.5819	0.014	14	18	24	IFWRTVR			
1044.5948	1044.6017	0.0069	7	101	108	EKAKIHYR			
1108.6248	1108.631	0.0062	6	128	136	IDKYTEVLK			
1267.7303	1267.7238	-0.0065	-5	22	32	TVRGMLPHKTK			
2866.4885	2866.5105	0.022	8	74	98	FAYLGRLAHEVGWKYQA VTATLEDK			

3	CCDC71 protein [Homo sapiens]	gi|48735006	24879.5	35	0	

Peptide Information

Calc. Mass	Obsrv. Mass	± da	± ppm	Start Seq.	End Seq.	Sequence	Ion Score	C. I. %	Modification
827.4846	827.4941	0.0095	11	120	126	VARTQPR			
845.5025	845.5119	0.0094	11	1	7	PKCLTRK			
853.5254	853.513	-0.0124	-15	163	169	DLPPKKR			
895.522	895.5322	0.0102	11	7	15	KGPGAGPRR			
944.5635	944.5654	0.0019	2	67	75	TQAKAAKAR			
945.5662	945.564	-0.0022	-2	100	108	VMAARAKAK			
1013.5962	1013.6022	0.006	6	127	136	GRGRPKGSAK			
1026.6166	1026.608	-0.0086	-8	118	126	AKVARTQPR			
1040.6072	1040.6086	0.0014	1	120	128	VARTQPRGR			
1041.6276	1041.613	-0.0146	-14	57	66	AARAQAKVAR			
1100.635	1100.6407	0.0057	5	223	232	LQPLLPYSAV			
1105.6146	1105.6022	-0.0124	-11	34	44	RMKGGSALGTK			
1171.6906	1171.678	-0.0126	-11	60	70	AQAKVARTQAK			
1184.6494	1184.6377	-0.0117	-10	146	155	NRPETVGQKR			

6	PREDICTED: similar to H3 histone, family 3B [Homo sapiens]	gi|88976633	15216.4	32	0	

Peptide Information

Calc. Mass	Obsrv. Mass	± da	± ppm	Start Seq.	End Seq.	Sequence	Ion Score	C. I. %	Modification
832.4999	832.4979	-0.002	-2	4	10	TKQTARK			
844.5073	844.514	0.0067	8	117	123	RVTIMPK			

858.5155	858.5172	0.0017	2	20	27	QLATKAAR	
931.5432	931.5523	0.0091	10	2	9	ARTKQTAR	
945.5727	945.564	-0.0087	-9	58	65	STELLVRK	
992.5635	992.5674	0.0039	4	51	57	EIRRYQK	
1032.5948	1032.6097	0.0149	14	42	50	YRPGTVALR	
1052.5847	1052.5978	0.0131	12	124	132	DIQLAHSIR	
1218.6841	1218.6906	0.0065	5	71	80	LVREIAQDFK	
1229.6959	1229.6937	-0.0022	-2	25	37	AARKSAPSTGGVK	

25 PREDICTED: similar to ribosomal protein L13a isoform 1 [Homo sapiens] gi|89037070 23428.2 26 0

Peptide Information

Calc. Mass	Obsrv. Mass	± da	± ppm	Start Seq.	End Seq.	Sequence	Ion Score	C. I. %	Modification
813.5305	813.533	0.0025	3	26	32	QVLLGRK			
844.5151	844.514	-0.0011	-1	166	171	IHYRKK			
872.5312	872.5234	-0.0078	-9	177	183	LRKQAEK			
915.5522	915.5591	0.0069	8	164	170	AKIHYRK			
915.5522	915.5591	0.0069	8	164	170	AKIHYRK			
971.5632	971.5668	0.0036	4	95	103	GQAALDRLK			
973.5676	973.571	0.0034	3	184	191	NVEKKIDK			
1018.5865	1018.5967	0.0102	10	117	125	RMVVPAAFK			
1044.5948	1044.6017	0.0069	7	162	169	EKAKIHYR			
1108.6248	1108.631	0.0062	6	189	197	IDKYTEVLK			
1267.7303	1267.7238	-0.0065	-5	83	93	TVRGMLPHKTK			
2000.009	2000.002	-0.007	-3	32	49	KVVVVCCEGINISGNFYR			

Spot Idx/Pos	146/F20	14	**Instr./Spot Origin**	ab4700/042810	**Process Status** Analysis Succeeded
Plate [#] Name	[1] 042810		**4700 Sample Name**		**Spectra** 13

Rank	Protein Name	Accession No.	Protein MW	Protein Score	Protein C. I. %	Total Ion Score	Total Ion C. I. %
11	H1 histone family, member 0 [Homo sapiens]	gi|20810	20872.2	21	0		

Peptide Information

Calc. Mass	Obsrv. Mass	± da	± ppm	Start Seq.	End Seq.	Sequence	Ion Score	C. I. %	Modification
870.577	870.5884	0.0114	13	162	169	TVKAKPVK			
895.6087	895.6135	0.0048	5	175	182	KAKPVKPK			
899.6036	899.61	0.0064	7	157	164	AKKPKTVK			
966.6458	966.6421	-0.0037	-4	176	184	AKPVKPKAK			
986.6356	986.6431	0.0075	8	74	82	RLVTTGVLK			
996.6564	996.6554	-0.001	-1	137	145	KPKATPVKK			
1053.6779	1053.6901	0.0122	12	165	174	AKPVKASKPK			

Spot Idx/Pos	147/F22	15	**Instr./Spot Origin**	ab4700/042810	**Process Status** Analysis Succeeded
Plate [#] Name	[1] 042810		**4700 Sample Name**		**Spectra** 13

Rank	Protein Name	Accession No.	Protein MW	Protein Score	Protein C. I. %	Total Ion Score	Total Ion C. I. %
2	ARP3 actin-related protein 3 homolog [Homo sapiens]	gi|5031573	47341	38	0	2	0

Peptide Information

Calc. Mass	Obsrv. Mass	± da	± ppm	Start Seq.	End Seq.	Sequence	Ion Score	C. I. %	Modification
958.5792	958.5829	0.0037	4	341	348	RTVDARLK			
1214.5687	1214.5781	0.0094	8	266	275	EFSIDVGYER			
1409.7787	1409.7894	0.0107	8	199	209	DITYFIQQLLR			
1409.7787	1409.7894	0.0107	8	199	209	DITYFIQQLLR	2	0	
1499.6947	1499.7078	0.0131	9	80	91	HGIVEDWDLMER			
1499.6947	1499.7078	0.0131	9	80	91	HGIVEDWDLMER			
1768.9075	1768.9175	0.01	6	210	225	DREVGIPPEQSLETAK			
1769.9254	1769.9199	-0.0055	-3	226	240	AVKERYSYVCPDLVK			
1795.9799	1795.9689	-0.011	-6	212	228	EVGIPPEQSLETAKAVK			
1912.981	1912.9827	0.0017	1	318	334	NIVLSGGSTMFRDFGRR			
2154.2183	2154.1975	-0.0208	-10	192	209	HIPIAGRDITYFIQQLLR			
2482.1885	2482.1809	-0.0076	-3	103	123	AEPEDHYFLLTEPPLNTP ENR			
2482.1885	2482.1809	-0.0076	-3	103	123	AEPEDHYFLLTEPPLNTP ENR			

4 translation initiation factor [Homo sapiens] gi|496902 46803.1 38 0

Peptide Information

Calc. Mass	Obsrv. Mass	± da	± ppm	Start Seq.	End Seq.	Sequence	Ion Score	C. I. %	Modification
1159.647	1159.6617	0.0147	13	330	339	VLISTDVWAR			
1212.6946	1212.7087	0.0141	12	106	116	ETQALILAPTR			
1417.7109	1417.7208	0.0099	7	196	206	GFKEQIYDVYR			
1469.7495	1469.7535	0.004	3	153	166	LDYGQHVVAGTPGR			
1588.8805	1588.8656	-0.0149	-9	374	387	KGVAINFVKNDDIR			
1827.9387	1827.9484	0.0097	5	52	67	GIYAYGFEKPSAIQQR			
1827.9387	1827.9484	0.0097	5	52	67	GIYAYGFEKPSAIQQR			
1994.0592	1994.0331	-0.0261	-13	244	260	DELTLEGIKQFFVAVER			
2140.1396	2140.1401	0.0005	0	340	358	GLDVPQVSLIINYDLPNN R			
2140.1548	2140.1401	-0.0147	-7	52	70	GIYAYGFEKPSAIQQRAIK			
2870.395	2870.373	-0.022	-8	388	411	ILRDIEQYYSTQIDEMPM NVADLI			

5 Growth-arrest-specific protein 7 (GAS-7) gi|12643625 47236.7 36 0

Peptide Information

Calc. Mass	Obsrv. Mass	± da	± ppm	Start Seq.	End Seq.	Sequence	Ion Score	C. I. %	Modification
873.4901	873.4961	0.006	7	278	284	ALTERQR			
1393.7321	1393.7365	0.0044	3	179	189	ERIKIEEDYAK			
1478.8074	1478.7898	-0.0176	-12	264	276	QLASRYASVEKAR			
1644.8591	1644.8368	-0.0223	-14	217	231	SLADEAEVHLKFSAK			
1707.8507	1707.8685	0.0178	10	87	103	KSTGDSQNLGSSPSKK			
1759.937	1759.913	-0.024	-14	283	296	QRDLEMKTQQLEIK			
1762.9128	1762.9265	0.0137	8	254	268	CDHHIADLRKQLASR			
1772.954	1772.9673	0.0133	8	216	231	KSLADEAEVHLKFSAK			
1786.9333	1786.9213	-0.012	-7	146	162	DPQGNGTVAGFELLLQK			
2460.2363	2460.2466	0.0103	4	194	216	LSQNSLASQEEGSLGEA WAQVKK			

15 translation elongation factor 1 alpha 1-like 14 [Homo sapiens] gi|15277711 42997.3 28 0

Peptide Information

Calc. Mass	Obsrv. Mass	± da	± ppm	Start Seq.	End Seq.	Sequence	Ion Score	C. I. %	Modification
1025.6101	1025.6255	0.0154	15	192	202	IGGIGTVPVGR			
1314.7416	1314.7347	-0.0069	-5	71	82	EHALLAYTLGVK			
1316.7355	1316.7366	0.0011	1	364	375	DMRQTVAVGVIK			
1404.7269	1404.7406	0.0137	10	21	32	YYVTIIDAPGHR			
1776.9313	1776.9458	0.0145	8	1	15	MQSERGITIDISLWK			
1908.0013	1908.0121	0.0108	6	21	36	YYVTIIDAPGHRDFIK			
1908.0013	1908.0121	0.0108	6	21	36	YYVTIIDAPGHRDFIK			
2515.3838	2515.3674	-0.0164	-7	203	226	VETGVLKPGMVVTFAPV NVTTEVK			
2515.3838	2515.3674	-0.0164	-7	203	226	VETGVLKPGMVVTFAPV NVTTEVK			
2938.3782	2938.3569	-0.0213	-7	332	359	SGDAAIVDMVPGKPMCV ESFSDYPPLGR			
2938.3782	2938.3569	-0.0213	-7	332	359	SGDAAIVDMVPGKPMCV ESFSDYPPLGR			

Spot Idx/Pos	148/F24	16	**Instr./Spot Origin**	ab4700/042810	**Process Status** Analysis Succeeded
Plate [#] Name	[1] 042810		**4700 Sample Name**		**Spectra** 13

Rank	Protein Name	Accession No.	Protein MW	Protein Score	Protein C. I. %	Total Ion Score	Total Ion C. I. %

								Score	C. I. %	Score	C. I. %
3	ARP3 actin-related protein 3 homolog [Homo sapiens]				gi|5031573		47341	37	0	4	0

Peptide Information

Calc. Mass	Obsrv. Mass	± da	± ppm	Start Seq.	End Seq.	Sequence	Ion Score	C. I. %	Modification
1214.5687	1214.5735	0.0048	4	266	275	EFSIDVGYER			
1281.6619	1281.6547	-0.0072	-6	318	329	NIVLSGGSTMFR			
1409.7787	1409.7798	0.0011	1	199	209	DITYFIQQLLR			
1409.7787	1409.7798	0.0011	1	199	209	DITYFIQQLLR	4	0	
1499.6947	1499.6978	0.0031	2	80	91	HGIVEDWDLMER			
1499.6947	1499.6978	0.0031	2	80	91	HGIVEDWDLMER			
1768.9075	1768.9159	0.0084	5	210	225	DREVGIPPEQSLETAK			
1795.9799	1795.9746	-0.0053	-3	212	228	EVGIPPEQSLETAKAVK			
2040.1534	2040.1238	-0.0296	-15	358	374	LKPKPIDVQVITHHMQR			
2154.2183	2154.1868	-0.0315	-15	192	209	HIPIAGRDITYFIQQLLR			
2482.1885	2482.1848	-0.0037	-1	103	123	AEPEDHYFLLTEPPLNTPENR			
2482.1885	2482.1848	-0.0037	-1	103	123	AEPEDHYFLLTEPPLNTPENR			
2954.469	2954.4314	-0.0376	-13	80	102	HGIVEDWDLMERFMEQVIFKYLR			

4	translation initiation factor [Homo sapiens]				gi|496902		46803.1	36	0	2	0

Peptide Information

Calc. Mass	Obsrv. Mass	± da	± ppm	Start Seq.	End Seq.	Sequence	Ion Score	C. I. %	Modification
1159.647	1159.6421	-0.0049	-4	330	339	VLISTDVWAR			
1262.6772	1262.6842	0.007	6	16	25	RLLKEEDMTK			
1417.7109	1417.7123	0.0014	1	196	206	GFKEQIYDVYR			
1469.7495	1469.7374	-0.0121	-8	153	166	LDYGQHVVAGTPGR			
1567.7903	1567.7986	0.0083	5	253	264	QFFVAVEREEWK			
1597.8445	1597.84	-0.0045	-3	152	166	KLDYGQHVVAGTPGR			
1640.8207	1640.8435	0.0228	14	1	16	MATTATMATSGSARKR			
1827.9387	1827.9415	0.0028	2	52	67	GIYAYGFEKPSAIQQR			
1827.9387	1827.9415	0.0028	2	52	67	GIYAYGFEKPSAIQQR			
2140.1396	2140.1318	-0.0078	-4	340	358	GLDVPQVSLIINYDLPNNR			
2140.1396	2140.1318	-0.0078	-4	340	358	GLDVPQVSLIINYDLPNNR	3	0	
3489.665	3489.6687	0.0037	1	17	46	LLKEEDMTKVEFETSEEVDVTPTFDTMGLR			

6	translation elongation factor 1 alpha 1-like 14 [Homo sapiens]				gi|15277711		42997.3	34	0		

Peptide Information

Calc. Mass	Obsrv. Mass	± da	± ppm	Start Seq.	End Seq.	Sequence	Ion Score	C. I. %	Modification
1025.6101	1025.6062	-0.0039	-4	192	202	IGGIGTVPVGR			
1314.7416	1314.7267	-0.0149	-11	71	82	EHALLAYTLGVK			
1314.7416	1314.7267	-0.0149	-11	71	82	EHALLAYTLGVK			
1404.7269	1404.729	0.0021	1	21	32	YYVTIIDAPGHR			
1776.9313	1776.9452	0.0139	8	1	15	MQSERGITIDISLWK			
1908.0013	1907.9967	-0.0046	-2	21	36	YYVTIIDAPGHRDFIK			
1997.0126	1997.0341	0.0215	11	16	32	FETSKYYVTIIDAPGHR			
2515.3838	2515.387	0.0032	1	203	226	VETGVLKPGMVVTFAPVNVTTEVK			
2515.3838	2515.387	0.0032	1	203	226	VETGVLKPGMVVTFAPVNVTTEVK			
2852.4167	2852.4299	0.0132	5	37	65	NMITGTSQADCAVLIVAAGVGEFEAGISK			
2938.3782	2938.3789	0.0007	0	332	359	SGDAAIVDMVPGKPMCVESFSDYPPLGR			
2938.3782	2938.3789	0.0007	0	332	359	SGDAAIVDMVPGKPMCVESFSDYPPLGR			

11	phosphogluconate dehydrogenase [Homo sapiens]				gi|40068518		53105.9	27	0		

Peptide Information

Calc. Mass	Obsrv. Mass	± da	± ppm	Start Seq.	End Seq.	Sequence	Ion Score	C. I. %	Modification
1411.7766	1411.7815	0.0049	3	332	343	IISYAQGFMLLR			
1493.7893	1493.7993	0.01	7	435	447	HEMLPASLIQAQR			
1591.8074	1591.8191	0.0117	7	120	136	GILFVGSGVSGGEEGAR			
1790.9393	1790.9468	0.0075	4	118	136	AKGILFVGSGVSGGEEGAR			
2160.1182	2160.1196	0.0014	1	88	107	LVPLLDTGDIIIDGGNSEYR			
2310.1399	2310.1406	0.0007	0	378	396	DAFDRNPELQNLLLDDFFK			
2463.3281	2463.311	-0.0171	-7	266	288	WTAISALEYGVPVTLIGEAVFAR			
2551.3191	2551.3152	-0.0039	-2	376	396	IKDAFDRNPELQNLLLDDFFK			
2595.1863	2595.2024	0.0161	6	185	206	MVHNGIEYGDMQLICEAYHLMK			

13	glucocorticoid receptor AF-1 specific elongation factor [Homo sapiens]				gi|7108915		46240	27	0		

Peptide Information

Calc. Mass	Obsrv. Mass	± da	± ppm	Start Seq.	End Seq.	Sequence	Ion Score	C. I. %	Modification
1025.6101	1025.6062	-0.0039	-4	220	230	IGGIGTVPVGR			
1314.7416	1314.7267	-0.0149	-11	99	110	EHALLAYTLGVK			
1314.7416	1314.7267	-0.0149	-11	99	110	EHALLAYTLGVK			
1404.7269	1404.729	0.0021	1	49	60	YYVTIIDAPGHR			
1908.0013	1907.9967	-0.0046	-2	49	64	YYVTIIDAPGHRDFIK			
1997.0126	1997.0341	0.0215	11	44	60	FETSKYYVTIIDAPGHR			
2515.3838	2515.387	0.0032	1	231	254	VETGVLKPGMVVTFAPVNVTTEVK			
2515.3838	2515.387	0.0032	1	231	254	VETGVLKPGMVVTFAPVNVTTEVK			
2852.4167	2852.4299	0.0132	5	65	93	NMITGTSQADCAVLIVAAGVGEFEAGISK			
2938.3782	2938.3789	0.0007	0	360	387	SGDAAIVDMVPGKPMCVESFSDYPPLGR			
2938.3782	2938.3789	0.0007	0	360	387	SGDAAIVDMVPGKPMCVESFSDYPPLGR			

Spot Idx/Pos	161/G2	17	**Instr./Spot Origin**	ab4700/042810	**Process Status** Analysis Succeeded
Plate [#] Name	[1] 042810		**4700 Sample Name**		**Spectra** 13

Rank	Protein Name	Accession No.	Protein MW	Protein Score	Protein C. I. %	Total Ion Score	Total Ion C. I. %
1	electron-transfer-flavoprotein, beta polypeptide isoform 1 [Homo sapiens]	gi|4503609	27826.2	135	100	14	78.09

Peptide Information

Calc. Mass	Obsrv. Mass	± da	± ppm	Start Seq.	End Seq.	Sequence	Ion Score	C. I. %	Modification
828.5301	828.5347	0.0046	6	249	255	LKEIGRI			
853.5253	853.5312	0.0059	7	99	106	LGPLQVAR			
1050.5652	1050.5626	-0.0026	-2	192	200	YATLPNIMK			
1054.6255	1054.6179	-0.0076	-7	177	186	LPAVVTADLR			
1102.5739	1102.5786	0.0047	4	165	174	EIDGGLETLR			

	1102.5739	1102.5786	0.0047	4	165	174	EIDGGLETLR			4	0	
	1295.8044	1295.8088	0.0044	3	175	186	LKLPAVVTADLR					
	1295.8044	1295.8088	0.0044	3	175	186	LKLPAVVTADLR			5	0	
	1339.7216	1339.7217	0.0001	0	222	233	LSVISVEDPPQR					
	1339.7216	1339.7217	0.0001	0	222	233	LSVISVEDPPQR					
	1403.7277	1403.735	0.0073	5	86	98	GIHVEVPPAEAER			5	0	
	1403.7277	1403.735	0.0073	5	86	98	GIHVEVPPAEAER					
	1470.8274	1470.8271	-0.0003	0	22	35	VKPDRTGVVTDPGVK					
	1486.7859	1486.7898	0.0039	3	162	174	VEREIDGGLETLR					
	1554.9464	1554.9446	-0.0018	-1	111	124	LAEKEKVDLVLLGK					
	1683.9526	1683.9391	-0.0135	-8	206	221	IEVIKPGDLGVDLTSK					
	1831.8464	1831.8707	0.0243	13	36	51	HSMNPFCEIAVEEAVR					
	1831.8464	1831.8707	0.0243	13	36	51	HSMNPFCEIAVEEAVR					
	1905.1279	1905.1251	-0.0028	-1	175	191	LKLPAVVTADLRLNEPR					
	2238.2351	2238.2393	0.0042	2	86	106	GIHVEVPPAEAERLGPLQVAR					
	2688.3118	2688.3362	0.0244	9	27	51	TGVVTDGVKHSMNPFCEIAVEEAVR					

4	PREDICTED: similar to Adenylate kinase isoenzyme 4, mitochondrial (Adenylate kinase 3-like 1) (ATP-	gi|113423642	25224.2	84	99.998	7	5.016

Peptide Information

Calc. Mass	Obsrv. Mass	± da	± ppm	Start Seq.	End Seq.	Sequence	Ion Score	C. I. %	Modification
949.5002	949.506	0.0058	6	127	134	WIHPPSGR			
949.5002	949.506	0.0058	6	127	134	WIHPPSGR			
1045.5524	1045.5605	0.0081	8	93	102	TLGQAEALDK			
1105.6013	1105.6149	0.0136	12	126	134	RWIHPPSGR			
1122.5282	1122.5358	0.0076	7	72	80	LMMSELENR			
1122.5282	1122.5358	0.0076	7	72	80	LMMSELENR			
1249.7262	1249.7363	0.0101	8	61	71	SLLVPDHVITR	4	0	
1249.7262	1249.7363	0.0101	8	61	71	SLLVPDHVITR			
1278.6293	1278.6471	0.0178	14	72	81	LMMSELENRR			
1325.6749	1325.6909	0.016	12	82	92	GQHWLLDGFPR			
1325.6749	1325.6909	0.016	12	82	92	GQHWLLDGFPR	3	0	
1639.8948	1639.9193	0.0245	15	8	24	AVILGPPGSGKGTVCQR			
1925.0139	1925.0304	0.0165	9	25	41	IAQNFGLQHLSSGHFLR			
1925.0139	1925.0304	0.0165	9	25	41	IAQNFGLQHLSSGHFLR			
2409.2786	2409.2932	0.0146	6	25	45	IAQNFGLQHLSSGHFLRENIK			
3984.936	3984.9592	0.0232	6	135	170	VYNLDFNPPHVHGIDDVTGEPLVQQEDDKPEAVAAR			

Spot Idx/Pos	162/G4	18	**Instr./Spot Origin**	ab4700/042810	**Process Status**	Analysis Succeeded
Plate [#] Name	[1] 042810		**4700 Sample Name**		**Spectra**	13

Rank	Protein Name	Accession No.	Protein MW	Protein Score	Protein C. I. %	Total Ion Score	Total Ion C. I. %
1	electron-transfer-flavoprotein, beta polypeptide isoform 1 [Homo sapiens]	gi|4503609	27826.2	92	100	24	97.868

Peptide Information

Calc. Mass	Obsrv. Mass	± da	± ppm	Start Seq.	End Seq.	Sequence	Ion Score	C. I. %	Modification
853.5253	853.5281	0.0028	3	99	106	LGPLQVAR			
1102.5739	1102.5658	-0.0081	-7	165	174	EIDGGLETLR			
1102.5739	1102.5658	-0.0081	-7	165	174	EIDGGLETLR			
1295.8044	1295.8074	0.003	2	175	186	LKLPAVVTADLR			
1295.8044	1295.8074	0.003	2	175	186	LKLPAVVTADLR	18	90.519	
1339.7216	1339.7192	-0.0024	-2	222	233	LSVISVEDPPQR			
1339.7216	1339.7192	-0.0024	-2	222	233	LSVISVEDPPQR			
1403.7277	1403.7322	0.0045	3	86	98	GIHVEVPPAEAER			
1403.7277	1403.7322	0.0045	3	86	98	GIHVEVPPAEAER	6	0	
1831.8464	1831.8613	0.0149	8	36	51	HSMNPFCEIAVEEAVR			
1831.8464	1831.8613	0.0149	8	36	51	HSMNPFCEIAVEEAVR			
1905.1279	1905.1244	-0.0035	-2	175	191	LKLPAVVTADLRLNEPR			
1905.1279	1905.1244	-0.0035	-2	175	191	LKLPAVVTADLRLNEPR			
2238.2351	2238.2378	0.0027	1	86	106	GIHVEVPPAEAERLGPLQVAR			
2290.1606	2290.1719	0.0113	5	77	98	TALAMGADRGIHVEVPPAEAER			

4	PREDICTED: similar to Adenylate kinase isoenzyme 4, mitochondrial (Adenylate kinase 3-like 1) (ATP-	gi|113423642	25224.2	69	99.906		

Peptide Information

Calc. Mass	Obsrv. Mass	± da	± ppm	Start Seq.	End Seq.	Sequence	Ion Score	C. I. %	Modification
949.5002	949.5016	0.0014	1	127	134	WIHPPSGR			
949.5002	949.5016	0.0014	1	127	134	WIHPPSGR			
1105.6013	1105.5948	-0.0065	-6	126	134	RWIHPPSGR			
1249.7262	1249.7294	0.0032	3	61	71	SLLVPDHVITR			
1249.7262	1249.7294	0.0032	3	61	71	SLLVPDHVITR			
1278.6293	1278.6423	0.013	10	72	81	LMMSELENRR			
1325.6749	1325.6772	0.0023	2	82	92	GQHWLLDGFPR			
1325.6749	1325.6772	0.0023	2	82	92	GQHWLLDGFPR			
1481.776	1481.7815	0.0055	4	81	92	RGQHWLLDGFPR			
1639.8948	1639.8844	-0.0104	-6	8	24	AVILGPPGSGKGTVCQR			
1925.0139	1925.0172	0.0033	2	25	41	IAQNFGLQHLSSGHFLR			
1925.0139	1925.0172	0.0033	2	25	41	IAQNFGLQHLSSGHFLR			
2409.2786	2409.2827	0.0041	2	25	45	IAQNFGLQHLSSGHFLRENIK			

Spot Idx/Pos	163/G6	19	**Instr./Spot Origin**	ab4700/042810	**Process Status**	Analysis Succeeded
Plate [#] Name	[1] 042810		**4700 Sample Name**		**Spectra**	7

Rank	Protein Name	Accession No.	Protein MW	Protein Score	Protein C. I. %	Total Ion Score	Total Ion C. I. %

Spot Idx/Pos	164/G8	20				**Instr./Spot Origin**	ab4700/042810				**Process Status**	Analysis Succeeded
Plate [#] Name	[1] 042810					**4700 Sample Name**					**Spectra**	13
Rank	**Protein Name**					**Accession No.**	**Protein MW**	**Protein Score**	**Protein C. I. %**	**Total Ion Score**	**Total Ion C. I. %**	
3	myosin, heavy polypeptide 9, non-muscle [Homo sapiens]					gi|12667788	226391.6	33	0			

Peptide Information

Calc. Mass	Obsrv. Mass	± da	± ppm	Start Seq.	End Seq.	Sequence	Ion Score	C. I. %	Modification
1045.571	1045.5795	0.0085	8	1558	1566	LEVNLQAMK			
1155.6632	1155.6715	0.0083	7	1924	1933	GDLPFVVPRR			
1155.6632	1155.6715	0.0083	7	1923	1932	RGDLPFVVPR			
1524.8057	1524.8043	-0.0014	-1	290	301	TDLLLEPYNKYR			
1558.8588	1558.8754	0.0166	11	719	731	QRYEILTPNSIPK			
1571.854	1571.8658	0.0118	8	374	387	VSHLLGINVTDFTR			
1571.854	1571.8658	0.0118	8	374	387	VSHLLGINVTDFTR			
1579.8438	1579.834	-0.0098	-6	765	778	AGVLAHLEEERDLK			
1615.8181	1615.8287	0.0106	7	328	341	IMGIPEEEQMGLLR			
1615.8181	1615.8287	0.0106	7	328	341	IMGIPEEEQMGLLR			
1623.839	1623.8448	0.0058	4	706	718	QGFPNRVVFQEFR			
1643.8097	1643.8097	0	0	1	14	MAQQAADKYLYVDK			
1643.8097	1643.8097	0	0	1	14	MAQQAADKYLYVDK			
1727.856	1727.8778	0.0218	13	126	139	NLPIYSEEIVEMYK			
1815.9082	1815.9271	0.0189	10	1816	1830	IAQLEEQLDNETKER			
1869.9664	1869.9609	-0.0055	-3	1755	1770	ANLQIDQINTDLNLER			
1949.9927	1950.0028	0.0101	5	1418	1433	LQQELDDLLVDLDHQR			
1949.9927	1950.0028	0.0101	5	1418	1433	LQQELDDLLVDLDHQR			
2048.9626	2048.9705	0.0079	4	1677	1694	SMEAEMIQLQEELAAAER			

2048.9626	2048.9705	0.0079	4	1677	1694	SMEAEMIQLQEELAAAER	
2299.1345	2299.1677	0.0332	14	1175	1193	TLEEEAKTHEAQIQEMRQ K	
2333.0562	2333.0798	0.0236	10	941	959	MQQNIQELEEQLEEEES AR	
2749.3274	2749.3521	0.0247	9	1302	1324	DFSALESQLQDTQELLQE ENRQK	
3017.4797	3017.47	-0.0097	-3	1136	1162	DLGEELEALKTELEDTLD STAAQQELR	

Rank	Protein Name	Accession No.	Protein MW	Protein Score	Protein C. I. %	Total Ion Score	Total Ion C. I. %
7	KIAA0678 protein [Homo sapiens]	gi|71891673	255972.3	30	0		

Peptide Information

Calc. Mass	Obsrv. Mass	± da	± ppm	Start Seq.	End Seq.	Sequence	Ion Score	C. I. %	Modification
1045.5887	1045.5795	-0.0092	-9	105	113	TELLTEALR			
1083.5656	1083.5759	0.0103	10	1406	1414	YAGYPMLIR			
1491.7437	1491.7435	-0.0002	0	1457	1469	ENGLEVLQEAFSR			
1504.6854	1504.708	0.0226	15	864	874	SYEFFNELYHR			
1504.6854	1504.708	0.0226	15	864	874	SYEFFNELYHR			
1513.7756	1513.7799	0.0043	3	114	126	FRTDFSEGKITGR			
1550.7849	1550.7935	0.0086	6	225	236	EPLEFEQYLNLR			
1586.8285	1586.8195	-0.009	-6	207	221	SAIDHAGNYIGISLR			
1586.8285	1586.8195	-0.009	-6	207	221	SAIDHAGNYIGISLR			
1643.7958	1643.8097	0.0139	8	627	640	HLHTAMFTISSDQR			
1643.7958	1643.8097	0.0139	8	627	640	HLHTAMFTISSDQR			
1647.8448	1647.8569	0.0121	7	1456	1469	RENGLEVLQEAFSR			
1699.9026	1699.9037	0.0011	1	1	14	GWSLSSLPRRFEHK			
1712.9329	1712.9464	0.0135	8	193	206	LHLFASEQREEIIK			
1736.8754	1736.8877	0.0123	7	375	390	FLATPPNGNFADAVFR			
1736.8754	1736.8877	0.0123	7	375	390	FLATPPNGNFADAVFR			
1916.9487	1916.96	0.0113	6	240	256	YSTDESITSLAEFVVQK			
1940.0269	1940.0266	-0.0003	0	967	984	ATVPLQSNVIEAAPDMKR			
1948.0176	1948.0352	0.0176	9	2099	2116	AMASLETIGPLMNGMKK R			
1958.9817	1958.9923	0.0106	5	1603	1620	LGGYLAEEQATPENPTIR			
2087.0767	2087.0789	0.0022	1	1603	1621	LGGYLAEEQATPENPTIR K			
2110.0637	2110.072	0.0083	4	357	374	WGLLSMPVDEEVESLHL R			
2266.219	2266.2039	-0.0151	-7	140	160	KPVILEVTPGGFDQINPA TNR			
2266.219	2266.2039	-0.0151	-7	140	160	KPVILEVTPGGFDQINPA TNR			
2511.334	2511.3438	0.0098	4	669	691	ILPPGLLAYLESSDLVPEK DADR			

Rank	Protein Name	Accession No.	Protein MW	Protein Score	Protein C. I. %	Total Ion Score	Total Ion C. I. %
11	DnaJ (Hsp40) homolog, subfamily C, member 13 [Homo sapiens]	gi|112421122	254252.4	26	0		

Peptide Information

Calc. Mass	Obsrv. Mass	± da	± ppm	Start Seq.	End Seq.	Sequence	Ion Score	C. I. %	Modification
1045.5887	1045.5795	-0.0092	-9	91	99	TELLTEALR			
1083.5656	1083.5759	0.0103	10	1392	1400	YAGYPMLIR			
1491.7437	1491.7435	-0.0002	0	1443	1455	ENGLEVLQEAFSR			
1504.6854	1504.708	0.0226	15	850	860	SYEFFNELYHR			
1504.6854	1504.708	0.0226	15	850	860	SYEFFNELYHR			
1513.7756	1513.7799	0.0043	3	100	112	FRTDFSEGKITGR			
1550.7849	1550.7935	0.0086	6	211	222	EPLEFEQYLNLR			
1586.8285	1586.8195	-0.009	-6	193	207	SAIDHAGNYIGISLR			
1586.8285	1586.8195	-0.009	-6	193	207	SAIDHAGNYIGISLR			
1643.7958	1643.8097	0.0139	8	613	626	HLHTAMFTISSDQR			
1643.7958	1643.8097	0.0139	8	613	626	HLHTAMFTISSDQR			
1647.8448	1647.8569	0.0121	7	1442	1455	RENGLEVLQEAFSR			
1712.9329	1712.9464	0.0135	8	179	192	LHLFASEQREEIIK			
1736.8754	1736.8877	0.0123	7	361	376	FLATPPNGNFADAVFR			
1736.8754	1736.8877	0.0123	7	361	376	FLATPPNGNFADAVFR			
1916.9487	1916.96	0.0113	6	226	242	YSTDESITSLAEFVVQK			
1940.0269	1940.0266	-0.0003	0	953	970	ATVPLQSNVIEAAPDMKR			
1948.0176	1948.0352	0.0176	9	2085	2102	AMASLETIGPLMNGMKK R			
1958.9817	1958.9923	0.0106	5	1589	1606	LGGYLAEEQATPENPTIR			
2087.0767	2087.0789	0.0022	1	1589	1607	LGGYLAEEQATPENPTIR K			
2110.0637	2110.072	0.0083	4	343	360	WGLLSMPVDEEVESLHL R			
2266.219	2266.2039	-0.0151	-7	126	146	KPVILEVTPGGFDQINPA TNR			
2266.219	2266.2039	-0.0151	-7	126	146	KPVILEVTPGGFDQINPA TNR			
2511.334	2511.3438	0.0098	4	655	677	ILPPGLLAYLESSDLVPEK DADR			

Spot Idx/Pos	165/G10	21	**Instr./Spot Origin**	ab4700/042810	**Process Status** Analysis Succeeded
Plate [#] Name	[1] 042810		**4700 Sample Name**		**Spectra** 13

Rank	Protein Name	Accession No.	Protein MW	Protein Score	Protein C. I. %	Total Ion Score	Total Ion C. I. %
1	DEAD (Asp-Glu-Ala-Asp) box polypeptide 1 [Homo sapiens]	gi|4826686	82379.8	82	99.996	7	35.986

Peptide Information

Calc. Mass	Obsrv. Mass	± da	± ppm	Start Seq.	End Seq.	Sequence	Ion Score	C. I. %	Modification
975.5006	975.5065	0.0059	6	452	458	TDRLWER			
1048.6149	1048.6255	0.0106	10	491	499	ILKGEYAVR			
1111.6832	1111.6978	0.0146	13	320	330	ELLIIGGVAAR			
1111.6832	1111.6978	0.0146	13	320	330	ELLIIGGVAAR	7	35.986	
1380.8684	1380.8784	0.01	7	318	330	LRELLIIGGVAAR			
1386.7239	1386.7271	0.0032	2	422	432	IMHFPTWVDLK			
1467.7664	1467.7736	0.0072	5	211	223	DLGLAFEIPPHMK			
1610.8068	1610.8232	0.0164	10	387	400	MHNQIPQVTSDGKR			
1663.8948	1663.8997	0.0049	3	563	577	KGDVRFLICTDVAAR			
1766.9258	1766.9036	-0.0222	-13	208	223	NGKDLGLAFEIPPHMK			
1916.0421	1916.0293	-0.0128	-7	400	416	RLQVIVCSATLHSFDVK			
1968.0396	1968.0426	0.003	2	331	349	DQLSVLENGVDIVVGTPG R			
1968.0396	1968.0426	0.003	2	331	349	DQLSVLENGVDIVVGTPG R			
2002.9287	2002.9384	0.0097	5	473	490	DNTRPGANSPEMWSEAI K			
2002.9287	2002.9384	0.0097	5	473	490	DNTRPGANSPEMWSEAI K			
2025.0399	2025.0447	0.0048	2	433	451	GEDSVPDTVHHVVVPVN PK			
2079.1121	2079.1104	-0.0017	-1	578	596	GIDIHGVPYVINVTLPDEK			
2134.1079	2134.1169	0.009	4	721	738	EAQTSFLHLGYLPNQLFR			
2134.1079	2134.1169	0.009	4	721	738	EAQTSFLHLGYLPNQLFR			
2138.1814	2138.1704	-0.011	-5	289	307	ALIVEPSRELAEQTLNNIK			
2372.1768	2372.178	0.0012	1	366	386	FLVLDEADGLLSQGYSDF INR			
2372.1768	2372.178	0.0012	1	366	386	FLVLDEADGLLSQGYSDF INR			
2876.5051	2876.4907	-0.0144	-5	578	602	GIDIHGVPYVINVTLPDEK QNYVHR			

2876.5051	2876.4907	-0.0144	-5	578	602	GIDIHGVPYVINVTLPDEK QNYVHR	
2896.5261	2896.4885	-0.0376	-13	331	358	DQLSVLENGVDIVVGTPG RLDDLVSTGK	

3 chaperone protein HSP90 beta [Homo sapiens] gi|9082289 72827.8 58 98.916

Peptide Information

Calc. Mass	Obsrv. Mass	± da	± ppm	Start Seq.	End Seq.	Sequence	Ion Score	C. I. %	Modification
829.5505	829.5417	-0.0088	-11	106	112	VKEVVKK			
886.5468	886.5516	0.0048	5	358	364	RLSELLR			
1236.6371	1236.6489	0.0118	10	246	255	RAPFDLFENK			
1237.6283	1237.6427	0.0144	12	77	88	ADHGEPIGRGTK			
1348.6643	1348.6775	0.0132	10	228	238	HFSVEGQLEFR			
1348.6643	1348.6775	0.0132	10	228	238	HFSVEGQLEFR			
1513.7856	1513.8082	0.0226	15	287	300	GVVDSEDLPLNISR			
1649.8744	1649.8676	-0.0068	-4	180	192	IKEKYIDQEELNK			
1782.9497	1782.9545	0.0048	3	533	547	HLEINPDHPIVETLR			
1782.9497	1782.9545	0.0048	3	533	547	HLEINPDHPIVETLR			
1808.9581	1808.9552	-0.0029	-2	113	127	HSQFIGYPITLYLEK			
1911.0446	1911.0511	0.0065	3	532	547	KHLEINPDHPIVETLR			
2015.0443	2015.0457	0.0014	1	89	104	VILHLKEDQTEYLEER			
2015.0443	2015.0457	0.0014	1	89	104	VILHLKEDQTEYLEER			
2171.1455	2171.146	0.0005	0	89	105	VILHLKEDQTEYLEERR			
2176.9451	2176.9678	0.0227	10	365	383	YHTSQSGDEMTSLSEYV SR			
2176.9451	2176.9678	0.0227	10	365	383	YHTSQSGDEMTSLSEYV SR			
2255.9587	2255.9744	0.0157	7	57	76	HNDDEQYAWESSAGGS FTVR			
2255.9587	2255.9744	0.0157	7	57	76	HNDDEQYAWESSAGGS FTVR			
2317.1243	2317.0999	-0.0244	-11	268	286	VFIMDSCDELIPEYLNFIR			
2391.1826	2391.1809	-0.0017	-1	390	410	SIYYITGESKEQVANSAF VER			

4 ribonucleotide reductase M1 subunit [Homo sapiens] gi|5006420 89984.5 58 98.839

Peptide Information

Calc. Mass	Obsrv. Mass	± da	± ppm	Start Seq.	End Seq.	Sequence	Ion Score	C. I. %	Modification
1096.5819	1096.5847	0.0028	3	13	21	VMFDKITSR			
1126.6003	1126.6104	0.0101	9	71	80	HPDYAILAAR			
1344.748	1344.7441	-0.0039	-3	119	130	STLDIVLANKDR			
1367.7035	1367.7137	0.0102	7	163	173	VAERPQHMLMR			
1367.7035	1367.7137	0.0102	7	163	173	VAERPQHMLMR			
1509.7842	1509.7776	-0.0066	-4	10	21	QERVMFDKITSR			
1570.87	1570.869	-0.001	-1	741	754	TRPAANPIQFTLNK			
1693.9635	1693.9425	-0.021	-12	629	643	VLSGEFQIVNPHLLK			
1828.0074	1827.9912	-0.0162	-9	741	756	TRPAANPIQFTLNKEK			
1850.0646	1850.0602	-0.0044	-2	628	643	RVLSGEFQIVNPHLLK			
2064.1533	2064.1414	-0.0119	-6	498	516	HRPIGIGVQGLADAFILM R			
2093.0444	2093.0535	0.0091	4	257	277	ATGSYIAGTNGNSNGLVP MLR			
2108.0845	2108.0823	-0.0022	-1	480	497	IIDINYYPVPEACLSNKR			
2302.1462	2302.1604	0.0142	6	699	719	GAFIDQSQSLNIHIAEPNY GK			
2333.1235	2333.1125	-0.011	-5	131	149	LNSAIIYDRDFSYNYFGFK			
2391.2019	2391.1809	-0.021	-9	140	158	DFSYNYFGFKTLERSYLL K			
2572.3252	2572.3203	-0.0049	-2	174	196	VSVGIHKEDIDAAIETYNL LSER			
3579.7998	3579.7856	-0.0142	-4	595	627	NSLLIAPMPTASTAQILGN NESIEPYTSNIYTR			

Spot Idx/Pos	166/G12	22	**Instr./Spot Origin**	ab4700/042810	**Process Status** Analysis Succeeded
Plate [#] Name	[1] 042810		**4700 Sample Name**		**Spectra** 13

Rank	Protein Name	Accession No.	Protein MW	Protein Score	Protein C. I. %	Total Ion Score	Total Ion C. I. %
1	heat shock 90kDa protein 1, beta [Homo sapiens]	gi|20149594	83212.1	134	100	1	0

Peptide Information

Calc. Mass	Obsrv. Mass	± da	± ppm	Start Seq.	End Seq.	Sequence	Ion Score	C. I. %	Modification
829.5294	829.5364	0.007	8	331	337	ALLFIPR			
886.5468	886.5482	0.0014	2	450	456	RLSELLR			
901.5254	901.524	-0.0014	-2	285	291	TKPIWTR			
1194.6477	1194.6538	0.0061	5	73	82	IDIIPNPQER			
1236.6371	1236.6494	0.0123	10	338	347	RAPFDLFENK			
1249.6171	1249.635	0.0179	14	492	502	EQVANSAFVER			
1348.6643	1348.6707	0.0064	5	320	330	HFSVEGQLEFR			
1348.6643	1348.6707	0.0064	5	320	330	HFSVEGQLEFR	1	0	
1364.7321	1364.7297	-0.0024	-2	338	348	RAPFDLFENKK			
1513.7856	1513.7952	0.0096	6	379	392	GVVDSEDLPLNISR			
1513.7856	1513.7952	0.0096	6	379	392	GVVDSEDLPLNISR			
1544.8278	1544.8197	-0.0081	-5	42	55	ELISNASDALDKIR			
1564.8693	1564.8527	-0.0166	-11	70	82	ELKIDIIPNPQER			
1649.8744	1649.8595	-0.0149	-9	272	284	IKEKYIDQEELNK			
1782.9497	1782.9604	0.0107	6	625	639	HLEINPDHPIVETLR			
1782.9497	1782.9604	0.0107	6	625	639	HLEINPDHPIVETLR			
1808.9581	1808.9512	-0.0069	-4	205	219	HSQFIGYPITLYLEK			
1847.797	1847.8038	0.0068	4	292	306	NPDDITQEEYGEFYK			
1911.0446	1911.0476	0.003	2	624	639	KHLEINPDHPIVETLR			
1911.0446	1911.0476	0.003	2	624	639	KHLEINPDHPIVETLR			
2015.0443	2015.0425	-0.0018	-1	181	196	VILHLKEDQTEYLEER			
2015.0443	2015.0425	-0.0018	-1	181	196	VILHLKEDQTEYLEER			
2034.0654	2034.0372	-0.0282	-14	276	291	YIDQEELNKTKPIWTR			
2059.0051	2059.009	0.0039	2	412	428	CLELFSELAEDKENYKK			
2171.1455	2171.155	0.0095	4	181	197	VILHLKEDQTEYLEERR			
2176.9451	2176.9622	0.0171	8	457	475	YHTSQSGDEMTSLSEYV SR			
2176.9451	2176.9622	0.0171	8	457	475	YHTSQSGDEMTSLSEYV SR			
2255.9587	2255.97	0.0113	5	149	168	HNDDEQYAWESSAGGS FTVR			
2255.9587	2255.97	0.0113	5	149	168	HNDDEQYAWESSAGGS FTVR			
2317.1243	2317.1086	-0.0157	-7	360	378	VFIMDSCDELIPEYLNFIR			
2358.1968	2358.1667	-0.0301	-13	379	399	GVVDSEDLPLNISREMLQ QSK			
2369.1882	2369.1697	-0.0185	-8	429	448	FYEAFSKNLKLGIHEDST NR			
2391.1826	2391.1763	-0.0063	-3	482	502	SIYYITGESKEQVANSAF VER			
2988.5312	2988.5474	0.0162	5	653	679	DLVVLLFETALLSSGFSLE DPQTHSNR			

6 DEAD (Asp-Glu-Ala-Asp) box polypeptide 1 [Homo sapiens] gi|4826686 82379.8 87 99.999 1 0

Peptide Information

Calc. Mass	Obsrv. Mass	± da	± ppm	Start Seq.	End Seq.	Sequence	Ion Score	C. I. %	Modification
901.5253	901.524	-0.0013	-1	455	461	LWERLGK			
975.5006	975.4911	-0.0095	-10	452	458	TDRLWER			

1048.6149	1048.6185	0.0036	3	491	499	ILKGEYAVR			
1111.6832	1111.6936	0.0104	9	320	330	ELLIIGGVAAR			
1111.6832	1111.6936	0.0104	9	320	330	ELLIIGGVAAR	1	0	
1380.8684	1380.8829	0.0145	11	318	330	LRELLIIGGVAAR			
1386.7239	1386.7163	-0.0076	-5	422	432	IMHFPTWVDLK			
1467.7664	1467.7673	0.0009	1	211	223	DLGLAFEIPPHMK			
1610.8068	1610.8152	0.0084	5	387	400	MHNQIPQVTSDGKR			
1663.8948	1663.8977	0.0029	2	563	577	KGDVRFLICTDVAAR			
1759.941	1759.9385	-0.0025	-1	401	416	LQVIVCSATLHSFDVK			
1766.9258	1766.9109	-0.0149	-8	208	223	NGKDLGLAFEIPPHMK			
1968.0396	1968.0535	0.0139	7	331	349	DQLSVLENGVDIVVGTPGR			
1968.0396	1968.0535	0.0139	7	331	349	DQLSVLENGVDIVVGTPGR			
1972.0724	1972.047	-0.0254	-13	417	432	KLSEKIMHFPTWVDLK			
2002.9287	2002.9343	0.0056	3	473	490	DNTRPGANSPEMWSEAIK			
2002.9287	2002.9343	0.0056	3	473	490	DNTRPGANSPEMWSEAIK			
2079.1121	2079.095	-0.0171	-8	578	596	GIDIHGVPYVINVTLPDEK			
2134.1079	2134.1172	0.0093	4	721	738	EAQTSFLHLGYLPNQLFR			
2134.1079	2134.1172	0.0093	4	721	738	EAQTSFLHLGYLPNQLFR			
2138.1814	2138.1819	0.0005	0	289	307	ALIVEPSRELAEQTLNNIK			
2372.1768	2372.179	0.0022	1	366	386	FLVLDEADGLLSQGYSDFINR			
2372.1768	2372.179	0.0022	1	366	386	FLVLDEADGLLSQGYSDFINR			
2564.3606	2564.3567	-0.0039	-2	53	75	TGAFSIPVIQIVYETLKDQQEGK			
2876.5051	2876.5066	0.0015	1	578	602	GIDIHGVPYVINVTLPDEKQNYVHR			
2896.5261	2896.5046	-0.0215	-7	331	358	DQLSVLENGVDIVVGTPGRLDDLVSTGK			

Spot Idx/Pos	167/G14	23	**Instr./Spot Origin**	ab4700/042810	**Process Status** Analysis Succeeded
Plate [#] Name	[1] 042810		**4700 Sample Name**		**Spectra** 13

Rank	Protein Name	Accession No.	Protein MW	Protein Score	Protein C. I. %	Total Ion Score	Total Ion C. I. %
1	crystallin, zeta variant [Homo sapiens]	gi|62089008	35384.7	83	99.996	10	70.02

Peptide Information

Calc. Mass	Obsrv. Mass	± da	± ppm	Start Seq.	End Seq.	Sequence	Ion Score	C. I. %	Modification
1054.564	1054.5559	-0.0081	-8	235	244	DLSLLSHGGR			
1221.6512	1221.6334	-0.0178	-15	15	25	VFEFGGPEVLK			
1221.6512	1221.6334	-0.0178	-15	15	25	VFEFGGPEVLK			
1249.6755	1249.6769	0.0014	1	1	11	ITMATGQKLMR			
1527.7954	1527.7863	-0.0091	-6	127	140	QGAAIGIPYFTAYR			
1527.7954	1527.7863	-0.0091	-6	127	140	QGAAIGIPYFTAYR	10	70.02	
1557.7842	1557.7848	0.0006	0	44	57	VHACGVNPVETYIR			
1633.8557	1633.8478	-0.0079	-5	190	203	IVLQNGAHEVFNHR			
1633.8557	1633.8478	-0.0079	-5	190	203	IVLQNGAHEVFNHR			
1773.0269	1773.0081	-0.0188	-11	28	43	SDIAVPIPKDHQVLIK			
2123.1025	2123.1028	0.0003	0	150	172	AGESVLVHGASGGVGLAACQIAR			
2123.1025	2123.1028	0.0003	0	150	172	AGESVLVHGASGGVGLAACQIAR			
2391.26	2391.2693	0.0093	4	37	57	DHQVLIKVHACGVNPVETYIR			
2551.2351	2551.2666	0.0315	12	95	118	VFTSSTISGGYAEYALAADHTVYK			
2716.4192	2716.4446	0.0254	9	64	90	KPLLPYTPGSDVAGVIEAVGDNASAFK			
2804.4436	2804.4668	0.0232	8	178	203	VLGTAGTEEGQKIVLQNGAHEVFNHR			
2844.5142	2844.4875	-0.0267	-9	64	91	KPLLPYTPGSDVAGVIEAVGDNASAFKK			

2	mitochondrial malate dehydrogenase 2, NAD [Homo sapiens]	gi|89574129	31948.8	77	99.986	20	97.029		

Peptide Information

Calc. Mass	Obsrv. Mass	± da	± ppm	Start Seq.	End Seq.	Sequence	Ion Score	C. I. %	Modification
1147.6581	1147.6473	-0.0108	-9	171	182	VNVPVIGGHAGK			
1233.7201	1233.7104	-0.0097	-8	145	155	IFGVTTLDIVR			
1233.7201	1233.7104	-0.0097	-8	145	155	IFGVTTLDIVR	14	87.003	
1281.6982	1281.6901	-0.0081	-6	71	83	GCDVVVIPAGVPR			
1454.7056	1454.6948	-0.0108	-7	221	236	AGAGSATLSMAYAGAR			
1454.7056	1454.6948	-0.0108	-7	221	236	AGAGSATLSMAYAGAR			
1560.8016	1560.7906	-0.011	-7	195	208	VDFPQDQLTALTGR	6	30.843	
1560.8016	1560.7906	-0.011	-7	195	208	VDFPQDQLTALTGR			
1793.0894	1793.0842	-0.0052	-3	6	24	VAVLGASGGIGQPLSLLLK			
1916.9309	1916.9399	0.009	5	259	275	SQETECTYFSTPLLLGK			
2143.1658	2143.1716	0.0058	3	137	155	HGVYNPNKIFGVTTLDIVR			
2143.1658	2143.1716	0.0058	3	137	155	HGVYNPNKIFGVTTLDIVR			
2365.2397	2365.2437	0.004	2	32	53	LTLYDIAHTPGVAADLSHIETK			
2365.2397	2365.2437	0.004	2	32	53	LTLYDIAHTPGVAADLSHIETK			
2695.3945	2695.4033	0.0088	3	58	83	GYLGPEQLPDCLKGCDVVVIPAGVPR			
2855.5334	2855.554	0.0206	7	183	208	TIIPLISQCTPKVDFPQDQLTALTGR			

7	glyceraldehyde-3-phosphate dehydrogenase [Homo sapiens]	gi|31645	36031.4	72	99.957				

Peptide Information

Calc. Mass	Obsrv. Mass	± da	± ppm	Start Seq.	End Seq.	Sequence	Ion Score	C. I. %	Modification
1330.6493	1330.6451	-0.0042	-3	324	335	VVDLMAHMASKE			
1473.7729	1473.7878	0.0149	10	235	248	VPTANVSVVDLTCR			
1613.9009	1613.8972	-0.0037	-2	67	80	LVINGNPITIFQER			
1613.9009	1613.8972	-0.0037	-2	67	80	LVINGNPITIFQER			
1646.8933	1646.8862	-0.0071	-4	220	234	VIPELDGKLTGMAFR			
1763.8022	1763.7977	-0.0045	-3	310	323	LISWYDNEFGYSNR			
1763.8022	1763.7977	-0.0045	-3	310	323	LISWYDNEFGYSNR			
2041.1075	2041.1089	0.0014	1	67	84	LVINGNPITIFQERDPSK			
2041.1075	2041.1089	0.0014	1	67	84	LVINGNPITIFQERDPSK			
2113.1399	2113.1384	-0.0015	-1	62	80	AENGKLVINGNPITIFQER			
2277.0378	2277.0623	0.0245	11	87	107	WGDAGAEYVVESTGVFTTMEK			
2369.2104	2369.2415	0.0311	13	118	139	RVIISAPSADAPMFVMGVNHEK			
2518.2168	2518.2429	0.0261	10	85	107	IKWGDAGAEYVVESTGVFTTMEK			
2540.3467	2540.3274	-0.0193	-8	62	84	AENGKLVINGNPITIFQERDPSK			
2595.3599	2595.3623	0.0024	1	163	186	VIHDNFGIVEGLMTTVHAITATQK			

2933.4534	2933.4802	0.0268	9	119	145	VIISAPSADAPMFVMGVN HEKYDNSLK	

12 uracil DNA glycosylase [Homo sapiens] gi|35053 35470.1 57 98.784

Peptide Information

Calc. Mass	Obsrv. Mass	± da	± ppm	Start Seq.	End Seq.	Sequence	Ion Score	C. I. %	Modification
1473.7729	1473.7878	0.0149	10	234	247	VPTANVSVVDLTCR			
1613.9009	1613.8972	-0.0037	-2	67	80	LVINGNPITIFQER			
1613.9009	1613.8972	-0.0037	-2	67	80	LVINGNPITIFQER			
1763.8022	1763.7977	-0.0045	-3	309	322	LISWYDNEFGYSNR			
1763.8022	1763.7977	-0.0045	-3	309	322	LISWYDNEFGYSNR			
2041.1075	2041.1089	0.0014	1	67	84	LVINGNPITIFQERDPSK			
2041.1075	2041.1089	0.0014	1	67	84	LVINGNPITIFQERDPSK			
2113.1399	2113.1384	-0.0015	-1	62	80	AENGKLVINGNPITIFQER			
2277.0378	2277.0623	0.0245	11	87	107	WGDAGAEYVVESTGVFT TMEK			
2369.2104	2369.2415	0.0311	13	118	139	RVIISAPSADAPMFVMGV NHEK			
2518.2168	2518.2429	0.0261	10	85	107	IKWGDAGAEYVVESTGV FTTMEK			
2540.3467	2540.3274	-0.0193	-8	62	84	AENGKLVINGNPITIFQER DPSK			
2595.3599	2595.3623	0.0024	1	163	186	VIHDNFGIVEGLMTTVHAI TATQK			
2933.4534	2933.4802	0.0268	9	119	145	VIISAPSADAPMFVMGVN HEKYDNSLK			

Spot Idx/Pos	168/G16	24	**Instr./Spot Origin**	ab4700/042810	**Process Status** Analysis Succeeded
Plate [#] Name	[1] 042810		**4700 Sample Name**		**Spectra** 13

Rank	Protein Name	Accession No.	Protein MW	Protein Score	Protein C. I. %	Total Ion Score	Total Ion C. I. %
1	glyceraldehyde-3-phosphate dehydrogenase [Homo sapiens]	gi|89573929	24604.7	107	100	2	0

Peptide Information

Calc. Mass	Obsrv. Mass	± da	± ppm	Start Seq.	End Seq.	Sequence	Ion Score	C. I. %	Modification
1473.7729	1473.845	0.0721	49	210	223	VPTANVSVVDLTCR			
1613.9009	1613.9684	0.0675	42	42	55	LVINGNPITIFQER			
1613.9009	1613.9684	0.0675	42	42	55	LVINGNPITIFQER	2	0	
1645.9093	1645.9619	0.0526	32	195	209	VIPELNGKLTGMAFR			
2041.1075	2041.1807	0.0732	36	42	59	LVINGNPITIFQERDPSK			
2041.1075	2041.1807	0.0732	36	42	59	LVINGNPITIFQERDPSK			
2113.1399	2113.2173	0.0774	37	37	55	AENGKLVINGNPITIFQER			
2213.1091	2213.1819	0.0728	33	94	114	VIISAPSADAPMFVMGVN HEK			
2213.1091	2213.1819	0.0728	33	94	114	VIISAPSADAPMFVMGVN HEK			
2277.0378	2277.1165	0.0787	35	62	82	WGDAGAEYVVESTGVFT TMEK			
2369.2104	2369.3091	0.0987	42	93	114	RVIISAPSADAPMFVMGV NHEK			
2518.2168	2518.3201	0.1033	41	60	82	IKWGDAGAEYVVESTGV FTTMEK			
2540.3467	2540.3562	0.0095	4	37	59	AENGKLVINGNPITIFQER DPSK			
2595.3599	2595.4463	0.0864	33	138	161	VIHDNFGIVEGLMTTVHAI TATQK			
2595.3599	2595.4463	0.0864	33	138	161	VIHDNFGIVEGLMTTVHAI TATQK			
2617.5034	2617.417	-0.0864	-33	176	202	GALQNIIPASTGAAKAVG KVIPELNGK			
2933.4534	2933.5596	0.1062	36	94	120	VIISAPSADAPMFVMGVN HEKYDNSLK			
3308.5642	3308.6765	0.1123	34	3	30	VDIVAINDPFIDLNYMVYM FQYDSTHGK			

10 MDH2 [Homo sapiens] gi|49168580 35536.8 70 99.935 16 78.164

Peptide Information

Calc. Mass	Obsrv. Mass	± da	± ppm	Start Seq.	End Seq.	Sequence	Ion Score	C. I. %	Modification
1221.6837	1221.6976	0.0139	11	325	335	ASIKKGEDFVK			
1233.7201	1233.7793	0.0592	48	166	176	IFGVTTLDIVR			
1233.7201	1233.7793	0.0592	48	166	176	IFGVTTLDIVR	16	78.164	
1281.6982	1281.7611	0.0629	49	92	104	GCDVVVIPAGVPR			
1327.6714	1327.7172	0.0458	34	258	269	FVFSLVDAMNGK			
1352.8372	1352.7809	-0.0563	-42	2	14	LSALVRPVSAALR			
1454.7056	1454.7694	0.0638	44	242	257	AGAGSATLSMAYAGAR			
1515.8451	1515.8148	-0.0303	-20	315	328	MISDAIPELKASIK			
1560.8016	1560.8658	0.0642	41	216	229	VDFPQDQLTALTGR			
1560.8016	1560.8658	0.0642	41	216	229	VDFPQDQLTALTGR			
1601.8645	1601.8942	0.0297	19	177	191	ANTFVAELKGLDPAR			
1793.0894	1793.1414	0.052	29	27	45	VAVLGASGGIGQPLSLLL K			
2143.1658	2143.2273	0.0615	29	158	176	HGVYNPNKIFGVTTLDIV R			
2365.2397	2365.3191	0.0794	34	53	74	LTLYDIAHTPGVAADLSHI ETK			
2365.2397	2365.3191	0.0794	34	53	74	LTLYDIAHTPGVAADLSHI ETK			

4 uracil DNA glycosylase [Homo sapiens] gi|35053 35470.1 52 96.065

Peptide Information

Calc. Mass	Obsrv. Mass	± da	± ppm	Start Seq.	End Seq.	Sequence	Ion Score	C. I. %	Modification
1645.9093	1645.9619	0.0526	32	219	233	VIPELNGKLTGMAFR			
1763.8022	1763.8685	0.0663	38	309	322	LISWYDNEFGYSNR			
1763.8022	1763.8685	0.0663	38	309	322	LISWYDNEFGYSNR			
2041.1075	2041.1807	0.0732	36	67	84	LVINGNPITIFQERDPSK			
2041.1075	2041.1807	0.0732	36	67	84	LVINGNPITIFQERDPSK			
2113.1399	2113.2173	0.0774	37	62	80	AENGKLVINGNPITIFQER			
2213.1091	2213.1819	0.0728	33	119	139	VIISAPSADAPMFVMGVN HEK			
2213.1091	2213.1819	0.0728	33	119	139	VIISAPSADAPMFVMGVN HEK			
2277.0378	2277.1165	0.0787	35	87	107	WGDAGAEYVVESTGVFT TMEK			
2540.3467	2540.3562	0.0095	4	62	84	AENGKLVINGNPITIFQER DPSK			
2595.3599	2595.4463	0.0864	33	163	186	VIHDNFGIVEGLMTTVHAI TATQK			
2595.3599	2595.4463	0.0864	33	163	186	VIHDNFGIVEGLMTTVHAI TATQK			
2933.4534	2933.5596	0.1062	36	119	145	VIISAPSADAPMFVMGVN HEKYDNSLK			
3308.5642	3308.6765	0.1123	34	28	55	VDIVAINDPFIDLNYMVYM FQYDSTHGK			

Spot Idx/Pos	169/G18	25	**Instr./Spot Origin**	ab4700/042810	**Process Status** Analysis Succeeded
Plate [#] Name	[1] 042810		**4700 Sample Name**		**Spectra** 13

Rank	Protein Name	Accession No.	Protein MW	Protein Score	Protein C. I. %	Total Ion Score	Total Ion C. I. %

							Score	C. I. %	Score	C. I. %
1	NME1-NME2 protein [Homo sapiens]				gi|66392203	30117.6	172	100	14	88.077

Peptide Information

Calc. Mass	Obsrv. Mass	± da	± ppm	Start Seq.	End Seq.	Sequence	Ion Score	C. I. %	Modification
977.5964	977.5933	-0.0031	-3	150	157	LVAMKFLR			
984.6199	984.6278	0.0079	8	134	142	GLVGEIIKR			
984.6199	984.6278	0.0079	8	19	27	GLVGEIIKR			
1069.5636	1069.5635	-0.0001	0	230	239	NIIHGSDSVK			
1175.6571	1175.6639	0.0068	6	172	181	DRPFFPGLVK			
1175.6571	1175.6639	0.0068	6	172	181	DRPFFPGLVK			
1344.7633	1344.7697	0.0064	5	122	133	TFIAIKPDGVQR			
1344.7633	1344.7697	0.0064	5	7	18	TFIAIKPDGVQR	15	90.107	
1516.8845	1516.8929	0.0084	6	19	31	GLVGEIIKRFEQK			
1516.8845	1516.8929	0.0084	6	134	146	GLVGEIIKRFEQK			
1710.8809	1710.8773	-0.0036	-2	158	171	ASEEHLKQHYIDLK			
1785.9163	1785.9221	0.0058	3	204	220	VMLGETNPADSKPGTIR			
1785.9163	1785.9221	0.0058	3	89	105	VMLGETNPADSKPGTIR			
1895.9789	1895.9728	-0.0061	-3	244	258	EISLWFKPEELVDYK			
2073.1279	2073.1257	-0.0022	-1	165	181	QHYIDLKDRPFFPGLVK			
2073.1279	2073.1257	-0.0022	-1	165	181	QHYIDLKDRPFFPGLVK			
2093.0557	2093.0549	-0.0008	0	182	200	YMNSGPVVAMVWEGLN VVK			
2311.1855	2311.1824	-0.0031	-1	240	258	SAEKEISLWFKPEELVDY K			
2311.1855	2311.1824	-0.0031	-1	240	258	SAEKEISLWFKPEELVDY K			
2407.2261	2407.2288	0.0027	1	182	203	YMNSGPVVAMVWEGLN VVKTGR			
2867.5203	2867.5078	-0.0125	-4	158	181	ASEEHLKQHYIDLKDRPF FPGLVK			
2867.5203	2867.5078	-0.0125	-4	158	181	ASEEHLKQHYIDLKDRPF FPGLVK			
3361.7312	3361.741	0.0098	3	230	258	NIIHGSDSVKSAEKEISLW FKPEELVDYK			

4	Putative nucleoside diphosphate kinase (NDK) (NDP kinase)				gi|3914116	15519	51	95.159		

Peptide Information

Calc. Mass	Obsrv. Mass	± da	± ppm	Start Seq.	End Seq.	Sequence	Ion Score	C. I. %	Modification
1069.5636	1069.5635	-0.0001	0	100	109	NIIHGSDSVK			
1175.6571	1175.6639	0.0068	6	42	51	DRPFFPGLVK			
1175.6571	1175.6639	0.0068	6	42	51	DRPFFPGLVK			
1785.9163	1785.9221	0.0058	3	74	90	VMLGETNPADSKPGTIR			
1785.9163	1785.9221	0.0058	3	74	90	VMLGETNPADSKPGTIR			
2073.1279	2073.1257	-0.0022	-1	35	51	QHYIDLKDRPFFPGLVK			
2073.1313	2073.1257	-0.0056	-3	17	34	GFRLVAMKFLPASEEHLK			
2093.0557	2093.0549	-0.0008	0	52	70	YMNSGPVVAMVWEGLN VVK			
2407.2261	2407.2288	0.0027	1	52	73	YMNSGPVVAMVWEGLN VVKTGR			

Spot Idx/Pos	170/G20	26	**Instr./Spot Origin**	ab4700/042810	**Process Status** Analysis Succeeded
Plate [#] Name	[1] 042810		**4700 Sample Name**		**Spectra** 13

Rank	Protein Name	Accession No.	Protein MW	Protein Score	Protein C. I. %	Total Ion Score	Total Ion C. I. %
1	NME1-NME2 protein [Homo sapiens]	gi|66392203	30117.6	163	100	29	99.785

Peptide Information

Calc. Mass	Obsrv. Mass	± da	± ppm	Start Seq.	End Seq.	Sequence	Ion Score	C. I. %	Modification
911.4733	911.4702	-0.0031	-3	143	149	FEQKGFR			
984.6199	984.6236	0.0037	4	19	27	GLVGEIIKR	6	52.426	
984.6199	984.6236	0.0037	4	134	142	GLVGEIIKR			
994.4774	994.4841	0.0067	7	221	229	GDFCIQVGR			
994.4774	994.4841	0.0067	7	106	114	GDFCIQVGR	9	76.913	
1069.5636	1069.5569	-0.0067	-6	230	239	NIIHGSDSVK			
1175.6571	1175.6576	0.0005	0	172	181	DRPFFPGLVK			
1175.6571	1175.6576	0.0005	0	172	181	DRPFFPGLVK			
1344.7633	1344.764	0.0007	1	122	133	TFIAIKPDGVQR			
1344.7633	1344.764	0.0007	1	7	18	TFIAIKPDGVQR	17	96.204	
1516.8845	1516.88	-0.0045	-3	134	146	GLVGEIIKRFEQK			
1710.8809	1710.8801	-0.0008	0	158	171	ASEEHLKQHYIDLK			
1785.9163	1785.9178	0.0015	1	89	105	VMLGETNPADSKPGTIR			
1785.9163	1785.9178	0.0015	1	204	220	VMLGETNPADSKPGTIR			
1895.9789	1895.9713	-0.0076	-4	244	258	EISLWFKPEELVDYK			
2073.1279	2073.1345	0.0066	3	165	181	QHYIDLKDRPFFPGLVK			
2093.0557	2093.0532	-0.0025	-1	182	200	YMNSGPVVAMVWEGLN VVK			
2311.1855	2311.1882	0.0027	1	240	258	SAEKEISLWFKPEELVDY K			
2761.376	2761.376	0	0	204	229	VMLGETNPADSKPGTIR GDFCIQVGR			
2867.5203	2867.4978	-0.0225	-8	158	181	ASEEHLKQHYIDLKDRPF FPGLVK			

7	Putative nucleoside diphosphate kinase (NDK) (NDP kinase)				gi|3914116	15519	63	99.649	9	76.913

Peptide Information

Calc. Mass	Obsrv. Mass	± da	± ppm	Start Seq.	End Seq.	Sequence	Ion Score	C. I. %	Modification
911.4733	911.4702	-0.0031	-3	13	19	FEQKGFR			
994.4774	994.4841	0.0067	7	91	99	GDFCIQVGR			
994.4774	994.4841	0.0067	7	91	99	GDFCIQVGR	9	76.913	
1069.5636	1069.5569	-0.0067	-6	100	109	NIIHGSDSVK			
1175.6571	1175.6576	0.0005	0	42	51	DRPFFPGLVK			
1175.6571	1175.6576	0.0005	0	42	51	DRPFFPGLVK			
1785.9163	1785.9178	0.0015	1	74	90	VMLGETNPADSKPGTIR			
1785.9163	1785.9178	0.0015	1	74	90	VMLGETNPADSKPGTIR			
2073.1313	2073.1345	0.0032	2	17	34	GFRLVAMKFLPASEEHLK			
2093.0557	2093.0532	-0.0025	-1	52	70	YMNSGPVVAMVWEGLN VVK			
2761.376	2761.376	0	0	74	99	VMLGETNPADSKPGTIR GDFCIQVGR			

8	RNA binding motif protein 3 isoform a [Homo sapiens]				gi|5803137	17160	41	41.804		

Peptide Information

Calc. Mass	Obsrv. Mass	± da	± ppm	Start Seq.	End Seq.	Sequence	Ion Score	C. I. %	Modification
867.4067	867.4026	-0.0041	-5	132	138	SRDYNGR			
1437.5665	1437.5724	0.0059	4	146	157	YSGGNYRDNYDN			
1437.5665	1437.5724	0.0059	4	146	157	YSGGNYRDNYDN			
1606.6992	1606.7145	0.0153	10	139	152	NQGGYDRYSGGNYR			
1730.7556	1730.754	-0.0016	-1	117	131	YYDSRPGGYGYGYGR			
1730.7556	1730.754	-0.0016	-1	117	131	YYDSRPGGYGYGYGR			
1981.9589	1981.9657	0.0068	3	48	65	GFGFITFTNPEHASVAMR			
1981.9589	1981.9657	0.0068	3	48	65	GFGFITFTNPEHASVAMR			
2225.092	2225.1077	0.0157	7	46	65	SRGFGFITFTNPEHASVA MR			
2227.9023	2227.9102	0.0079	4	139	157	NQGGYDRYSGGNYRDN YDN			
2227.9023	2227.9102	0.0079	4	139	157	NQGGYDRYSGGNYRDN			

YDN

Spot Idx/Pos	171/G22	27	Instr./Spot Origin	ab4700/042810	Process Status	Analysis Succeeded
Plate [#] Name	[1] 042810		4700 Sample Name		Spectra	13

Rank	Protein Name	Accession No.	Protein MW	Protein Score	Protein C. I. %	Total Ion Score	Total Ion C. I. %
1	type 1 RNA helicase pNORF1	gi|1885356	122976	202	100	1	0

Peptide Information

Calc. Mass	Obsrv. Mass	± da	± ppm	Start Seq.	End Seq.	Sequence	Ion Score	C. I. %	Modification
942.5843	942.5868	0.0025	3	858	865	RLNVALTR			
952.5502	952.5402	-0.01	-10	342	349	IAYFTLPK			
1099.5742	1099.5775	0.0033	3	245	253	IPSEQEQLR			
1107.5792	1107.5828	0.0036	3	678	687	AGLSQSLFER			
1129.6476	1129.64	-0.0076	-7	333	341	WDLGLNKKR			
1135.7673	1135.7693	0.002	2	688	697	LVVLGIRPIR			
1135.7673	1135.7693	0.002	2	688	697	LVVLGIRPIR			
1182.6953	1182.6874	-0.0079	-7	918	928	KLVNTINPGAR			
1182.6953	1182.6874	-0.0079	-7	918	928	KLVNTINPGAR			
1206.5282	1206.5366	0.0084	7	929	938	FMTTAMYDAR			
1206.5282	1206.5366	0.0084	7	929	938	FMTTAMYDAR	1	0	
1219.6317	1219.6475	0.0158	13	939	949	EAIIPGSVYDR			
1219.6317	1219.6475	0.0158	13	939	949	EAIIPGSVYDR			
1222.6249	1222.6318	0.0069	6	908	917	ESLMQFSKPR			
1286.7578	1286.7528	-0.005	-4	866	877	ARYGVIIVGNPK			
1286.7578	1286.7528	-0.005	-4	866	877	ARYGVIIVGNPK			
1322.7136	1322.7274	0.0138	10	833	843	EKDFIILSCVR			
1380.6542	1380.6582	0.004	3	1106	1118	AYQHGGVTGLSQY			
1431.7954	1431.8054	0.01	7	499	511	TVTSATIVYHLAR			
1431.7954	1431.8054	0.01	7	499	511	TVTSATIVYHLAR			
1490.7822	1490.7893	0.0071	5	149	162	GNTSGSHIVNHLVR			
1490.7822	1490.7893	0.0071	5	149	162	GNTSGSHIVNHLVR			
1531.8074	1531.809	0.0016	1	320	332	LKESQTQDNITVR			
1567.7611	1567.761	-0.0001	0	844	857	ANEHQGIGFLNDPR			
1567.7611	1567.761	-0.0001	0	844	857	ANEHQGIGFLNDPR			
1603.7961	1603.8101	0.014	9	383	396	VPDNYGDEIAIELR			
1657.8254	1657.8335	0.0081	5	342	355	IAYFTLPKTDSDMR			
1723.8622	1723.8701	0.0079	5	844	858	ANEHQGIGFLNDPRR			
1816.8751	1816.8944	0.0193	11	429	444	TFAVDETSVSGYIYHK			
1824.9126	1824.9191	0.0065	4	817	832	LYQEVEIASVDAFQGR			
1824.9126	1824.9191	0.0065	4	817	832	LYQEVEIASVDAFQGR			
1862.0857	1862.0919	0.0062	3	481	498	TVLQRPLSLIQGPPGTGK			
1862.0857	1862.0919	0.0062	3	481	498	TVLQRPLSLIQGPPGTGK			
1896.8933	1896.9064	0.0131	7	1089	1105	SQIDVALSQDSTYQGER			
1910.0129	1910.0242	0.0113	6	550	566	EAIDSPVSFLALHNQIR			
1910.0129	1910.0242	0.0113	6	550	566	EAIDSPVSFLALHNQIR			
1914.0078	1914.0186	0.0108	6	783	800	AGAKPDQIGIITPYEGQR			
1947.9486	1947.9583	0.0097	5	296	311	YEDAYQYQNIFGPLVK			
1953.0118	1953.0227	0.0109	6	656	673	QLILVGDHCQLGPVVMCK			
1988.0236	1988.0309	0.0073	4	463	480	FTAQGLPDLNHSQVYAVK			
2000.946	2000.9686	0.0226	11	221	236	DINWDSSQWQPLIQDR			
2047.0302	2047.0461	0.0159	8	577	594	LQQLKDETGELSSADEKR			
2082.05	2082.0237	-0.0263	-13	817	834	LYQEVEIASVDAFQGREK			
2144.1245	2144.1235	-0.001	0	462	480	RFTAQGLPDLNHSQVYAVK			
2246.124	2246.1479	0.0239	11	397	416	SSVGAPVEVTHNFQVDFVWK			
2253.1543	2253.1572	0.0029	1	512	533	QGNGPVLVCAPSNIAVDQLTEK			
2308.2295	2308.2256	-0.0039	-2	376	396	GIGHVIKVPDNYGDEIAIELR			
2530.2778	2530.3091	0.0313	12	632	655	SILIDESTQATEPECMVPVVLGAK			
2538.1406	2538.157	0.0164	6	96	116	TSQLLAELNFEEDEEDTYYTK			
2815.4106	2815.4187	0.0081	3	271	295	ENPSATLEDLEKPGVDEEPQHVLLR			

31	transcription activator	gi|292496	114659.1	22	0			

Peptide Information

Calc. Mass	Obsrv. Mass	± da	± ppm	Start Seq.	End Seq.	Sequence	Ion Score	C. I. %	Modification
1094.6027	1094.597	-0.0057	-5	427	435	VLIFSQMTR			
1115.5844	1115.6006	0.0162	15	229	237	YLVIDEAHR			
1159.6371	1159.646	0.0089	8	865	873	YKAPFHQLR			
1159.6371	1159.646	0.0089	8	865	873	YKAPFHQLR			
1174.6327	1174.6414	0.0087	7	102	111	GGPLRDYQIR			
1222.6248	1222.6318	0.007	6	182	192	VICFVGDKDAR			
1237.6575	1237.6388	-0.0187	-15	467	476	FLEVEFLGQR			
1305.6909	1305.7035	0.0126	10	740	751	NPDIPNPALAQR			
1308.6946	1308.6876	-0.007	-5	774	784	LLTQGFTNWTK			
1397.8223	1397.8152	-0.0071	-5	562	573	LRLDSIVIQQGR			
1619.7964	1619.8162	0.0198	12	705	717	QPNVQDFQFFPPR			
1645.8809	1645.87	-0.0109	-7	867	880	APFHQLRIQYGTSK			
1670.9119	1670.9052	-0.0067	-4	837	850	IMAQIERGEARIQR			
1686.902	1686.8951	-0.0069	-4	544	557	LITDNTVEERIVER			
1819.9297	1819.9084	-0.0213	-12	740	755	NPDIPNPALAQREEQK			

43	Tax1-binding protein 2 [Homo sapiens]	gi|76560593	148167.9	21	0			

Peptide Information

Calc. Mass	Obsrv. Mass	± da	± ppm	Start Seq.	End Seq.	Sequence	Ion Score	C. I. %	Modification
1159.6317	1159.646	0.0143	12	245	255	ETLTGELAGLR			
1159.6317	1159.646	0.0143	12	245	255	ETLTGELAGLR			
1190.6375	1190.6339	-0.0036	-3	411	421	STVNALTSELR			
1320.6212	1320.637	0.0158	12	453	463	DSCLREAEELR			
1333.6957	1333.6971	0.0014	1	945	956	EVLDASESRTVK			
1407.7703	1407.7583	-0.012	-9	682	693	QQLDHARGLELK			
1486.772	1486.7902	0.0182	12	487	498	LRESQEGREVQR			
1540.7754	1540.7549	-0.0205	-13	1299	1313	RSSAPFSPPSGPPEK			
1584.8088	1584.8094	0.0006	0	1195	1208	SHEDTVRLSAEKGR			
1669.9119	1669.8969	-0.015	-9	56	69	LDLNRLVAQLEEEK			
1670.9071	1670.9052	-0.0019	-1	61	75	LVAQLEEEKSALQGR			
1747.9224	1747.9001	-0.0223	-13	207	221	LEKEALEGSLFEVQR			
1947.9552	1947.9583	0.0031	2	833	849	TQTSALNRQLAEMEAER			
2000.9744	2000.9686	-0.0058	-3	489	505	ESQEGREVQRQEAGELR			
2284.1638	2284.176	0.0122	5	1124	1143	QRQEGEAAALNTVQKLQDER			
2287.2039	2287.1743	-0.0296	-13	210	229	EALEGSLFEVQRQLAQLEAR			

Spot Idx/Pos	172/G24	28	Instr./Spot Origin	ab4700/042810	Process Status	Analysis Succeeded
Plate [#] Name	[1] 042810		4700 Sample Name		Spectra	13

Rank	Protein Name	Accession No.	Protein MW	Protein Score	Protein C. I. %	Total Ion Score	Total Ion C. I. %
1	Regulator of nonsense transcripts 1 (ATP-dependent helicase RENT1) (Nonsense mRNA reducing factor 1	gi|17380291	124266.7	216	100		

Peptide Information

Calc. Mass	Obsrv. Mass	± da	± ppm	Start Seq.	End Seq.	Sequence	Ion Score	C. I. %	Modification
942.5843	942.5738	-0.0105	-11	869	876	RLNVALTR			

952.5502	952.5398	-0.0104	-11	342	349	IAYFTLPK
1059.6196	1059.6069	-0.0127	-12	879	888	YGVIIVGNPK
1099.5742	1099.5876	0.0134	12	245	253	IPSEQEQLR
1107.5792	1107.5837	0.0045	4	689	698	AGLSQSLFER
1135.7673	1135.7666	-0.0007	-1	699	708	LVVLGIRPIR
1135.7673	1135.7666	-0.0007	-1	699	708	LVVLGIRPIR
1182.6953	1182.7019	0.0066	6	929	939	KLVNTINPGAR
1206.5282	1206.5421	0.0139	12	940	949	FMTTAMYDAR
1206.5282	1206.5421	0.0139	12	940	949	FMTTAMYDAR
1218.7244	1218.7244	0	0	190	200	NVFLLGFIPAK
1222.6249	1222.6359	0.011	9	919	928	ESLMQFSKPR
1223.7106	1223.699	-0.0116	-9	908	918	VLVEGPLNNLR
1223.7106	1223.699	-0.0116	-9	908	918	VLVEGPLNNLR
1286.7578	1286.7611	0.0033	3	877	888	ARYGVIIVGNPK
1286.7578	1286.7611	0.0033	3	877	888	ARYGVIIVGNPK
1364.7783	1364.7693	-0.009	-7	456	467	LLGHEVEDVIIK
1380.6542	1380.671	0.0168	12	1117	1129	AYQHGGVTGLSQY
1431.7954	1431.8002	0.0048	3	510	522	TVTSATIVYHLAR
1431.7954	1431.8002	0.0048	3	510	522	TVTSATIVYHLAR
1490.7822	1490.7894	0.0072	5	149	162	GNTSGSHIVNHLVR
1490.7822	1490.7894	0.0072	5	149	162	GNTSGSHIVNHLVR
1567.7611	1567.7598	-0.0013	-1	855	868	ANEHQGIGFLNDPR
1567.7611	1567.7598	-0.0013	-1	855	868	ANEHQGIGFLNDPR
1588.827	1588.8282	0.0012	1	893	904	QPLWNHLLNYYK
1603.7961	1603.7972	0.0011	1	394	407	VPDNYGDEIAIELR
1630.8435	1630.8455	0.002	1	350	363	TDSGNEDLVIIWLR
1723.8622	1723.861	-0.0012	-1	855	869	ANEHQGIGFLNDPRR
1723.8622	1723.861	-0.0012	-1	855	869	ANEHQGIGFLNDPRR
1816.8751	1816.8787	0.0036	2	440	455	TFAVDETSVSGYIYHK
1824.9126	1824.9178	0.0052	3	828	843	LYQEVEIASVDAFQGR
1824.9126	1824.9178	0.0052	3	828	843	LYQEVEIASVDAFQGR
1862.0857	1862.0867	0.001	1	492	509	TVLQRPLSLIQGPPGTGK
1862.0857	1862.0867	0.001	1	492	509	TVLQRPLSLIQGPPGTGK
1888.9261	1888.934	0.0079	4	812	827	SYLVQYMQFSGSLHTK
1910.0129	1910.0179	0.005	3	561	577	EAIDSPVSFLALHNQIR
1910.0129	1910.0179	0.005	3	561	577	EAIDSPVSFLALHNQIR
1914.0078	1914.0145	0.0067	4	794	811	AGAKPDQIGIITPYEGQR
1947.9486	1947.9462	-0.0024	-1	296	311	YEDAYQYQNIFGPLVK
1988.0236	1988.0115	-0.0121	-6	474	491	FTAQGLPDLNHSQVYAVK
2000.946	2000.9602	0.0142	7	221	236	DINWDSSQWQPLIQDR
2047.0302	2047.033	0.0028	1	588	605	LQQLKDETGELSSADEKR
2144.1245	2144.1265	0.002	1	473	491	RFTAQGLPDLNHSQVYAVK
2153.146	2153.1426	-0.0034	-2	559	577	SREAIDSPVSFLALHNQIR
2308.2295	2308.23	0.0005	0	387	407	GIGHVIKVPDNYGDEIAIELR
2308.2295	2308.23	0.0005	0	387	407	GIGHVIKVPDNYGDEIAIELR
2538.1406	2538.147	0.0064	3	96	116	TSQLLAELNFEEDEEDTYYTK
2815.4106	2815.4021	-0.0085	-3	271	295	ENPSATLEDLEKPGVDEEPQHVLLR
2893.3936	2893.3936	0	0	715	741	MHPALSAFPSNIFYEGSLQNGVTAADR

Spot Idx/Pos	187/H2	29	**Instr./Spot Origin**	ab4700/042810	**Process Status**	Analysis Succeeded
Plate [#] Name	[1] 042810		**4700 Sample Name**		**Spectra**	13

Rank	Protein Name	Accession No.	Protein MW	Protein Score	Protein C. I. %	Total Ion Score	Total Ion C. I. %
1	glutamate dehydrogenase 1 variant [Homo sapiens]	gi|62897195	61301.2	107	100	13	86.964

Peptide Information

Calc. Mass	Obsrv. Mass	± da	± ppm	Start Seq.	End Seq.	Sequence	Ion Score	C. I. %	Modification
956.52	956.5281	0.0081	8	454	460	LTFKYER			
956.52	956.5281	0.0081	8	454	460	LTFKYER			
963.5258	963.5309	0.0051	5	528	535	YNLGLDLR			
995.5342	995.5436	0.0094	9	204	211	RFTMELAK			
1000.4556	1000.4669	0.0113	11	69	76	MVEGFFDR			
1000.4556	1000.4669	0.0113	11	69	76	MVEGFFDR			
1059.533	1059.5468	0.0138	13	445	453	NLNHVSYGR			
1059.533	1059.5468	0.0138	13	445	453	NLNHVSYGR			
1394.746	1394.748	0.002	1	524	535	TAMKYNLGLDLR			
1425.6281	1425.6279	-0.0002	0	125	136	DDGSWEVIEGYR			
1425.6281	1425.6279	-0.0002	0	125	136	DDGSWEVIEGYR	1	0	
1488.828	1488.8413	0.0133	9	35	50	GQPAAAPQPGLALAAR			
1491.726	1491.7263	0.0003	0	504	516	DIVHSGLAYTMER			
1543.8325	1543.8275	-0.005	-3	77	90	GASIVEDKLVEDLR			
1543.8325	1543.8275	-0.005	-3	77	90	GASIVEDKLVEDLR	12	81.881	
1581.7291	1581.7305	0.0014	1	124	136	RDDGSWEVIEGYR			
1737.8918	1737.8822	-0.0096	-6	481	496	HGGTIPIVPTAEFQDR			
1737.8918	1737.8822	-0.0096	-6	481	496	HGGTIPIVPTAEFQDR			
1748.89	1748.8826	-0.0074	-4	303	318	TFVVQGFGNVGLHSMR			
1748.89	1748.8826	-0.0074	-4	303	318	TFVVQGFGNVGLHSMR			
1837.0516	1837.0535	0.0019	1	108	123	IIKPCNHVLSLSFPIR			
1837.0516	1837.0535	0.0019	1	108	123	IIKPCNHVLSLSFPIR			
1915.9218	1915.9131	-0.0087	-5	213	231	GFIGPGIDVPAPDMSTGER			
1920.912	1920.9061	-0.0059	-3	461	476	DSNYHLLMSVQESLER			
1920.912	1920.9061	-0.0059	-3	461	476	DSNYHLLMSVQESLER			
1958.0381	1958.0212	-0.0169	-9	347	363	ELEDFKLQHGSILGFPK			
1993.1527	1993.1251	-0.0276	-14	108	124	IIKPCNHVLSLSFPIRR			
2044.0167	2044.0094	-0.0073	-4	212	231	KGFIGPGIDVPAPDMSTGER			
2049.0068	2049.0005	-0.0063	-3	461	477	DSNYHLLMSVQESLERK			
2164.0703	2164.0613	-0.009	-4	497	516	ISGASEKDIVHSGLAYTMER			
2164.0703	2164.0613	-0.009	-4	497	516	ISGASEKDIVHSGLAYTMER			
2242.1714	2242.1565	-0.0149	-7	400	420	IIAEGANGPTTPEADKIFLER			
2242.1714	2242.1565	-0.0149	-7	400	420	IIAEGANGPTTPEADKIFL			

Rank	Protein Name	Accession No.	Protein MW	Protein Score	Protein C. I. %	Total Ion Score	Total Ion C. I. %
7	ATP synthase, H+ transporting, mitochondrial F1 complex, beta subunit precursor [Homo sapiens]	gi|32189394	56524.6	40	25.028		

Peptide Information

Calc. Mass	Obsrv. Mass	± da	± ppm	Start Seq.	End Seq.	Sequence	Ion Score	C. I. %	Modification
1385.7092	1385.7094	0.0002	0	144	155	IMNVIGEPIDER			
1406.681	1406.6974	0.0164	12	226	239	AHGGYSVFAGVGER			
1435.7539	1435.7715	0.0176	12	311	324	FTQAGSEVSALLGR			
1439.7892	1439.7858	-0.0034	-2	282	294	VALTGLTVAEYFR			
1601.8103	1601.8223	0.012	7	265	279	VALVYGQMNEPPGAR			
1650.9172	1650.9092	-0.008	-5	95	109	LVLEVAQHLGESTVR			
1650.9172	1650.9092	-0.008	-5	95	109	LVLEVAQHLGESTVR			
1780.9625	1780.9495	-0.013	-7	144	159	IMNVIGEPIDERGPIK			
1815.8694	1815.8885	0.0191	11	407	422	IMDPNIVGSEHYDVAR			
1988.0334	1988.0197	-0.0137	-7	388	406	AIAELGIYPAVDPLDSTSR			
2023.0105	2023.0178	0.0073	4	463	480	FLSQPFQVAEVFTGHMGK			
2266.0842	2266.0862	0.002	1	325	345	IPSAVGYQPTLATDMGTMQER			
2318.1445	2318.1326	-0.0119	-5	240	259	TREGNDLYHEMIESGVIN			

							LK
3338.7014		3338.7253	0.0239	7	295	324	DQEGQDVLLFIDNIFRFT QAGSEVSALLGR

Spot Idx/Pos	188/H4	30	**Instr./Spot Origin**	ab4700/042810	**Process Status**	Analysis Succeeded
Plate [#] Name	[1] 042810		**4700 Sample Name**		**Spectra**	13

Rank	Protein Name	Accession No.	Protein MW	Protein Score	Protein C. I. %	Total Ion Score	Total Ion C. I. %
1	Chain A, Structure Of Human Glutamate Dehydrogenase-Apo Form	gi|20151	55973.4	198	100	23 #	

Peptide Information

Calc. Mass	Obsrv. Mass	± da	± ppm	Start Seq.	End Seq.	Sequence	Ion Score	C. I. %	Modification
905.4323	905.4658	0.0335	37	40	46	ESEEQKR			
956.52	956.5453	0.0253	26	401	407	LTFKYER			
956.52	956.5453	0.0253	26	401	407	LTFKYER			
963.5258	963.5499	0.0241	25	475	482	YNLGLDLR			
1000.4556	1000.4904	0.0348	35	16	23	MVEGFFDR	6	0	
1000.4556	1000.4904	0.0348	35	16	23	MVEGFFDR			
1059.533	1059.5614	0.0284	27	392	400	NLNHVSYGR			
1394.746	1394.7701	0.0241	17	471	482	TAMKYNLGLDLR			
1425.6281	1425.6548	0.0267	19	72	83	DDGSWEVIEGYR			
1425.6281	1425.6548	0.0267	19	72	83	DDGSWEVIEGYR	6	0	
1491.726	1491.7567	0.0307	21	451	463	DIVHSGLAYTMER			
1543.8325	1543.8599	0.0274	18	24	37	GASIVEDKLVEDLR	10	37.458	
1543.8325	1543.8599	0.0274	18	24	37	GASIVEDKLVEDLR			
1581.7291	1581.7565	0.0274	17	71	83	RDDGSWEVIEGYR			
1737.8918	1737.9161	0.0243	14	428	443	HGGTIPIVPTAEFQDR			
1737.8918	1737.9161	0.0243	14	428	443	HGGTIPIVPTAEFQDR			
1748.89	1748.9139	0.0239	14	250	265	TFVVQGFGNVGLHSMR			
1748.89	1748.9139	0.0239	14	250	265	TFVVQGFGNVGLHSMR			
1837.0516	1837.0806	0.029	16	55	70	IIKPCNHVLSLSFPIR			
1837.0516	1837.0806	0.029	16	55	70	IIKPCNHVLSLSFPIR			
1915.9218	1915.9493	0.0275	14	160	178	GFIGPGIDVPAPDMSTGE R			
1920.912	1920.9424	0.0304	16	408	423	DSNYHLLMSVQESLER			
1920.912	1920.9424	0.0304	16	408	423	DSNYHLLMSVQESLER			
1933.0024	1932.9475	-0.0549	-28	131	147	AGVKINPKNYTDNELEK			
1958.0381	1958.0604	0.0223	11	294	310	ELEDFKLQHGSILGFPK			
1958.0381	1958.0604	0.0223	11	294	310	ELEDFKLQHGSILGFPK			
1993.1527	1993.1589	0.0062	3	55	71	IIKPCNHVLSLSFPIRR			
2044.0167	2044.0457	0.029	14	159	178	KGFIGPGIDVPAPDMSTG ER			
2044.0167	2044.0457	0.029	14	159	178	KGFIGPGIDVPAPDMSTG ER			
2049.0068	2049.0439	0.0371	18	408	424	DSNYHLLMSVQESLERK			
2164.0703	2164.1028	0.0325	15	444	463	ISGASEKDIVHSGLAYTM ER			
2164.0703	2164.1028	0.0325	15	444	463	ISGASEKDIVHSGLAYTM ER			
2242.1714	2242.2017	0.0303	14	347	367	IIAEGANGPTTPEADKIFL ER			
2242.1714	2242.2017	0.0303	14	347	367	IIAEGANGPTTPEADKIFL ER			
2318.1975	2318.209	0.0115	5	250	269	TFVVQGFGNVGLHSMRY LHR			
2441.3035	2441.3164	0.0129	5	345	367	AKIIAEGANGPTTPEADKI FLER			
2497.2139	2497.2927	0.0788	32	405	424	YERDSNYHLLMSVQESL ERK			
2603.3384	2603.3323	-0.0061	-2	95	118	GGIRYSTDVSVDEVKALA SLMTYK			
2742.4211	2742.4666	0.0455	17	368	391	NIMVIPDLYLNAGGVTVS YFEWLK			
3045.4885	3045.5374	0.0489	16	266	293	YLHRFGAKCIAVGESDGS IWNPDGIDPK			
3782.9363	3782.9573	0.021	6	368	400	NIMVIPDLYLNAGGVTVS YFEWLKNLNHVSYGR			

Rank	Protein Name	Accession No.	Protein MW	Protein Score	Protein C. I. %	Total Ion Score	Total Ion C. I. %
6	ATP synthase, H+ transporting, mitochondrial F1 complex, beta subunit precursor [Homo sapiens]	gi|32189	56524.6	84	99.997		

Peptide Information

Calc. Mass	Obsrv. Mass	± da	± ppm	Start Seq.	End Seq.	Sequence	Ion Score	C. I. %	Modification
1385.7092	1385.7341	0.0249	18	144	155	IMNVIGEPIDER			
1406.681	1406.7242	0.0432	31	226	239	AHGGYSVFAGVGER			
1435.7539	1435.782	0.0281	20	311	324	FTQAGSEVSALLGR			
1439.7892	1439.8136	0.0244	17	282	294	VALTGLTVAEYFR			
1601.8103	1601.8384	0.0281	18	265	279	VALVYGQMNEPPGAR			
1650.9172	1650.9451	0.0279	17	95	109	LVLEVAQHLGESTVR			
1748.8561	1748.9139	0.0578	33	45	62	DYAAQTSPSPKAGAATG R			
1748.8561	1748.9139	0.0578	33	45	62	DYAAQTSPSPKAGAATG R			
1780.9625	1780.9805	0.018	10	144	159	IMNVIGEPIDERGPIK			
1815.8694	1815.9052	0.0358	20	407	422	IMDPNIVGSEHYDVAR			
1988.0334	1988.0648	0.0314	16	388	406	AIAELGIYPAVDPLDSTSR			
2023.0105	2023.0638	0.0533	26	463	480	FLSQPFQVAEVFTGHMG K			
2060.9956	2061.0601	0.0645	31	242	259	EGNDLYHEMIESGVINLK			
2164.1145	2164.1028	-0.0117	-5	35	55	AAPTAVHPVRDYAAQTS PSPK			
2164.1145	2164.1028	-0.0117	-5	35	55	AAPTAVHPVRDYAAQTS PSPK			
2228.1128	2228.1885	0.0757	34	407	426	IMDPNIVGSEHYDVARGV QK			
2266.0842	2266.1287	0.0445	20	325	345	IPSAVGYQPTLATDMGT MQER			
2318.1445	2318.209	0.0645	28	240	259	TREGNDLYHEMIESGVIN LK			
2732.6045	2732.5076	-0.0969	-35	19	44	RLTPSASLPPAQLLRAA PTAVHPVR			
3031.6824	3031.5806	-0.1018	-34	63	91	IVAVIGAVVDVQFDEGLP PILNALEVQGR			
3714.886	3714.8579	-0.0281	-8	352	387	GSITSVQAIYVPADDLTD PAPATTFAHLDATTVLSR			

Spot Idx/Pos	189/H6	31	**Instr./Spot Origin**	ab4700/042810	**Process Status**	Analysis Succeeded
Plate [#] Name	[1] 042810		**4700 Sample Name**		**Spectra**	13

Rank	Protein Name	Accession No.	Protein MW	Protein Score	Protein C. I. %	Total Ion Score	Total Ion C. I. %
1	lactate dehydrogenase A [Homo sapiens]	gi|5031857	36665.4	150	100	21	97.755

Peptide Information

Calc. Mass	Obsrv. Mass	± da	± ppm	Start Seq.	End Seq.	Sequence	Ion Score	C. I. %	Modification
833.3748	833.3673	-0.0075	-9	100	106	QQEGESR			
913.5829	913.5765	-0.0064	-7	91	99	LVIITAGAR			
913.5829	913.5765	-0.0064	-7	91	99	LVIITAGAR	21	97.755	
1071.5404	1071.5294	-0.011	-10	170	177	FRYLMGER			
1071.5404	1071.5294	-0.011	-10	170	177	FRYLMGER			

1134.5636	1134.5571	-0.0065	-6	306	315	VTLTSEEEAR	
1167.6666	1167.6621	-0.0045	-4	269	278	RVHPVSTMIK	
1167.6666	1167.6621	-0.0045	-4	269	278	RVHPVSTMIK	
1191.5786	1191.5812	0.0026	2	158	169	VIGSGCNLDSAR	
1494.748	1494.7413	-0.0067	-4	158	171	VIGSGCNLDSARFR	
1556.8138	1556.8066	-0.0072	-5	100	112	QQEGESRLNLVQR	
1633.7825	1633.7809	-0.0016	-1	60	73	GEMMDLQHGSLFLR	
1633.7825	1633.7809	-0.0016	-1	60	73	GEMMDLQHGSLFLR	
1644.9835	1644.9662	-0.0173	-11	113	126	NVNIFKFIIPNVVK	
1874.9614	1874.9647	0.0033	2	58	73	LKGEMMDLQHGSLFLR	
1874.9614	1874.9647	0.0033	2	58	73	LKGEMMDLQHGSLFLR	
1906.0392	1906.0281	-0.0111	-6	82	99	DYNVTANSKLVIITAGAR	
1910.9606	1910.9519	-0.0087	-5	213	228	TLHPDLGTDKDKEQWK	
2074.0815	2074.0828	0.0013	1	6	22	DQLIYNLLKEEQTPQNK	
2112.0681	2112.0447	-0.0234	-11	246	265	GYTSWAIGLSVADLAESIMK	
2232.158	2232.1401	-0.0179	-8	285	305	DDVFLSVPCILGQNGISDLVK	
2353.2471	2353.2388	-0.0083	-4	244	265	LKGYTSWAIGLSVADLAESIMK	
2390.3401	2390.3481	0.008	3	77	99	IVSGKDYNVTANSKLVIITAGAR	
2863.5273	2863.5417	0.0144	5	279	305	GLYGIKDDVFLSVPCILGQNGISDLVK	

4	heterogeneous nuclear ribonucleoprotein A2/B1 isoform A2 [Homo sapiens]	gi|4504447	35983.9	48	89.163	

Peptide Information

Calc. Mass	Obsrv. Mass	± da	± ppm	Start Seq.	End Seq.	Sequence	Ion Score	C. I. %	Modification
1013.4434	1013.4584	0.015	15	192	201	GGNFGFGDSR			
1377.6293	1377.627	-0.0023	-2	202	216	GGGGNFGPGPGSNFR			
1377.6293	1377.627	-0.0023	-2	202	216	GGGGNFGPGPGSNFR			
1410.6873	1410.6952	0.0079	6	162	173	YHTINGHNAEVR			
1798.9221	1798.938	0.0159	9	11	26	LFIGGLSFETTEESLR			
1879.9659	1879.9691	0.0032	2	102	117	LFVGGIKEDTEEHHLR			
1927.017	1927.0332	0.0162	8	10	26	KLFIGGLSFETTEESLR			
2189.9053	2189.9114	0.0061	3	314	338	NMGGPYGGGNYGPGGSGGSGGYGGR			
2189.9053	2189.9114	0.0061	3	314	338	NMGGPYGGGNYGPGGSGGSGGYGGR			
2220.0706	2220.0769	0.0063	3	118	135	DYFEEYGKIDTIEIITDR			
2277.155	2277.1479	-0.0071	-3	142	161	GFGFVTFDDHDPVDKIVLQK			
2495.0393	2495.0474	0.0081	3	227	254	GFGDGYNGYGGGPGGGNFGGSPGYGGGR			

32	Phosphodiesterase 6A, cGMP-specific, rod, alpha [Homo sapiens]	gi|112180437	99482.8	22	0	

Peptide Information

Calc. Mass	Obsrv. Mass	± da	± ppm	Start Seq.	End Seq.	Sequence	Ion Score	C. I. %	Modification
929.5665	929.5605	-0.006	-6	32	40	LISDLLGAK			
1011.5581	1011.5488	-0.0093	-9	621	629	LHGSSILER			
1542.8525	1542.8413	-0.0112	-7	318	330	VIDYILHGKEDIK			
1784.9146	1784.9069	-0.0077	-4	751	765	TVLQQNPIPMMDRNK			
1784.9146	1784.9069	-0.0077	-4	751	765	TVLQQNPIPMMDRNK			
1886.9969	1886.9821	-0.0148	-8	198	213	VDGSHFTKRDEEILLK			
2249.1138	2249.0938	-0.02	-9	12	29	FLDSNIGFAKQYYNLHYR			
2438.2529	2438.2637	0.0108	4	751	771	TVLQQNPIPMMDRNKADELPK			
2806.4246	2806.4207	-0.0039	-1	556	579	ITYHNWRHGFNVGQTMFSLLVTGK			
2934.5195	2934.5176	-0.0019	-1	555	579	KITYHNWRHGFNVGQTMFSLLVTGK			
3682.876	3682.8433	-0.0327	-9	207	236	DEEILLKYLNFANLIMKVYHLSYLHNCETR			

Spot Idx/Pos	190/H8	32	**Instr./Spot Origin**	ab4700/042810	**Process Status**	Analysis Succeeded
Plate [#] Name	[1] 042810		**4700 Sample Name**		**Spectra**	13

Rank	Protein Name	Accession No.	Protein MW	Protein Score	Protein C. I. %	Total Ion Score	Total Ion C. I. %
1	lactate dehydrogenase A [Homo sapiens]	gi|50318	36665.4	119	100		

Peptide Information

Calc. Mass	Obsrv. Mass	± da	± ppm	Start Seq.	End Seq.	Sequence	Ion Score	C. I. %	Modification
833.4152	833.4354	0.0202	24	223	228	DKEQWK			
1011.5656	1011.6007	0.0351	35	270	278	VHPVSTMIK			
1264.6782	1264.7018	0.0236	19	233	243	QVVESAYEVIK			
1644.9835	1645.0377	0.0542	33	113	126	NVNIFKFIIPNVVK			
1657.853	1657.8906	0.0376	23	43	57	DLADELALVDVIEDK			
1799.0359	1799.0052	-0.0307	-17	269	284	RVHPVSTMIKGLYGIK			
1899.032	1899.064	0.032	17	43	59	DLADELALVDVIEDKLK			
1906.0392	1906.1049	0.0657	34	82	99	DYNVTANSKLVIITAGAR			
1910.9606	1911.0211	0.0605	32	213	228	TLHPDLGTDKDKEQWK			
1933.0682	1933.118	0.0498	26	23	42	ITVVGVGAVGMACAISILMK			
1944.1204	1944.1799	0.0595	31	133	149	LLIVSNPVDILTYVAWK			
2112.0681	2112.1367	0.0686	32	246	265	GYTSWAIGLSVADLAESIMK			
2112.0681	2112.1367	0.0686	32	246	265	GYTSWAIGLSVADLAESIMK			
2353.2471	2353.3394	0.0923	39	244	265	LKGYTSWAIGLSVADLAESIMK			
2390.3401	2390.4207	0.0806	34	77	99	IVSGKDYNVTANSKLVIITAGAR			
2495.2961	2495.2114	-0.0847	-34	246	268	GYTSWAIGLSVADLAESIMKNLR			
2863.5273	2863.6221	0.0948	33	279	305	GLYGIKDDVFLSVPCILGQNGISDLVK			
3513.7966	3513.8669	0.0703	20	43	73	DLADELALVDVIEDKLKGEMMDLQHGSLFLR			
3611.7886	3611.8848	0.0962	27	178	212	LGVHPLSCHGWVLGEHGDSSVPVWSGMNVAGVSLK			

Spot Idx/Pos	191/H10	33	**Instr./Spot Origin**	ab4700/042810	**Process Status**	Analysis Succeeded
Plate [#] Name	[1] 042810		**4700 Sample Name**		**Spectra**	13

Rank	Protein Name	Accession No.	Protein MW	Protein Score	Protein C. I. %	Total Ion Score	Total Ion C. I. %
1	NME1-NME2 protein [Homo sapiens]	gi|66392203	30117.6	118	100		

Peptide Information

Calc. Mass	Obsrv. Mass	± da	± ppm	Start Seq.	End Seq.	Sequence	Ion Score	C. I. %	Modification
994.4774	994.4921	0.0147	15	106	114	GDFCIQVGR			
994.4774	994.4921	0.0147	15	221	229	GDFCIQVGR			
1149.6415	1149.6565	0.015	13	57	66	DRPFFAGLVK			
1149.6415	1149.6565	0.015	13	57	66	DRPFFAGLVK			
1181.587	1181.5825	-0.0045	-4	40	49	FMQASEDLLK			
1344.7633	1344.7744	0.0111	8	122	133	TFIAIKPDGVQR			
1344.7633	1344.7744	0.0111	8	7	18	TFIAIKPDGVQR			

1516.8845	1516.8854	0.0009	1	134	146	GLVGEIIKRFEQK	
1516.8845	1516.8854	0.0009	1	19	31	GLVGEIIKRFEQK	
1785.9163	1785.927	0.0107	6	89	105	VMLGETNPADSKPGTIR	
1785.9163	1785.927	0.0107	6	204	220	VMLGETNPADSKPGTIR	
2034.0806	2034.0894	0.0088	4	50	66	EHYVDLKDRPFFAGLVK	
2034.0806	2034.0894	0.0088	4	50	66	EHYVDLKDRPFFAGLVK	
2066.0261	2066.0259	-0.0002	0	40	56	FMQASEDLLKEHYVDLK	
2066.0261	2066.0259	-0.0002	0	40	56	FMQASEDLLKEHYVDLK	
2116.0718	2116.074	0.0022	1	67	85	YMHSGPVVAMVWEGLN VVK	
2116.0718	2116.074	0.0022	1	67	85	YMHSGPVVAMVWEGLN VVK	
3196.6499	3196.6282	-0.0217	-7	40	66	FMQASEDLLKEHYVDLK DRPFFAGLVK	

Rank	Protein Name	Accession No.	Protein MW	Protein Score	Protein C. I. %	Total Ion Score	Total Ion C. I. %
11	Chain A, Nucleoside Triphosphate, Nucleoside Diphosphate Mol_id: 1; Molecule: Nucleoside Diphosphat	gi|1421609	17155.9	25	0		

Peptide Information

Calc. Mass	Obsrv. Mass	± da	± ppm	Start Seq.	End Seq.	Sequence	Ion Score	C. I. %	Modification
994.4774	994.4921	0.0147	15	105	113	GDFCIQVGR			
994.4774	994.4921	0.0147	15	105	113	GDFCIQVGR			
1344.7633	1344.7744	0.0111	8	6	17	TFIAIKPDGVQR			
1344.7633	1344.7744	0.0111	8	6	17	TFIAIKPDGVQR			
1516.8845	1516.8854	0.0009	1	18	30	GLVGEIIKRFEQK			
1516.8845	1516.8854	0.0009	1	18	30	GLVGEIIKRFEQK			
1785.9163	1785.927	0.0107	6	88	104	VMLGETNPADSKPGTIR			
1785.9163	1785.927	0.0107	6	88	104	VMLGETNPADSKPGTIR			

Spot Idx/Pos	192/H12	34	**Instr./Spot Origin**	ab4700/042810	**Process Status**	Analysis Succeeded
Plate [#] Name	[1] 042810		**4700 Sample Name**		**Spectra**	13

Rank	Protein Name	Accession No.	Protein MW	Protein Score	Protein C. I. %	Total Ion Score	Total Ion C. I. %
1	NME1-NME2 protein [Homo sapiens]	gi|66392203	30117.6	135	100	17	86.888

Peptide Information

Calc. Mass	Obsrv. Mass	± da	± ppm	Start Seq.	End Seq.	Sequence	Ion Score	C. I. %	Modification
911.4733	911.4838	0.0105	12	143	149	FEQKGFR			
984.6199	984.6309	0.011	11	19	27	GLVGEIIKR	9	5.908	
984.6199	984.6309	0.011	11	134	142	GLVGEIIKR			
1149.6415	1149.6497	0.0082	7	57	66	DRPFFAGLVK			
1149.6415	1149.6497	0.0082	7	57	66	DRPFFAGLVK			
1344.7633	1344.7748	0.0115	9	122	133	TFIAIKPDGVQR			
1344.7633	1344.7748	0.0115	9	7	18	TFIAIKPDGVQR	10	31.837	
1516.8845	1516.8903	0.0058	4	134	146	GLVGEIIKRFEQK			
1516.8845	1516.8903	0.0058	4	19	31	GLVGEIIKRFEQK			
1785.9163	1785.9252	0.0089	5	204	220	VMLGETNPADSKPGTIR			
1785.9163	1785.9252	0.0089	5	89	105	VMLGETNPADSKPGTIR			
2034.0806	2034.0925	0.0119	6	50	66	EHYVDLKDRPFFAGLVK			
2034.0806	2034.0925	0.0119	6	50	66	EHYVDLKDRPFFAGLVK			
2066.0261	2066.0303	0.0042	2	40	56	FMQASEDLLKEHYVDLK			
2116.0718	2116.0618	-0.01	-5	67	85	YMHSGPVVAMVWEGLN VVK			
2116.0718	2116.0618	-0.01	-5	67	85	YMHSGPVVAMVWEGLN VVK			

Rank	Protein Name	Accession No.	Protein MW	Protein Score	Protein C. I. %	Total Ion Score	Total Ion C. I. %
23	nucleoside diphosphate kinase B	gi|924935	2058.1	21	0	10	31.837

Peptide Information

Calc. Mass	Obsrv. Mass	± da	± ppm	Start Seq.	End Seq.	Sequence	Ion Score	C. I. %	Modification
1344.7633	1344.7748	0.0115	9	7	18	TFIAIKPDGVQR			
1344.7633	1344.7748	0.0115	9	7	18	TFIAIKPDGVQR	10	31.837	

References

AHMED, A. & DANESHTALAB, M. 2012. Nonclassical biological activities of quinolone derivatives. *J Pharm Pharm Sci,* 15**,** 52-72.

ALCARAZ-ESTRADA, S. L., YOCUPICIO-MONROY, M., DEL ANGEL, R.M. 2010. Insights into dengue virus genome replication. *Future Virology,* 5**,** 575-592.

ALEN, M. M., DALLMEIER, K., BALZARINI, J., NEYTS, J. & SCHOLS, D. 2012. Crucial role of the N-glycans on the viral E-envelope glycoprotein in DC-SIGN-mediated dengue virus infection. *Antiviral Res,* 96**,** 280-7.

ALEN, M. M. & SCHOLS, D. 2012. Dengue virus entry as target for antiviral therapy. *J Trop Med,* 2012**,** 628475.

BACK, A. T. & LUNDKVIST, A. 2013. Dengue viruses - an overview. *Infect Ecol Epidemiol,* 3.

BARBAN, V., GIRERD, Y., AGUIRRE, M., GULIA, S., PETIARD, F., RIOU, P., BARRERE, B. & LANG, J. 2007. High stability of yellow fever 17D-204 vaccine: a 12-year restrospective analysis of large-scale production. *Vaccine,* 25**,** 2941-50.

BARONTI, C., SIRE, J., DE LAMBALLERIE, X. & QUERAT, G. 2010. Nonstructural NS1 proteins of several mosquito-borne *Flavivirus* do not inhibit TLR3 signaling. *Virology,* 404**,** 319-30.

BHATT, S., GETHING, P. W., BRADY, O. J., MESSINA, J. P., FARLOW, A. W., MOYES, C. L., DRAKE, J. M., BROWNSTEIN, J. S., HOEN, A. G., SANKOH, O., MYERS, M. F., GEORGE, D. B., JAENISCH, T., WINT, G. R., SIMMONS, C. P., SCOTT, T. W., FARRAR, J. J. & HAY, S. I. 2013. The global distribution and burden of dengue. *Nature,* 496**,** 504-7.

CARLSON, D. A., FRANKE, A. S., WEITZEL, D., SPEER, B. L., HUGHES, P. F., HAGERTY, L., FORTNER, C. N., VEAL, J. M., BARTA, T. E., ZIEBA, B. J., SOMLYO, A. V., SUTHERLAND, C., DENG, J. T., WALSH, M. P., MACDONALD, J. A. & HAYSTEAD, T. A. 2013. Fluorescence Linked Enzyme Chemoproteomic Strategy for Discovery of a Potent and Selective DAPK1 and ZIPK Inhibitor. *ACS Chem Biol*.

CARRINGTON, C. V., FOSTER, J. E., PYBUS, O. G., BENNETT, S. N. & HOLMES, E. C. 2005. Invasion and maintenance of dengue virus type 2 and type 4 in the Americas. *J Virol,* 79**,** 14680-7.

CDC. 2012. *Epidemiology* [Online]. CDC. Available: http://www.cdc.gov/dengue/epidemiology/ [Accessed 10/12/2013 2013].

CHE, P., TANG, H. & LI, Q. 2013. The interaction between claudin-1 and dengue viral prM/M protein for its entry. *Virology,* 446**,** 303-13.

CHUA, J. J., BHUVANAKANTHAM, R., CHOW, V. T. & NG, M. L. 2005. Recombinant non-structural 1 (NS1) protein of dengue-2 virus interacts with human STAT3beta protein. *Virus Res,* 112**,** 85-94.

CREGAR-HERNANDEZ, L., JIAO, G. S., JOHNSON, A. T., LEHRER, A. T., WONG, T. A. & MARGOSIAK, S. A. 2011. Small molecule pan-dengue and West Nile virus NS3 protease inhibitors. *Antivir Chem Chemother,* 21**,** 209-17.

DEL ANGEL, R. M. & VALLE, J. R. 2013. Dengue vaccines: strongly sought but not a reality just yet. *PLoS Pathog,* 9**,** e1003551.

DENG, J., LI, N., LIU, H., ZUO, Z., LIEW, O. W., XU, W., CHEN, G., TONG, X., TANG, W., ZHU, J., ZUO, J., JIANG, H., YANG, C. G., LI, J. & ZHU, W. 2012. Discovery of novel small molecule inhibitors of dengue viral NS2B-NS3 protease using virtual screening and scaffold hopping. *J Med Chem,* 55**,** 6278-93.

DUNCAN, J. S., GYENIS, L., LENEHAN, J., BRETNER, M., GRAVES, L. M., HAYSTEAD, T. A. & LITCHFIELD, D. W. 2008. An unbiased evaluation of CK2 inhibitors by chemoproteomics: characterization of inhibitor effects on CK2 and identification of novel inhibitor targets. *Mol Cell Proteomics,* 7**,** 1077-88.

DUNCAN, J. S., HAYSTEAD, T. A. & LITCHFIELD, D. W. 2012. Chemoproteomic characterization of protein kinase inhibitors using immobilized ATP. *Methods Mol Biol,* 795**,** 119-34.

DURBIN, A. P., KIRKPATRICK, B. D., PIERCE, K. K., SCHMIDT, A. C. & WHITEHEAD, S. S. 2011. Development and clinical evaluation of multiple investigational monovalent DENV vaccines to identify components for inclusion in a live attenuated tetravalent DENV vaccine. *Vaccine,* 29**,** 7242-50.

EKKAPONGPISIT, M., WANNATUNG, T., SUSANTAD, T., TRIWITAYAKORN, K. & SMITH, D. R. 2007. cDNA-AFLP analysis of differential gene expression in human hepatoma cells (HepG2) upon dengue virus infection. *J Med Virol,* 79**,** 552-61.

FADDEN, P., HUANG, K. H., VEAL, J. M., STEED, P. M., BARABASZ, A. F., FOLEY, B., HU, M., PARTRIDGE, J. M., RICE, J., SCOTT, A., DUBOIS, L. G., FREED, T. A., SILINSKI, M. A., BARTA, T. E., HUGHES, P. F., OMMEN, A., MA, W., SMITH, E. D., SPANGENBERG, A. W., EAVES, J., HANSON, G. J., HINKLEY, L., JENKS, M., LEWIS, M., OTTO, J., PRONK, G. J., VERLEYSEN, K., HAYSTEAD, T. A. & HALL, S. E. 2010a. Application of chemoproteomics to drug discovery: identification of a clinical candidate targeting hsp90. *Chem Biol,* 17**,** 686-94.

FANG, S., WU, Y., WU, N., ZHANG, J. & AN, J. 2013. Recent advances in DENV receptors. *ScientificWorldJournal,* 2013**,** 684690.

FRANCICA, J. R., VARELA-ROHENA, A., MEDVEC, A., PLESA, G., RILEY, J. L. & BATES, P. 2010. Steric shielding of surface epitopes and impaired immune recognition induced by the ebola virus glycoprotein. *PLoS Pathog,* 6**,** e1001098.

FREIFELD, C., BROWNSTEIN, J. 2013. *Dengue Map: A CDC-HealthMap Collaboration* [Online]. Available: http://www.healthmap.org/dengue/ [Accessed 10/12/2013 2013].

GRANT, D., TAN, G. K., QING, M., NG, J. K., YIP, A., ZOU, G., XIE, X., YUAN, Z., SCHREIBER, M. J., SCHUL, W., SHI, P. Y. & ALONSO, S. 2011. A single amino acid in nonstructural protein NS4B confers virulence to dengue virus in AG129 mice through enhancement of viral RNA synthesis. *J Virol,* 85**,** 7775-87.

GRAVES, P. R. & HAYSTEAD, T. A. 2002. Molecular biologist's guide to proteomics. *Microbiol Mol Biol Rev,* 66**,** 39-63; table of contents.

GRAVES, P. R., KWIEK, J. J., FADDEN, P., RAY, R., HARDEMAN, K., COLEY, A. M., FOLEY, M. & HAYSTEAD, T. A. 2002. Discovery of novel targets of quinoline drugs in the human purine binding proteome. *Mol. Pharmacol.,* 62**,** 1364-72.

GUIRAKHOO, F., PUGACHEV, K., ZHANG, Z., MYERS, G., LEVENBOOK, I., DRAPER, K., LANG, J., OCRAN, S., MITCHELL, F., PARSONS, M., BROWN, N., BRANDLER, S., FOURNIER, C., BARRERE, B., RIZVI, F., TRAVASSOS, A., NICHOLS, R., TRENT, D. & MONATH, T. 2004. Safety and efficacy of chimeric

yellow Fever-dengue virus tetravalent vaccine formulations in nonhuman primates. *J Virol,* 78**,** 4761-75.

HANNEMANN, H., SUNG, P. Y., CHIU, H. C., YOUSUF, A., BIRD, J., LIM, S. P. & DAVIDSON, A. D. 2013. Serotype-specific differences in dengue virus non-structural protein 5 nuclear localization. *J Biol Chem,* 288**,** 22621-35.

HAYSTEAD, T. A. 2006. The purinome, a complex mix of drug and toxicity targets. *Curr Top Med Chem,* 6**,** 1117-27.

HEATON, N. S., PERERA, R., BERGER, K. L., KHADKA, S., LACOUNT, D. J., KUHN, R. J. & RANDALL, G. 2010. Dengue virus nonstructural protein 3 redistributes fatty acid synthase to sites of viral replication and increases cellular fatty acid synthesis. *Proc Natl Acad Sci U S A,* 107**,** 17345-50.

HEINZ, F. X. & STIASNY, K. 2012a. Flaviviruses and *Flavivirus* vaccines. *Vaccine,* 30**,** 4301-6.

HEINZ, F. X. & STIASNY, K. 2012b. Flaviviruses and their antigenic structure. *J Clin Virol,* 55**,** 289-95.

LAMBETH, C. R., WHITE, L. J., JOHNSTON, R. E. & DE SILVA, A. M. 2005. Flow cytometry-based assay for titrating dengue virus. *J Clin Microbiol,* 43**,** 3267-72.

LASHLEY, F., DURHAM, J. 2002. *Emerging infectious diseases: trends and issues,* New York, Springer Publishing Company, Sheridan Press.

LIBRATY, D. H., YOUNG, P. R., PICKERING, D., ENDY, T. P., KALAYANAROOJ, S., GREEN, S., VAUGHN, D. W., NISALAK, A., ENNIS, F. A. & ROTHMAN, A. L. 2002. High circulating levels of the dengue virus nonstructural protein NS1 early in dengue illness correlate with the development of dengue hemorrhagic fever. *J Infect Dis,* 186**,** 1165-8.

LIEW, K. J. & CHOW, V. T. 2004. Differential display RT-PCR analysis of ECV304 endothelial-like cells infected with dengue virus type 2 reveals messenger RNA expression profiles of multiple human genes involved in known and novel roles. *J Med Virol,* 72**,** 597-609.

LIM, S. P., SONNTAG, L. S., NOBLE, C., NILAR, S. H., NG, R. H., ZOU, G., MONAGHAN, P., CHUNG, K. Y., DONG, H., LIU, B., BODENREIDER, C., LEE,

G., DING, M., CHAN, W. L., WANG, G., JIAN, Y. L., CHAO, A. T., LESCAR, J., YIN, Z., VEDANANDA, T. R., KELLER, T. H. & SHI, P. Y. 2011. Small molecule inhibitors that selectively block dengue virus methyltransferase. *J Biol Chem,* 286**,** 6233-40.

LIN, C. F., WAN, S. W., CHENG, H. J., LEI, H. Y. & LIN, Y. S. 2006. Autoimmune pathogenesis in dengue virus infection. *Viral Immunol,* 19**,** 127-32.

LINDENBACH, B. D. 2009. Measuring HCV infectivity produced in cell culture and in vivo. *Methods Mol Biol,* 510**,** 329-36.

LU, H., XU, X. F., GAO, N., FAN, D. Y., WANG, J. & AN, J. 2013. Preliminary evaluation of DNA vaccine candidates encoding dengue-2 prM/E and NS1: their immunity and protective efficacy in mice. *Mol Immunol,* 54**,** 109-14.

MA, L., JONES, C. T., GROESCH, T. D., KUHN, R. J. & POST, C. B. 2004. Solution structure of dengue virus capsid protein reveals another fold. *Proc Natl Acad Sci U S A,* 101**,** 3414-9.

MARKOFF, L., FALGOUT, B. & CHANG, A. 1997. A conserved internal hydrophobic domain mediates the stable membrane integration of the dengue virus capsid protein. *Virology,* 233**,** 105-17.

MCARTHUR, J. H., DURBIN, A. P., MARRON, J. A., WANIONEK, K. A., THUMAR, B., PIERRO, D. J., SCHMIDT, A. C., BLANEY, J. E., JR., MURPHY, B. R. & WHITEHEAD, S. S. 2008. Phase I clinical evaluation of rDEN4Delta30-200,201: a live attenuated dengue 4 vaccine candidate designed for decreased hepatotoxicity. *Am J Trop Med Hyg,* 79**,** 678-84.

MCDOWELL, M., GONZALES, S. R., KUMARAPPERUMA, S. C., JESELNIK, M., ARTERBURN, J. B. & HANLEY, K. A. 2010. A novel nucleoside analog, 1-beta-d-ribofuranosyl-3-ethynyl-[1,2,4]triazole (ETAR), exhibits efficacy against a broad range of Flaviviruses in vitro. *Antiviral Res,* 87**,** 78-80.

MILLER, S., KASTNER, S., KRIJNSE-LOCKER, J., BUHLER, S. & BARTENSCHLAGER, R. 2007. The non-structural protein 4A of dengue virus is an integral membrane protein inducing membrane alterations in a 2K-regulated manner. *J Biol Chem,* 282**,** 8873-82.

MILLER, S., SPARACIO, S. & BARTENSCHLAGER, R. 2006. Subcellular localization and membrane topology of the Dengue virus type 2 Non-structural protein 4B. *J Biol Chem,* 281**,** 8854-63.

MISHRA, K. P., SHWETA, DIWAKER, D. & GANJU, L. 2012. Dengue virus infection induces upregulation of hn RNP-H and PDIA3 for its multiplication in the host cell. *Virus Res,* 163**,** 573-9.

MONATH, T. P. 2008. Treatment of yellow fever. *Antiviral Res,* 78**,** 116-24.

MULLER, D. A. & YOUNG, P. R. 2013. The *Flavivirus* NS1 protein: molecular and structural biology, immunology, role in pathogenesis and application as a diagnostic biomarker. *Antiviral Res,* 98**,** 192-208.

MUNOZ-JORDAN, J. L., SANCHEZ-BURGOS, G. G., LAURENT-ROLLE, M. & GARCIA-SASTRE, A. 2003. Inhibition of interferon signaling by dengue virus. *Proc Natl Acad Sci U S A,* 100**,** 14333-8.

NEMESIO, H., PALOMARES-JEREZ, F. & VILLALAIN, J. 2012. NS4A and NS4B proteins from dengue virus: membranotropic regions. *Biochim Biophys Acta,* 1818**,** 2818-30.

NETSAWANG, J., NOISAKRAN, S., PUTTIKHUNT, C., KASINRERK, W., WONGWIWAT, W., MALASIT, P., YENCHITSOMANUS, P. T. & LIMJINDAPORN, T. 2010. Nuclear localization of dengue virus capsid protein is required for DAXX interaction and apoptosis. *Virus Res,* 147**,** 275-83.

NGUYEN, N. M., TRAN, C. N., PHUNG, L. K., DUONG, K. T., HUYNH HLE, A., FARRAR, J., NGUYEN, Q. T., TRAN, H. T., NGUYEN, C. V., MERSON, L., HOANG, L. T., HIBBERD, M. L., AW, P. P., WILM, A., NAGARAJAN, N., NGUYEN, D. T., PHAM, M. P., NGUYEN, T. T., JAVANBAKHT, H., KLUMPP, K., HAMMOND, J., PETRIC, R., WOLBERS, M., NGUYEN, C. T. & SIMMONS, C. P. 2013. A randomized, double-blind placebo controlled trial of balapiravir, a polymerase inhibitor, in adult dengue patients. *J Infect Dis,* 207**,** 1442-50.

NIYOMRATTANAKIT, P., ABAS, S. N., LIM, C. C., BEER, D., SHI, P. Y. & CHEN, Y. L. 2011. A fluorescence-based alkaline phosphatase-coupled polymerase assay for identification of inhibitors of dengue virus RNA-dependent RNA polymerase. *J Biomol Screen,* 16**,** 201-10.

NIYOMRATTANAKIT, P., CHEN, Y. L., DONG, H., YIN, Z., QING, M., GLICKMAN, J. F., LIN, K., MUELLER, D., VOSHOL, H., LIM, J. Y., NILAR, S., KELLER, T. H. & SHI, P. Y. 2010. Inhibition of dengue virus polymerase by blocking of the RNA tunnel. *J Virol,* 84**,** 5678-86.

NIYOMRATTANAKIT, P., WINOYANUWATTIKUN, P., CHANPRAPAPH, S., ANGSUTHANASOMBAT, C., PANYIM, S. & KATZENMEIER, G. 2004. Identification of residues in the dengue virus type 2 NS2B cofactor that are critical for NS3 protease activation. *J Virol,* 78**,** 13708-16.

NOVAK, R. 1992. The asian tiger mosquito, Aedes albopictus. *Wing Beats,* 3.

OOI, E. E. & GUBLER, D. J. 2009. Dengue in Southeast Asia: epidemiological characteristics and strategic challenges in disease prevention. *Cad Saude Publica,* 25 Suppl 1**,** S115-24.

PARK, B. K., BOOBIS, A., CLARKE, S., GOLDRING, C. E., JONES, D., KENNA, J. G., LAMBERT, C., LAVERTY, H. G., NAISBITT, D. J., NELSON, S., NICOLL-GRIFFITH, D. A., OBACH, R. S., ROUTLEDGE, P., SMITH, D. A., TWEEDIE, D. J., VERMEULEN, N., WILLIAMS, D. P., WILSON, I. D. & BAILLIE, T. A. 2011. Managing the challenge of chemically reactive metabolites in drug development. *Nat Rev Drug Discov,* 10**,** 292-306.

PATTANAKITSAKUL, S. N., RUNGROJCHAROENKIT, K., KANLAYA, R., SINCHAIKUL, S., NOISAKRAN, S., CHEN, S. T., MALASIT, P. & THONGBOONKERD, V. 2007. Proteomic analysis of host responses in HepG2 cells during dengue virus infection. *J Proteome Res,* 6**,** 4592-600.

PERERA, R., KHALIQ, M. & KUHN, R. J. 2008. Closing the door on Flaviviruses: entry as a target for antiviral drug design. *Antiviral Res,* 80**,** 11-22.

PERERA, R. & KUHN, R. J. 2008. Structural proteomics of dengue virus. *Curr Opin Microbiol,* 11**,** 369-77.

RAJAN, A., KELLY, R. J., TREPEL, J. B., KIM, Y. S., ALARCON, S. V., KUMMAR, S., GUTIERREZ, M., CRANDON, S., ZEIN, W. M., JAIN, L., MANNARGUDI, B., FIGG, W. D., HOUK, B. E., SHNAIDMAN, M., BREGA, N. & GIACCONE, G. 2011. A phase I study of PF-04929113 (SNX-5422), an orally bioavailable heat shock protein 90 inhibitor, in patients with refractory solid tumor malignancies and lymphomas. *Clin Cancer Res,* 17**,** 6831-9.

RATHORE, A. P., PARADKAR, P. N., WATANABE, S., TAN, K. H., SUNG, C., CONNOLLY, J. E., LOW, J., OOI, E. E. & VASUDEVAN, S. G. 2011. Celgosivir treatment misfolds dengue virus NS1 protein, induces cellular pro-survival genes and protects against lethal challenge mouse model. *Antiviral Res,* 92**,** 453-60.

RAWLINSON, S. M., PRYOR, M. J., WRIGHT, P. J. & JANS, D. A. 2006. Dengue virus RNA polymerase NS5: a potential therapeutic target? *Curr Drug Targets,* 7**,** 1623-38.

RAWLINSON, S. M., PRYOR, M. J., WRIGHT, P. J. & JANS, D. A. 2009a. CRM1-mediated nuclear export of dengue virus RNA polymerase NS5 modulates interleukin-8 induction and virus production. *J Biol Chem,* 284**,** 15589-97.

RODENHUIS-ZYBERT, I. A., WILSCHUT, J. & SMIT, J. M. 2010. Dengue virus life cycle: viral and host factors modulating infectivity. *Cell Mol Life Sci,* 67**,** 2773-86.

RODENHUIS-ZYBERT, I. A., WILSCHUT, J. & SMIT, J. M. 2011. Partial maturation: an immune-evasion strategy of dengue virus? *Trends Microbiol,* 19**,** 248-54.

ROEHRIG, J. 2013. Current status of dengue vaccine development. *SAGE/Immunization Meeting.* National Center for Emerging and Zoonotic Infectious Disease, Division of Vector-Borne DIseases, Arboviral Branch.

ROGERS, D. J., WILSON, A. J., HAY, S. I. & GRAHAM, A. J. 2006. The global distribution of yellow fever and dengue. *Adv Parasitol,* 62**,** 181-220.

SABCHAREON, A., WALLACE, D., SIRIVICHAYAKUL, C., LIMKITTIKUL, K., CHANTHAVANICH, P., SUVANNADABBA, S., JIWARIYAVEJ, V., DULYACHAI, W., PENGSAA, K., WARTEL, T. A., MOUREAU, A., SAVILLE, M., BOUCKENOOGHE, A., VIVIANI, S., TORNIEPORTH, N. G. & LANG, J. 2012. Protective efficacy of the recombinant, live-attenuated, CYD tetravalent dengue vaccine in Thai schoolchildren: a randomised, controlled phase 2b trial. *Lancet,* 380**,** 1559-67.

SAMPATH, A. & PADMANABHAN, R. 2009. Molecular targets for *Flavivirus* drug discovery. *Antiviral Res,* 81**,** 6-15.

SAN MARTIN, J. L., BRATHWAITE, O., ZAMBRANO, B., SOLORZANO, J. O., BOUCKENOOGHE, A., DAYAN, G. H. & GUZMAN, M. G. 2010. The

epidemiology of dengue in the americas over the last three decades: a worrisome reality. *Am J Trop Med Hyg,* 82**,** 128-35.

STAHLA-BEEK, H. J., APRIL, D. G., SAEEDI, B. J., HANNAH, A. M., KEENAN, S. M. & GEISS, B. J. 2012. Identification of a novel antiviral inhibitor of the *Flavivirus* guanylyltransferase enzyme. *J Virol,* 86**,** 8730-9.

STEVENS, A. J., GAHAN, M. E., MAHALINGAM, S. & KELLER, P. A. 2009. The medicinal chemistry of dengue fever. *J Med Chem,* 52**,** 7911-26.

TAN, G. K. & ALONSO, S. 2009. Pathogenesis and prevention of dengue virus infection: state-of-the-art. *Curr Opin Infect Dis,* 22**,** 302-8.

TANG, K. F. & OOI, E. E. 2012. Diagnosis of dengue: an update. *Expert Rev Anti Infect Ther,* 10**,** 895-907.

VILIBIC-CAVLEK, T., LJUBIN-STERNAK, S., BABIC-ERCEG, A., SVIBEN, M. & MLINARIC-GALINOVIC, G. 2012. [Virology diagnosis of re-emergent infections: dengue virus]. *Lijec Vjesn,* 134**,** 164-7.

WAN, S. W., LIN, C. F., WANG, S., CHEN, Y. H., YEH, T. M., LIU, H. S., ANDERSON, R. & LIN, Y. S. 2013. Current progress in dengue vaccines. *J Biomed Sci,* 20**,** 37.

WARKE, R. V., XHAJA, K., MARTIN, K. J., FOURNIER, M. F., SHAW, S. K., BRIZUELA, N., DE BOSCH, N., LAPOINTE, D., ENNIS, F. A., ROTHMAN, A. L. & BOSCH, I. 2003. Dengue virus induces novel changes in gene expression of human umbilical vein endothelial cells. *J Virol,* 77**,** 11822-32.

WHO. 2013. *Better environmental management for control of dengue* [Online]. WHO.org. Available: http://www.who.int/heli/risks/vectors/denguecontrol/en/ [Accessed 10/12/2013 2013].

WILSON, J. R., DE SESSIONS, P. F., LEON, M. A. & SCHOLLE, F. 2008. West Nile virus nonstructural protein 1 inhibits TLR3 signal transduction. *J Virol,* 82**,** 8262-71.

XIE, X., GAYEN, S., KANG, C., YUAN, Z. & SHI, P. Y. 2013. Membrane topology and function of dengue virus NS2A protein. *J Virol,* 87**,** 4609-22.

XIE, X., WANG, Q. Y., XU, H. Y., QING, M., KRAMER, L., YUAN, Z. & SHI, P. Y. 2011. Inhibition of dengue virus by targeting viral NS4B protein. *J Virol,* 85**,** 11183-95.

XU, T., SAMPATH, A., CHAO, A., WEN, D., NANAO, M., CHENE, P., VASUDEVAN, S. G. & LESCAR, J. 2005. Structure of the Dengue virus helicase/nucleoside triphosphatase catalytic domain at a resolution of 2.4 A. *J Virol,* 79**,** 10278-88.

YAP, T. L., XU, T., CHEN, Y. L., MALET, H., EGLOFF, M. P., CANARD, B., VASUDEVAN, S. G. & LESCAR, J. 2007. Crystal structure of the dengue virus RNA-dependent RNA polymerase catalytic domain at 1.85-angstrom resolution. *J Virol,* 81**,** 4753-65.

YAUCH, L. E. & SHRESTA, S. 2008. Mouse models of dengue virus infection and disease. *Antiviral Res,* 80**,** 87-93.

YIN, Z., CHEN, Y.-L., KONDREDDI, R. R., CHAN, W. L., WANG, G., NG, R. H., LIM, J. Y. H., LEE, W. Y., JEYARAJ, D. A., NIYOMRATTANAKIT, P., WEN, D., CHAO, A., GLICKMAN, J. F., VOSHOL, H., MUELLER, D., SPANKA, C., DRESSLER, S., NILAR, S., VASUDEVAN, S. G., SHI, P.-Y. & KELLER, T. H. 2009a. N-Sulfonylanthranilic Acid Derivatives as Allosteric Inhibitors of Dengue Viral RNA-Dependent RNA Polymerase. *Journal of Medicinal Chemistry,* 52**,** 7934-7937.

YIN, Z., CHEN, Y. L., KONDREDDI, R. R., CHAN, W. L., WANG, G., NG, R. H., LIM, J. Y., LEE, W. Y., JEYARAJ, D. A., NIYOMRATTANAKIT, P., WEN, D., CHAO, A., GLICKMAN, J. F., VOSHOL, H., MUELLER, D., SPANKA, C., DRESSLER, S., NILAR, S., VASUDEVAN, S. G., SHI, P. Y. & KELLER, T. H. 2009b. N-sulfonylanthranilic acid derivatives as allosteric inhibitors of dengue viral RNA-dependent RNA polymerase. *J Med Chem,* 52**,** 7934-7.

YIN, Z., CHEN, Y. L., SCHUL, W., WANG, Q. Y., GU, F., DURAISWAMY, J., KONDREDDI, R. R., NIYOMRATTANAKIT, P., LAKSHMINARAYANA, S. B., GOH, A., XU, H. Y., LIU, W., LIU, B., LIM, J. Y., NG, C. Y., QING, M., LIM, C. C., YIP, A., WANG, G., CHAN, W. L., TAN, H. P., LIN, K., ZHANG, B., ZOU, G., BERNARD, K. A., GARRETT, C., BELTZ, K., DONG, M., WEAVER, M., HE, H., PICHOTA, A., DARTOIS, V., KELLER, T. H. & SHI, P. Y. 2009c. An adenosine nucleoside inhibitor of dengue virus. *Proc Natl Acad Sci U S A,* 106**,** 20435-9.

ZHANG, M., ZHENG, X., WU, Y., GAN, M., HE, A., LI, Z., ZHANG, D., WU, X. & ZHAN, X. 2013. Differential proteomics of Aedes albopictus salivary gland, midgut and C6/36 cell induced by dengue virus infection. *Virology,* 444**,** 109-18.

ZOMPI, S. & HARRIS, E. 2012. Animal models of dengue virus infection. *Viruses,* 4**,** 62-82.

Biography

Brittany Lauren Speer

Born on May 14, 1987 at Overlook Hospital in Summit, New Jersey, USA

Education:

Aug. 2009 - May 2014	Doctor of Philosophy Department of Pharmacology Duke University Durham, NC, USA
Aug. 2005 - May 2009	Bachelor of Science Department of Chemistry The College of New Jersey Ewing, NJ, USA (Summa Cum Laude, Phi Beta Kappa)

Publications:

Carlson, D., Franke, A., Weitzel, D., Speer, B., Hughes, P., Hagerty, L., Fortner, C., Veal, J., Barta, T., Zieba, B., Somlyo, A., Sutherland, C., Deng, J., Walsh, M., MacDonald, J., Haystead, T. **Fluorescence linked enzyme chemoproteomic strategy for discovery of a potent and selective DAPK1 and ZIPK inhibitor.** *ACS Chem Bio* 2013. PMID: 24070067

Hughes, P., Barrot, J., Carlson, D., Loiselle, D., Speer, B., Bodoor, K., Rund, L., Haystead, T. **A highly selective Hsp90 affinity chromatography resin with a cleavable linker.** *Bioorg Med Chem* 2012 May 15;20(10):3298-305 PMID: 22520629

Awards:

2012 - 2013	Preparing Future Faculty Fellow, Duke University Graduate School
2012	Duke Graduate School Conference Travel Award (Cartagena, Colombia)